

Characterization and Formation of High-Chroma Features
in Loamy Soils of Southern Minnesota

A Dissertation
SUBMITTED TO THE FACULTY OF
UNIVERSITY OF MINNESOTA
BY

Douglas Wayne Pribyl

IN PARTIAL FULFILLMENT OF THE REQUIREMENTS
FOR THE DEGREE OF
DOCTOR OF PHILOSOPHY

James C. Bell, Adviser

December 2012

Acknowledgements

Many people both inside and outside the University of Minnesota have helped make this dissertation possible. The Department of Soil, Water, and Climate has supported me in many ways not least of which was the office staff, who were always ready with a friendly greeting, and willing and able to solve any problem: Karen Mellem, Kari Jarcho, Jenny Brand, and Marjorie Bonse. I especially want to thank my adviser, Jay Bell, for his continuous enthusiasm and encouragement. Ed Nater, together with Jay Bell, is responsible for introducing me to soil genesis and enabling me to pursue the interest they created. The rest of my committee, Paul Bloom and Carrie Jennings, have provided inspiration and motivation. Terry Cooper and John Lamb imparted wisdom and confidence in ways that only the best teachers can. I am profoundly grateful to have been their teaching assistant.

Parts of this work were carried out in the Characterization Facility, University of Minnesota, which receives partial support from NSF through the MRSEC program. A special thanks to the staff who trained, listened, suggested, and encouraged: Bob Hafner, Ozan Ugurlu, Jinping Dong, John Nelson, Alice Ressler, Maria Torija Juana, Fang Zhou, and Nicholas Seaton.

My earliest microscopy imaging and analysis work was with Gib Ahlstrand at the Biological Imaging Center, now part of the University Imaging Centers at the University of Minnesota. Later imaging and analysis work at the Imaging Center required the able assistance of Tracy Anderson, Gail Celio, and Mark Sanders, who were most generous with their time and resources to help a non-biologist in time of need.

Also, I want to thank Thelma Berquó, Subir Banerjee, and others at the Institute for Rock Magnetism, Paroma Chakravarty at Dr. Raj Suryanarayanan's Pharmaceutics Lab for use of their FT-Raman, Roger Eliason and Russell Anderson at the University of Minnesota Soil Testing Lab, Donna Whitney in the Geology Department who made her lab available for thin sectioning and Valerie Morgan who took the time to train me.

I am truly fortunate to have had the loving support of my wife, whose quiet, unwavering confidence kept me on course and whose companionship kept me grounded.

Finally for my parents, who encouraged me to pursue my interests and continue my education, a more tangible acknowledgement: the choice of Palatino Linotype as the type font used for this dissertation.

Dedication

This dissertation is dedicated to my parents, Vernon and Myra Pribyl, whose love of family knows no bounds.

ABSTRACT

High-chroma features have not been adequately defined under existing terminology or classified under existing systems. The terms “masses” as a subclass of concentrations used in field definitions and “loose infillings” used in micromorphological classifications come closest but are not fully satisfactory. Defined descriptively, high-chroma features have a typical color of 7.5YR 5/8, are usually less than 1 to 2 mm in diameter, are poorly cemented, and have a sharp external boundary with the soil matrix. They are found in well-drained to poorly drained soils with first-appearance typically at depths of 50 to 100 cm. A study was undertaken to more fully characterize and classify high-chroma features and to provide more accurate interpretations of feature morphology for applications in environmental and soil quality, plant nutrition, and soil genesis.

High-chroma features found within peds having varying degrees of hydromorphic expression were assigned to classes depending on internal color and color patterns. Material removed from features, halos, and the soil matrix was analyzed using a low-power stereomicroscope, SEM/EDS, TEM/ED, μ -XRD, ICP, and stain tests to determine properties and composition.

Four formation hypotheses are proposed: (1) a non-pedogenic origin, features having developed from the weathering of an inherited precursor mineral; (2) a pedogenic origin resulting from the formation and infilling of vesicles that formed at depth shortly after deglaciation but are no longer actively forming; (3) a pedogenic origin but features are actively forming; (4) formation by dissolution of a soluble mineral fragment and subsequent infilling of the resulting void, analogous to the formation of a geode.

Although high-chroma features might develop by more than one pathway, a non-pedogenic origin is favored. Non-pedogenic hypothesis (1) and the hybrid geodic hypothesis (4) offer the most efficient explanations for the presence of silt, iron, and manganese within high-chroma features. A proposed weathering sequence based on feature classification and evidence for the presence of manganese nodules in the till-source bedrock also support a non-pedogenic origin. Pedogenic hypotheses require a sequence of events of uncertain and in some cases seemingly low probability.

Existing classification systems offer little insight into genesis. Most importantly, given the evidence for a non-pedogenic origin, high-chroma features should not be interpreted or classified as redoximorphic features as the term is typically used in the field. Although high-chroma features may result from alternating periods of oxidation and reduction, when used alone they are ambiguous indicators of seasonal wetness.

Table of Contents

Acknowledgements	i
Dedication	ii
Abstract	iii
List of Tables	v
List of Figures	vi
Introduction	1
General description of high-chroma features	3
Historical and interpretive sciences	6
General description of the study area	10
Development of the soils	17
Literature Review	26
Part I: Further characterization of the till	26
Part II: Classification systems	50
Part III: Properties and formation of nodules and concretions	75
Methods	101
Sampling methods	102
Sample sites	104
Initial sample preparation	109
Thin sections	109
Characterization and analysis	111
Results and Discussion	137
Classification of peds by hydromorphology	137
Characterization of high-chroma features	144
Classification of high-chroma features	203
Classification as redoximorphic features	209
Comparison of data: non-pedogenic and pedogenic hypotheses	215
Discussion of proposed formation hypotheses	220
Non-pedogenic, inherited	223
Pedogenic, inherited	230
Pedogenic, coeval	256
Geode hypothesis	258
Other hypotheses	261
Conclusion	264
References	271
Appendices	294
Appendix A: Corrected ICP data	295
Appendix B: Reagents and Stains	296
Appendix C: Discussion and Evaluation of Analytical Methods	297

List of Tables

Table 1	Physical characteristics associated with high-chroma features	5
Table 2	Climate summary from monitoring stations in southern Minnesota	13
Table 3	Chemical analysis of Manitoba Paleozoic deposits	33
Table 4	Chemical analysis of the Pierre shale	37
Table 5	Chemical analysis of surface deposits and nodule	41
Table 6	Drainage class and taxonomic classification for the soil series mapped in the study area	105
Table 7	Occurrence of features for soil series mapped in the study area	106
Table 8	Classification of peds by hydromorphic expression	139
Table 9	Field data for soils in and near sample sites	145
Table 10	OSD data for soils in and near sample sites	148
Table 11	Summary of physical properties of high-chroma features	153
Table 12	Summary of physical properties of high-chroma features and halos by class	154
Table 13	Micro-XRD data	186
Table 14	Alizarin Red S and Titan Yellow stain test sequences	199
Table 15	Alizarin Red S and potassium ferricyanide stain reactions	200
Table 16	Some iron and manganese (hydr)oxides relevant to the formation of high-chroma features	249

List of Figures

Figure 1	Locations of climate stations	12
Figure 2	Major glacial landforms of southern Minnesota	14
Figure 3	Soil moisture regimes	16
Figure 4	Soil temperature regimes	16
Figure 5	Ternary diagrams comparing texture and grain composition	19
Figure 6	Relationship between iron and manganese in nodules near Chamberlain, S.D.	45
Figure 7	Structure of a high-chroma feature	103
Figure 8	Classification of high-chroma features	121
Figure 9	Boundary versus halo	138
Figure 10	Feature-to-matrix comparison with VP-SEM	178
Figure 11	EDS of feature-to-matrix comparison with VP-SEM	180
Figure 12	SEM image of high-chroma feature	181
Figure 13	EDS of a feature similar to that of Figure 12	183
Figure 14	TEM image with ED pattern	184
Figure 15	Micro-XRD spectrum of a high-chroma feature in situ	187
Figure 16	Micro-XRD comparison of samples 2A and 2B	189
Figure 17	Raman spectra	192
Figure 18	Raman reference spectra	193
Figure 19	Enrichment factors from ICP results	196
Figure 20	Field key to soil concentrations	204

INTRODUCTION

Concentrations of iron minerals are arguably the most easily recognized of all soil features. Distinctive colors and patterns produced by the presence or absence of iron are often used to distinguish horizons and to infer the degree of saturation, past or present, in a soil. If formed under conditions of alternating saturation, reduction, and oxidation, mottled patterns of gray depletions and brown, yellow, or red concentrations are correctly called redoximorphic features. Discrete concentrations of iron may occur in soils without an apparent association with depletions or a water table. These features, sometimes having high Munsell chroma, are of particular interest because they pose a serious and vexing problem of interpretation. These are the features of interest in this study.

Many land use decisions including wetland delineation, land development, agricultural activities, and septic tank and waste disposal siting, are based on the degree of saturation or wetness as indicated by the presence of redoximorphic features. Assignment of the term "redoximorphic" to a soil feature is an interpretation based on morphology. Their appearance in a soil profile, high above a known water table, is sometimes interpreted to mean that the features are relict, having formed sometime in the past under different environmental conditions. Such an interpretation must be approached with caution not just because of the limited state of our knowledge about how redoximorphic features form, but also because of the consequences of misinterpretation. Misinterpreting a feature as an actively forming redoximorphic feature can lead to excessive and unnecessary construction expense to protect soil and groundwater quality, while incorrectly identifying a feature as a relict or as a non-redoximorphic feature when they are actively

forming redoximorphic features may result in the contamination of groundwater or failure of a waste disposal or septic system, with unpleasant consequences for the owner.

Identification of features as being of redoximorphic origin is problematic. No tests or set of properties exist to conclusively identify a feature as having a redoximorphic origin or to establish whether it is actively forming. Concentrations are particularly troublesome since they can have non-redoximorphic origins but have morphologies that resemble redoximorphic features.

The objectives of this research are to (1) characterize and classify Fe-Mn concentrations in a way that reflects possible origins; (2) to provide more accurate interpretations of nodule morphology for applications in environmental and soil quality, plant nutrition, and soil genesis; (3) to answer the question of whether features are aggrading or degrading.

Initially, three hypotheses were considered: (1) high-chroma features are weathered iron or iron-manganese mineral clasts present in the parent material (inherited origin); (2) high-chroma features are concentrations of iron-manganese minerals that oxidized out of soil solution (pedogenic origin); (3) high-chroma features are degradational. Possible precursor minerals under the inherited hypothesis include iron sulfides such as pyrite, iron and manganese carbonates such as siderite and rhodochrosite, and iron silicate minerals such as olivine and pyroxene.

To test these hypotheses, high-chroma features taken from soils with differing hydromorphology were characterized and compared on the basis of physical, chemical, and mineralogical properties. Methods used for

characterization include electron and optical microscopy and microanalysis, x-ray diffraction, inductively coupled plasma for chemical analysis, and microchemical stain tests for carbonate mineral identification.

A thorough understanding of feature genesis is necessary for making accurate interpretations. Therefore, the ultimate goal is to understand the formational environment, origin, and genesis of high-chroma features by closely examining the features themselves, an approach first set forth by Nicolaus Steno in his *Prodromus* written in 1669. Steno stated that the fundamental problem of studying solids within solids is: “given a substance possessed of a certain figure, and produced according to the laws of nature, to find in the substance itself evidences disclosing the place and manner of its production” (Steno 1968:209). Finding and properly interpreting those “evidences” in high-chroma features is the challenge taken up by this research.

General Description of High-Chroma Features

The term “high-chroma feature” was chosen as one that was purely descriptive. Most other terms, such as mottle, nodule or concretion, Brewer’s glaeble, Kubiena’s amygdule, Vepraskas’ redoximorphic feature, all had or have specific connotations associated implicitly or explicitly with genesis. “Mottle” has been defined and used as a generic term (Soil Science Society of America 2001) but has connotations of wetness (Ciolkosz and Dobos 1990) and most recently has been restricted to lithochromic colors (Schoeneberger et al. 2002). Nodule or concretion can also carry connotations of genesis but also by the NRCS field definition are “cemented bodies,” (Schoeneberger et al. 2002:2-18) a characteristic that is absent in the high-chroma features of this study. “Concentrations,” a term that refers to concentrations of color different from the

matrix, could be a suitable term, but with the relatively recent adoption of the terms “redoximorphic feature,” and “redoximorphic concentrations,” now has the connotation of wetness. “Redoximorphic feature” is a purely interpretive term so is completely unsuitable for use in this context. Redoximorphic features are also referred to as “masses” (Schoeneberger et al. 2002:2-14) making that term also unsuitable.

Use of the term “pedological feature,” has long-standing formal support in the literature. Bullock et al. (1985) modified the definitions of pedological features as given by Brewer and Sleeman (1960) and Brewer (1964). They define pedofeatures as “discrete fabric units present in soil materials that are recognizable from an adjacent material by a difference in concentration in one or more components or by a difference in internal fabric” This definition is repeated by Stoops (2003:101). Weathered fragments of rock, nodules, or concretions are not included in the definition of pedofeatures but are considered part of the groundmass. The term pedofeatures as defined by Bullock et al. (1985) and Stoops (2003) seems most suitable as a generic term for high-chroma pedofeatures, or just high-chroma features.

High-chroma features identified and defined in this study generally have the physical characteristics summarized in Table 1.

In the field, the most outstanding characteristics are color, sharp boundary, and lack of cementation. In the laboratory, better cemented features will survive sieving and sometimes can be removed from the ped intact if extra care is taken. There is some question, however, as to whether these features are truly high-chroma features of interest. Under the microscope, the halo surrounding the feature becomes more apparent and the internal fabric

Table 1. Physical characteristics associated with high-chroma features. Color and induration are the most consistent properties and size the most variable.

Property	Modal Value and Range
Color	Munsell 5YR 5/8 to most commonly 7.5YR 5/8, often with dark occlusions and internal variations of color that range from darker red to purple.
Contrast	Prominent contrast with the surrounding matrix.
Size	Range of size is approximately 0.5 to 1.0 mm in diameter. They are seldom larger than 2 millimeters in maximum dimension in well-drained soils.
Basic shape	Usually spherical to elliptical; sometimes irregular
Boundary	Sharp with matrix
Halo	Typically a halo of 10YR hue surrounds the feature
Rind	Some features have a surrounding shell or coating
Induration	Loose; Usually not possible to remove intact

including occlusions of darker material and red to pink or purple colors adjacent to the darker material can be discerned. Occasionally a coarser-textured rind at least partially surrounds the feature.

High-chroma features can be found in any landscape position from well-drained summits to poorly drained footslopes. Previous studies based on limited field work and Official Series Descriptions have shown no relation with Bk horizons, depth, or drainage class (unpublished data). They are not consistently found above or in Bt horizons but may occur in any B-horizon and are somewhat more common in C-horizons. Typical first appearance in a soil profile is at 50 to 100 cm depth in a B or C horizon.

Historical and Interpretive Sciences

The search for evidence and explanation differs between historical sciences such as paleontology, astronomy, cosmology, geology, and pedology and experimental sciences such as physics and chemistry. Historical sciences seek to explain particular events using generalized principles similar to laws rather than searching for generalized laws themselves (van Bemmelen 1961:490). Historical sciences such as pedology and geology are also interpretive, known in the philosophy of science as “hermeneutic,” literally the art and science of reading texts. The pedologist finds and evaluates clues from careful observations of a soil profile or a pedological feature, a “reading” of the pedological text, to formulate an explanation and pose a hypothesis (Frodeman 1995). Frodeman (1995:963) uses the analogy of a physician interpreting symptoms of an illness or a detective building a circumstantial case against a suspect.

Historical sciences have been regarded as inferior to experimental science but that view continues to be effectively challenged. Experimental methods and

falsification, in the traditional Popperian approach to defining the “scientific method,” are not the only legitimate ways to formulate and test hypotheses. Historical sciences look for positive evidence, evidence that supports one hypothesis over the others as providing the best explanation of the observed facts (Cleland 2001). In some cases, it is our assumptions rather than the hypothesis that may be faulty. Falsification may then involve the rejection of assumptions rather than an entire hypotheses. Failure to reject a given hypothesis, leading to its tentative acceptance, is based both on the accumulation of positive evidence and the lack of refuting evidence, an approach actually used more generally in science, including experimental sciences, than may be generally admitted (van Bemmelen 1961). The claim of “experimental confirmation” carries considerable weight in science but the more general “empirical confirmation” that includes the observation of positive evidence unrestricted to direct experimentation only, is equally valid.

Our knowledge about pedologic processes and events are limited in six possible ways: some are rare, extensive in space and time, and complex; our powers of measurement and observation may be inadequate, and our ability to understand them is limited (Watson 1969). Formational events may have happened far in the past, are slow to manifest themselves, and take place on a relatively large geographic scale, limiting the amount of data available to the observer and hindering formulation and testing of working hypotheses. The records left by past processes are often incomplete and obliterated by later events. Furthermore, it is often difficult or impossible to verify observations because of the inaccessibility of the area or its destruction through natural or anthropogenic causes (van Bemmelen 1961:455-456). As a result, greater

subjectivity of interpretations is introduced than would otherwise be the case (Pannekoek 1956). Davis (1926) went even further by referring to “the immensely speculative nature” of geology as a pathway to challenge existing concepts, citing examples of what were formerly “outrageous” explanations that are now accepted into the geological canon. In light of such difficulties, it becomes necessary to use different methods of explanation and exploration, including reasoning by analogy, narrative logic, (Frodeman 1995:965), and the Method of Multiple Working Hypotheses (van Bemmelen 1961).

Analogy between past and present is fundamental to geology as manifested in the principle of uniformitarianism (Frodeman 1995). Use of analogy extends beyond consideration of past-and-present to include similarities of processes in different contexts, processes that produce similar results or objects. Analogy with related geologic events that produce morphologically similar objects in the soil is used to help interpret observations made in this study.

Unlike experimental sciences, historical sciences do not usually make predictions or explain events on the basis of universal laws or generalizations. Instead, narrative logic is used to explain an event by considering its place in a larger whole, thus giving it context and meaning (Frodeman 1995). An event or object may not make sense by itself but only through its contribution to a larger story. Our understanding of each part comes from understanding the whole, while an understanding of the whole comes from an understanding of the parts. This circular reasoning is fundamental to hermeneutics and is considered to be the way understanding actually progresses. Cycles of comparison are used to evaluate each piece of evidence and individual observation based on its fit with

the whole that is being constructed. Evidence is kept or discarded based on its relationship with the whole.

At least partly because of the complexity of pedologic/geologic processes, the Method of Multiple Working Hypotheses as advocated by the geologist T.C. Chamberlain is often applied to problems of geological research. Chamberlain (1890) advocated the formulation of as many hypotheses as reasonably possible. Each hypothesis is then tested either sequentially or in parallel leading to the elimination, modification, or combination of hypotheses (Schumm 1991). Developing Multiple Working Hypotheses is said to prevent the investigator from having a favorite hypothesis, which can result in the development of a ruling theory. When observations and interpretations are made only through the lens of the favored hypothesis or ruling theory, an investigator risks unconsciously matching facts to fit that theory. Chamberlain (1890) stressed that a working hypothesis exists to guide the collection of facts and suggest lines of inquiry rather than to find only supporting evidence for a ruling theory. Development of multiple working hypotheses strengthens that approach. Chamberlain's method has been a guiding principle in this research project.

Questions of interpretation permeate all levels of geographic scale. Interpretations of micromorphological features for example, are often inadequate, being based on comparisons with macromorphological features and laboratory data, or simply on the authority of an author, sometimes without any supporting laboratory data. A hypothesis often is proposed and then becomes gradually regarded as fact without any further supporting evidence (Stoops 2009; Stoops et al. 2010) a situation resembling that of Chamberlain's criticism of ruling theories discussed earlier.

Frodeman (1995:966) regards the methods of interpretive and historical sciences as more relevant to the uncertainties and complexities of modern life:

“We are seldom in possession of all the data we would like for making a decision, and it is not always clear that the data we possess are unbiased or objective. We are forced to fill in the gaps in our knowledge with interpretation and reasonable assumptions that we hope will be subsequently confirmed. Thus, the methods of a hermeneutic and historical science better mirror the complexities we face as historical beings.

“It is likely that this type of reasoning will become more crucial in the next century. Many of the issues we face (global warming, and various types of risk and resource assessment) are by their nature both scientific and ethical, with the scientific aspect of the problem influenced by interpretation and uncertainty.” ... geology provides another, and I believe better, model for reasoning than has our traditional model of the sciences.”

Perhaps his is an outrageous proposal. Perhaps not. Regardless, many times throughout this project, for perhaps all of the six reasons given above, the ability to render even a mildly satisfactory interpretation and hypothesis was difficult or impossible without resorting to subjectivity and in some cases, speculation. The purpose of this discussion is to justify the need for greater subjectivity and even speculation given the nature of the subject. Hopefully, it is clear when that has happened during the subsequent discussion.

General Description of the Study Area

For the purposes of this study, southern Minnesota is defined as that portion of the state south of 45° 25', approximately the northern boundary of Kandiyohi County. Of particular interest is a roughly triangular area extending from Kandiyohi County in west-central Minnesota to Wright County to Carver County in the east central and to Lincoln County in the extreme southwest. The extreme southwest and southeast corners of the state are specifically excluded from the study area, as they were marginal to the Des Moines lobe. Soil

characteristics based primarily on their characteristic silty texture are notably dissimilar to most of the rest of southern Minnesota.

Location of sites that provided climate data is given in Figure 1. Rainfall and temperatures in southern Minnesota vary substantially by season, typical of a continental climate (Table 2). No strong east-west or north-south temperature trends are apparent from the data. Precipitation is heaviest in the east, least in the southwest, while the trend in snow depth is reversed.

Maximum relief in southern Minnesota is approximately 400 meters. The highest elevations are in southwest Minnesota along Buffalo Ridge in Pipestone and Murray Counties, about 600 meters above sea level. The lowest elevation is in the east near the juncture of Minnehaha Creek and the Mississippi River in Minneapolis at an elevation of about 200 meters above sea level.

The most prominent topographic features in southwest Minnesota are a series of U-shaped moraines draped across the southern part of the state, variations of the Bemis and Altamont moraines (Figure 2). These represent the farthest advances of the Des Moines lobe during the final two phases of the Wisconsin glaciation (Patterson 1996). The Altamont ground moraine extends throughout much of south central Minnesota. The Pine City Moraine borders the study area in the northeast while the Alexandria Moraine, belonging to the Wadena lobe extends into northern Kandiyohi County.

Older till and bedrock have in some instances also helped shape the topography. The Bemis moraine, known locally as Buffalo Ridge, is an end moraine of Des Moines lobe till deposited on top of the Coteau des Prairie, an area that escaped erosion during the last glacial period. The coteau is cored by a series of pre-Wisconsin tills overlying Cretaceous Pierre Shale (Patterson 1996).



Figure 1. Locations of climate stations. Locations marked with an (F) supplied frost depth. Underlined locations supplied all other climate data. Marshall supplied both.

Table 2. Climate summary from monitoring stations in southern Minnesota. Numbers in parentheses give the range of values from four stations in Willmar, Hutchinson, Chaska, and Marshall. Frost depths are from the winters 1999-2000 or 2003-2004 to 2010-2011 depending on the station location. Frost depth stations are in Starbuck, Otsego, Worthington, and Marshall. Winter is December, January, February; summer is June, July, August. Locations are found in Figure 1.

Variable	Description
Temperature	Average annual temperature in southern Minnesota is 7(2)°C, warmest in Marshall and Chaska, coolest in Willmar. Seasonal averages range from -9(3) °C (-11 - -8) in the winter to 21(1)°C in the summer (MRCC 2011). Willmar is the coldest and Marshall the warmest during both winter and summer, although Chaska in the east is within 0.5C° of Marshall in the summer.
Precipitation	Average annual precipitation is 707(120)mm with Chaska the wettest and Marshall the driest. Winters are relatively dry compared to summer. Average winter precipitation is 53(4)mm compared to 308(69)mm in the summer (MRCC 2011).
Snowfall	Average annual snowfall is 1,100(230)mm with the highest in Willmar, lowest in Hutchinson. The three winter months account for less than 60% of the total annual snowfall (MRCC 2011). Significant snowfall occurs in the transitional seasons, especially in spring.
Snow depth	Snow depth averages 130(50) (102 -152)mm for the months November through May (HPRCC 2011). Snow accumulates deepest in Marshall with Hutchinson and Chaska tied for least.
Growing season	The number of frost-free days averages 155(4) for a 0°C base and 197(26) for a -4°C base, a difference of about 10 weeks (MRCC 2011; HPRCC 2011). No clear pattern of max/min emerges between east-west or north south. In all cases, differences are less than 5 days except for an unusually short season at Hutchinson reported only in the MRCC data with the -4°C base. Eliminating the questionable data from Hutchinson reduces the range from 26 days to 6 days.
Frost depth	Frost depths average 1190mm with minimum of 760mm and a maximum of 1524mm (MnDOT 2011). The minimum occurred at all four stations during the winter of 2005–2006. Maximum frost depth was recorded at Starbuck during 2007–2008 and again in 2010–2011.

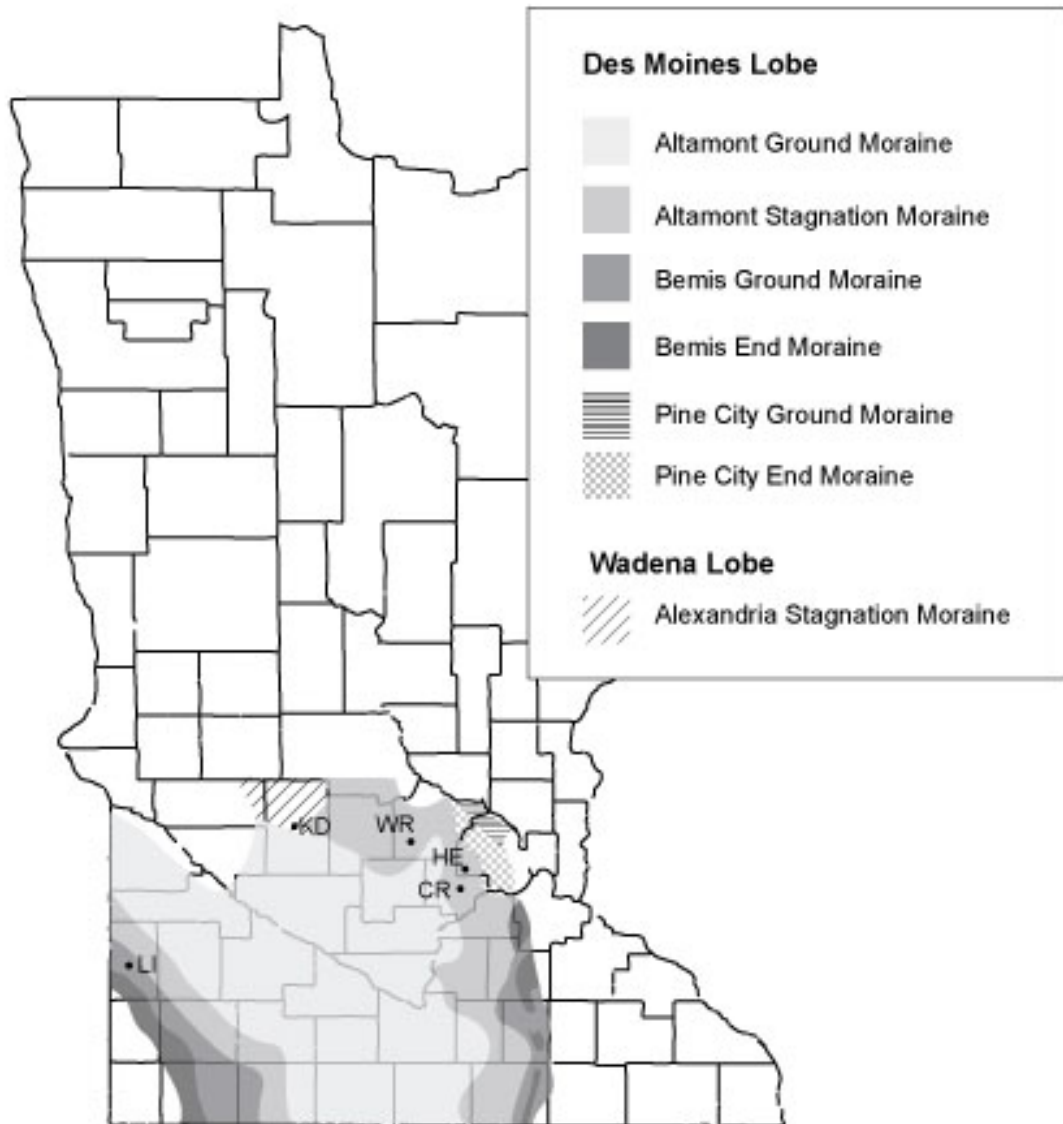


Figure 2. Major glacial landforms of southern Minnesota that are relevant to this study. Sites are identified by a two-letter abbreviation of the county in which they are found: LI = Lincoln KD = Kandiyohi; WR = Wright; HE = Hennepin; CR = Carver.

In northern Kandiyohi County, Des Moines lobe till overlies the older Wadena lobe sediments of the Alexandria Moraine near the boundary with the Altamont ground moraine to the south (Hobbs and Goebel 1982).

Vegetation at the time of European settlement was primarily tall-grass prairie with patches of wet prairie in the southwest changing to hardwood forest in the southeast and east-central (Anderson et al. 2001). A zone of transition, the prairie-forest border lies in a narrow band running from southeast to northwest. Most of the land is now used for agriculture (MGIO 2011).

Three soil moisture regimes, Aquic and Udic, and Udic-Ustic are present in southern Minnesota (Figure 3). Aquic and Udic comprise about 95% of southern Minnesota. The Aquic moisture regime exists at the locations of former glacial lakes, Glacial Lake Benson in the west and Glacial Lake Minnesota in the south central. No sampling sites are located in the Aquic moisture regime. An Udic-Ustic transition in the extreme southwest makes up 5% of southern Minnesota and is not represented in the study area.

Two soil temperature regimes are found in southern Minnesota: Frigid and Mesic (Figure 4). Southern Minnesota is on the northern edge of the mesic temperature regime, which dominates the region. The site in Lincoln County is in the Frigid temperature regime where it intrudes into extreme southwest Minnesota.

Presently, soils are predominantly Udolls and Aquolls in the southwest with a change to Udalfs and Udolls to the northeast, especially along the forest-prairie border (Anderson et al. 2001).

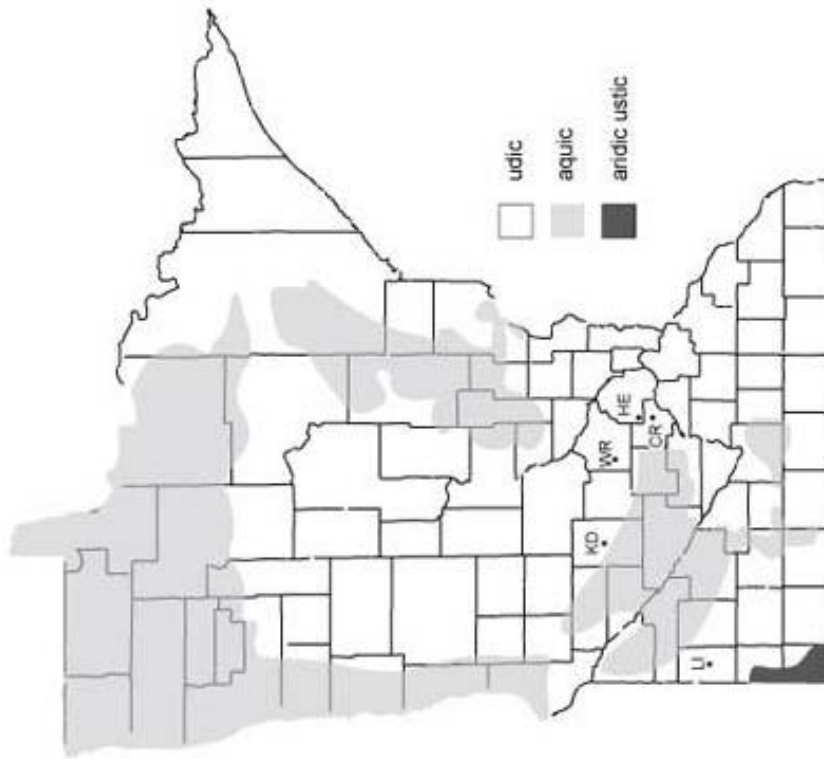


Figure 3. Soil moisture regimes and study sites. Modified from “Soil Temperature Regimes of the Contiguous United States” published by the USDA/NRCS. Some areas of aquatic moisture regimes are highly generalized.

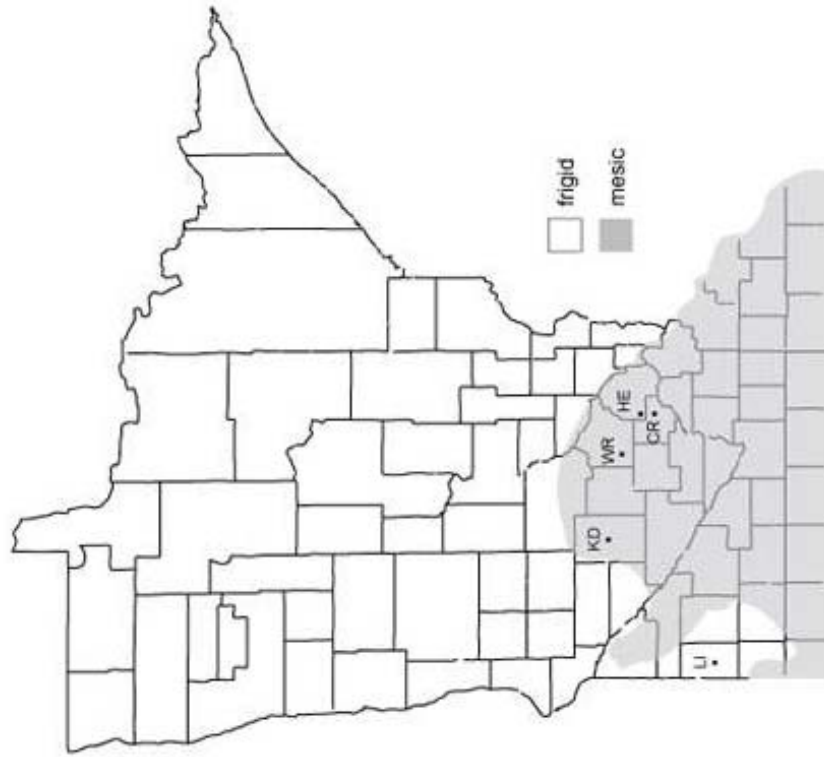


Figure 4. Soil temperature regimes and study sites. Modified from “Soil Temperature Regimes of the Contiguous United States” published by the USDA/NRCS.

Development of the soils

Parent material of glacial origin is distinguished from till since much of the original till, defined as the material laid down directly by glacial ice (Pettijohn 1957:266), has been reworked by water and gravity after deposition. Parent material then might include supraglacial, englacial, and subglacial tills as well as till that has been reworked, stratified, and transported. Soils begin to form only after stabilization of the till. Once stabilized, the parent material may now begin to differ in texture, chemical, and mineral composition from the original deposit.

Till and Topography

Till, whether deposited directly by a melting glacier or reworked by water and gravity, influences soil development in two ways: first by its influence on topography and hydrology, and second by its lithologic composition. These in turn are influenced by the topography and lithology of earlier glacial deposits and by the nature of the underlying material over which the glacier passed. Source region and flow direction of the ice determine the bedrock and sediments with which the advancing glacier has potential contact. Ice flow into Minnesota was primarily from the northwest (Lusardi et al. 2011). Bedrock sources of till for glaciers advancing into Minnesota are Cretaceous Shale to the northwest in North Dakota and the Red River Valley, and Paleozoic limestone and dolomite to the north and northwest in the Williston Basin of North Dakota and southwest Manitoba (Moran et al. 1976). Igneous crystalline material might be from local granitic sources or from earlier glacial incursions that came out of the Canadian Shield to the northeast and have been incorporated into the later Des Moines lobe till. Variability in till composition and texture may also result from sorting

by water and gravity either through surface transport or deposition of fine material beneath areas of ponded water that exist on the surface of stagnant ice (Patterson 1996: 51).

Despite the attention given to limestone and shale, crystalline material is present in significant amounts in tills from all three regions. Crystalline minerals make up approximately 40% to 60% of the mineral composition of the till while carbonates make up approximately 30% to 35% and shale 10% to 25% (Lusardi 1998a). Crystalline minerals include felsite, basalt-gabbro-diabase, granitic rocks, quartzite, and some iron-formation minerals often of Precambrian age sourced from the northeast and North Shore region (Arneman and Wright 1959; Hobbs 1998). Some of these minerals are durable and are able to survive generations of glacial transport so their usefulness as diagnostic indicators of till is limited (Arneman and Wright 1959).

Of primary interest in this study are the tills left behind by two major ice lobe advances, the Wadena lobe of the Middle to early Late Wisconsin and the Des Moines lobe of the Late Wisconsin. They differ significantly in both texture and mineral composition (Figure 5).

The Wadena lobe of the Middle or Early Late Wisconsin may have advanced out of Winnipeg from the north and northwest approximately 30,000 to 40,000 radiocarbon years before the present (rcbp) (Wright 1972: 524-25; Ojakangas and Matsch 1982; Goldstein 1998:75). Retreat of the Wadena lobe during this time exposed the Alexandria moraine, an ice stagnation feature present in northern Kandiyohi County and extending to the northwest. The underlying Wadena lobe till has a sandy to sandy loam texture and contains a relatively high proportion of Paleozoic carbonate fragments, but little Cretaceous

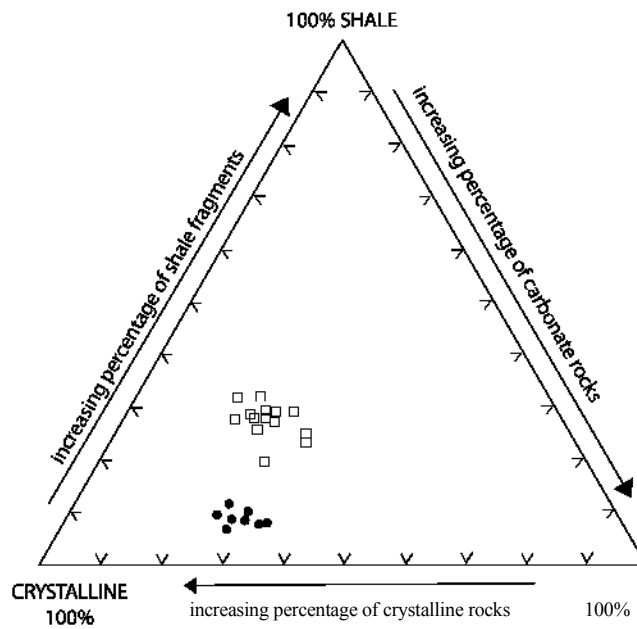
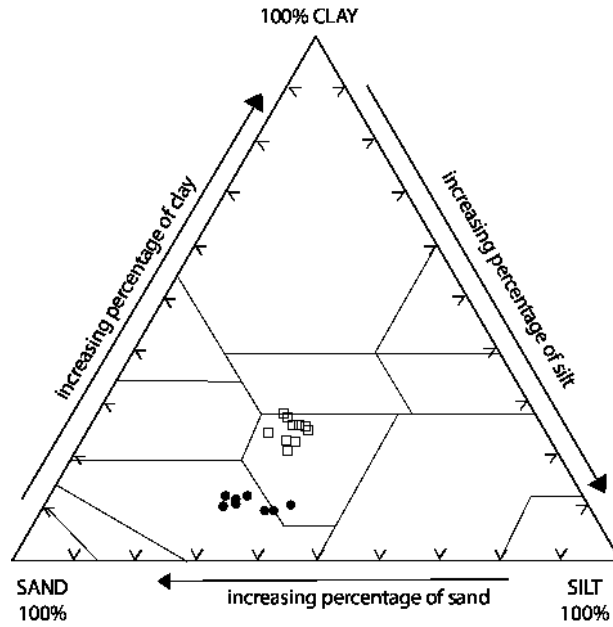


Figure 5. Ternary diagrams comparing texture (top) and grain composition (bottom) in the 1 to 2 mm sand fraction for two different tills. Granite Falls till from the Wadena lobe is shown as filled circles and New Ulm till from the Des Moines lobe is shown as open squares. Adapted from Lusardi (1998).

Shale, suggesting a more northerly source out of Manitoba. The upper till in the part of the Alexandria Moraine not covered by the later Des Moines lobe deposits is known as Granite Falls Till and may overly even older calcareous tills such as Browerville and Kandiyohi, tills that may have helped shape its underlying form (Goldstein 1998). Goldstein (1998) suggests that the Wadena lobe actually advanced from the northeast but incorporated high-carbonate, low-shale Browerville till in central Minnesota and the similar Kandiyohi till near the Alexandria Moraine. Browerville and Kandiyohi tills were sourced from the northwest, the dominant direction of pre-Wisconsin ice incursions. Incorporation of Browerville and Kandiyohi tills into the later Wadena till gave Wadena till its “northwest” characteristics along with a high proportion of “northeastern” crystalline materials.

Des Moines lobe till, deposited during the Late Wisconsin approximately 20,000 to 12,000 rcbp, is similar in color to Wadena lobe till but is finer textured, typically loam to clay loam, and contains abundant Paleozoic limestone and Cretaceous (Pierre) shale fragments (Gienke 1987). The presence of Pierre Shale has been considered diagnostic for Des Moines lobe tills (Goldstein 1998). In places, Des Moines lobe till may overlie and mix with Wadena lobe till (Lueth 1974:147; Ojakangas and Matsch 1982:104; Goldstein (1998); Morey et al. (2000)).

Des Moines lobe till, associated with ice flow from the northwest, was derived from shale, siltstone, limestone, and preexisting glacial deposits, a combination that resulted in a till containing significant amounts of smectite (Mickelson et al. 1983:5). High shrink-swell clays such as smectite decrease the permeability of the till, reducing the loss of subglacial water and increasing the likelihood of collapse of supraglacial till, resulting in characteristic flow-till

hummocks (Mickelson et al. 1983:7,8). Associated with hummocky terrain are ice-walled lake plains: flat-topped hills that are filled with supraglacial sediments, typically till and finer-textured lacustrine material. Thick supraglacial till is present where regional topography permitted ice movement by compressive flow upslope. Thin supraglacial till occurs near the centerlines of lobes that are on flat beds or downhill slopes (Mickelson et al. 1983:6,29,30). Supraglacial, proglacial, and subglacial sediments, pushed to the present position or formed as the result of a fluctuating position of the ice lobe, may occasionally be found together as mixtures as in the Bemis moraine of southwest Minnesota (Patterson 1996:46, 48).

The Bemis ground moraine was deposited about 14,000 rcbp (Patterson 1996). An adjacent and slightly younger moraine called the Altamont was deposited about 13,400 rcbp. Both moraines have hummocky, stagnation topography. The so-called Altamont is not a true moraine but is actually an area of repeated contact between active and stagnant ice (Patterson 1996). Extending north from the Altamont stagnation Moraine is an extensive ground moraine covering most of south central Minnesota also attributed to the Altamont. Ice block lakes, depressions, and hollows are present or have been present throughout this region (Birks 1976). The Alexandria Moraine from the earlier Wadena glacial period, is also known for its hummocky, stagnation topography.

Climate and Vegetation

Climate, along with vegetation, has changed dramatically in Minnesota since the last glaciation although expected correlations between vegetation, glacial extent, and climate are sometimes lacking (Wright 1976).

The last glacial lobe advanced over spruce (*Picea*) forest between 20,000 to 14,700 rcbp (Mickelson 1983). At the maximum extent of the Des Moines lobe, spruce continued to exist marginally to the glacier suggesting that permafrost was not generally present (Mickelson 1983). Limited areas of tundra vegetation may have existed along glacial margins and small local areas not covered by ice but there is evidence of this only in northern (Wright 1976:128), central (Barry 1983; Watts 1983; Birks 1976) and eastern Minnesota (Watts 1983). Marginal tundra may have existed until ice retreat 13,000 rcbp. The extent of tundra to the south is unknown. There is no evidence of tundra or permafrost in southern Minnesota other than along the extreme eastern margin of the glacier as ice-wedge casts (Péwé 1983). It seems more likely that boreal forest rather than tundra-forest existed in south central Minnesota (Ashworth et al. 1981). On the other hand, permafrost was widespread in Wisconsin during the Wisconsin glaciation but evidence of permafrost is often overlooked (Clayton et al. 2001) or under reported (Zanner 1998:133). Failure to find periglacial features might reflect “the intensity of investigations in these areas and not a quantitative difference in the appearance of these phenomena” between those areas that have confirmed periglacial features and the rest of the glacial margin (Zanner 1998:48). Zanner (1998:133) found support for the idea that areas in southeastern Minnesota were influenced by periglacial conditions and permafrost and suggested that the presence of these features indicate a sequence of changing climatic conditions that influenced the evolution of the landscape.

When glacial retreat began with climate warming about 13,000 to 12,000 rcbp (Ojakangas and Matsch 1982:108), a late-glacial forest of spruce and scattered hardwoods grew up to the edge of the glacier advancing faster than the

glacier retreated (Wright 1976:119; Barry 1983). Spruce still dominated up to 10,000 rcbp (Webb et al. 1983) and may have mantled large areas of stagnant ice (Birks 1976). In Eastern Minnesota, spruce forest was quickly replaced with a forest of pine, fir, and northern hardwoods (Watts 1983:304, 308) between 11,000 and 10,000 rcbp, while hardwoods expanded west and south (Birks 1976; Webb et al. 1983). Expansion of deciduous forest implies that the early Holocene, being influenced by the melting ice sheet, was cooler and wetter than the later Holocene (Webb et al. 1983).

Prairie followed the northward retreat of the spruce forest and began to make a presence in west central and southwest Minnesota by about 10,000 rcbp following a brief transition to deciduous woodland (Webb et al 1983; Watts 1983). Prairie expanded northeastward during a warmer and dryer period beginning about 8,000 rcbp and continuing until about 5,000 rcbp. This period was thought to be at least as dry as the 1930s (Moran et al. 1976). Spruce retreated to the north nearly disappearing from Minnesota. By 7,000 to 6,000 rcbp, prairie reached its maximum extent, covering most of Minnesota. After 5,000 rcbp, prairie retreated westward accompanied by the expansion of pine (*Pinus*). A cooler, wetter climate established by 4,000 rcbp encouraged the development of the patterned peatlands in northern Minnesota. At 3,000 rcbp, scattered spruce had returned in the north. By 2,000 rcbp, the prairie was essentially at its present position (Ruhe 1983). After 2,000 rcbp, pine continued to spread westward into the prairie/deciduous forest of northwest Minnesota while spruce returned to the north. Within the last 500 years, the forest/prairie ecotone became more diffuse than it was 3,000 rcbp, when the boundary was more abrupt. (Watts 1983; Webb et al. 1983; Ruhe 1983).

Vegetation and climate conditions are important when considering soil formation over the last 10,000 to 12,000 years. Present conditions are markedly different from past conditions that existed over most of the soil's history. Although claiming our soils are 10,000 years old, considering past climate and vegetation changes, they are much younger, or when considering heritable properties, much older.

Soils and Soil Development in Summary

Soil development is linked to Jenny's five factors of climate, organisms, relief, parent material, and time. We have reasonably accurate estimates of the time that these soils have been developing, and can characterize the parent material as well as the local relief, but the necessary specifics of local climate and vegetation are lacking. At best, with a few exceptions of well-preserved pollen in wetlands, we can only make broad generalizations about vegetation and from these, infer climate. Because of the paucity of data and suitable sampling sites, inferences about early soil development can be little more than speculation.

Soil development would be expected to begin shortly after deglaciation. Limited vegetation cover immediately following ice melt, however, would likely result in increased runoff and erosional loss. Solifluction and frost heave also may have contributed to an increased erosion rate (Davis 1983) prior to stabilization by vegetation. Permafrost was found to increase regional erosion in Wisconsin (Clayton et al. 2001). There is evidence of increased erosion rates in Iowa following deglaciation between 13,000 and 10,500 rcbp (Ruhe 1983). Numerous episodes of landscape instability seem to alternate with periods of stability and soil development throughout the Holocene (Ruhe 1983), which has been characterized by alternating cycles of warm, dry periods and cool, moist

periods. During the dry periods, steep slopes are unstable and in places, are accompanied by deposition of loess on more gentle slopes. During cooler and wetter periods, soils developed (Moran et al. 1976).

Local relief and hydrology over large areas of the Des Moines lobe from 14,000 to 12,000 rcbp have been influenced by the presence of stagnant ice or ice-block hollows that remain after the slow melting of ice buried by supraglacial till (Ashworth et al. 1981). In southwest Minnesota, the final stages of ice melt produced shallow lake basins, some having filled with lacustrine sediment and others, but for drainage would still be filled with water (Patterson 1996:53). Soils that form in these areas would be expected to have aquic morphology. The overlying till may have been forested before melt out formed depressions, which later filled in. Slopes along these melt-out features are unstable but stabilization may require only a few centuries. During this early, unstable period, vegetation may grade from pioneer shrubs to spruce forest on older surfaces in a repeating but lengthening cycle as the landscape stabilizes.

Major vegetational changes occurring approximately every 3,000 years give each climate and vegetation regime an opportunity to make its imprint on the developing soil. How much of that contribution is permanent and remains visible in the soil today is an open question (Ruhe 1983) but may become important when interpreting soil morphology for land use. As with tundra, permafrost and so-called periglacial conditions may have existed locally. Their former existence is difficult to demonstrate especially if such conditions were marginal or short-lived, making only a subtle imprint on soil morphology that is no longer recognized in the modern soil but whose former presence could have influenced subsequent soil development (Ruhe 1983).

Changes in climate, vegetation, and hydrology, interacting at varying geographic scales, have influenced soil development in southern Minnesota over the last 12,000 years. It seems likely that the soils present on the landscape today contain a record of their past history. Although this record is incomplete and in some cases might be completely lost, the influence of past genetic processes makes polygenetic rather than monogenetic soils more typical even in young glaciated landscapes that have seen dramatic changes in climate and vegetation over a relatively short time. Stable, resistant soil features formed under earlier conditions but resembling modern features may still be present in the soil. Likewise, modern features may closely resemble earlier formed features. Such interpretations require caution.

LITERATURE REVIEW

Part I: Further characterization of the till

The starting point for the formation of pedofeatures and surrounding soil matrix is till, composed of bedrock fragments and previously existing soils and sediments that were transported by the glacier and redeposited as the glacier retreated. The term “till” as used here is limited to material deposited directly by the ice. Till is often reworked by wind and water after being released from the ice, changing its texture and composition (Patterson 1996:51).

Understanding the composition of the till is important for two reasons, both related to weathering. First, weathering of rocks and minerals influences the chemistry of pore waters. The chemical composition of concentration features that form by precipitation of material out of solution depends on the chemical composition of that solution. Since we cannot know what the chemistry of the soil solution has been at any time in the past, the best we can do is to speculate

based on a study of the initial starting materials, some assumptions about weathering and formation processes, and studies of subglacial water and young tills of similar composition.

Second, some minerals in the till weather to pseudomorphs or alteromorphs of precursor minerals. Of special interest are minerals containing reduced iron and manganese that weather to iron oxides and oxyhydroxides. Examples are the end members siderite (FeCO_3) and rhodochrosite (MnCO_3) and their intermediates. Precursors or the oxidized minerals themselves can be inherited during subsequent soil formation and identified as nodules or inherited minerals.

The intent of the discussion that follows is twofold: to establish the existence of raw material sources as the basis for the more speculative existence of a geochemical system dominated early in its history by calcium, magnesium, iron, and manganese carbonates and to establish the presence of precursor minerals with alteromorphic potential.

Source Areas

With only a single exception in southwest Minnesota (other exceptions are reported but are outside of the study area), the source of New Ulm till is Riding Mountain Provenance (Thorleifson et al. 2007), an area of Paleozoic carbonate and Cretaceous shale bedrock in southwestern Manitoba and north central to northeast North Dakota and extreme northwest Minnesota, an area that includes the northeastern margin of the Williston Basin. Calcite and dolomite each comprise as much as 20% of the $<63 \mu\text{m}$ matrix till material; carbonates total as much as 35 to 40%. Shale comprises as much as 30% of the 8 to 16 mm fraction of

till material (Thorleifson et al. 2007). Silicates, or crystalline minerals, make up the balance.

The other source area for till in southern Minnesota is the Winnipeg Provenance, an area to the northeast of the Riding Mountain Provenance. In one instance, at the Windom site, New Ulm lithology is reported to be of Winnipeg Provenance (Thorleifson et al. 2007). A Winnipeg source is not usually associated with the most recently deposited tills such as New Ulm but rather with earlier deposits of Granite Falls till and its correlates, such as the Lower Red Lake Falls till (Matsch 1972; Meyer 1986; Thorleifson et al. 2007). Winnipeg lobe tills (the Winnipeg lobe was formerly known as the Wadena lobe) have a lower shale content but higher carbonate content than those of Riding Mountain (Figure 5). No Granite Falls till or its correlates were identified in the study area. That result was unexpected since deposits associated with the Wadena lobe are found across northern Kandiyohi County (Hobbs and Goebel 1982; Giencke 1987). Des Moines till is known to be thin (usually less than 1 to 3 meters thickness) where it overlays the Wadena till at the southern edge of the Alexandria Moraine in Kandiyohi and Meeker counties and may not have completely covered the existing till in some places (Goldstein 1998:73). Coarser-textured soils such as Sunburg, Wadenill, and Koronis, thought to have formed in Wadena till, are found in northern Kandiyohi County. Possibly the underlying Wadena till was sufficiently diluted by the more recent Des Moines lobe till or it may a probabilistic outcome of sampling.

Glacial sediments in western Manitoba are fine-textured, high in silt content, and contain abundant carbonates, reflecting the composition of the underlying bedrock (Manitoba Geological Survey 2011a). These sediments,

where present, are generally thin but overlie thick Paleozoic dolomite or dolomitic limestone beds 200 to 250 meters thick that outcrop where not covered by glacial sediments (Bannatyne 1988). Intermittent glacial sediments also overlay Cretaceous shale (Spector 1941:43).

Characterization of Bedrock Sources

Bedrock sources for the tills correspond roughly with their primary mineralogy. Tills from a northerly source region are rich in Paleozoic carbonates; tills from a northwesterly source are rich in Cretaceous shale; tills from the northeast are rich in crystalline rock. Each will be discussed in terms of their dominant mineralogy, that is, their dominant contribution to till composition.

Paleozoic carbonates

Paleozoic strata in Manitoba lie on the northeastern margin of the Williston Basin. They are comprised almost entirely of dolomite, dolomitic limestone, and limestone with minor layers of clay and/or sand. An exception is the basal sandstone-shale sequence of the Winnipeg formation (Manitoba Geological Survey 2011a). Mineralogical variants of limestone and dolomite such as calcitic limestone; argillaceous, micritic, and arenaceous dolomite; and dolomitic and calcareous shale can be found throughout the strata (Bannatyne 1988:2).

One of the most notable characteristics of much of the Paleozoic dolomite is mottling. Mottles have made Manitoba dolomite a popular dimension stone world-wide (Kendall 1977). A particular type of mottled limestone-dolomite from the Ordovician Red River Formation is Tyndall stone, also known as “tapestry stone” (Coniglio 2011). A reddish limestone-dolomite quarried further

to the northeast is sold under the name “Manitoba Prairie Rose Marble” (Manitoba Geological Survey 2011b).

Dolomite mottles are discussed here because the generally accepted process of their formation in rock, while geologic, has parallels with the formation of high-chroma features (mottles) in soil, to be discussed later. Mottled carbonates occur along a continuum from undolomitized mottled limestone to so-called color-mottled dolomite (Kendall 1977:483). One end member is dolomitized mottles within a surrounding limestone rock as exemplified by Tyndall Stone. The other end member contains dolomite mottles within a fully dolomitized matrix.

Mottles are thought to have formed by the infilling of channels or burrows made by crustaceans such as the Ordovician decapod *Thalassinoides* (Coniglio 2011). Their burrows were either backfilled by the burrowing organism or filled with material after the burrow was abandoned. This reworked material subsequently became fine-textured dolomite. The surrounding matrix material lithified into limestone or dolomite earlier than sediment in the channels resulting in a permeability difference between the infilled burrow channels and the surrounding rock. Later, possibly when overlying evaporite sediments were being deposited, magnesium-rich brine permeated the lower sediments and deposited preferentially in the more permeable burrows, resulting in the formation of a distinct dolomite in the burrows, replacing the original calcitic material. Even slight chemical and permeability differences between the material in the burrows and that of the matrix may have been enough to cause the dolomite/limestone differentiation. Iron may have been brought into the burrow channels with the same magnesium brine that contributed to their

dolomitization. The darker color of the mottles may have resulted from the oxidation of the iron or from the oxidation of pyrite that precipitated along with the dolomite within the mottles or from the oxidization of pyrite linings surrounding some of the burrows (Coniglio 2011). It seems more likely, however, that contrast differences between mottles and matrix that are primarily differences in color value (lightness or darkness) would result from only slight differences in texture and the calcium-magnesium composition rather than from the presence of minor elements. Differences in hue or chroma would result from the presence of pigmenting agents, elements such as iron and manganese.

Manitoba dolomite occurs in a wide range of colors and color patterns described without standardization or use of a standardized reference. Bannatyne (1988) describes various outcrops as varicolored, gray and brownish-gray, mauve, buff, bluish-gray, bleached to buff, buff to purplish, deep maroon to orange and buff, gray, grayish buff, red, greenish-gray, rose, orange, purple, mottled red and buff, purplish-orange, yellowish-gray, white to cream, orange-buff, brick red, yellow-buff, reddish-buff, mottled gray and brown, grayish mottled, buff to brownish buff mottled, orange and reddish buff with rose-red and purplish patches, ochre-red, purple and olive to buff with traces of orange and green. In addition, red, green, brown, and reddish brown argillaceous layers and pore infillings have been noted. No relationships have been reported between color variations and variations in chemistry, mineralogy, or geographical distribution. The possibility does exist, however, that even minor constituents, for example iron and manganese, are responsible for the color patterns, and which upon weathering and release from the parent rock, contribute to the geochemical composition of the till and pore water.

The average chemical composition of 22 samples taken throughout the Paleozoic strata are shown in Table 3. Medians are preferred as a measure of average composition because a few shale-rich and argillaceous layers skew the means for Si, Al, Fe, Ti, Na, K, Mn to the high end and skew Ca to the low end. Variations in silica and alumina of less than 1% are considered significant enough to alter the properties of the rock and reflect different formational environments (Bannatyne 1988:19–20). The lower median value for magnesium compared to calcium likely reflects the presence of limestone in addition to dolomite in some layers. The ratio Ca:Mg should be close to 1:1 for dolomite, higher for limestone. Most Middle Ordovician dolomitic rocks in the Upper Midwest are stoichiometric (Mossler 1985:23).

Little mention is made of other carbonate minerals or pyrite in the Paleozoic strata, with the exception of the Winnipeg Formation. The Winnipeg Formation, the basal unit of the Paleozoic strata in southwestern Manitoba, is comprised of sandstone and shale rather than limestone or dolomite of the overlying Red River Formation (Bannatyne 1988:2). Dolomite, calcite, ankerite, and anhydrite are present primarily as pore-filling cements with only minor iron cementation (Last and Shum 1991:16). Pyrite is found in small amounts in many of the samples. In addition, a widespread pyrite-cemented zone and pyrite concretion/oolite bed has been reported by several investigators near the top of the Black Island Member in outcrop and subsurface cores (Last and Shum 1991:15).

Some additional insight into the composition of the Winnipeg and Red River Formations can be gained by studying similar deposits of similar age that formed in similar environments. The Platteville Formation in southeast

Table 3. Chemical analysis of Manitoba Paleozoic deposits. Oxides are sorted in terms of decreasing values of medians. LOI refers to loss-on-ignition, a procedure that is assumed to estimate the content of organic matter in a sample. Data are compiled from Bannatyne (1988) from 22 samples.

Component	Mean (%)	Median (%)	Minimum (%)	Maximum (%)
LOI	46.01	46.81	38.23	47.95
CaO	32.36	30.75	26.70	47.80
MgO	19.08	20.60	4.90	30.40
SiO ₂	1.84	1.02	0.08	12.00
Fe ₂ O ₃	0.40	0.25	0.08	2.13
Al ₂ O ₃	0.50	0.17	0.00	3.90
K ₂ O	0.21	0.07	0.00	1.56
Na ₂ O	0.02	0.02	0.00	0.09
MnO	0.02	0.02	0.00	0.04
TiO ₂	0.03	0.01	0.00	0.20
P ₂ O ₅	0.02	0.01	0.00	0.06

Minnesota, a sedimentary deposit contemporary with the Winnipeg and Red River Formations, was deposited on the southeastern margin of the Transcontinental Arch in the Hollandale embayment (Webers 1972). At the same time, Winnipeg and Red River Formations were deposited along the northwestern side of the Transcontinental Arch in the Williston Basin. In addition to dolomite, trace amounts of pyrite, limonite, collophane, glauconite, chert, gypsum, authigenic feldspar, sphalerite, fluorite, and galena are present. Though the volume of these minerals is low, their presence is significant (Mossler 1985:13). (Limonite is an old field term for poorly crystalline, hydrated goethite and other iron oxides. It is still useful for describing a nodule or coating of brownish iron oxides of unknown composition.)

Although relatively uncommon, pyrite is widespread. (Mossler 1985:13). It occurs in fracture veins that are filled with ferroan calcite (Fe^{2+} substitution for some Ca is fairly common but iron-bearing calcites are probably less common than iron-bearing dolomites and ankerites (Deer et al. 1992:626)) and in small (<0.6 cm diameter) pyrite-lined borings or burrows and some pyrite-lined vugs (Mossler 1985:8). Limonite is a common alteration product of pyrite and chamosite (Mossler 1985:13). Gypsum and sparry calcite are found as infillings of vugs formed by dissolved brachiopod shells, fractures, and joints. Most vugs are filled with blocky equant calcite spar whose crystals increase in size from the margin towards the center of the former void. Some of the most recent void-filling calcite and associated coarse dolomite is ferroan (Mossler 1985:15). (Ferroan dolomite has up to 20% of Mg positions occupied by Fe^{2+} or Mn (Deer et al. 1992:650).) Sphalerite was associated with slightly ferroan void-filling dolomite and calcite. Chalcopyrite has also been observed in deposits near the

Twin Cities area (Mossler 1985:15). No other iron-bearing carbonates besides the limited amounts commonly found in calcite and dolomite were reported.

The dolomite itself is diagenetic, selectively replacing fossil fragments and the limestone matrix along animal burrows and borings. Blue staining of thin sections and polished slabs resulting from application of a potassium ferricyanide solution indicates the presence of ferrous iron in the carbonate lattice and therefore that the dolomite must have formed under reducing conditions (Mossler 1985:13). The amount of substitution is only on the order of 1% to 2%. Most of the iron reported in the analysis is probably present as pyrite or limonite (Mossler 1985:23).

In northwest Minnesota, Pleistocene deposits overlie the Ordovician Red River formation that in turn overlies the Winnipeg Formation, both of which closely resemble corresponding occurrences in Manitoba (Mossler 1978:12). The dolomite is classified as finely crystalline and biogenic. Dolomite content in the upper part of the Red River Formation exceeds 70% of total carbonate but decreases at the base of the formation to less than 10% of total carbonate. The dolomite occurs as very fine to fine, silt-sized (0.05 to 0.065 mm), crystalline rhombs. The Red River Formation contains numerous shale partings in the lower part and is "intensely color mottled" (Mossler 1978:12) consistent with mottled dolomite found in Manitoba.

Dolomite and limestone from southern Manitoba that were incorporated into the till of recent Pleistocene glaciers appear to be potentially major sources of calcium and magnesium and minor sources of silica, iron, and aluminum released during weathering of the till. Their presence in pore water may play a significant role in subsequent soil formation and in the nature and composition

of concentrations that form prior to soil development or in the developing soil and are then inherited. Pyrite, which occurs initially as linings of pores, voids, and burrows in the dolomite, weathers to iron nodules of limonite even though it may become fragmented as a result of glacial transport. Pyrite or its weathering product, limonite, could then be found in soils as inherited mineral concentrations.

Cretaceous shale

Mesozoic formations of the Riding Mountain region are comprised almost entirely of shales and sandstones, with some limestone and gypsum in the older Jurassic strata (Manitoba Geological Survey 2011a). Siliceous, calcareous, and carbonaceous shales are also present. Cretaceous shales are described as highly siliceous; dark, greenish gray color when moist to light steel or slightly greenish gray when dry; surfaces of joints show black or reddish brown staining; manganiferous ironstone nodules occur in bands in the shale (Kirk 1929).

Pierre Shale is perhaps the most well-known formation of the Cretaceous rocks in the Riding Mountain area because of its relative abundance in Des Moines lobe (New Ulm) till. Pierre Shale is dark-gray clay shale with numerous bentonite layers. Calcareous and ferruginous concretions are relatively common in some members. Minor amounts of colloidal silica are also present. A single thin sandy layer appears at the base of the Sully Member (Gries and Rothrick 1941; United States Geological Survey 2011).

Chemical analysis of four samples of Pierre Shale are given in Table 4. The difference between the Pierre Shale and Paleozoic carbonates (Table 3) is notable. The silica content of the shale is higher than the total of calcium plus magnesium in the Paleozoic rock. Iron and aluminum are about 10 and 45 times higher in the

Table 4. Chemical analysis of Pierre shale. Data are compiled from Leonard (1906) from four samples, with the following exceptions: organic matter and carbon dioxide are from a single sample and sulphur trioxide is from three samples.

Component	Mean (%)	Median (%)	Minimum (%)	Maximum (%)
SiO ₂	76.99	78.94	68.14	81.94
Al ₂ O ₃	7.54	7.65	6.52	8.35
Moisture (>100°)	7.70	7.52	6.06	9.71
Organic matter	3.00	3.00	3.00	3.00
Fe ₂ O ₃	2.75	2.50	1.90	4.10
CO ₂	1.44	1.44	1.44	1.44
Alkalies	1.40	1.24	1.11	2.01
CaO	1.22	1.21	0.80	1.67
MgO	1.22	1.15	0.93	1.65
SO ₃	0.20	0.16	0.05	0.39

shale respectively, while calcium and magnesium are 4 to 6% of the values in the carbonate rock.

Cretaceous deposits from northwest Minnesota at the extreme eastern margin of the Williston Basin are similar to those in southeastern Manitoba (Mossler 1978:10). Data from a test well showed an upper layer of light olive-gray to medium gray shale directly below Pleistocene deposits that is weathered to white or pale reddish-brown in the upper 5 meters (Mossler 1978:8). Texture of the lower shale is 1-15-84% sand-silt-clay. The clay is mainly illite with less than 10% kaolinite. Lack of kaolinite calls into question a Cretaceous age of this deposit since this basal Cretaceous layer found elsewhere throughout the state is highly kaolinitic (Mossler 1978:14). A layer of interbedded sandstone and sandy shale lies at the base of the unit (Mossler 1978:9). Beneath this questionably Cretaceous shale unit lies an interval of dolomite, marl, and red mudstone known informally as the Hallock red beds. The top of the bed is dolomite and dolomitic marl. An interval of shale lies below the carbonate bed. The upper 2 meters of the shale is light gray, in contrast with the remaining 20 meters that is a pale reddish brown containing numerous silt-sized, pink, euhedral rhombs of dolomite and minor amounts of interstitial satin spar gypsum. The predominant clay is illite. Its age is uncertain (Mossler 1978:10,14).

One important characteristic of the Pierre shale is the presence of iron-manganese nodules. Manganese deposits of potential economic value have been discovered in southwest Manitoba and central South Dakota, and may exist in southwest Minnesota (Spector 1941; Gries and Rothrock 1941; Jirsa and Southwick 2011). In central South Dakota, manganese is found in layers of bedrock shale as extractable nodules (Gries and Rothrock 1941), while in

Manitoba manganese deposits are also found in secondary Quaternary sediments as bog or wad manganese formed as a result of the weathering of Cretaceous iron-manganese-carbonate nodules (Spector 1941).

Manganese occurrences in Manitoba are typical wad or bog deposits: loose and friable, “porous when dry” and mostly “earthy and amorphous” making sectioning and preparation difficult (Spector 1941:46). Some nodules 1/8 to 1-inch (3 to 25 mm) in size were coated with limonite. Occasionally, travertine and limonite appeared as bands or lenses cutting or interbedding with the manganese deposits. The manganese may also be mixed with limonite or calcareous tufa (Spector 1941:52). They typically occur along the base of steep slopes where springs flow outward into a bog area depositing manganese and travertine at the spring outlet and manganese in the bog. Bog deposits are of recent age, having formed since glaciation (Spector 1941:47). Some manganese deposits are free of clay, shale, or other impurities but in others they are mixed with clay or shale (Spector 1941:49). Pyrolusite was identified as the only manganese mineral present in the deposits but no x-ray studies were performed (Spector 1941:46).

The manganiferous ironstone nodules themselves vary in diameter from 2 to 6 inches (5 to 15 cm). They are scattered throughout the Odana layer of the Pierre shale. These nodules are a light gray color and often have a flat or ellipsoidal shape. They are composed of iron, manganese, calcium, and magnesium carbonates. Most have a shell of oxidized iron or manganese about 1/8 to 1/4-inch (3 to 6 mm) thick; others found at the base of steep slopes or rock cuts are oxidized throughout, suggesting a longer period of weathering. In some cases the dark material grades into the gray core, the transition zone being a

reddish color; in others the dark material makes a sharp boundary with the core. A blue-black coating of manganese oxides is common on the outer surface of nodules taken from the Riding Mountain Member. The nodules there are not very numerous (Spector 1941:57).

Composition of the surface or secondary deposits differs in several respects from that of the nodules (Table 5). Most noticeable is the “exchange” of iron for manganese between the nodules and secondary deposits. Ironstone nodules are composed of iron carbonate with moderate amounts of manganese, calcium, and magnesium. Manganese in secondary deposits has been concentrated to a considerable extent, from 4.5% (as MnO) in the nodules to 43% (Mn) and 89% (Mn₃O₄) in the secondary surface deposits. The iron content is less than 2 to 3% in the surface deposits compared to 38% in the nodules. If, as hypothesized by Spector (1941), dissolution of the nodules in groundwater is the source of the secondary manganese deposits, the iron released from the nodules could be a significant source of iron in the groundwater and possibly also in any subsequently developed soils. Iron might be expected to accumulate as bog iron deposits in quantities similar to that of manganese but apparently it has not. No explanation, speculative or otherwise, is given on the fate of the released iron. The shale itself contains very little manganese and that is in a relatively insoluble form (Spector 1941:58).

Manganiferous nodules found in Pierre Shale near Chamberlain, South Dakota are similar to those found in Manitoba (Spector 1941:35). Hewitt (1930) first described the nodules in the Oacoma beds where they are most abundant:

“The manganiferous iron nodules commonly range from 2 to 3 inches in thickness and 3 to 8 inches in diameter and form persistent layers in the shale; where the quantity is low the nodules are separated, but where the quantity is high many nodules have

Table 5. Chemical analysis of samples of two surface deposits and one source nodule. Data are from Spector (1941:49, 51, 55).

Component	Surface deposit 1 (%)	Surface deposit 2 (%)	Ironstone nodule (%)
SiO ₂	3.11	11.72	7.98
Fe ₂ O ₃	0.51	—	—
FeO	—	—	37.61
Al ₂ O ₃	2.58	—	4.50
Fe ₂ O ₃ +Al ₂ O ₃	[3.09]†	3.03	—
Mn	—	42.85	—
MnO	—	—	4.44
Mn ₃ O ₄	88.88	—	—
CaO	2.88	2.52	5.44
MgO	—	3.23	4.91§
P	0.07‡	0.05	—
CO ₂	—	—	35.12

† Fe₂O₃+Al₂O₃ were not reported directly but were summed from their separate results

‡ P was determined on an unignited sample

§ MgO was assumed by difference.

coalesced to form continuous [sic] layers 3, 4, or even 5 feet long. The color of the fresh nodules ranges from pale gray to olive-green; under the influence of weathering the carbonates change to oxides and become black. Oxidation is complete to a depth of only a foot or two, but films of oxides are found to a depth of 6 or 8 feet. Even the unweathered nodules separate easily from the shale; with exposure to air the shale dries, cracks, and falls away from the nodules. Invertebrate marine fossils are very common in the concretions, and the organic matter which these shells once contained has probably caused the development of concretions. Fragments of bones, especially vertebrae, of both terrestrial and marine vertebrate animals are common in the concretion bed.

“Many geologic problems arise in the study of such concretion zones, but it will be sufficient to state here that the concretions appear to have developed in the sediments of a shallow sea shortly after burial. They are not related to processes of recent weathering that have produced the present surface but without doubt persist under the upland plains many miles east and west beyond the outcrop along the Missouri Valley.”

There is considerable difference in the size and abundance of the nodules in the different layers (Gries and Rothrock 1941:64) but the average thickness is about 2 inches. Comparing the total thickness of the concretionary layers with the total thickness of the zone in which they occur shows that on average about 10% of each zone (ten zones measured) is made up of carbonate nodules, with a range of 8 to 25%.

The Oacoma Zone consists of gray shale characterized by abundant black iron-manganese carbonate concretions and numerous thin bentonite beds. An alternating sequence of layers of shale, bentonite, shale, concretions is common in the upper beds. The lower bentonite bed contains numerous biotite flakes and is known as the lower micaceous bentonite. Concretions are found in layers that vary from continuous ledges 2 to 6 inches thick to 1-inch thick zones of purplish nodules no larger than marbles. Chemical analysis shows that the concretions consist of iron, manganese, and calcium carbonates. Many of the nodules contain fossil fragments. In addition, barite rosettes ranging from 1/2-inch to 5 to 6 inches

in diameter have been found at three exposures. Near the top of the zone, a 1/2 to 2-inch layer of fibrous calcite is common (Gries and Rothrock 1941:19, 21, 23).

The Verendrye Beds at the top of the Sully Member and lying above the Oacoma Zone consist of shale containing large, flat concentrations of iron-manganese in rather well-defined layers. These concretions range from several feet in diameter to 6 inches or less. The interior of these concretions is usually green or greenish gray but weathers to purplish black on the surface (Gries and Rothrock 1941:26).

The main mineral constituent of the nodules is siderite (FeCO_3) belonging to the variety known as clay ironstone (Gries and Rothrock 1941:66). An analysis of samples also found mangano-calcite ($\text{CaCO}_3 \cdot \text{MnCO}_3$) also called spartite. Spartite turns black upon exposure to air, a characteristic of the nodules found in this area. Chemical analysis confirmed that the samples contain sufficient carbon dioxide to form carbonates of all the calcium, magnesium, iron, or manganese present in the nodules. The manganese in these nodules may exist in both the oxide form and as carbonates with calcite (spartite) or siderite (oligonite) (Gries and Rothrock 1941:68). A list of minerals reported to have been found during investigations of the nodules include: siderite, calcite, aragonite, dolomite, mangano-calcite, pyrolusite, manganite, apatite, and quartz. Chemical content includes manganese, iron, aluminum, calcium, magnesium, carbonate, phosphorus, and silica. Iron, manganese, and carbonate are the main constituents (Gries and Rothrock 1941:69).

Data published in Gries and Rothrock (1941:72–76) does suggest an inverse relationship between iron and manganese content, as they noted. They interpret this as an indication of a chemical relation between iron and manganese

rather than a mechanical mixture without specifying further. Plotting a best-fit regression line on their data for Fe versus Mn content returned an r^2 of 66% (Figure 6). Iron content tends to decrease approximately linearly with increasing manganese content until a manganese content of about 18% when a second population of nodules with a low iron content appears. The plot suggests a minimum allowable value for iron of about 2.5%; values appear to “bottom out” near this value. The minimum iron content reported is 2.3%. The average manganese content is 19% with a range from 8% to 28%. The average iron content is 10% with a range of 2% to 23%. It is also worth noting that the average iron content of the nodules is relatively high with a range that nearly matches that of manganese. Again, as nodules weather out, they would appear to be a potentially significant source of iron as well as manganese but the iron apparently was never concentrated as a uniform deposit.

Nodules are brittle and tend to shatter on weathering. Once shattered, they are easily carried away by the river and incorporated into river sediments where they are lost (Gries and Rothrock 1941:62). Similarly, the nodules would likely be crushed and broken into small fragments when encountering advancing ice and easily weathered in the resultant till and its subsequent soil.

Crystalline and other minerals

This category includes silicates, heavy minerals, and accessory minerals found in the till and in bedrock sources. In addition to being useful indicators of glacial ice provenance, these minerals are important because many contain iron, manganese, and other elements that can be released into the soil solution by weathering or can oxidize into new minerals. Release of elements into solution can be followed by reprecipitation and neof ormation of new minerals as masses,

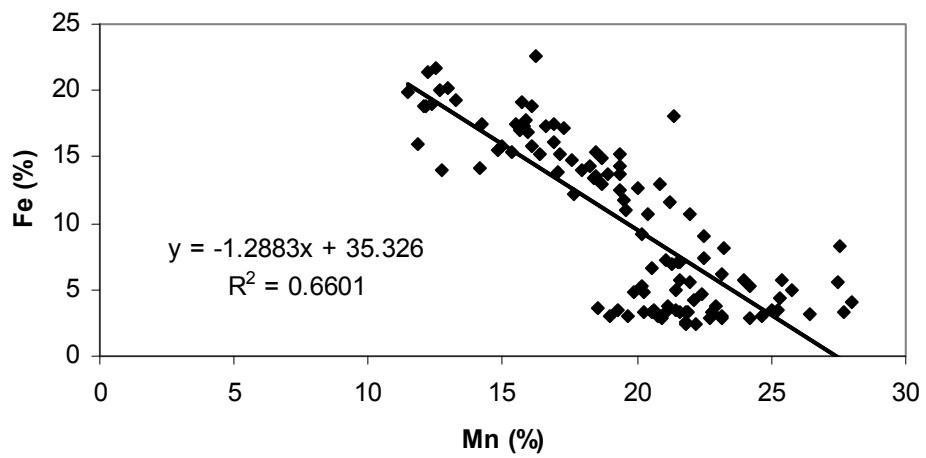


Figure 6. Relationship between iron and manganese in nodules sampled near Chamberlain, S.D. Statistical significance was not calculated since the figure is intended only to show a general relationship and reveal any patterns that might exist. Data from Gries and Rothrock 1941:72–74.

crystals, nodules or concentrations. The chemical and mineral composition of a mineral fragment can be altered by weathering into a new mineral such as pyrite that oxidizes into limonite, an example of “inherited minerals” of Schoenberger et al. (2002).

Among the minerals identified in Minnesota tills are the non-magnetic heavy minerals pyrite, hematite, ilmenite, rutile, goethite, siderite, monazite, garnet, zircon, kyanite, staurolite, titanite, epidote, orthopyroxine, bronzite, clinopyroxine, diopside, clinoamphibole hornblende, and leucoxene. Magnetite is the most abundant magnetic, heavy mineral (Thorleifson et al. 2007).

Samples collected by Thorleifson et al. (2007) clearly show the distinction in till composition between source regions. An end member sample of till from the Riding Mountain provenance (8-16 mm fraction) contains predominantly Cretaceous shale and Paleozoic carbonate, with minor amounts of felsic intrusive and high grade metamorphic, dark metasedimentary and metavolcanic, reddish volcanic, ironstone, and quartzite. An end member of Winnipeg provenance till (8-16 mm fraction) contains predominantly Paleozoic carbonate, lesser amounts of felsic intrusive and high grade metamorphic, and minor amounts of Cretaceous shale, mafic intrusive and high grade metamorphic, dark metasedimentary and metavolcanic, quartzite, reddish volcanic, and ironstone (Minnesota Geological Survey 2011).

New Ulm till (Des Moines lobe) and Granite Falls till (Wadena lobe) contain about 10–40% and as much as 30% granitic clasts respectively (Gowan 1998:164–165) in addition to limestone and carbonates. Samples of the greater than 1 mm fraction of Granite Falls till contains no or little shale (1 to 5%). Carbonate and granitic rocks are present in approximately equal amounts and

together comprise at least 80% of this size range. Rocks from the Lake Superior region are not uncommon (Matsch 1972:553). The coarse-sand fraction of New Ulm till contains siliceous shale, fine-grained dolomite and limestone, and granitic rocks including igneous quartz (Matsch 1972:554).

Although granite varies in exact color and composition, it always contains feldspar and quartz. Granites usually contain about 8% mica or hornblende. Biotite mica is most common but muscovite may also be present. Accessory minerals include zircon, titanite, apatite, magnetite, and ilmenite (Klein and Hurlbut 1993:564).

Fragments of clasts classified as basalt-gabbro-diabase by Hobbs (1998:201–202) are usually present in samples of Des Moines lobe till. Basalt and its textural variants are rich in iron, magnesium, aluminum, silicon, and oxygen (Ojakangas and Matsch 1982:4) and are composed primarily of calcic plagioclase and pyroxene. Apatite, magnetite, and olivine are almost always present (Bates and Jackson 1984; Klein and Hurlbut 1993:568). The source area for the class basalt-gabbro-diabase is usually considered to be the North shore of Lake Superior although other source areas are possible. Red sandstone and iron-formation clasts are also present although in minor amounts. Pebbles are primarily granitic (Hobbs 1998:201–202).

Considering possible bedrock sources of crystalline material, the Black Island Member of the Winnipeg Formation, the basal sandstone and shale layer of the Paleozoic strata, is composed of 75% quartz in whole-rock samples and over 90% quartz in the framework components. Whole-rock mineralogy also contains minor amounts of K-feldspar, plagioclase, illite, dolomite, calcite, anhydrite, and pyrite, and less than 0.2% kaolinite and halite. The framework

components contain orthoclase and microcline feldspars, igneous rock fragments, and heavy minerals dominated by pyrite, tourmaline, diopside, and zircon. As noted earlier, a widespread pyrite cemented zone and pyrite concretion bed occurs near the top of the Black Island Member.

In northwest Minnesota, a Paleozoic section correlative with that of North Dakota and Manitoba taken from a test well is comprised of an upper sandstone layer, an intermediate shale with thin sandstone stringers, and a basal sandstone. The upper layer is a fine-to-medium quartzose sandstone composed of calcareous orthoquartzite. The basal sandstone is medium-to-coarse quartzose sandstone that contains jasper and white, quartzitic siltstone grains (Mossler 1978:10).

Crow Creek, a layer of sand and marl at the base of the Sully Member of the Pierre Shale, is composed of almost equal amounts of silt and very fine sand. The particles themselves are sub-angular quartz grains cemented with iron oxide and clay. The cementing materials are present in such a large amount that the layer could be considered a sandy or silty limestone (Gries and Rothrock 1941:15–16).

Summary

Paleozoic limestone and dolomite supplied in the main, calcium, magnesium, and carbonates to the soil solution. Cretaceous shale supplied iron, manganese, and silica. Both were sources of silica primarily in the form of quartz, predominantly as silt grains. Silica in the shale was also present as clay minerals and as amorphous silica possibly available as gels that infill voids.

Although the large manganese deposits studied in Manitoba are secondary, their manganese source was thought to be iron-manganese nodules in

the Pierre shale. The manganese concentration of the ironstone nodules reported by Spector (1941) is only about 4.5% (Table 5). Ferromagniferous nodules found in the Pierre shale near Chandler, South Dakota contain on average 19% manganese (Gries and Rothrock 1941). It is uncertain whether the lower manganese content of the ironstone nodules resulted from weathering and removal of manganese or whether the manganese content was never as high as in the ferromagniferous nodules found near Chandler. A manganese content of 4.5% in the ironstone calls into question whether they are the source of the manganese deposits in Manitoba or if the source is ferromagniferous nodules of considerably higher manganese content similar to those found in the Pierre shale near Chandler.

Pierre shale is a bedrock source material found in New Ulm till that was deposited throughout western and southern Minnesota. Manganese nodules incorporated into glacial sediments became fragmented and dispersed throughout the glacial sediment as a result of glacial transport. Weathering processes that formed the secondary deposits in Manitoba can reasonably be assumed to be similar to those active in southern Minnesota and thus would have been capable of weathering fragmented nodules into secondary deposits in Minnesota. Fragmentation and dispersion, however, likely diluted the manganese concentration in the till sufficiently to preclude the formation of larger and more widespread deposits of secondary manganese as in Manitoba. Absence of suitable relief and hydrology may also have played a part.

Both end-member samples from Thorleifson et al. (2007) and Minnesota Geological Society (2011) contain ironstone clasts that appear to be oxidized and

may be weathered fragments of ironstone nodules from the Cretaceous shale discussed earlier.

This conclusion is not completely satisfying. To better understand the formation of high-chroma features, additional investigative work is needed to characterize the pore water chemistry at the time of glacial retreat or even shortly before, and subsequent changes to that chemistry as tills weather and soils form. One formational hypothesis is that high-chroma features are relict, having developed under conditions more conducive to their formation than at present. Immediate post-glacial conditions might have been suitable. That possibility is, of course, difficult to confirm. Another highly speculative approach is to follow soil development in general terms from the retreat of the last glacier to the appearance of modern soils with a special awareness of factors that may have contributed to the formation of high-chroma features. This approach would consider subglacial weathering, cryogenic weathering, and the appearance of a "protoil," the first functioning sediment that supports any kind of vegetative cover, including lichens, and lead finally to the formation of a developed soil. The subglacial environment is a unique environment of pre-soil development in the absence of vegetation and for the most part, oxygen, specialized microbes being the dominant organism factor. Data and information on immediate post-glacial protoils are limited but a consideration of how they developed may provide understanding of early soil formation including soil features and soil change on a broader time scale than is usually considered.

Part II: Classification systems

"Precision in classification leads to precision in thought and so is of vast value as a mental discipline" (Grabau 1913 in Pettijohn 1949:177).

Introduction

The purpose of this section is to classify high-chroma features using existing classification systems and definitions under the hypothesis that proper classification will suggest a genetic pathway or provide clues as to their origin and genesis. Field classifications and definitions are compared to those used in micromorphological and thin-section work. A comparison is made between genetic and descriptive classification systems using the example of high-chroma features. The concept of redoximorphic features is discussed.

Classification Systems

Classification systems have two objectives: to organize knowledge, and to provide a better understanding of formational processes (Pettijohn 1949, 1957). Establishing a classification system to meet those objectives requires the development of acceptable terminology, the identification of properties that uniquely define classes, and the establishment of boundaries between classes (Pettijohn 1957). The purpose of this section is to use existing terminology for classifying soil features as a starting point towards the ultimate goal of understanding their genesis.

Different users of classification systems have different needs. Field workers require a descriptive classification. Laboratory workers are interested in an analytical classification. Descriptive terms that have the highest correlation with genesis will result in the most useful analysis. As a result, both descriptive and genetic classification schemes are needed, and because our knowledge of formational processes is limited, the most practical system is one that achieves a balance between the two (Rodgers 1950).

There seems to be no successful classification system that is based solely on genetic factors. Todd (1903) proposed a genetic classification of sedimentary rocks based on mode of growth. Grabau (1913) attempted to develop a genetic classification of limestones. Neither was successful. Kubiëna (1938) attempted to develop a soil classification based on genetic interpretations of soil fabrics and soil features found within each fabric type. His system failed because it did not generalize beyond the particular soils he described, and similar soil fabrics often had different genetic pathways (Stoops 2003). Bryan (1952) classified the gravel fraction of soil at the highest level into two genetic categories: those “Derived from Parent Rock” and those “Developed in the Soil Itself” His classification is heavily genetic interspersed with descriptive criteria and did not receive widespread recognition or acceptance.

The most well-known classification systems are those of organisms. The *Systema Naturae* and *Species Plantarum* of Linnaeus that introduced the binomial classification system are based on arbitrary morphological traits ascribed to the ideal type species that have a similar appearance in related organisms. The morphology of other specimens can be compared to the type species for identification and determination of class membership (Arms and Camp 1987). Natural classification systems use these similarities to map out a branching or splitting pattern of relationships. Each split that results in a new species or branch arises from a common ancestor, a true genetic relationship.

Attempting to classify inorganic materials such as minerals and soils using the same approach as organic or biological entities presents considerable difficulties. No naturally defined discrete entity such as a species exists. Minerals and soils occur on a continuum based on variability of composition that gives a

range of properties. They lack the continuity of development and the reproductive distinctiveness of an organic species. Identical minerals can form from different sources (Grabau 1904) and pathways. There are no principles of descent and no common ancestors (Smith 1986:15). Furthermore, classifying soils requires a consideration of variability over time and over space, a consideration that represents a major difference between the taxonomy of soils and the taxonomy of living organisms. Therefore, the taxonomy of soils must be approached differently than the taxonomy of living organisms (Smith 1986:16).

Linnaeus attempted a binomial classification of minerals in the tenth edition of his *Systema Naturae* published in 1758. In 1757, following the *Systema Naturae* of Linnaeus, Emmanuel Mendes de Costa also published a classification of minerals by series, chapter, genus, section, member, species. Robert Jameson published a *System of Mineralogy* in 1816, self-described as a “System of oryctognosy [mineralogy],” using class, order, species, and subspecies. It was not until the appearance of James Dana’s hierarchical mineral classification by chemistry and crystal structure that first appeared in his *System of Mineralogy* in 1837 has any lasting success been achieved in mineral classification. Karl Strunz developed a classification system similar to Dana’s original classification based on similar criteria. (His *Mineralogische Tabellen* was first published in 1941 and updated in 2001. It is now known as the Nickel-Strunz classification.) Neither of these latter two systems are based on genetic relationships and inheritance but rather on composition and texture, the two fundamental properties of all solids (Krynine 1948). Composition refers to the components that make up the solid material. Texture refers to how those components are put together. Minerals for example, are composed of certain elements that are put together as crystals

having a definite order and structure. (Krynine (1948) admitted structure as a possible third fundamental of solids.) While chemical composition can vary with isomorphic substitution, crystal form is constant, except in the case of pseudomorphic replacement. Likewise, soils and features within soils are composed of “elements,” “textures,” and “structures,” only a few of which are useful for classification purposes.

The present system of U.S. Soil Taxonomy is an example of a mixed system, containing elements that are both genetic and descriptive (Smith 1986:36). With only two exceptions, Aridisols and Gelisols, soils at the highest and most inclusive level, Order, are largely recognized by the factors and processes responsible for their formation, but the actual placement of a soil into a particular Order is based on objective morphological, physical, and chemical properties. Soil Taxonomy does not address the description and classification of soil features, however. Much of that work has been done outside the Soil Survey by soil micromorphologists.

Soil features have been used as objects of classification in their own right and also used as a criterion for classification of the soil in which they occur. An early example of the former is that of Bennett and Allison (1928) who developed a classification of soil concretions based on color, size, consistency, and quantitative chemical analysis. An example of the latter is that of Kubiëna (1938), who used specific soil features to explain genesis and classify soils on the basis of their fabric (Stoops 2003). Soil features were considered only as components of particular soil fabrics.

Brewer (1964) introduced the term “pedological features.” Pedological features are recognizable units within the soil that can be distinguished from the

surrounding soil material for any reason, such as origin, differences in composition, or differences in fabric. Pedological features that formed on surfaces (cutans or coatings) or in voids (pedotubules or channel infillings) are distinguished from those that did not form on surfaces or within voids (glaebules). In addition, a glaebule is a pedological feature recognized as a discrete entity because of a greater concentration of some constituent material, a difference in fabric compared with the enclosing soil material, or because it has a distinct boundary with the enclosing soil. Nodules and concretions are well-known examples of glaebules. Note that the distinction Brewer (1964) makes between pedological features formed within voids and those that did not form within voids is a distinction based on an aspect of presumed genesis. Thus, the identification or classification of a pedological feature as a glaebule restricts the relevant formational process to one that takes place outside of a void (other than packing voids) and is unrelated to surfaces. Likewise, classification of a feature as a channel infilling or simply an infilling, restricts the relevant formational process to one that takes place within a void. It is not clear, however, that the process itself would be different in each case, only *where* the process takes place is different.

Bullock et al. (1985) developed a classification system deliberately based almost exclusively on morphology and description rather than genetics and interpretation. They redefined and renamed Brewer's term, pedological features, to "pedofeatures," which they defined as "discrete fabric units present in soil materials recognizable from adjacent material by a difference in concentration in one or more components, e.g., a granulometric fraction, organic matter, crystals, chemical components, or an internal fabric" (Bullock et al. 1985:95). Replacement

of the term “pedological features” with the term “pedofeatures” was done to emphasize the basic differences between the two systems (Stoops 2003:101). At the highest level of classification, features are separated into two categories: those related to voids, such as coatings and infillings, equivalent to Brewer’s (1964) cutans and pedotubules, and those unrelated to voids, such as crystal intergrowths and nodules, equivalent to Brewer’s (1964) glaeboles.

One genetically based difference between Brewer’s (1964) definition and that of Bullock et al. (1985) is that Brewer (1964) considered rock fragments, weathered grains, and fragments of inherited nodules to be pedological features, while Bullock et al. (1985) consider them to be part of the groundmass, approximately equivalent to Brewer’s (1964) s-matrix. Brewer’s definition would seem to imply that rock fragments, weathered grains, and nodule fragments are pedological features because they have been acted upon by pedogenic processes. Such a broad definition could easily be extended to include individual sand and silt grains that have been separated from their surrounding matrix, rendering the concept nearly useless. The interpretation of Bullock et al. (1985) is less genetic and more “process neutral” but Brewer’s (1964) interpretation is not without merit and bears consideration in certain instances where such an interpretation leads to a clearer understanding of genesis.

Stoops (2003) updated and clarified some concepts and terminology in Bullock et al. (1985). He also expanded some descriptions and developed identification keys for pedofeatures that use two different bases for classification: their relation to groundmass and their relation to morphology. He considers them to be equivalent classifications and states that both are needed for complete identification of the features (Stoops 2003:102). Features formed from a change

within the groundmass are called matrix pedofeatures while those formed outside the groundmass are called intrusive pedofeatures. As with Brewer (1964) and Bullock et al. (1985), Stoops' (2003:104) morphological classification distinguishes pedofeatures that are related to voids and natural surfaces, and those that are not related to voids and natural surfaces. It is not clear how the initial classification based on a relationship with voids and surfaces is morphological and not genetic unless the term "related to" is intended to be descriptive rather than interpretive, but that distinction is not overtly stated. It is possible that "Morphological Classification" (the full heading is: "Morphological Classification of Pedofeatures as Related to Their Fabric") is used as a convenient label for the initial classification since the crystallinity and related distribution pattern of pedofeatures also play a significant role in their classification.

Sedimentary geologists have developed similar criteria and descriptions for geological features. Accretionary bodies, defined by Pettijohn (1957:196-200) as "segregations of the rarer constituents of the rock," could be considered the geological equivalent of pedofeatures except for its strong genetic meaning that includes only features that formed through the specific process of accretion. Actually, the term "segregations" is perhaps more general and inclusive (even if it carries genetic overtones) and thus may be more analogous to the term "pedofeatures" than is "accretionary bodies." Pettijohn identified four groups of segregations, a grouping that can be extended in modified form to soil features: (1) nodules, (2) spherulites and other regular crystal growths, (3) true concretions, and (4) geodes, septaria, and other forms related in that they have a partially or completely filled interior cavity. He identified these as four different

types of structures that are fundamentally different in morphology and *origin* [italics mine] (Pettijohn 1949, 1957).

Field and micromorphological classifications

Field terminology, as promulgated by Schoeneberger et al. (2002) and the Natural Resources Conservation Service, combines accretionary bodies, segregations, glaeboles, and pedofeatures into the general concept of “concentrations” (Schoeneberger et al. 2002:2-18). Seven types of concentrations are recognized. Each is discussed below in relation to its micromorphological or thin-section description and later to the genesis of high-chroma features. Field terminology is used as the basis for discussion since field classifications are used as the basis for all later analysis and interpretations regardless of scale.

Finely Disseminated Materials

Finely disseminated materials are physically small precipitates (e.g., salts, carbonates) dispersed throughout the matrix of a horizon. The materials cannot be readily seen (10X lens), but can be detected by a chemical reaction (e.g., effervescence of CaCO₃ by HCl) or other proxy indicators (Schoeneberger et al. 2002:2-18).

The concept of finely disseminated materials corresponds approximately to the micromorphological concept of a partial fabric, defined as all fabric units, which on a given scale are identical with the criteria being considered. This definition requires the additional definition of fabric unit, which is “a finite three-dimensional unit delimited by natural boundaries, statistically homogeneous on the scale under consideration, and that can be distinguished from other fabric units by the methods of study applied and at the scale of observation used” (Bullock et al. 1985, Stoops 2003). In the case of finely disseminated CaCO₃, each precipitated crystal is a fabric unit. All the crystals

together comprise a partial fabric. Matrix material that is not precipitated CaCO_3 comprises the remainder of the fabric, which could be further divided into other partial fabrics by identifying other fabric units. Increasing the magnification (change of scale) could reveal the presence of other homogeneous partial fabrics constituting the fabric that appeared homogeneous under lower magnification.

The field definition given above is to a certain extent genetic and operational, applies to an entire soil horizon, and is bounded by that horizon. The micromorphological definition of partial fabric does not require a concentration of material nor a specific boundary, only that the boundary be "natural." Boundaries can be contained within a horizon. Partial fabrics may be grouped on virtually any conceptual basis from descriptive to genetic. An obvious example of finely disseminated materials would be a pedogenic accumulation of finely divided CaCO_3 in a Bk horizon.

Masses

Masses are noncemented (... Extremely Weakly Cemented or less) bodies of accumulation of various shapes that cannot be removed as discrete units, and do not have a crystal structure that is readily discernible in the field (10X hand lens). This includes finely crystalline salts and redox concentrations that do not qualify as nodules or concretions (Schoeneberger et al. 2002:2-18).

Cementation is not considered a valid criterion in micromorphology because it cannot be assessed in thin section (Stoops 2003:117). Despite this limitation, the micromorphological concept of a loose infilling would seem to give the closest correspondence to the field concept of masses. Infillings are voids other than packing voids that are filled or partially filled by soil material (Bullock et al. 1985:103; Stoops 2003:113). Loose infillings consist of grains, aggregates, crystals, or excrements loosely packed throughout the void. Loose infillings may

be either continuous or discontinuous. Discontinuous loose infillings consist of loosely packed material grouped into clusters rather than being continuously distributed throughout the void. Although intended to be descriptive, the term “infilling,” carries with it a genetic connotation.

Kubiëna (1938) presented specific soil features in the larger context of soil fabrics but in the discussion that follows, features will be considered independently of fabric. Kubiëna’s insights into the genesis of soil features are worthy of consideration despite the warning that his opinion is often accepted without support from laboratory analysis (Stoops et al. 2010:3). In many instances, however, he does support his conclusions either with simple laboratory experiments he himself performed or with those performed by colleagues. Although Kubiëna’s (1938) soil classification scheme was never accepted, his identification of certain soil features warrants inclusion here as potentially relevant to the concept of masses and high-chroma features, beginning with his concept of crystal formations.

According to Kubiëna (1938), three types of crystal formations are produced by evaporation of the soil solution: efflorescences, interflorescences, and depositions. Kubiëna did not define efflorescences in anything but genetic terms. Bates and Jackson (1984) define an efflorescence as “a white powder, produced on the surface of a rock or soil in an arid region by evaporation of water, or by loss of water of crystallization on exposure to the air.” There seems to be no particular reason to limit the definition to any specific color, an external surface, or to an arid region. Upon drying of a soil, internal pores and voids would likely meet the requirement that there be a surface in an arid region available for evaporation. It becomes a matter of scale. Color is dependent on the

particular composition of the soil solution. Kubiëna (1938) allowed that the precipitating surface was not limited to external surfaces but could take place within the soil profile. In typical fashion he defined efflorescences genetically, as features in which the soil solution has been drawn from the interior of the soil body by evaporation and dissolved substances are precipitated on the surface. Efflorescence refers to both the product and process (Kubiëna 1938:164). Interflorescences occur when the soil solution dries and its constituents precipitate before reaching the surface. Deposition is the precipitation of the constituents of a soil solution onto the wall surface of a "fabric body" from the outside. Deposition can be distinguished from efflorescences by their tendency to fill in surface relief; efflorescences tend to follow surface relief (Kubiëna 1938:165-166). All three types of crystal formations may appear in the soil at the same time since they represent the last stage in the drying process. He claimed that every accumulation is completed by efflorescence or interflorescence. Distinguishing between them may be difficult. For example, he maintained that many interflorescences turn out to be efflorescences "after more careful investigation" Kubiëna (1938:165). These concepts were never incorporated into the micromorphology literature possibly in part because of the difficulty of distinguishing between efflorescences and interflorescences.

Crystal formations, even of the same salt, can occur in a variety of sizes, shapes, and patterns. Factors that influence the resultant morphology include size and shape of the spaces in which they form; air and water content; the concentration, composition, and pH of the soil solution; the nature of the capillary system; and the presence of colloids and colloidal gels. Crystals forming from gel masses do not take the same shape as those formed under normal

conditions but take on peculiar shapes including powdery precipitations (Kubiëna 1938:166), a description that would seem to match the loose infillings of Bullock et al. (1985) and also of high-chroma features.

Efflorescences of salts as “crystalline crusts or powdery precipitations” are common in soils (Kubiëna 1938:183). The appearance of powdery precipitations indicate precipitation from a concentrated soil solution, alkaline pH, and a rapid rate of evaporation. Under these conditions, precipitation takes place rapidly producing rounded, very small crystals (1-1.5 μm diameter). Lower concentrations of salts and acid to neutral soil solutions produce long, thin needles and threads (Kubiëna 1938:152, 167-183, 212). The appearance of a hemispherical shape result from the lack of a uniform system of fine capillaries, which in turn, results from a lack of colloidal material in the soil (Kubiëna 1938:183).

Kubiëna (1938) also discusses what he calls “amygdalus formations,” defined as round-shaped spaces filled with colloidal or crystalline substances (Kubiëna 1938:191). If the space is partially filled with air, growth of the amygdalus can take place by the process of efflorescence. Salts or colloids in the soil solution precipitate initially on the walls of the space and gradually grow inwards towards the center. According to Kubiëna (1938), the process can be recognized by the visible presence of different stages of formation. It is not immediately apparent how amygduli differ from efflorescences, although given the qualification above, an amygdulus may form if the space is entirely filled with soil solution rather than completely or partially filled with air. An amygdulus may also be required to have a round shape, a requirement that would stand in contrast to the literal meaning the word “amygdulus.” Amygduli

are discussed in a chapter titled, “compact soil fabrics” so Kubiëna might consider their occurrence to be restricted to a specific soil class. Efflorescences are discussed as features within “spongy soil fabric.”

Crystal chambers, crystal formations, are similar to amygduli but are entirely filled with “grain-like salt crystals” (Kubiëna 1938:189). Colloidal material is excluded. Crystal chamber diameters vary from 100 μm to 1 mm. Individual crystal grains of calcite vary from 50 to 100 μm and gypsum from 10 to 400 μm . All grains tend to be of uniform size, indicating that conditions of formation were identical throughout the precipitation process or during each precipitation event (Kubiëna 1938:190). Finer crystal grains indicate a more rapid rate of drying. Again, as with amygduli, it is not apparent how crystal formations differ from efflorescences except that, if sufficiently abundant, they are considered to comprise a unique soil fabric called “crystal chamber fabric” (Kubiëna 1938:189).

What crystal formations, crystal chambers, and amygduli all seem to have in common is that they are formed by the process of secretion, defined by Bates and Jackson (1984) as material deposited from solution within a cavity; deposition is inward rather than outward from a center. What distinguishes them from each other is less clear.

Because cementation is not considered in the definition of amygduli or crystal chambers, it is not clear whether they should be included under the field concept of masses. On the other hand, if the precipitate is loose and uncemented and they occur within the soil profile rather than at the surface, they would be considered masses under Schoeneberger et al. (2002) and infillings by Bullock et al. (1985).

Nodules

Nodules are cemented (Very Weakly Cemented or greater) bodies of various shapes (commonly spherical or tubular) that can be removed as discrete units from the soil. Crystal structure is not discernible with a 10X hand lens (Schoeneberger et al. 2002:2-18).

Bryan (1952:45) proposed a succinct yet complete if not over-generalized definition of nodules as “rounded lumps, whatever their nature, that have been produced within the soil and as a result of soil-forming processes.” Bryan’s (1952) definition addresses physical properties (rounded lumps), occurrence (within the soil), composition (whatever their nature), and formation (a result of soil-forming processes). His genetic definition raises one of the most fundamental challenges in feature analysis: determining whether or not a feature formed in the present soil through pedogenic processes (and what those processes might be). (The other fundamental challenge is to determine whether a feature is actively forming, is stable, or is degrading.)

The most modern micromorphological definition of nodules is that they are approximately equidimensional pedofeatures unrelated to natural surfaces or voids and do not consist of single crystals or crystal intergrowths (Stoops 2003). Nodules cannot have formed in voids, but as with other genetic definitions, that may be difficult to prove. Furthermore, morphology taken by itself can be ambiguous. For example, a section taken through a dense continuous infilling may be mistaken for a nodule (Stoops 2003:117).

As with masses, using cementation to define nodules requires that they be evaluated on a property that cannot be verified in thin section. Cementation, therefore, is considered to be an invalid criterion with which to define nodules

micromorphologically (Stoops 2003:117). Since cementation is not a consideration when defining nodules micromorphologically, lack of cementation does not disqualify a feature from being classified as a nodule. In micromorphology then, the only distinguishing criterion between nodules and infillings is whether or not the feature formed within a void. Field and micromorphological definitions of a nodule have no diagnostic criteria in common: one requires cementation and does not recognize any formational criteria; the other requires formation within a void and does not recognize cementation. Nodules, along with concretions discussed later, are probably the only two feature types with completely descriptive field definitions.

Nodules are accretionary structures (Pettijohn 1957), referring to a process “by which inorganic bodies grow larger, by addition of fresh material to the outside” (Bates and Jackson 1984), or growth outward, in contrast to the process of secretion, or growth inward, discussed earlier under masses. Nodules have a composition different from the surrounding material and are formed by precipitation of material from solution within the host material, which distinguishes a nodule from a pebble (Pettijohn 1975:462), a simple rock fragment generally rounded by abrasion (Bates and Jackson 1984).

Kubiëna (1938:191) describes what he calls “invasion amyguli,” found within the larger intergranular spaces of the skeletal material in “ground-water soils.” These “round-shaped and well demarked accumulation[s]” consist of colloidal materials interspersed with mineral grains. His description of invasion amygduli resembles that of nodules formed in wet soils, a relationship discussed later in the section on redoximorphic features.

Nodules with a loose internal fabric may actually be proto-nodules, nodules in the early stages of formation, that are as yet uncemented. According to Bryan (1952:46), "Incipient nodules are sometimes little more than ill-defined efflorescences or soft white spots or rusty flecks." Such nodules would be classified as masses in the field. No completely satisfactory criteria for distinguishing nodules having a loose internal fabric from loose infillings seems to exist. Differentiation between the two requires the micromorphologist to determine whether the feature formed in a void (infilling) or not in a void (nodule).

Concretions

Concretions are cemented (Very Weakly Cemented or greater) bodies similar to nodules, except for the presence of visible, concentric layers of material around a point, line, or plane. The terms "nodule" and 'concretion" are not interchangeable (Schoeneberger et al. 2002:2-18).

Definitions of nodules and concretions are often blurred to the extent that sometimes the two terms are used interchangeably, resulting in the loss of any meaningful distinction that formerly existed between the two (Pettijohn 1957; Brewer 1964). The field definitions of nodules and concretions given by Schoeneberger et al. (2002) clearly distinguish between the two on the basis of the concentric layering that is present in nodules. Pettijohn (1949:151) also considers true concretions to have a concentric structure while nodules are structureless.

Bullock et al. (1985) and Stoops (2003) do not distinguish between nodules and concretions. They consider a concretion as a nodule with a concentric fabric having more than one ring and approximately circular in shape, a type of nodule they call a "concentric nodule" (Bullock et al. 1985:104; Stoops 2003:119). For

micromorphological descriptions, concretions, nodules, mottles, and flecks are treated together as a single concept, that of nodules (Stoops 2003).

As discussed earlier under masses, Kubiena (1938) assigned the term “amygduli” to microscopic formations that fill round-shaped spaces with colloidal or crystalline substances. He considered larger forms, or macroscopic amygduli, to be concretions (Kubiena 1938:191). It is not clear if he was referring to concretions in the restricted sense or to a more generic definition that would also include nodules. Conceivably, his invasion amygduli (Kubiëna 1938:191) discussed above under nodules, could also be considered concretions or concentric nodules if they are layered.

Concretions, like nodules, are accretionary structures (Pettijohn 1957) having a composition different from the surrounding material formed by precipitation of material from solution within the host material (Pettijohn 1975:462). More specifically, Pettijohn considered that “true *concretions* are concentrically laminated structures ... normally subspherical, though commonly very oblate, to irregular bodies formed generally by orderly precipitation of mineral matter in the pores of a sediment adjacent to a nucleus” (Pettijohn 1949:149; Pettijohn 1957:197). Again, although it is possible to confirm the morphology, it is considerably more difficult to demonstrate that any particular concentrically laminated structure actually formed by orderly precipitation in the pores of a sediment. The requirement stated by Pettijohn above that concretions have an identifiable nucleus is used by other authors to define concretion to an extent that the presence of a nucleus seems diagnostic for concretions. Neither Schoeneberger et al. (2002) or Stoops (2003) include such a requirement in their definitions. Stoops (2003), based on Bullock et al. (1985), assigns a nodule with a

nucleus to its own separate class called “nucleic” distinct from “concentric.” A concentration with a nucleus but no layering would be considered a nodule by Schoeneberger et al. (2002), a nucleic nodule by Stoops (2003), or a concretion by Bates and Jackson (1984). If one considers that concentric layering around a point, line, or plane (as in Schoeneberger et al. 2003) implies that a nucleus is present even if not directly visible, then the requirement that concretions have a nucleus does exist in the field definition of concretion.

Some authors define what they mean by nodule and concretion early in their work. Others might assume that the reader already knows the distinction or can discover it through context, and some authors seem to use the terms interchangeably, whether intentional or not. Since a standard, uniform, and widely accepted terminology does not exist, defining terms early seems most prudent.

Crystals

Crystals are macro-crystalline forms of relatively soluble salts (e.g., halite, gypsum, carbonates) that form in situ by precipitation from soil solution. The crystalline shape and structure is readily discernible in the field with a 10X hand lens (Schoeneberger et al. 2002:2-18).

No requirement for cementation is given in the field definition. Therefore, the presence of loose crystals identifiable under a 10X hand lens may be the single deciding factor as to whether a feature is classified as a crystal or a mass.

Since the field definition also contains no references to voids or surfaces, the field concept of crystals could include the micromorphological concepts of “infillings by crystals” (Stoops 2003:115) and “crystals and crystal intergrowths” defined as “single crystals and crystal intergrowths larger than 20 μm , euhedral or subhedral, embedded in the groundmass, and that are not part of the parent

material” (Stoops 2003:116). Crystal intergrowths include crystal complexes such as fibrous goethite, spherulites of calcite or siderite, or aggregations of small spherical particles such as framboids of pyrite (Stoops 2003:116).

Considering 200 μm as a practical limit of resolution for the human eye, the specified size limit of 20 μm will make crystals just visible with the use of a 10X hand lens (depending on the quality of the lens, lighting conditions, and contrast).

The field definition given by Schoeneberger et al. (2002) matches the concept of amygduli and crystal chambers proposed by Kubiëna (1938). Both are genetic and the requirements may be difficult to verify.

Biological Concentrations

Biological concentrations are discrete bodies accumulated by a biological process (e.g. fecal pellets), or pseudomorphs of biota or biological processes (e.g. insect casts) formed or deposited in soil (Schoeneberger et al. 2002:2-18).

Micromorphology recognizes only the narrower concept of excrement pedofeatures. No specific definition of excrement pedofeatures is given, but any definition of a pedofeature related to a biological process, is of necessity, genetic (Bullock et al. 1985:133). The ability of micromorphologists to make an interpretation of biological origin will vary greatly (Bullock et al. 1985:133).

Variations in color and morphology, and similarities to inorganic features make the identification of excrement pedofeatures particularly challenging. Colors range from black through brown to yellow. While usually composed of organic or organic and mineral material, some consisting of only mineral composition do occur (Bullock et al. 1985:136). These can be composed of clay and/or iron compounds or very fine calcite. While it is nearly impossible to relate particular excrements to the kind of animal that produced them, shape,

composition, size, and color usually are recorded. Ageing alters their appearance and must be taken into consideration (Stoops 2003:124–125).

Amorphous and cryptocrystalline pedofeatures described by Bullock et al. (1985:126) include material that may form partial or complete pseudomorphs or impregnations of plant tissues, animal remains, and rock or soil fabrics.

Filled insect casts or burrows are considered fabric pedofeatures. Krotovina are classified as “Special Features” in the field classification (Schoeneberger et al. 2002:2-67).

One intriguing question is why redoximorphic features are not included in the field definition of “biological concentrations” in a manner similar to that of masses, which in their definition include “redox concentrations that do not qualify as nodules or concretions.” Although a discussion of redoximorphic features is deferred until later, the underlying process is microbiological and often results in an accumulation of material. The phrasing of the definition seems directed towards the exclusion of redoximorphic concentrations but does not overtly exclude them: “discrete bodies accumulated by a biological process” is a definition consistent with other definitions of redoximorphic concentrations.

Inherited Minerals

Inherited minerals are field-observable particles (e.g., mica flakes) or aggregates (e.g., glauconite pellets) that impart distinctive soil characteristics and formed by geologic processes in the original Parent Material and subsequently inherited by the soil rather than formed or concentrated by pedogenic processes (Schoeneberger et al. 2002:2-18). They are included as concentrations “due to historical conventions” (Schoeneberger et al. 2002:2-18).

Rock fragments, inherited nodules, and fragments of pedofeatures were considered glaeboles by Brewer (1965). Brewer (1965:143-146) further subdivided pedological features into orthic pedofeatures (those formed in situ by soil-

forming processes) and inherited pedofeatures (relicts of parent rock or parent material). He recognized three types of inherited pedofeatures: lithorelicts, pedorelicts, and sedimentary relicts. Such a distinction is no longer made. All are now considered to be coarse material and part of the groundmass (Bullock et al. 1985; Stoops 2003:104).

Stoops (2003:117–118) acknowledges that it is not always clear if a nodule is pedogenic or was inherited with the parent material and therefore should be considered part of the groundmass. He placed nodules into three classes: anorthic nodules (nodular bodies inherited from the parent material but may have a pedogenic origin), orthic nodules (formed in-situ), and disorthic nodules (formed in-situ but have been locally translocated). He admits that distinguishing orthic from anorthic nodules may be rather difficult and sometimes impossible.

Anorthic nodules that are not pedogenic would be considered inherited minerals under the field classification but would not be considered pedofeatures under Bullock et al. (1985) and Stoops (2003) but part of the groundmass.

Redoximorphic Features

Redoximorphic Features (RMF) are a color pattern in a soil due to loss (depletion) or gain (concentration) of pigment compared to the matrix color, formed by oxidation/reduction of Fe and/or Mn coupled with their removal, translocation, or accrual; or a soil matrix color controlled by the presence of Fe⁺². The composition and process of formation for a soil color or color pattern must be known or inferred before describing it as a RMF. Because of this inference, RMF are described separately from other mottles, concentrations; e.g., salts; or compositional features; e.g., clay films (Schoeneberger et al. 2002:2-14).

Redoximorphic features are not included in the concept of concentrations discussed in Schoeneberger et al. (2002) but instead are given their own

dedicated chapter between a chapter titled “Mottles” and a chapter titled “Concentrations.”

The National Resources Conservation Service has a simpler and completely genetic definition: “Features formed by the processes of reduction, translocation, and/or oxidation of Fe and Mn oxides” (Vasilas et al. 2010:39-40). Redox concentrations are defined as “bodies of apparent accumulation of Fe-Mn oxides. Redox concentrations include soft masses, pore linings, nodules, and concretions” (Vasilas et al. 2010:39). In the field, redoximorphic concentrations are considered to be masses, nodules, or concretions (Schoeneberger et al. 2002:2-14). Redox depletions are defined as “bodies of low chroma (2 or less) having value of 4 or more where Fe-Mn oxides have been stripped or where both Fe-Mn oxides and clay have been stripped Redox depletions contrast distinctly or prominently with the matrix” (Vasilas et al. 2010:39). Redoximorphic features, both concentrations and depletions, are associated with anaerobic or alternating aerobic/anaerobic conditions in the soil (Vepraskas 1999).

No micromorphological classification system recognizes redoximorphic features specifically by that name. This omission might be at least in part because the term has come into the lexicon only within the last 30 years, postdating Bullock et al. (1985) but Stoops makes no mention of them in his later classification schemes including his most recent 2003 monograph. The omission may also exist because the term is somewhat uniquely American (Jay Bell, pers. comm.). Notably, thirteen scientists are acknowledged at the beginning of Bullock et al. (1985); none are from the United States. It should be noted, however, that Stoops does give an example of one possible grouping of features that are related to oxidation-reduction into a “redoximorphic partial fabric,”

noting that similar examples “are no longer purely descriptive but involve interpretations” Stoops (2003:37). Redoximorphism is so completely genetic that its exclusion from a system based intentionally on description and morphology alone seems obvious.

Bullock et al. (1985) devote an entire chapter to depletion pedofeatures, but do not mention concentrations as a specific type of pedofeature. Stoops (2003:103) includes depletion pedofeatures as a subclass of matrix pedofeatures but he emphasizes that the term “depletion pedofeature” does not refer to a process, only that the feature includes less of a material than the surrounding matrix. As with Bullock et al. (1985), he makes no mention of a corresponding term, “concentration pedofeatures.”

In micromorphological taxonomy, a system developed deliberately on the basis of descriptive criteria, a “redoximorphic concentration” might correspond to any recognizable soil feature composed of pedogenic iron and/or manganese. For example, amorphous and cryptocrystalline pedofeatures described by Bullock et al. (1985:126) are concentrations that impregnate soil material. If composed of iron oxides, they could be considered redoximorphic concentrations (amorphous and cryptocrystalline pedofeatures are defined on the basis of their appearance under a polarized light microscope, a definition that is not of practical use in the field). Coatings, hypocoatings, quasicoatings, and infillings are concentrations of material that are associated with pores and surfaces. If they are concentrations of pedogenic iron and/or manganese oxides they could also be considered redoximorphic features. The only necessary condition is that the concentrated elements are formed pedogenically by the processes of oxidation and reduction.

Certain types of precipitations have been regarded as indicators of aerobic or anaerobic conditions. Kubiëna (1938:212) regarded salt efflorescences in the interior of a soil as an indicator of aerobic conditions since their appearance is always restricted to air-filled spaces as long as no other forms of salt or colloidal precipitations are present. Crystal chambers and crystal tubes are indicators of predominantly anaerobic conditions. Alternating aerobic/anaerobic conditions may be indicated by the formation of crystal chambers and of neoformed empty spaces with efflorescences or crystal deposits forming on their walls or interior surfaces. Strictly anaerobic conditions are indicated by the formation of large intercalary crystals, more simply called, "intercalations." Intercalations are elongated, undulating pedofeatures that are unrelated to natural surfaces and do not consist of single crystals or crystal intergrowths (Stoops 2003:121). They appear similar to coatings of planar voids that are now closed. Little is known about the formation of intercalations. Heeding the warning given by Stoops et al. (2010:3), it should be mentioned that Kubiëna offers no evidence for the above claims, so their reliability is questionable.

Summary

Field classifications of concentrations provided by Schoeneberger et al. (2002) are useful adjuncts to field descriptions but only a subset of them are based on morphological properties, limiting their application and usefulness. Concentrations defined genetically require interpretations that may involve equipment and procedures that are not practical to use or undertake in the field.

Micromorphological descriptions are written with a more strictly morphological basis but the connections between morphology and genesis are often unclear or unknown. This is a problem that has plagued soil scientists

throughout our history. Morphological classifications help organize our knowledge about concentrations but without a more complete and certain understanding of genesis, the morphology-genesis connections remain, for the most part, speculative. Morphological classifications and genetic classifications remain separate and, in Stephen Jay Gould's words comparing religion and science, "non-overlapping magisteria."

The relatively recent concept of "redoximorphic features" has further complicated the picture. This strictly genetic concept often is applied as a descriptive term even when appropriate morphological terms are available and their use would provide more useful information. More discussion on the subject of redoximorphic features appears later in the Results section.

Part III: Properties and formation of nodules and concretions

No formal studies of "high-chroma features" as described in this study are known to have been published, so comparisons of physical, chemical, and mineralogical properties can only be made with features whose reported properties approximate those of high-chroma features. In many cases, however, not enough descriptive information is available to ascertain whether the features being discussed have sufficiently similar physical properties and composition to be regarded as equivalent to high-chroma features as defined in this study. Analogies and conclusions based on those published studies must be evaluated and considered in that light.

Papers included in this review date from the beginning of the twentieth century to the beginning of the twenty-first century. Much of the early work was truly pioneering work that later investigators built on, but for whom credit seems to have been lost over the decades since publication. Their early insights

provided explanations for the formation of nodules and concretions that are still relevant and accepted today.

This review is regrettably but necessarily incomplete, partly because of the large volume of literature on nodules and concretions and partly because of the inability to include foreign language sources, which contain important works both early and contemporary.

Physical properties

Sizes of nodules reported in the literature range from “minute” to 0.05 mm to larger than 20 mm (Thresh 1902; Wheeting 1936; Dawson et al. 1985). This reported size range brackets the size of high-chroma features. Most nodules and concretions that have been studied and reported in the literature are much larger than high-chroma features, especially those from well-drained soils. This is a sampling artifact likely based on a decision of practicality and convenience rather than scientific significance, and skews the results towards the larger sizes.

In addition to size, reported shapes of nodules and concretions resemble those of high-chroma features. Shapes have been found to be almost perfectly spherical to elliptical (Thresh 1902; Tsukunaga 1932; Drosdoff and Nikiforoff 1940), round to subround and polygonal (King et al. 1990), or irregular with a rough surface (Wheeting 1936; Drosdoff and Nikiforoff 1940; Sokolova and Polteva 1968). Smaller nodules sometimes are aggregates of even smaller particles (Wheeting 1936; Drosdoff and Nikiforoff 1940).

Nodule colors are often reported imprecisely in the literature as black, brown, or dark brown (Thresh 1902; Robinson 1929; Tsukunaga 1932), yellowish brown (Robinson 1929), reddish brown to almost black (Winters 1938), dark reddish brown (Pawluk and Dumanski 1973), light brown to black (Drosdoff and

Nikiforoff 1940), and red (Tsukunaga 1932). Whittig et al. (1957), however, described 7.5YR 5/6 “splotches” that generally grade to nearly black. Pawluk and Dumanski (1973) found 2.5 YR 3/4 particles and quartz grains cemented by 7.5YR 5/8 material in an A-horizon with 7.5YR 5/8 and a few 2.5YR 4/8 in a B-horizon. Gallaher et al. (1973:I) also found nodules with a 7.5YR 5/6 and 7.5YR 5/8 surface enclosing a 7.5YR 3/0 core. Note that 7.5YR 5/8 is an exact match with high-chroma features. In a theoretical explanation of the formation of iron-rich reddish rims around the reduced faces of peds (quasicoatings), Fanning et al. (1992) stated that the color of the rims was often 7.5YR 5/6 to 5/8.

Mottling is a dominant characteristic of high-chroma features. Clark and Brydon (1963) found variations in interior colors ranging from brown or yellowish-brown to dark gray or grayish brown, some with black mottling present.

Contrasting colors between an outer shell and an inner core are not uncommon as reported above by Whittig et al. (1957) and Gallaher et al. (1973:I). Drosdoff and Nikiforoff (1940) found larger nodules (15mm) with a metallic blue luster in the core and a rusty or ochre-yellow shell around a black nucleus. King et al. (1990) found nodules with a gray interior (N5) surrounded by a 5YR 3/3 or 7.5YR 6/6 outer layer.

Because of the imprecision with which colors have been reported, it is often difficult to say just how good the color match is between nodules and concretions reported in the literature and high-chroma features. The 7.5 YR 5/6 and 5/8 colors are the best match. Vitreous, metallic, metallic blue luster and mottled color patterns, especially those that include black, match more detailed descriptions of high-chroma features discussed later.

Contrast, another aspect of color, was recognized as an important criteria for identifying redoximorphic patterns in Virginia paleosols (Stolt et al. 1994). King et al. (1990) described an outer crust as “prominent.”

Although concentric banding or layering is often most visible as a color contrast, it is considered here as internal fabric. Concentric banding around a defined nucleus (Tsukunaga 1932; Winters 1938; Taylor and Schwertmann 1974) and differentiated fabric (Phillippe et al. 1972) are commonly observed in concretions although undifferentiated, non-concentric fabrics are also observed (Clark and Brydon 1963; Phillippe et al. 1972; Pawluk and Dumanski 1973; Arocena et al. 1994). More unusual but also relevant are scale-like deposits and loose black powder in cavities (Robinson 1929) and vitreous and metallic lusters (Drosdoff and Nikiforoff 1940; Pawluk and Dumanski 1973; King et al. 1990).

Nodule boundaries range from well-defined (Robinson 1929; King et al. 1990), distinct (Phillippe et al. 1972), and sharp (Phillippe et al. 1972), to diffuse (Phillippe et al. 1972). Sharp boundaries were found in a well-drained soil and distinct to diffuse boundaries in the lower part of a moderately well drained soil and in a somewhat poorly drained soil (Phillippe 1972).

No halos or rinds were reported except possibly a “ferruginous limestone weathering crust” (Taylor and Schwertmann 1974).

As with size and color, nodules exhibit a broad range of induration from very hard (Sokolova and Polteva 1968) to hard (Thresh 1902; Tsukunaga 1932; Winters 1938; Phillippe 1972; Schwertmann and Fanning 1976), harder (Winters 1938), medium (Schwertmann and Fanning 1976), soft (Robinson 1929; Sokolova and Polteva 1968; Gallaher et al. (1973:I), softer (Clark and Brydon 1963), very soft (King et al. 1990), soft easily pulverized (Winters 1938), soft but harden upon

dessication (Phillippe 1972), and well-cemented (Drosdoff and Nikiforoff 1940) to loose powder (Robinson 1929). Soft has been defined as having a Moh's hardness of less than 2 (Gallaher et al. 1973:I), still much harder than that of high-chroma features. Relative terms "softer" and "harder" are almost useless for comparison between studies. The only descriptions that are close to matching high-chroma features are possibly the soft easily pulverized bodies of Winters (1938) and loose black powder in cavities (Robinson 1929) although the color is not a match.

Composition

Ferruginous concretions are enriched with iron and usually manganese oxides (Thresh 1902; Drosdoff and Nikiforoff 1940; Pawluk and Dumanski 1973; Gallaher et al. 1973:II; Taylor and Schwertmann 1974; Schwertmann and Fanning 1976; King et al. 1990) although relative amounts of each element and their forms are variable. Iron mineral species include goethite (Pawluk and Dumanski 1973; Gallaher et al. 1973:II; Taylor and Schwertmann 1974; Schwertmann and Fanning 1976; King et al. 1990; Arocena et al. 1994; Sanz et al. 1996; Zhang and Karathanasis 1997) and hematite (Winters 1938; Pawluk and Dumanski 1973; Gallaher et al. 1973:II; Taylor and Schwertmann 1974; King et al. 1990; Arocena et al. 1994) in non-magnetic concretions as well as possible ferrihydrite (Taylor and Schwertmann 1974; Liu et al. 2002), and magnetite (Winters 1938; Sokolova and Polteva 1968) or maghemite (Pawluk and Dumanski 1973) in magnetic concretions. Lepidocrocite and lepidocrocite plus hematite were reported in one study (Arocena et al. 1994).

Manganese minerals include MnO₂ (Thresh 1902; Robinson 1929; Gallaher et al. 1973:II), birnessite in high-calcium manganese concretions (Taylor and Schwertmann 1974; Schwertmann and Fanning 1976), psilomelane (Gallaher et

al. 1973:I, II) in high-barium manganese concretions, and lithiophorite, vernadite, and possibly birnessite (Liu et al. 2002). Birnessite and vernadite could only be identified using differential x-ray diffraction techniques (Sanz et al. 1996).

Iron and manganese minerals are often poorly crystalline making identification difficult and in some cases inconclusive (Zhang and Karathanasis 1997; Sanz et al. 1986; Palumbo et al. 2001; Liu et al. 2002).

Calcium carbonate (Thresh 1902; Tsukunaga 1932), siderite (Taylor and Schwertmann 1974) and ferrous iron (Tsukunaga 1932) have also been identified in concretions. Sanz et al. (1996), however, did not find siderite or rhodochrosite, a result they found surprising since these two minerals are relatively common in a carbonate system with alternating redoximorphic cycles.

Superficially, concretions tend to resemble the whole soil or contain whole soil material with clays and quartz particles cemented by iron oxides (Thresh 1902; Whittig et al. 1957; Clark and Brydon 1963; Sokolova and Polteva 1968; Phillippe et al. 1972; Pawluk and Dumanski 1973; Gallaher et al. 1973:I; Taylor and Schwertmann 1974; Schwertmann and Fanning 1976).

Concentrations of minor elements vary relative to the surrounding soil, either higher or lower. Authors have reported enrichment of Na, S, Ca, Mg, Ba, Zn (Tsukunaga 1932; Wheeting 1936; Winters 1938; Gallaher et al. 1973:I; King et al. 1990), either enrichment or depletion of organic matter, Si, P, Al, K (Tsukunaga 1932; Wheeting 1936; Winters 1938; Whittig et al. 1957; Clark and Brydon 1963; Sokolova and Polteva 1968; Phillippe et al. 1972; Gallaher et al. 1973:I; Dawson et al. 1985; King et al. 1990), and depletion of Ti (King et al. 1990). Dawson et al. (1985) found enrichment in all trace elements while King et al. (1990) found enrichment in some and depletion in others.

Occurrence

Soil concretions occur in a wide variety of soils and geographic locations. A partial list from the studies reviewed here include boulder clay of Essex UK (Thresh 1902), residual limestone soils in Manchuria (Tsukunaga 1932), Podzols of the west coast of British Columbia and western Washington (Wheeting 1936), Illinois (Winters 1938), Tennessee and Georgia (Gallaher et al. 1973:I; Gallaher et al. 1973:II), Alberta, Canada (Pawluk and Dumanski 1973), Australia, Germany, The Netherlands (Taylor and Schwertmann 1974), New Zealand (Dawson et al. 1985), and Taiwan (King et al. 1990).

Depths of occurrence can begin at the surface or upper layers (Robinson 1936; Tsukunaga 1936) especially in poorly drained Podzols (Winters 1938). Starting from the shallowest depths, ranges of maximum occurrence reported are 6 to 25 cm in an A2-horizon and 15 to 75 cm in a B-horizon of an upland Podzol (Sokolova and Polteva 1968); 20 to 50 cm in a glacial Podzol (Wheeting 1936); 30 to 85 cm in a silt loam in a Podzolic Inceptisol (Whittig et al. 1957); at 7, 20, and 30 cm in a hydrosequence of wetter-to-dryer Braunerde-Pseudogley soils, although the shallowest depth may have resulted from anthropic disturbance (Schwertmann and Fanning 1976); 50 to 100 cm in a forested Inceptisol (King et al. 1990), 75 to 110 cm in a poorly drained Podzol (Winters 1938), 90 to 100 cm in Blakely loam from Georgia (Robinson 1929), and 125 to 150 cm in a well-drained Paleudalf in Kentucky (Phillippe et al. 1972).

Most often, depths are given by the horizons in which they are found. Maximum concentrations of concretions might occur at the surface, in upper layers, increase with depth then decrease (Wheeting 1936), decrease with depth (Winters 1938), in the lower layers (Robinson 1929), present in most horizons or

have no definite zone of development (Whittig 1936; Winters 1938), or even in all soils and all horizons (Phillippe et al. 1972). Concretions are found in the A-horizon (including A2-horizons) and upper B-horizons (Drosdoff and Nikiforoff 1940; Whittig et al. 1957; Sokolova and Polteva 1968; Schwertmann and Fanning 1976), are a minimum in the B-horizon (Drosdoff and Nikiforoff 1940) and increasing or highest in the C-horizon (Robinson 1929). Location in the profile varies by drainage class with a maximum of nodules in the C-horizon in a well-drained soil, nodules found throughout the A-horizon and at a maximum in the B-horizon of a moderately well drained soil, and a higher concentration of nodules in the surface of a somewhat poorly drained soil than in the well-drained or moderately well-drained soils studied (Phillippe et al. 1972; Schwertmann and Fanning 1976).

Concretions have a tendency to occur more frequently in soils with restricted drainage (Wheeting 1936) including those with underlying argillic horizons or fragipans (Whittig et al. 1957; Phillippe et al. 1972; Gallaher et al. 1973:I). They were not found in excessively drained or the most poorly drained soils (Wheeting 1936; Schwertmann and Fanning 1976) and are rare in sands (Winters 1938), although they were found in a sandy groundwater bog (Taylor and Schwertmann 1974). They are frequently found in finer-textured soils including glacial loams (Wheeting 1936; Clark and Brydon 1963; Sokolova and Polteva 1968; Cescas et al. 1970; Phillippe et al. 1972). Winters (1938) reported concretions in well-drained Podzols.

Manganese concretions are typically found where the pH is above 6.0 to 6.5 even as high as 8 (Robinson 1929) including limestone soils or horizons above

a layer of limestone or carbonates. They also are found under acid conditions as in many Podzols (Wheeting 1936; Sokolova and Polteva 1968).

Interpretation and Formation

Concentrations form by accumulation of material as a result of pedogenic processes that include removal, translocation, and deposition (Schoeneberger et al. 2002:2-18) or more generally as translocations and transformations (Zhang and Karathanasis 1997). Their formation is influenced by oxygen and carbon dioxide concentrations, pH, and organics (Tsukunaga 1932). Although discussed separately, formational processes are often linked inextricably and rarely, if ever, occur individually or in isolation within a soil profile.

At least as early as 1932, alternating cycles of wetting and drying were believed to be responsible for the accretionary growth of concretions with a concentric structure (Tsukunaga 1932). Iron carbonates and hydroxides in the soil weather to oxidized forms and reduced forms of iron minerals respectively under condition of alternating oxidation and reduction (Tsukunaga 1932). Other authors also have associated the formation of concretions, the appearance of variable Fe:Mn ratios, and zonal compositions within concretions with alternating cycles of oxidation and reduction (Winters 1938; Whittig et al. 1957; Cescas and Tyner 1967; White and Dixon 1996; Zhang and Karathanasis 1997; Liu et al. 2002; Gasparatos et al. 2005). Post-glacial climate fluctuations may have influenced local redox potentials resulting in zoning or nonzoning of concretions, but their ages often are unknowable, and any claims about previous redox potentials can only be speculation (Cescas et al. 1970). The seasonal distribution of rainfall appears to be as important as the total rainfall, and there must be a

pronounced moisture deficiency during the growing season for concretions to form (Schwertmann and Fanning 1976).

Removal

Iron and manganese are brought into solution through the processes of reduction, protonation, and chelation.

Reduction in wet soils takes place as a result of microbial activity. As the oxygen in pore water is depleted, microorganisms make use of oxidized forms of nitrogen, manganese, iron, and sulfur as electron acceptors to complete their metabolic cycle. Oxidized iron and manganese minerals containing Fe^{3+} , Mn^{3+} , or Mn^{4+} are reduced to Fe^{2+} or Mn^{2+} , which are soluble forms that can become mobile in the soil solution. Because reduction is microbially mediated, sufficient wetness, low oxygen, suitable energy sources (principally carbon), and temperatures above biological zero, are necessary for microbial activity and the reduction process to occur. Soils may be saturated without reduction occurring if any of the previous requirements are not met. Oxygenated rainwater or a high-oxygen groundwater source will prevent reduction despite saturation.

Iron and manganese solubility increases under acidic and reducing conditions that are found in waterlogged soils (Robinson 1930). Reduction and solubilization also take place during periods of unusual wetness or high rainfall (Cescas and Tyner 1967). Solubility also will increase with increasing time of submergence as long as there is sufficient organic matter present in the soil to provide an energy source for microbial reduction. Anaerobic bacteria develop rapidly under suitable conditions (Robinson 1930). Robinson (1930) observed an eight-fold increase in iron and a four-fold increase in manganese in soil water at depths of 40 to 48 inches. The effect was more pronounced in surface soils.

possibly because subsoils contain less organic matter, the particular form of manganese present is less soluble than at the surface, or simply because subsoils lack manganese.

In addition, the solubility of calcium, magnesium, potassium, and sodium also increases considerably under submerged conditions while silica solubility increases only slightly (Robinson 1930). As a result, bases may be largely removed from submerged soils. Aluminum solubility does not appear to increase. Sulfur is converted to sulfide under reducing conditions.

Reduction of iron and manganese is accompanied by the simultaneous production of carbon dioxide resulting from the oxidation of organic matter by anaerobic bacteria under submerged or poorly drained conditions. Carbon dioxide, which was found to be present in considerable quantities in all samples tested, maintains manganese, iron, calcium, and magnesium in solution as bicarbonates (Robinson 1930).

Levels of iron that are toxic to land plants have appeared under laboratory conditions in about eight days but under field conditions the time required is likely to be shorter (Robinson 1930). Toxic conditions for manganese take longer to develop. Toxic gases such as hydrogen sulfide produced in submerged soils are also present under certain conditions. Conditions that are toxic to microbes may also exist, especially in soils higher in organic matter such as peats (Jeffrey 1924). This toxicity may not be fatal but results in the bacteria assuming a dormant state, reappearing if and when conditions become more favorable.

Protonation, the binding of protons with surface metal oxides, is generally associated with low soil pH. In soils with higher pH, such as those developed in Des Moines loess till, soil acids produced through decomposition of organic

matter or the acidic excretions of soil organisms can act at a smaller scale to remove iron and manganese from silicate rocks (Thresh 1902; Robinson 1929). The solubility of iron and manganese was found to be greatly increased with increased hydrogen ion concentrations (Robinson 1930). In the early stages of soil formation, mineral weathering is dominated by the dissolution of iron- and manganese-bearing minerals like olivine, releasing relatively large amounts of Fe^{2+} that is quickly oxidized to Fe^{3+} leading to the formation of hematite or goethite (Arocena et al. 1994). Subsequent weathering results in increasing amounts of Al^{3+} and organic acids in the soil solution, making its composition more conducive for the formation of higher Al-substituted goethite.

The action of organic acids is enhanced by chelation. Many organic acids such as oxalic acid are bidentate or polydentate ligands capable of binding metal cations at multiple sites on the chelating molecule, forming a metal-organic complex. Chelation is capable of bringing oxidized forms of iron and manganese into solution thereby potentially mobilizing them.

Concretions might be expected to be larger and more abundant in upper horizons since these horizons have experienced the greatest weathering, but that is not always the case (Winters 1938). This expectation is based on the observation, discussed previously, that concretions are more common in soil horizons where alternating periods of oxidation and reduction are most frequent, typically at the surface of poorly drained soils. Since weathering is most active at the surface, however, removal of weathering products could prevent formation of concretions or result in the dissolution of any concretions that begin to form if the soil solution is able to move freely downward through the soil profile. Some concretions have been shown to result from the progressive weathering of small

soil peds or by the weathering of basalt fragments, which could not be distinguished from other aggregates (Clark and Brydon 1963).

Translocation

Once iron and manganese have been brought into solution, they are free to move within the soil profile. Translocation of soil material takes place in solution or suspension, soil material moving with water through soil pores by gravity, capillary action, or diffusion along concentration gradients (Brady and Weil 1999; Schaetzl and Anderson 2005).

Dissolved manganese can be transported considerable distances as manganous bicarbonate (Robinson 1929). Iron is transported with bicarbonate as well, but will come out of solution earlier than manganese as the redox potential in the soil increases, so tends not to move as great a distance (Schwertmann and Fanning 1976) and because manganese becomes soluble under milder reducing conditions than iron (Gasparantos et al. 2005), it can move independently of iron (Cescas and Tyner 1967). Dissolved iron and manganese follow the movement of soil moisture toward areas of smaller pore size as the soil dries (Whittig et al. 1957).

Slow removal of end products plays a major role in concretion formation (Winters 1938). Restricted subsurface drainage retards removal of weathering products and appears to be necessary for nodule formation (Clark and Brydon 1963). Restricted subsurface drainage maintains saturation, reducing the amount of moisture percolating through the soil during wet seasons and enhances drying in the summer (Clark and Brydon 1963; Gasparantos et al. 2005).

Fragipans restrict downward water movement, resulting in alternating wet and dry, oxidizing and reducing conditions. Water tables may fluctuate from

the upper boundary of the pan almost to the surface during wet seasons. (Phillippe et al. 1972). Lindbo et al. (2000) found that nodules had formed in remnants of a brittle fragipan matrix.

Under sufficiently strong conditions of removal and transport, concretions are not present (Tsukunaga 1932). Under these conditions, iron and manganese can be completely removed from the soil profile (Gaudette and Millette 1975). The high permeability of sandy soils removes secondary weathering products (Winters 1938) preventing formation of nodules or concretions. Few concretions are found in soils having permeable subsoils (Clark and Brydon 1963). Loss of materials is most significant in very wet coarse-textured ground water soils. (Schwertmann and Fanning 1976). Formation of concretions is not typical for coarse-textured podzolic soils (Sokolova and Polteva 1968).

Schwertmann and Fanning (1976) reasoned that because wetting and drying appear essential for concretion formation, maximum formation of concretions would not be expected to occur in the wettest nor in the driest zone but somewhere between the two. Some extremely wet Psuedogleys (Stagnogleys) were found to have no concretions at all, while maximum formation was in soils with medium to low air volume and conductivity but with a rapid change in aeration of large magnitude as described by Blume (1968). They noted that periodic oxidation and drying seem essential to this process whereas more permanent wetness leads to mottling or even complete loss of iron and manganese. This could explain why the maximum concentration of concretions is always found above the depth of maximum mottle development.

Free drainage of water is primarily a function of pore size (Cescas et al. 1970). A heterogeous matrix texture and porosity in the zone immediately above

a water table could result in non-uniform redox (Eh) gradients due to their influence on drainage, especially drainage of the smallest pores. Variations of porosity either facilitate or impede diffusion of gaseous as well as dissolved oxygen and carbon dioxide, the latter being important in controlling the pH under which either sequential or simultaneous Fe-Mn precipitation occurs. Manganese and iron diffuse towards the nodule along a redox gradient, with iron diffusing only during periods in which the solution is reduced with respect to iron (White and Dixon 1996; Lindbo et al. 2000). Thus, variations in redox gradients are responsible for the location and the relative Fe-Mn composition of concentrations that form.

During wet periods the soil must be reduced for mobilization of iron and manganese and growth of nodules. Fe-Mn nodules resist reduction because of the high concentration of reducible material (iron and manganese oxides) in a compact zone with low porosity (White and Dixon 1996). During the time lag between the reduction of the soil matrix and the reduction of the nodules, the nodules are centers of high redox potential in a reduced matrix. The difference in redox potential between nodules and matrix induces a concentration gradient and reduced iron and manganese diffuse towards the nodule where they are oxidized by the oxides already present. After some time, the nodule surface will become reduced and manganese can diffuse towards the surface of the nodule forming an outer band enriched in manganese. Banded and unbanded nodules likely have a different origin.

Horizontal movement of water through a soil profile has been found to be an important aspect of translocation. Lateral movement of dissolved soil material, resulting from prolonged soil wetness, resulted in the formation of

nodules in hollows where an excess of water accumulates in the spring and a deficit occurs in the summer (Dawson et al. 1985). The factors affecting horizontal mobilization may exert a greater influence on profile development than the factors of leaching (Drosdoff and Nikiforoff 1940). Horizontal movement tends to retain mobile compounds within the horizons. If this is true, then eluviation and illuviation may not be the main processes leading to the development of the general soil profile (Drosdoff and Nikiforoff 1940).

King et al. (1990) found that under balanced conditions of surface erosion, iron mobilization, and precipitation, the iron-accumulation zone in the profile remained between 0.3 and 2 meters, with iron being recycled in this zone resulting in a cycle of nodule formation, exposure from surface erosion, subsequent weathering, and reformation of nodules. In a more stable or more erosive site, iron would quit cycling and nodules would stop forming.

Podzolization combines chelation with translocation to move iron, manganese, and aluminum downward through the soil profiles of forested soils to accumulate in the B-horizons. In forested soils, podzolization likely accounts for the dissolution and translocation of iron and aluminum minerals and is the process most responsible for the formation of Spodosols or Podzols (Wheeting 1936). Bog iron soils (gley soils) have been found to obtain iron from surrounding podzolized upland soils (Taylor and Schwertmann 1974). A relatively high content of dithionite soluble iron in nodules has been interpreted as a recrystallization of iron that had been translocated to the iron nodules partly due to podzolization during a previous pedological episode (Pai et al. 2003).

Reprecipitation

Deposition, reprecipitation, and concentration of iron and manganese occurs through saturation, drying, oxidation, and freezing (Tsukunaga 1932; Schaetzl and Anderson 2005). Reprecipitation, the final step in the formation of concentrations, is of particular interest because the resulting features often reflect the environment in which the reprecipitation occurred (Kubiëna 1938).

Reoxidation and precipitation occur if, when the soil begins to dry, oxygen reenters pores and channels. Oxygen combines with reduced iron in solution to form iron oxides and (hydr)oxides. Reoxidation and precipitation also occur where reduced iron moving through the soil matrix encounters areas of high oxygen concentration such as pores or channels, places where oxygen has been trapped in the soil after saturation, or along root channels where oxygen is released by the roots or aerenchyma tissue of certain hydrophytic plants (Vepraskas 2001). Reoxidation may take place within the matrix in micropores to form soft masses or nodules, along root channels or ped faces to form pore linings, which may be hard or cemented, or in larger voids to form infillings or coatings. Iron oxidizes more readily in air than does manganese. Manganese at lower pH is difficult to oxidize in air and is more easily oxidized through the action of microorganisms (Tebo et al. 1997).

Although manganous solutions are more stable than ferrous solutions, they can be readily oxidized under certain conditions to precipitate the insoluble oxide, MnO_2 (Robinson 1929). Conditions that bring about the precipitation of manganese appear to be sharply defined since very pure deposits are found in soils containing only traces of manganese. Ferrous bicarbonate in solution is rapidly oxidized to ferric hydroxide upon exposure to air (Robinson 1930). Iron

precipitates before manganese (Cescas and Tyner 1967), manganese requiring long contact with air and even then is only partially removed (Robinson 1930).

Iron, and especially manganese, can be oxidized and precipitated by the action of certain bacteria (White and Dixon 1996; Sanz et al. 1996). Manganese is more easily oxidized by organisms than directly by oxygen (Tebo et al. 1996). Robinson (1930) attributed high concentrations of iron and manganese carbonates in bog soils to the possible action of microorganisms on organic matter. Tsukunaga (1932) and Nikiforoff (1937) concluded that the formation of concretions was almost certainly the result of certain microorganisms capable of segregating and precipitating iron and manganese. Waksman (1932) found various microorganisms capable of extracting iron from solution and depositing it on their surfaces as ferric hydroxide. He also cites Beijerinck who described several types of fungi and bacteria that oxidize manganese salts of organic acids to manganese carbonates. Thiel (1925) found that fungi able to precipitate manganese from organic and inorganic salts of manganese are present in peat bogs, loamy and manganiferous soils, and iron spring "slimes." In addition, sulfate-reducing organisms precipitate brown granules of manganese around the colonies. Further, some types of iron bacteria precipitate manganese as rapidly as iron. Palumbo et al. (2001) found an unusual tubular morphology composed of manganese oxides resembling those reported by Zhang and Karathanasis (1997) that they attributed to microbial action. They also reported finding fungal hyphae associated with the concretions, as did Arocena and Pawluk (1991).

Specialized microorganisms in Podzols decompose organo-metallic compounds releasing bound Fe, Mn, Al (Sokolova and Polteva 1968). Redox conditions and the presence of ferrous and manganous compounds necessary for

microorganisms exist in upper soil layers. Aristovskaya (1965) found concretions to consist of microcolonies of Fe-Mn bacteria with abundant precipitation of Fe-Mn hydroxides. Redox conditions and the presence of ferrous and manganous compounds, conditions favorable for the formation of high-chroma features exist in a variety of soils, not just Podzols.

High pH possibly plays a role in precipitation (Robinson 1929; Palumbo et al. 2001). Manganese concretions are typically found where the pH is above 6.0 to 6.5 even as high as 8 (Robinson 1929). Manganese dioxide appears to be dissolved in the soil solution when the pH is below 5.0 to 5.2. Robinson (1929) found that manganese is highest in the surface soil, reaches a minimum in the B-horizon, and increases in the C-horizon. In many soils, manganese features of manganese dioxide occur above a layer of carbonates or limestone. Precipitation of iron may also be caused by the presence of ammonia (Robinson 1930) as a result of organic matter decomposition under anaerobic conditions (Pettijohn 1957). Ammonia has been found to develop in waterlogged soils as a result of the decomposition of nitrogen compounds (Subramanian 1927a,b), possibly raising the pH to the extent that iron and manganese could precipitate out of solution.

In the presence of an alkali such as CaCO_3 , oxides of iron and manganese precipitate out of solution and continue to oxidize by exposure to soil air (Thresh 1902). Slight acidity, even as excess carbonic acid, prevents oxidation leading Thresh (1902) to conclude that nodules can form only in an alkali or "chalky" soil. This appears to be an overgeneralization and applies mostly to manganese.

Calcium carbonate appears to play a significant role in the formation of soil features containing manganese (Robinson 1929). Manganese oxides and calcium carbonate apparently replaced each other in manganese nodules (Thresh

1902; Robinson 1929). Manganese has been found to replace calcium in calcium carbonate, in one instance forming pseudomorphs of pyrolusite after calcite (Robinson 1929). Robinson (1929) found that solutions of manganous bicarbonate percolated through columns of calcium carbonate will precipitate dark particles within the mass of calcium carbonate. These dark particles react vigorously with hydrogen peroxide so were presumed to be manganese dioxide. Colloidal manganese dioxide will adsorb manganous salts from solution. Once a particle of manganese dioxide is formed by replacement of calcium or through microbial precipitation, the particle can continue to grow by adsorbing manganous salts from solution and oxidizing them to manganese dioxide, a process used to remove manganese from water supplies. The formation of manganese concretions may take place through a similar process (Robinson 1929). As will be discussed later, the oxidation of Mn^{2+} to Mn^{4+} is autocatalytic. Solid manganese oxide surfaces catalyze the oxidation of manganese in solution.

In surface soils, salts in the soil solution can be concentrated by oxidation and drying. Iron and manganese along with other colloidal materials move down the profile where they coagulate and precipitate as "sols" when soil moisture is depleted (Tsukunaga 1932). Cescas et al. (1970) describe "Billowy elongated plasmic masses" as probably either hydrated iron or iron-manganese oxides. Dessication of former gelatinous precipitates may account for the numerous submicron cracks and fissures apparent on the top and sides of the plasmic masses. The shape of these masses may have originated through filling or encapsulation of former pore channels.

Drying prevents downward movement of the soil solution (Wheeting 1936) and concentrates salts in smaller pores, leading to the precipitation of iron

and manganese and the development of concretions at the “points of final desiccation” (Smith 1936; Drosdoff and Nikiforoff 1940). The precipitate serves as a cementing agent around localized nuclei of coarse particles or other suitable material (Whittig et al. 1957; White and Dixon 1996; Sanz et al. 1996; Liu et al. 2002).

Precipitation of iron and manganese resembles crystallization, beginning at a particular point and incorporating neighboring sand particles as the nodule grows (Thresh 1902; White and Dixon 1996; Sanz et al. 1996; Palumbo et al. 2001). Inclusions of sand grains and other soil material strongly suggests that cementing material is deposited in pore spaces within the soil (Winters 1938). Cavity infillings of iron and manganese eventually produce the dense concretionary matrix structure. These infillings probably result from the diffusion of dissolved plasmic iron and manganese and subsequent precipitation within the pore volume of the concretion matrix (Zhang and Karanthanasis 1997). A sparseness of pores and their small cross-sectional sizes within the concretions emphasize the relative completeness with which the pores of the soil matrix may be infilled by plasmic iron and manganese oxides during the course of concretion formation (Sokolova and Polteva 1968). The precipitation of hydroxides presumably within the original matrices led to drastic reductions and loss of total porosity for both zoned and unzoned concretions. It appears that much of the original matrix porosity was infilled during concretion formation. High iron and manganese contents and more-or-less uniform cross sectional distribution of silica suggest that infilling is associated with processes of diffusion to and precipitation of iron and manganese within the pore volume of a concretion (Cescas et al. 1970). The extent of infilling, judged from the frequency

and distribution of pore sizes appeared to be similar for zoned and nonzoned concretions. Weathered coarse fragments of saprolite may act as a nucleus for iron surface coatings that accumulate on the fragments and move to the interior of the ped to form nodules (Pai et al. 2003).

Once cemented, an iron-manganese grain may be unavailable to microorganisms and grows by extraction of iron and manganese from the surrounding soil (Drosdoff and Nikiforoff 1940). The concretion grows until it is limited by pore space or until an accumulation of toxins terminates development of the colony. Concentric rings could be explained as seasonal growth resulting from alternating active and dormant stages of the colonies. A large number of concretions do not exhibit layering, however but these colonies may not experience periodic cycles of growth and dormancy but only a single, possibly continuous stage of growth. Whether of microbial origin or not, a single shell may result from the sole occurrence of environmental circumstances favorable for their formation but cannot be known (Cescas et al. 1970).

Concretions with a shelly concentric structure grow by accretion or “centrifugal enlargement” of colloidal clay and humus during alternating cycles of wetting and drying. Spherical or elliptical forms seem to be formed by concentration of salts (Tsukunaga 1932). Pellets start as small aggregates and grow as weathering proceeds (Wheeting 1936). In some cases, larger composite concretions were found consisting of aggregates of smaller concretions. (Gallaher et al. 1973:I). X-ray microdiffraction suggested that large nodules (100-300 μ m) are actually a conglomeration of very fine particles of Fe-oxide minerals in random orientation. Also, the formation of large goethite nodules can be the result of dissolution of earlier formed small goethite nodules and their

subsequent recrystallization, although cumulative crystallization may also be the cause (Arocena et al. 1994).

In Podzols, the formation of larger concretions proceeds as precipitation of iron-manganese compounds on the surface of these grains (Sokolova and Polteva 1968). Iron segregation dominated in the podzolic horizon while manganese compounds formed concretions in lower horizons since manganese compounds are more soluble and mobile than iron, being precipitated at higher pH and Eh. A minimum Eh (100mv or even negative) was observed in spring and autumn when soils were waterlogged with snowmelt and rain water. Lower horizons, including the B, remained oxidizing (400mv and higher). Also, pH increases with depth. As a result, iron compounds precipitate mainly in upper podzolic horizon and manganese compounds in the lower layers.

Pawluk and Dumanski (1973) found evidence of in-situ formation in a poorly drained soil by comparing fabrics. The internal fabric of the concretion closely resembled the fabric of the s-matrix of the surrounding soil. The possibility of an allogenic origin was discounted as there was no evidence of disruption of the internal fabric. Furthermore, concentrations of concretions were localized in zones of strongest mottling, were more common and of different mineralogical composition in the A as compared to the B horizon, and were absent below the solum. The appearance in thin-section of infused iron oxide within the soil s-matrix further suggested an accretionary origin even though concentric laminated structure was absent. On the other hand, Clark and Brydon (1963) concluded that formation of nodules or "shot" was from progressive weathering of small soil peds and not by accretion.

Nodule size may provide clues to origin. Arocena et al. (1994) used mineralogy and size to ascertain that the nodules in a C-horizon are probably inherited. The wide range of nodule sizes in the B-horizon suggests differences in formation: small nodules probably represent the unaltered allogenic iron nodules similar to those present in the C-horizon today. The larger nodules may have started forming early in the genesis of the soils and continue up to the present day.

The occurrence of several iron oxide associations within the sola points to changing conditions that existed during their formation. The association of goethite with hematite is typical for well-drained conditions while the presence of a goethite and lepidocrocite association is common in reductomorphic environments. The dominance of goethite over lepidocrocite suggests the prevalence of an oxidizing environment, which would be expected in a coarse-textured, well-drained soil. Reductomorphic conditions necessary for the formation of lepidocrocite is likely to occur only under certain microenvironmental conditions such as some isolated periods of flooding during soil formation.

Phosphorus apparently has little influence on the precipitation of iron. Phillippe et al. (1972) studied a residual soil developed from highly phosphatic limestone. A lower phosphorus content in concretions relative to the soil matrix was seen to minimize the role of phosphorus in precipitating iron and manganese.

An important consideration is the manner in which the segregation or concentration is placed within the surrounding material (Pettijohn 1975:463). Emplacement may happen in a variety of ways: by replacing or incorporating

existing host material, as with nodules; by deposition within or around existing voids, as in coatings, geodes, and infillings; by deposition within pores around nucleating centers in the host material as in concretions; or by simply pushing aside the surrounding matrix material as they grow, as in crystals and crystal intergrowths. The manner and location of deposition, therefore, determines at least in part, which type of feature will be present. Conversely, the type and location of the concentration within the matrix provides clues to the manner and location of its formation.

Relative time of emplacement is also an important consideration (Pettijohn 1975:463). The feature may have formed prior to, simultaneously with, or after development of the surrounding soil matrix. This can be a difficult determination to make (Stoops 2003).

Geologists do not clearly understand the factors of formation responsible for many of the segregational bodies found in rocks. Questions concerning size, shape, number, spacing, and orientation of concretions remain unanswered (Pettijohn 1975:464). Some segregations, such as those in carbonate rocks tend to replace their matrix while those in shale do not. Some concretions are microcrystalline while others are large crystals, crystal clusters, or radial aggregates. While Pettijohn's statement above was directed at geological features, it is as true of features that have formed in soils and regolith as it is of those that formed in rock and is analogous to similar statements by Brewer (1972) reported earlier pertaining to soil features.

Summary

The earliest successful descriptive classification of concentrations was that of Bennett and Allison (1928), who developed a classification of soil concretions

as part of their larger study of Cuban soils. The soil features they classified were iron-manganese concretions called *perdigón* that occur in certain soils of Cuba. Their summary description of the physical properties, composition, and occurrence, of this single type of nodule within a single geographic area, encompasses a range of characteristics that includes nearly all concretions or nodules that have been reported in the literature:

*“These vary in size from microscopic to nodules larger than a man’s fist and in amount from a few here and there through the soil to approximately 100 per cent of the mass of material. These are locally known as *perdigón*. They are usually of roundish shape, but often are of irregular form. The principal colors are black, brown, reddish-brown and yellowish. Most of these concretions occur at depths ranging from about 8 inches to 3 feet and are confined to the older soils, seldom or never occurring in very recent alluvial deposits. In the lower stream bottoms where there is freshly deposited soil, *perdigón* are never present except as water-transported material, but on the older, higher outer alluvial strips they are frequently present as a locally formed part of the mother soil.*

*“These *perdigón* are usually hard; some of those apparently more incipient character, however, are crumbly to only semi-hard. In composition, they are highly ferruginous, as a rule. Some contain considerable manganese. Chemical analysis show them as having a quite marked chemical difference from the soil matrix, such as the usual presence of more iron and phosphorus and of less silica in the concretions than in the unconsolidated mother material.*

*“In some types of *perdigón* a concentric structure is distinctly observable; in others, it is not. In the latter instances, the *perdigón* may constitute aggregates rather than concretions” (Bennett and Allison 1928:4-5).*

Soil nodules and concretions described in the literature occur in a wide variety of sizes, shapes, colors, induration, soils, horizons, and composition. Because of this range of properties, correlations of properties with hypothesized formational processes are tentative at best. Properties of high-chroma features represent a unique combinatorial subset of all property classes reported in the literature, again complicating attempts to correlate morphology with genesis.

High-chroma features appear to be a different entity from nodules and concretions reported in the literature, based on their consistently unique color, color pattern, lack of induration, and sharp boundary. They contain very little if any of the soil matrix. Although all of these properties have been reported to occur separately in various kinds of nodules, there is no evidence that they all appear simultaneously in a single type of concentration or class of concentrations reported in the literature.

Formation hypotheses almost universally emphasize the role of alternating cycles of wetting and drying, oxidation and reduction. Sequential processes of formation, removal, and translocation, have been used with reasonable success to explain the formation of iron and manganese concentrations generally. However, the singular combination of properties possessed by high-chroma features as described in this research means that they remain a unique entity for study.

Although concretions may seem relatively more common in Podzols, that may simply mean that more Podzols have been studied, more papers published, or more were selected unintentionally for review. One does well to remember, however, that immediately pre- and post-glaciation, the soils of southern Minnesota were under the influence of spruce and perhaps pine as well as hardwood forests in relatively fine-textured parent materials.

METHODS

Methods used for this project include field observations, optical microscopy, and laboratory analysis. Several analytical methods were considered but not used. Some methods were more successful than others. Only methods that produced a useable result or that were of particular interest in this

investigation are included in the methods section. All methods that were considered, whether used or not, are discussed in appendix C.

Initial investigations of high-chroma features revealed a basic structural framework (Figure 7). This framework provides the basis for subsequent descriptions and a simple classification scheme for high-chroma and similar features.

Sampling methods

The small size of high-chroma features along with their unpredictable occurrence complicated efforts to find suitable sampling locations. Attempts to locate productive sites by coring either with a probe or auger were unsuccessful. In dry upland soils, often much of the sample material was lost upon raising the probe or auger from the hole. Regardless of soil wetness or site location, collecting samples with a probe or auger could not produce a sufficient quantity of undisturbed features for analysis.

In a landscape of low relief, as is typical of much of southern Minnesota, natural exposures of soil profiles are uncommon. Some potential sites were found by word-of-mouth reports of new construction from local residents but most sites were found by driving county roads and exploring accessible construction sites looking for exposures that contained high-chroma features. Sites containing sufficient sample material were eventually located where building or road excavations produced loose soil material. Bulk material that contained a sufficient quantity of features for study was gathered from five sites.

Although depth information is lost using bulk collection, that loss was a trade-off that had to be made in order to obtain a sufficient quantity of features suitable for study. Since depth effects can be confounded with parent material,

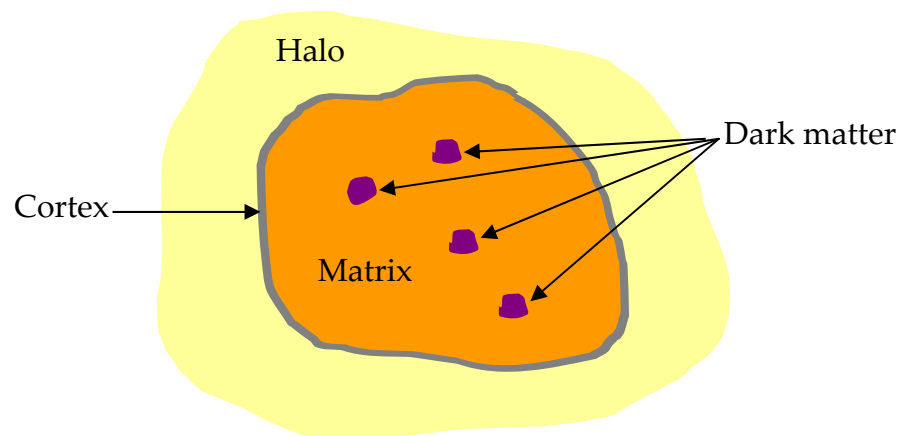


Figure 7. General structure of a high-chroma feature. Many features lack a visible cortex and dark matter. Dark matter may be purple or pink, sometimes iridescent, or black.

distance to a water table, and the effects of weathering, loss of depth information was not considered critical, although lack of depth information did have the potential to limit the ability to make later interpretations. Of primary importance is the feature itself and its formational environment, which could be inferred from examination of the ped that contains the feature.

Soil maps and information from the Soil Survey and Official Series Descriptions of the area were used to infer the soil profile expected to have been present at the sampling sites before disturbance. Ped morphology was compared to the Official Series Descriptions of the mapped soils at each location to match horizons, drainage class, and landscape position, information that was no longer available from the more disturbed sites. As in other historical sciences such as archaeology or paleontology, the loss of context should not preclude the study of an interesting object found, for example, at the base of a hill or washed downstream, having moved from its original location.

Sample sites

Locations of the sample sites are shown on the map in Figure 2. Details of the soils mapped at these sites by the Soil Survey are given in Tables 6 and 7. Sites are listed from southwest to southeast.

Lincoln County

The Lincoln County site is in Shaokotan Township, Section 26, less than one-half mile south of Lake Shaokotan. The site was found during reconstruction of County State Aid Highway 2 at N44°23.818' W96°21.706'. The site is a linear to convex shoulder or backslope on the Bemis ground moraine (Hobbs and Goebel 1982). Parent material is Des Moines lobe till (Hokanson et al. 1970). The Quaternary geology of the site is Des Moines lobe deposits of the Late Wisconsin,

Table 6. Drainage class and taxonomic classification for the soil series mapped in the study area. WD=well drained; MWD=moderately well drained; SPD=somewhat poorly drained; PD=poorly drained. (m) denotes morainic phase. Data from Official Series Descriptions.

County/Series	Drainage	Taxonomic Class
Kandiyohi		
Sunburg†	WD	Coarse-loamy, mixed, superactive, mesic Typic Eutrudepts
Wadenill†	WD	Coarse-loamy, mixed, superactive, mesic Typic Hapludolls
Lincoln		
Buse†	WD	Fine-loamy, mixed, superactive, frigid Typic Calcicudolls
Wilno†	WD	Fine-loamy, mixed, superactive, frigid Pachic Hapludolls
Hokans	WD	Fine-loamy, mixed, superactive, frigid Calcic Hapludolls
Svea	WD/MWD	Fine-loamy, mixed, superactive, frigid Pachic Hapludolls
Wright		
Hamel†	PD/SPD	Fine-loamy, mixed, superactive, mesic Typic Argiaquolls
Reedslake	WD	Fine-loamy, mixed, superactive, mesic Typic Argiudolls
Le Sueur	SPD	Fine-loamy, mixed, superactive, mesic Aquic Argiudolls
Cokato	WD	Fine-loamy, mixed, superactive, mesic Typic Argiudolls
Storden	WD	Fine-loamy, mixed, superactive, mesic Typic Eutrudepts
Hennepin		
Angus (m)†	WD	Fine-loamy, mixed, superactive, mesic Mollic Hapludalfs
Lester (m)	WD	Fine-loamy, mixed, superactive, mesic Mollic Hapludalfs
Le Sueur	SPD	Fine-loamy, mixed, superactive, mesic Aquic Argiudolls
Carver		
Lester†	WD	Fine-loamy, mixed, superactive, mesic Mollic Hapludalfs
Kilkenny†	MWD	Fine, smectitic, mesic Oxyaquic Vertic Hapludalfs

† indicates the soil series or complex mapped at the sampling site.

Table 7. Occurrence of concentrations and depletions for soil series mapped in the study area. Only horizons with concentrations or depletions are listed. Wilno had none but is included for completeness. (m) denotes morainic phase. Depths are in centimeters. Contrast applies only to concentrations. Columns labeled “A, S, C” refers to the abundance, size, and contrast respectively of features. Abundance: f=few, c=common, m=many; S: f=fine, m=medium, c=coarse; Contrast: f=faint, c=distinct, p=prominent (see Schoeneberger et al. 2002). Data from Official Series Descriptions.

County/Series	Horizon	Depth	Status	A, S, C	Concentrations	Depletions
Kandiyohi						
Sunburg	C	51	relic†	cmp	7.5YR 5/6	2.5Y 6/2
Wadenill	C	79	relic	cmd	10YR 5/6	10YR 5/2
Lincoln						
Buse	Bk2	56	relic	ffd	7.5YR 5/6	2.5Y 6/2
	C	102	relic	f-p	2.5Y 5/6	2.5Y 5/2
Wilno	—	—	—	—	—	—
Hokans	C	102		fmd	2.5Y 5/6	2.5Y 6/2
Svea	C	91		ffd	5YR 4/6	5Y 5/1
Wright						
Hamel	AB	41		mfp	7.5YR 4/4	—
	Btg1	61		mfp	7.5YR 4/4	—
	Btg2	102		mcp	7.5YR 4/4	—
	Cg1	117		mmp	10YR 5/6	—
	Cg2	140		mmp	10YR 5/6	—
Reedslake	Bk2	81		ffp	7.5YR 5/8	2.5Y 6/2
	C	122		ffp	7.5 YR 5/8	2.5Y 6/2
Le Sueur	Bt1	43		—	—	2.5Y 4/2
	Bt2	61		ffp	10YR 4/6	2.5Y 5/2
	C	117		m&cmp	10YR 4/4 & 4/6	—
Cokato	Bt3	89	relic	—	—	2.5Y 6/2
	Bk	104	relic	cmp	10YR 5/8	—
Storden	Bk1	18	relic	ffp	10YR 5/8	—
	Bk2	86	relic	ffd	10YR 5/8	10YR 6/2
	C	140	relic	cfp	10YR 5/8	10YR 6/1
Hennepin						
Angus (m)	C	102		cmd	10YR 5/6	2.5Y 5/2
Lester (m)	Bk2	127		cfp	10YR 5/6	—
	C	152		cmd	10YR 5/6	10YR 6/2
Le Sueur					(see above)	(see above)
Carver						
Lester					(see above)	(see above)
Kilkenny	Bt3	97		ffd	7.5YR 4/4	—
	2BC	135		—	—	7.5YR 4/4
	2C	165		cmp	10YR 4/6	2.5Y 5/1
				—	7.5YR 4/4 Fe-Mn	

† From the Official Series Description for the Sunburg series dated 4/2007. Remarks: "The redoximorphic features in this pedon could be relic. These redoximorphic features are typical on summits in the coarse-loamy till in central Minnesota."

supraglacial and hummocky till deposited on melting ice that was subject to repeated mass movements during deposition; yellow-brown; loam to clay loam; contains pebbles of carbonate, felsic and mafic igneous rocks, shale, chert, and some lignite (Patterson 1995). Soils at this site are mapped as Buse-Wilno complex (J100D2) with adjacent areas of Hokans-Svea (J101B).

Kandiyohi County

The Kandiyohi County site is in Dovre Township, section 26, approximately 4 miles north of Willmar at N45°10.70' W95°2.37'. The site was a building excavation in a housing development called Chadwick Estates. This site is on a convex summit on or near the stagnation moraine of the Alexandria Moraine complex associated with the Wadena lobe. It lies just north of the Olivia Till Plain, which is composed of New Ulm till deposited by the Des Moines lobe (Giencke 1987). It is possible that a thin layer of Des Moines lobe till has overridden or been incorporated with the Wadena Till at this site (Hobbs and Goebel 1982). Soils here are mapped as Sunburg-Wadenill complex (805C, 805D). Both soils are described as having formed in Wadena lobe till of Late Wisconsin age. Adjacent areas of lower landscape position and depressions are mapped as Delft loam (336).

Wright County

The Wright County site is in Cokato Township, Section 35, in a housing development one-half mile east of Cokato at N45°4.466' W94°10.377'. The site is on a linear to convex backslope on the Altamont stagnation moraine (Hobbs and Goebel 1982). Parent material is till from the most recent advance of the Des Moines lobe (Edwards 1968a:112). More details are given under the Hennepin County site description. The Quaternary geology of the site is Late Wisconsin

Des Moines lobe till and supraglacial sediment forming hummocky and rolling till plains with variable relief, loam to clay loam, 10YR to 2.5Y, calcareous, and characterized by the presence of shale (Lehr 1990). Soils at this site are mapped as Hamel loam (414) with Reedslake-LeSueur complex (1207B) to the north and Cokato-Storden (1213C) to the south and east.

Hennepin County

The Hennepin County site is in T117N R24W (Township unknown), Section 31, at the extreme southwest corner of the county in a housing development called Hunter's Crest on the west side of the city of St. Bonifacius at N44°53.89' W93°45.81'. The site is severely disturbed but a linear backslope landscape position was inferred from the surrounding landscape. It lies on the Altamont stagnation moraine near its westernmost boundary with the Altamont ground moraine (Hobbs and Goebel 1982). Parent material is Des Moines lobe till similar in composition and origin to the Wright County site: loam to clay loam texture, grayish brown to light olive brown where well-drained and olive gray where poorly drained, with abundant limestone, shale, granite and sandstone. It is calcareous with 15 to 25% carbonates (Lueth 1974). Surficial geology is high-relief loamy till, hummocky with irregular topography that includes circular flat-topped hills and collapsed channels, relief of approximately 18–30 meters, and shale content 25–40% of the 1–2 mm fraction (Meyer and Lusardi 2000). Soils at this site are mapped as Angus loam, morainic (L37B). Lester loam, morainic (L22C2) and Le Sueur loam (L25A) are adjacent.

Carver County

The Carver County site, in the northeast corner of the county, is in Laketown Township, Section 16 in a housing development called Lakebridge, 3

miles west of Victoria near N44°51.362' W93°41.301'. This site was also severely disturbed but was likely on a hillslope on the Altamont stagnation moraine near its eastern boundary with the Pine City end moraine of the Grantsburg sublobe. Topography here may still reflect the steep-hill-and-depression topography of the earlier deposited and underlying St. Croix moraine (Hobbs and Goebel 1982). Composition of the parent material till is similar in all respects to that of the Hennepin County and Wright County sites (Ref. Edwards 1968b). Surficial geology is high-relief loamy till deposited on top of stagnant ice, hummocky, with overall relief approximately 18–30 meters (Lusardi 1998b). Average composition of the very coarse sand fraction is approximately 40% crystalline rocks, 30% carbonate rocks, and 30% shale (Lusardi 1998b). Soils at this site are mapped as Lester-Kilkenny (KB) and Kilkenny-Lester (KB2).

Initial sample preparation

Samples containing high-chroma features consisted of irregular blocks of soil of varying sizes taken from the excavation sites. They were placed in plastic bags, brought back to the laboratory, and allowed to air dry. Larger blocks were then broken apart to make smaller soil fragments (*sensu* Kubierna 1938:154) about four centimeters in diameter to fit into a 60 cc polycarbonate jar for storage until needed. Since these blocks do represent the natural horizons of the soil from which they were obtained, and will separate along natural boundaries, they are considered peds and are referred to as peds in the subsequent discussion.

Thin sections

A few soil blocks were selected for thin sectioning from the Kandiyohi County site. Thin sections were prepared by impregnating with 3M Scotchcast epoxy cured at 90°C for two hours. Mineral transformations at 90°C were

assumed to be minimal. Sections were ground and polished to a final targeted thickness of 30 μ m with a 1 μ m finish. Polyethylene glycol was used for lubrication during all sawing, grinding, polishing, and cleaning operations. The use of water caused loss of clay and severe damage to the sample. Impregnation of these samples proved especially difficult even with the use of vacuum and the low viscosity Scotchcast at 90°C (9 cps). The best impregnation was achieved with Scotchcast that had exceeded its shelf life by at least two years. This was probably the result of a noticeably longer cure time, the epoxy remaining at a lower viscosity for a longer time giving better penetration into the smallest pores. Final properties of the epoxy seemed unaffected by the increased cure time, an observation supported in a discussion with the manufacturer's technical representative, except for a slightly darker color, unnoticeable in thin section.

Low-viscosity epoxies that cured at room temperature, such as Epotek 301-1, did not impregnate as well as the Scotchcast. The optical clarity of Epotek along with the convenience and safety of room temperature cure were attractive attributes but did not offset the problems resulting from the slightly higher viscosity and shorter cure time compared to Scotchcast. They also had a tendency to produce more bubbles. Thinning these epoxies with a variety of solvents including ethanol, methanol, isopropanol, and acetone, was not successful. Impregnation still was incomplete and resulted in a soft, rubbery block that took months to fully harden. Even a marginally acceptable cure took weeks to achieve. A modified Spurr resin also gave incomplete impregnation and in addition, droplets of wet, sticky material appeared on ground and polished surfaces and in larger voids, especially those that failed to impregnate completely.

Difficulty of impregnation may have been related to the relatively high shrink-swell clay content of the material and the use of air drying. Also, it is possible that the method of removal of the samples from the soil caused sufficient disturbance that many of the smaller pores closed up, preventing complete impregnation.

Characterization and Analysis

Physical properties of peds and features were initially studied using a Nikon SMZ800 low-power stereomicroscope with a P-Plan 1X apochromatic lens and 10X eyepieces. Zoom range is from 10X to 63X. Photographic documentation was made with a Nikon E8800 digital camera using an adapter manufactured by the Martin Microscope company. Chemical and mineralogical methods are discussed later in separate sections.

Peds

Profile morphology reflects the formational environment of the soil, and it is those processes, past and present, operating within that environment that are of interest to the study of high-chroma features. The morphological imprint left behind by those processes are distinctive throughout the depth of the profile and are visible as individual horizons within the profile. Peds, removed from horizons to which they belong, are representative samples of those horizons and therefore contain a localized history of soil forming processes at that site. The expression of hydromorphism within peds is a relevant indication of that history.

Peds, or blocks, were classified by their degree of hydromorphic expression, regardless of the drainage classification given in the Official Series Description for the soils mapped at the site. At least some variation in hydromorphic expression in the excavated blocks was expected as a result of

possible variability of actual map unit boundaries, transition and intergrading between map units, and the excavation of material from lower horizons mixing with material from upper horizons. Degree of hydromorphism was based primarily on the presence or absence of mottles on ped faces with Munsell values of 4 or above and chromas of 2 or below. Other hydromorphologic features that were used to aid in classification include manganese concentrations (Plate 2B), root channel or pore linings (Plate 3, 4B), and intercalations (Stoops 2003: 121) (Plate 5). Criteria are similar to those used by Veneman et al. (1976). Pore linings appear either as hypocoatings of manganese or iron (Plate 3), or as circumferential zones of low-chroma color that appear to be depleted of iron and manganese (Plate 4B). Depleted zones around a void were termed “neoalbans” by Veneman et al. (1976). In some cases, neoalban hypocoatings are surrounded by a quasiccoating of higher chroma material, which is likely iron or manganese or both (Plate 4B). Intercalations, which could be closed planar voids or infillings, have a morphology similar to pore linings but no pore or channel is visible. To be considered hydromorphic, concentrations were required to be unambiguously associated with depletions. The presence of concentrations alone was not used as a criterion for the hydromorphic classification.

Three classes reflecting the degree of hydromorphic expression were defined following Stoops and Eswaran (1985): weak (Plates 1A, 6), moderate (Plate 5), and strong (Plates 2A, 4A), with intergrades permitted. Hydromorphic features considered when making a classification are the presence of low chroma, gleying, neoalbans and quasiferrans, channel neoferrans or intercalations, ped ferrans, and manganese nodules (see Veneman et al. 1976; Veneman et al. 1998). Weak expression corresponds approximately to the hydromorphology expected

to be found in well-drained soil profiles, strong expression corresponds approximately to the hydromorphology expected to be found in poorly drained soil profiles, and moderate expression to the hydromorphology of moderately well-drained to somewhat poorly drained. At the extremes, very weak and very strong hydromorphologic classes could also be considered, corresponding to excessively well-drained and very poorly drained respectively. Class divisions are not precise but they do permit at least a reasonable relative ordering of peds into a hydromorphic gradient.

Peds were broken apart to reveal any high-chroma features that might be present internally. Because of the relatively high clay content, the peds were hard and brittle after drying and breaking them apart often required a hammer and chisel. Once a feature was exposed, it was described, and in some cases, removed from the ped for further analysis.

Features

Features were described on the basis of physical, chemical, and mineralogical properties. Descriptions of peds and features loosely followed Stoops (2003), and Bullock et al. (1985) but elements of Brewer (1964) and Fitzpatrick (1993) were incorporated when and where they seemed more suitable. Descriptive criteria chosen were those that seemed most likely to correlate with origin and to reveal relationships between feature, halo, and soil matrix or groundmass.

Features are three-dimensional but in most cases could be viewed essentially only in two dimensions. Breaking peds open to reveal any high-chroma features contained within, rather than making thin sections, enabled some useful three-dimensional views but in many instances the loose structure of

the feature material resulted in the feature fracturing randomly with some loss of feature material rather than cleaving neatly or separating cleanly along its outer boundary. Since intact removal of the feature from the enclosing matrix was in nearly every case impossible, size measurements and shape descriptors are almost exclusively two-dimensional.

Physical properties

The basic elements of landscape-scale photointerpretation are applicable to the collection and interpretation of optical data at a microscopic scale. The elements of size, shape, shadow, tone and color, texture, and pattern are considered the most fundamental elements (Rabben 1960). All except shadow, which is three-dimensional, were incorporated into the physical description of high-chroma features. Elements of height, site, and association were added by Estes et al. (1963), and time by Teng et al. (1997). Height is three-dimensional and no diurnal or seasonal variations in the appearance high-chroma features are present (in-situ features look the same in the morning as they do in the afternoon, the same on Monday as Thursday, and the same in winter as they do in summer) so both elements are of little relevance, but site and association are relevant. Physical components of features are associated with each other, in a way similar to mineral associations. Internal components of features have a relationship not just to each other but to boundary and even external components as well, such as the halo and groundmass. Associations can also be made between feature properties and composition, and the site at which they occur. Time is an element of importance and relevance but was not able to be incorporated into this study.

Physical properties of features are grouped into two categories: boundary properties and internal properties. Boundary properties include size, shape, transition (otherwise known as boundary sharpness), and surface. Internal properties include color, color pattern, cortex, induration, impregnation, texture, and chemical and mineralogical composition. A halo is often found surrounding high-chroma features. The halo is external to the feature itself and could be considered a distinct feature with its own properties (a hypocoating), but its adjacency to high-chroma features strongly suggests that its presence is linked to the feature, either by formational or degradational processes.

Size

Size was measured using a calibrated reticule in the eyepiece of a low-power stereomicroscope. $Feret_{\text{maximum}}$ and $Feret_{\text{minimum}}$ were measured. $Feret_{\text{maximum}}$, also called the Feret diameter or the caliper length, is the perpendicular distance between two parallel tangents across the maximum width of the feature. $Feret_{\text{minimum}}$ is similar except it is taken across the narrowest dimension. It can be compared to the width of the object that would pass through the corresponding sieve opening. Features were placed into nine size classes ranging from 0.5 mm or less to 6 mm or more in maximum dimension.

A size limit maximum, strict size uniformity, or size correlations with other properties, might indicate the presence of a controlling mechanism during formation.

Shape

Shape can give clues as to possible crystallinity (Bullock et al. 1985) and therefore to possible origin, formational environment, and history (Stoops 2003) but is a difficult and complex characteristic to describe and measure.

Mathematical formulas have been proposed for the quantification of shape (see Brewer 1964) but no system has become universally accepted or standard.

Feature shape is three-dimensional but often can be viewed in only two dimensions. Removal of loose feature material can destroy detailed shape information but can reveal underlying three-dimensional shapes that are not apparent when viewed in two-dimensions, such as an apparent circular feature in cross-section that is found to be elliptical when sectioned at 90° or when removed from the ped.

One approach has been to match feature shape with pre-defined patterns. In this study, matching a variety of standard shape patterns with feature shapes was considered unnecessary. Instead, four fundamental components of shape were identified: form, elongation, roundness, and smoothness, which together provide an effective description of feature shape.

Form

Form, as used here, refers to the underlying geometric pattern, such as circular, elliptical, square, rectangular, triangular, or irregular, shapes whose two-dimensional shapes possess common three-dimensional analogues.

Roundness

Pattern matching was initially attempted using pre-defined roundness patterns in Schoeneberger et al. (2002:2-39), Bullock et al. (1985:31), and Fitzpatrick (1993:48). That effort was abandoned as being unnecessarily complicated and difficult to apply three-dimensional shape criteria to small soil features visible primarily in two-dimensions.

Roundness, and its complement, angularity, are endpoints along a shape gradient. Three classes of roundness were used: angular, mixed, and rounded.

Angular features have sharp corners. Rounded features have rounded corners or more often, lack definite corners. Mixed features have both sharp and round corners or may have corners that are between round and angular. The central concept for class angular would be a cube or square, and for class rounded, a sphere or circle.

Features that result from broken mineral fragments might be expected to have sharp corners (and sharper boundaries) and classed as angular unless they have been rounded by transport (Stoops 2003) or weathering. Crystals, such as gypsum and calcite, that are able to grow relatively uninhibited within voids and pores in the soil, also would be angular unless altered by weathering.

Elongation

Elongation was quantified by the Feret Ratio, defined as $\text{Feret}_{\text{maximum}}/\text{Feret}_{\text{minimum}}$. A perfectly spherical or circular feature would have a Feret Ratio equal to 1. The Feret Ratio was used to place features into three qualitative categories: low, having a Feret Ratio of less than 1.5; medium, having a Feret Ratio of 1.5 to 2.0; and high, having a Feret Ratio of 2.0 or greater.

Transition

Transition refers to the rate of change of a defining property, most often color. A sharp transition between feature and groundmass is defined as a color change that is not discernable at 10X magnification, usually less than 0.1 mm wide; a clear transition is a color change that is one-half of the narrowest dimension of the feature; a diffuse transition is greater than one-half the narrowest dimension of the feature.

Surface

Surface corresponds approximately to roughness or waviness of the edge or boundary of a feature. A feature with a smooth surface, when viewed in two-dimensions, minimizes the perimeter relative to its underlying shape. A feature with a rough surface has a convoluted edge or boundary and increases the perimeter relative to its underlying shape.

Color

Color was described using the Munsell system. For reference, Munsell chroma is divided into three categories. Low chroma is considered to be a soil or feature color with a chroma of 2 or less, which matches the Hydric Soil Field Indicator criteria for an iron-depleted feature (Vasilas et al. 2010). High-chroma is considered to be greater than 5. A medium chroma is greater than 2 and 5 or less.

The color of larger features was measured using standard field methods. Colors of smaller features were obtained under a low-power stereomicroscope using a fiber optic ring light color corrected with a daylight filter. Smaller features and interior colors were estimated by matching the image color in a larger relatively homogeneous area of the ped with the color of that area estimated directly with a Munsell color chip using PhotoShop® (Adobe®) then converting the RGB values from PhotoShop® (Adobe®) to Munsell colors using the conversion software, CMC10c (WallkillColor). The image was finalized by color appearance matching the image of the feature and the surrounding soil matrix on a calibrated computer monitor with the direct microscope image.

Raw camera images were downloaded through Adobe Bridge® (Adobe®) into Photoshop Camera Raw® (Adobe®) where images were corrected for white balance and exposure. Careful adjustment of the Exposure setting and sometimes

the Tint in Photoshop Camera Raw[®] (Adobe[®]) at this point often saved considerable time later. Images were then brought into PhotoShop[®] (Adobe[®]) where final color corrections were made using adjustments to Hue, Saturation, and Lightness based on colors of selected areas defined with the Magic Wand Tool. Ped matrix color was corrected first followed by the feature color, if needed. Corrections were made in order to accurately match observed colors.

Most images of features were taken while the feature was in the ped and therefore had a depth dimension as well as area. Obtaining an image of the feature that was in focus throughout its depth required the use of image stacking within PhotoShop[®] (Adobe[®]) to create a single seamless layer composed of a series of images taken at different focus locations or depths on the feature and the immediately surrounding matrix.

An attempt was made to develop “mini-chips,” very small chips of Munsell colors that would be useable for comparisons under a microscope, but the halftoning process used by inkjet and laser printers to represent colors rather than the continuous toning of a single printing ink resulted in only a pattern of dots being visible under the microscope rather than a uniform color.

Color is a fundamental, and in large part definitional property of high-chroma features. Color can be influenced by several factors making mineral identification and other interpretations based color alone somewhat tenuous. It is these factors, however, that can also make color a meaningful criteria. Deviations of feature color from those of a “pure” mineral can point to variations in crystal or particle size, density, and composition that may be related to their formation. Color and color patterns, discussed below, may also be useful for making relative

comparisons between features, reflecting differences in their development and formational environment.

Color Class

One of the most significant characteristics of high-chroma features is the presence of color variations within the feature. Though similar patterns are found in nearly every feature, the pattern itself and the degree to which the pattern is expressed varied from feature-to-feature. This expression of a color pattern was regarded as an indication of compositional differences possibly pointing to genetic pathways. When used in a purely descriptive way, such patterns could also be useful for comparing the internal structures of different features. While it was possible to develop detailed descriptions of the color patterns observed in each feature, and in fact several were tried and found unsatisfactory, a simpler classification system was developed and applied to features that were broken open or sectioned while within the ped (Figure 8).

Cortex

Some features possess an outer shell or rind. This rind can be distinguished by a difference in color and texture, the rind often being darker with an irregular or rough surface or outer rim. In some features, the rind differs in texture compared with the internal fabric. Since not all features possess a visible rind, its presence may indicate the action of a particular genetic process or a specific origin not common to all features.

Induration

Induration, cementation, or hardness is difficult to measure in such small features and especially in thin sections. Induration corresponds roughly to the concept of consistence applied to peds. Three categories were used: loose,

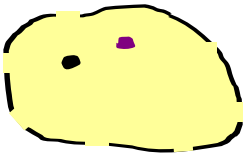
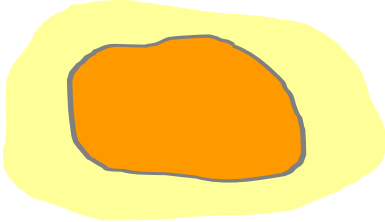
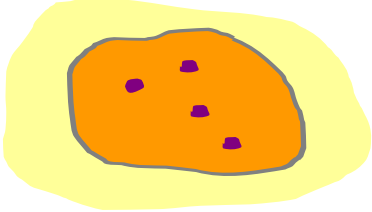
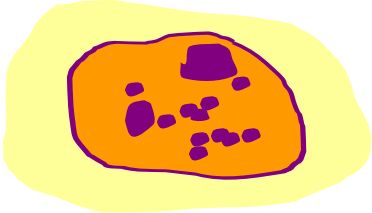
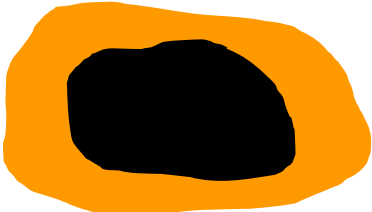
With Cortex and Halo	Description	
Class 1		<p>Single, nearly uniform yellow color. Less than 1% weak reddish or black mottles. No cortex, but may have a black external coating that does not completely cover the feature. Halo is not present.</p>
Class 2		<p>Strong brown color is dominant. Few weak reddish or black mottles (less than 2%). Most features lack a visible cortex.</p>
Class 3		<p>Strong brown matrix color with common weak red or black mottles (2% to 20%). Most features lack a visible cortex.</p>
Class 4		<p>Feature matrix is often darker and more purple than Classes 2 and 3. Darker mottle color dominates over strong brown. Many dark fragments (more than 20%) often have a metallic to submetallic luster with faint iridescence. Most features lack a cortex.</p>
Class 5		<p>Dark to black core surrounded by red to yellow outer layer. Metallic luster and iridescence on surface of dark core material. No cortex was ever found; halo is of a color similar to that of Class 2, 3, 4 features but often less prominent.</p>

Figure 8. Classification of high-chroma features.

moderate, and hard that correspond to the Dry Classes of Loose, Slightly Hard, and Hard in Schoeneberger et al. (2002:2-50). The degree of correlation with their more quantitative descriptions is unknown. Loose induration means that material falls apart into smaller aggregates or even single grains under only a slight touch of a micro-tool. Hard induration requires considerable force with a micro-tool to separate grains.

The degree of induration may indicate the relative quantity of cementing materials such as clay, carbonate, or iron oxides. Their absence in features found within a cemented matrix is also noteworthy.

Texture

Texture refers to the distribution of particle sizes present within the feature, and is analogous to the standard concept of soil texture. Where the distribution of particle sizes is limited, especially if the distribution is bimodal, the concept of c/f-related distribution (Stoops 2003:41–46, 92–93) provides a useful way to describe the internal fabric of features.

Impregnation

Features can enclose or impregnate the groundmass (impregnative) or they can intrude into the groundmass without any incorporation (intrusive). Impregnative and intrusive pedofeatures are defined by Stoops (2003:101–102). Matrix pedofeatures enclose the groundmass and often have a gradual or diffuse boundary. Impregnative pedofeatures are a subclass of matrix pedofeatures that are “recognizable because of a higher concentration of one or more components.” Noteworthy is his statement that “the use of the term *impregnative* does not imply any interpretation of the process of their formation” (Stoops 2003:102). Impregnative pedofeatures, then, are concentrations of material such as iron or

magnesium oxides or oxyhydroxides that enclose the groundmass to varying degrees.

Intrusive pedofeatures do not enclose the groundmass but form in preexisting voids outside the groundmass or in the groundmass by complete displacement or replacement of the other constituents (Stoops 2003:104).

Intrusive pedofeatures always have sharp boundaries, an example of a descriptive criterion that *may* correlate with genesis.

Because of obvious difficulties in determining if features formed in a void or by displacement, features were classified as being impregnative or intrusive based solely on whether or not the groundmass appears to have been incorporated into the feature. If the feature was impregnative, the degree of impregnation or “purity” was recorded as weak, moderate, or strong according to the definitions given by Stoops (2003:102–103).

Chemical and mineral analysis I: Beam methods and microspectroscopy

Beam methods in this context refers to the use of a high energy particle beam to produce and collect imaging, chemical, and structural information about a substance through direct interaction with the beam itself. Beam sources might be x-ray, electron, or laser.

Scanning electron microscopy and microanalysis

Several features were removed from soil blocks along with only enough surrounding matrix material to maintain their integrity in an SEM chamber. Chamber vacuum drawdown times became excessive the SEM if samples larger than about 3 mm were used. Samples were placed on carbon conductive tape on a half-inch aluminum stub. Some samples were uncoated and others were coated with 50Å of platinum. Because of the rough surface texture of the samples,

conductive coatings were difficult to apply uniformly and failed to coat effectively below the surface in cavities or pores. Loose material removed from features was also placed on carbon conductive tape or carbon adhesive painted to a half-inch aluminum stub.

A Hitachi S3500N variable-pressure SEM (VP-SEM) with EDS capability in the Biological Imaging Center and a JEOL 6500 with EDS capability in the Characterization Facility, both at the University of Minnesota, were used for sub-microscopic imaging and analysis. Variable pressure SEM, which is able to operate at a higher chamber pressure than conventional SEMs, was used without a conductive coating. In high-pressure mode, the VP-SEM is similar to what is called an “environmental SEM” but the VP-SEM is also capable of operation at high vacuum similar to a conventional SEM.

Transmission electron microscopy and microanalysis

A Technai T12 TEM with electron diffraction capability operating at 130KV was also used for characterization in the Characterization Facility at the University of Minnesota. Scheduling conflicts were accommodated by the use of a JEOL 1200 EXII at the Nils Hasselmo facility at the University of Minnesota and a Philips CM12 at the Biological Imaging Center at the University of Minnesota.

Samples of high-chroma features were prepared by a crush-and-float method. A feature was removed from the ped. It was then ground in an agate mortar and several drops of isopropanol were added to the ground mixture. The suspension was then pipetted into a small glass vial and an additional quantity of isopropanol was added. The dilute solution was agitated and a copper TEM grid immersed in the solution for several seconds, then removed and air dried.

X-ray diffraction

Conventional XRD using a Siemens D500 with cobalt radiation to eliminate possible fluorescence from iron was initially used on a ground sample of a larger feature. A Bruker AXS micro-diffractometer and rapid XRD with copper sources were used on smaller undisturbed samples and on an impregnated section. These instruments enabled simultaneous detection of a variety of minerals over a small area. Extended times, up to 24 hours were used to detect small amounts of iron minerals. The classification system for features had not been developed when XRD was completed. As a result, sample data are not class specific and cannot be associated with any color class.

Raman spectroscopy

Raman spectroscopy was first demonstrated in 1928 (Raman and Krishnan 1928) but its use has only become practical with the development of sensitive spectrophotometers and sophisticated analytical software. Micro-Raman, which projects a laser beam backwards through the lens of an ordinary optical microscope, produces a spot size of approximately 1 μm diameter depending on the lens used.

Raman spectroscopy provides information about molecular vibrations that can be used for sample identification, quantification, and imaging. The technique involves shining a monochromatic light source (laser) on a sample and detecting the scattered light. Most of the scattered light is of the same frequency as the excitation source and is known as Rayleigh or elastic scattering. A very small amount of the scattered light (about 0.00005% of the incident light intensity) is shifted in energy from the laser frequency as a result of interactions between the incident light waves and the vibrational energy levels of the

molecules in the sample. This scattering effect is known as Raman scattering. Plotting the intensity of these shifts versus frequency results in a Raman spectrum of the sample. Generally, Raman spectra are plotted with respect to the laser frequency such that the Rayleigh band representing the laser frequency lies at 0 cm^{-1} . When plotted in this way, band positions will lie at frequencies that correspond to the energy levels of different functional group vibrations. The Raman spectrum can therefore be interpreted in a similar way to an infrared absorption spectrum (InPhotonics 1999) although the mechanism of Raman scattering is different from that of IR absorption and the peaks do not always correspond. A notch filter is often used to remove the reflected laser light (Rayleigh scattering) from the spectrum. Minerals can be identified based on the unique spectrum of reflected light. Peaks in the fingerprint region, between 400 cm^{-1} and 1600 cm^{-1} , give bonding information based on characteristic surface reflections that are most useful for mineral identification.

A Witek spectrophotometer and software were used in conjunction with an argon-ion laser at 514.5 nm and an Olympus optical microscope. Output power was reduced to 0.1 mW using a mechanical shutter, resulting in scan times of 10 to 20 minutes per sample. Spectra were obtained by averaging 3 runs. Low power was necessary to avoid heat buildup from the laser beam within the sample that could cause transformations of iron minerals.

Very little sample preparation is needed to use Raman spectroscopy. In most cases, the only preparation needed was to trim soil blocks to fit under the optical microscope. Samples were placed on half-inch aluminum SEM stubs held upright in a plastic storage box or placed on glass slides. Essentially any size sample that can be accommodated under the microscope is suitable. The stub

and box with cover open or the sample and glass slide were placed under the objective lens of the microscope. The microscope stage was moved to position areas of interest under the laser beam for analysis. Powdered material removed from features was simply placed on a glass microscope slide clamped under the lens of the microscope.

Attempts to solve problems with fluorescence were unsuccessful. The first approach was to reduce laser power to as low as 0.01 mW and increase collection times to 30 minutes. In all cases, either fluorescence continued or no spectrum was collected. Continued problems of fluorescence from iron minerals at 514.5 nm led to the use of a Krypton laser at 752.5 nm since fluorescence can sometimes be reduced by use of longer or shorter wavelengths. Longer wavelength lasers can be operated at higher power but give lower resolution, making identification of diagnostic peaks in the fingerprint region more difficult. Shorter wavelengths increase the risk of damage to the sample even with short-term exposure. Neutral density filters were used to reduce the power applied to the sample. Samples were run at power levels ranging from 20 mW to 500 mW.

Fourier Transform Raman (FT-Raman) also was attempted using a Nd:YAG laser at a wavelength of 1024 nm operating at a power of 100 to 300 mW depending on the sample. Samples were lightly crushed and placed in glass sample tubes to a depth of 3 to 5 mm. Spectra were collected and averaged based on 32 scans.

Chemical and mineral analysis II: Wet methods

Wet chemical methods were also used to obtain additional information about the features and surrounding matrix material. Limited sample durability meant it was not possible to perform every available test on every sample. The

choice of which tests were made on any particular sample was a subjective judgment as to appropriateness and their ability to maximize the amount of information collected based on sample morphology.

Removal of material for sampling

Soil blocks were broken apart to reveal any additional high-chroma features present within the block. Since the features are so small, this required breaking the fragment into ever-smaller sizes in order to reveal the features. When found, features were described, measured and classified, then removed from the surrounding matrix by carefully scooping or scraping out first the feature material then any halo material using a micro-chisel under a stereomicroscope onto a small piece of weighing paper. Features and their halos were sorted on the basis of color classes previously discussed. Feature and halo material was transferred into small tared plastic vials labeled according to the color classification of the feature and weighed. Material was collected until a minimum of 1 mg of each color class of features and haloes was obtained from each sample site. A sample of matrix material was taken from the “spoils” remaining after breaking the peds apart and removing any features. Because the matrix possesses a high degree of variability within a short distance, a representative sample was best obtained by taking a mixed sample or homogenized sample rather than a local scraping as in the case of features and halos. Minimum sample size for each class was considered to be 1 to 2 milligrams. Individual sample quantities from larger features were in the range of one to two milligrams. Smaller features weighed less than one a tenth of a milligram.

Some features were recovered by carefully breaking apart the peds into smaller and smaller fragments, then probing through the residue with a micro-forceps under a stereomicroscope to remove features that remained intact. A third method of recovery was by wet sieving. About 1 gram of soil was placed in a 63 μm sieve. The sieve was placed in a round plastic container filled with enough deionized water to keep the sample fully immersed. The sieve was agitated gently in a circular motion to remove the finer material. The water was changed when it became cloudy. After several rounds of rinsing, the water remained clear. The sieve and residue were then dried in a low temperature oven at 105°C. The residue was then placed on a sheet of clean white paper and gently probed with a scalpel while examining the residue for high-chroma features under a stereomicroscope. Any features discovered were removed with a micro-forceps and collected in a plastic vial. This method was abandoned for two reasons. First, the yield was low relative to the time and labor required. Second, the method selected for those features that were cohesive enough to survive crushing and sieving, no matter how gentle. These features may possess properties different from other high-chroma features and may have a different origin from those too poorly cemented to survive sieving, posing an interesting question for further study.

Acid ammonium oxalate

Acid ammonium oxalate (AAO) (or ammonium oxalate-oxalic acid in the dark) (Loeppert and Inskeep 1996) was used to compare the relative amounts of amorphous or poorly crystalline minerals to the amount of crystalline minerals. 0.1 ml of an acid ammonium oxalate mixture at pH 3 was added to a small amount of sample material that had been previously placed in a well of a spot

plate. The spot plate and sample were kept in the dark for two hours. The sample was photographed before and after AAO. By comparing the two images, the percentage of poorly crystalline material was estimated by comparing the loss of color before and after treatment. Percentages were recorded as belonging to one of three classes: less than 25%, 25% to 75%, and greater than 75%. The broader mid-range reflects the difficulty of distinguishing and classifying changes that do not involve complete removal of oxides.

Extraction for inductively coupled plasma

Since sulfur was an element of interest in the analysis, dithionite, the standard treatment to extract crystalline iron minerals, could not be used. Instead, ascorbic acid with a reducing agent was used to dissolve more crystalline iron and manganese minerals. After documenting the changes resulting from two hours in the dark, 0.1 mL of 0.1 M ascorbic acid and 1 mL of hydroxylamine hydrochloride (HH) at pH 2 (see Table 14, page 199) were added to the acid ammonium oxalate (AAO) solution in the spot plate (Chao 1972; Chao and Zhou 1983; Shuman 1982, 1985). The spot plate was covered with a glass plate to prevent evaporation and placed under a 60 watt incandescent soft-white light bulb in an aluminum reflector held 5 cm above the spot plate for 30 minutes resulting in a solution temperature of approximately 90°C. The light and heat from the incandescent bulb induced photoreduction and increased the rate of dissolution of metal oxides and oxyhydroxides.

The extractant solution prepared above was transferred from the spot plate with a micro-pipette and placed in a 10 cc polyethylene test tube that had been immersed in 10% HCl solution overnight and rinsed with deionized water to remove any contaminants in the tube or caps.

Iron, manganese, aluminum, amorphous silica, and some sulfur minerals such as jarosite, are soluble in AAO (Burt 2004:312; Welch et al. 2007; Welch et al. 2008). Following the AAO/HH extraction, a drop of 10% HCl was placed in the spot plate well with the remaining material and heated to 90°C for 30 minutes to dissolve any remaining gypsum and dolomite and other less soluble carbonate minerals. This solution was added to the AAO-extractant solution already present in the polyethylene test tubes.

The residue remaining after the extractions was collected and described. Any colorless or white fragments remaining in the spot plate were placed in a clean spot plate well and stain tested for the presence of carbonates. Darker fragments were immersed in a drop of 30% H₂O₂ to dissolve any manganese that might be present and oxidize any pyrite to soluble sulfate (Borah et al. 2005). This extractant solution was also added to the extractant solution obtained from the previous steps.

Deionized water was added to the test tube to bring the total solution quantity to 5 mL, the minimum required for ICP-AES analysis. A blank was prepared for each set of analyses. Samples were then brought to the Soil Testing Lab at the University of Minnesota for elemental analysis.

Inductively coupled plasma

Inductively coupled plasma-atomic emission spectroscopy (ICP-AES) was used for chemical analysis. ICP-AES was chosen after unsuccessful attempts at isolating and identifying the chemical and mineral composition using XRD, SEM-EDX, TEM-ED, and Raman spectroscopy. Poor crystallinity, small sample sizes, difficulty in isolating and locating the features of interest, and relatively low concentrations of important elements such as manganese made detection by

these methods unsuccessful. Although the use of ICP required destruction of the sample and precluded the study of localized areas within the feature, it provided a fast but highly sensitive method for detecting a range of elements at low concentrations. Following the extraction procedure described above, samples were analyzed for Fe, Mn, Al, Si, Ca, Mg, P, S, K, Ti, Na, Cu, Zn, Co, Ni, Pb, Ba, Sr, Cd, Li. Only samples from the Kandiyohi County site were submitted for analysis.

Quantitative analysis on the basis of sample mass was possible after collecting a sufficient quantity of sample material but its accuracy is questionable. The small size and volume of features, which meant sample masses in the low milligram range, and the close relationship between feature, halo, and matrix complicated sample collection and added to the problem of obtaining samples sufficiently free of contaminating material from neighboring areas, which affected the reliability of subsequent analysis. Even small quantities of contaminating material represent a relatively large proportion of the sample. Handling a ped under the microscope to remove material from a feature or halo often caused unwanted material to drop off the ped and onto the collection area, which had to be removed. Removal of as much contaminating material as possible was done under the microscope with a small brush and forceps but removing unwanted material also increased the risk of losing desirable material.

Stain tests

Stain tests are a quick, simple, and generally reliable method of identifying certain minerals in small sample volumes. Stain tests for carbonates have proven especially useful, having been used in thin sections and drill cores (Dickson 1966; Hitzman 1999). They have been used since the late nineteenth

century to distinguish calcite and dolomite but methods have been developed for identifying a variety of carbonate species, feldspars, and clays, and for enhancing the contrast of biological specimens (Allman and Lawrence 1972). Specific carbonate tests have been published by Warne (1962), Friedman (1959), Dickson (1965, 1966), and Evamy (1963). Warne (1962) seems to have based his test procedure on Friedman's (1959) Procedure I but expanded the tests to include ankerite, strontianite, cerrusite, siderite, a test to distinguish calcite and witherite using rhodizonic acid, and a test to separate dolomite from rhodochrosite using benzidine. Evamy (1963) modified Dickson's (1965) procedure by lowering the concentration of HCl in the reagent solutions to avoid formation of CO₂ bubbles on the surface that could prevent staining. Friedman's (1959) Procedure II provides an independent test procedure for the same carbonate minerals as in Procedure I. Procedure I is based primarily on and begins with alizarin red S while Procedure II begins with titan yellow. With the exception of Feigl's solution, the two procedures use a completely different suite of reagents to test for the same suite of carbonate minerals providing an independent verification of mineral identity.

Successful stain tests require that the dyes used are selective, so that a particular dye will stain only a specific material even when similar materials are present. Getting the mineral to take up the dye, either as a surface precipitate or absorbed into the mineral structure, depends on several factors including surface preparation, strength and age of reagents, temperature, surface finish, and staining time. Although the technique is relatively simple and inexpensive, considerable experimentation is required to establish which stains are most effective on the minerals being tested, as well as determining the most effective

temperatures and times (Miller 1988). Staining procedures were verified on samples of calcite, dolomite, siderite, ankerite, and gypsum obtained from Wards™ Natural Science.

Stain tests can be very sensitive but also at times, unreliable. The concern, as with any other test, is with false positives and false negatives. False positives can occur because the dye reacts with other mineral species similar in structure or composition to the target species. Contaminated reagents can also produce false positives. False negatives can be caused by interfering materials present in the test solution that prevent the reaction of the target mineral with the indicator dye. Extractants such as the complexing agents oxalic acid and ascorbic acid can sometimes interfere by binding with the target element and must be removed before completing spot or stain tests on residues remaining after an extraction. Interferences were investigated before data collection began. To minimize potential problems with interferences, samples were rinsed after pipetting off the remaining extractant solution by placing a drop of DI water into the spot plate well, then pipetting off the DI rinse water. Whenever possible, this procedure was repeated at least once. Care had to be taken to minimize loss of sample material from pipetting. These losses were inevitable and were one reason why only limited testing could be performed on any one sample.

Thin surface coatings of oxides and other contaminants can also prevent reaction. They can usually be removed by pretreating the sample in dilute hydrochloric acid. Mineral residues remaining after extraction had been exposed to acidified solutions so no pretreatment in dilute HCl was deemed necessary and would have led to additional sample loss. Samples of matrix material were pre-treated for no more than 30 seconds to minimize loss of calcite or other

soluble carbonates that might be present in small quantities or as small fragments.

Stain solutions were standard concentrations and formulations found in Friedman (1959) and Warne (1962) (see Tables 14, 15, B1). The most comprehensive staining procedures use a sequence of stains to reduce or eliminate ambiguous results, but lack of sufficient test material often prevented completion of a complete sequence. No single feature contained sufficient material to complete the entire sequence. As a result, partial test sequences were conducted on two or more different samples. Stains that give a “No color” response are also important in order to eliminate ambiguity. The staining sequences in Table 14 are also laid out as flow charts in Friedman (1959) and Warne (1962).

Alizarin red S and potassium ferricyanide can be used individually or in combination (Table 15). When used in combination, they act independently and give stain colors that are a response to either the alizarin red S, the potassium ferricyanide, or the combination, depending on the sample composition.

Tests shown in Tables 14 and 15 were all conducted, but not all tests were conducted on all samples. Approximately 10% of samples were subjected to stain testing. Three stains said to be specific for gypsum were also applied to some samples: titan yellow, rhodamine B base, and alizarin cyanin green (acid green) (Allman and Lawrence 1972:103).

Samples were placed in a glass or ceramic spot plate and a drop or two of the indicator solution added by micropipette. Colors usually appear within a few seconds but ferroan dolomites can take 5 minutes or longer to produce color when using potassium ferricyanide. Heat is sometimes required for ferroan

dolomites and is always required for siderite when staining with potassium ferricyanide (Warne 1962). Sodium hydroxide mixtures with alizarin red S and titan yellow require heating. When required, the test solution was heated to 90°C under a 60 watt incandescent light bulb mounted in a metal reflector clamped 3 cm above the spot plate. With one exception discussed later in the Results and Discussion section, stain tests followed complete removal of iron oxide coatings following AAO treatment.

A method for staining siderite was developed by Hallimond (1925). After a light surface etch in dilute hydrochloric acid, the sample is immersed in a solution of hot concentrated potassium hydroxide for 5 to 10 minutes. A small amount of hydrogen peroxide is added from time to time during heating. Any siderite present will be stained brown. Ferroan dolomite is stained a lighter brown while dolomite remains unstained.

In addition to stains, reagents used for selective dissolution and identification include 10% HCl (carbonates), hydrogen peroxide (manganese), hydroxylamine hydrochloride (manganese), sodium hypochlorite (organic matter), nitric acid (pyrite), acid ammonium oxalate, and ascorbic acid (both for iron and manganese oxides).

Spot tests as found in Feigl (1972) also were valuable as quick, easy methods to confirm the presence of absence of particular elements. Spot tests were used primarily for the detection of manganese after extraction into solution with acid ammonium oxalate or hydroxylamine hydrochloride. Indicators used were sodium bismuthate, sodium periodate, and tetrabase solution (Table B1). Problems of interference with extractant solutions limited their usefulness,

however. Commercially available test strips were used to test for sulfate in solution.

Halo

A halo is a yellowish ring of varying width surrounding the high-chroma feature itself. Its chroma is higher than that of the matrix but lower than that of the feature. A halo is different from a diffuse boundary (Figure 9). The presence of a halo surrounding a feature may indicate either accretion or degradation. Presence or absence of a halo may also be influenced by the mineralogy and elemental composition of the feature since some minerals are more easily weathered than others and may leave a weathering signature in the form of a halo. Physical extent of the halo was reported using an index defined as the ratio of average halo width to average feature width. Categories used are less than one-half the average feature width, between one-half and one feature width, and greater than one feature width. An index of 1 indicates that the average width of the halo is equal to the average width of the feature.

RESULTS AND DISCUSSION

Classification of peds by hydromorphology

Hydromorphic classes assigned to peds and drainage classes assigned to the corresponding soil profiles at sample sites did not always match (Table 8). Matching of drainage class with ped morphology depends on the accurate placement of the sampling location on the soil map, consistent descriptions and interpretations of both soil profiles and peds, and the depth or horizon to which the peds belonged.

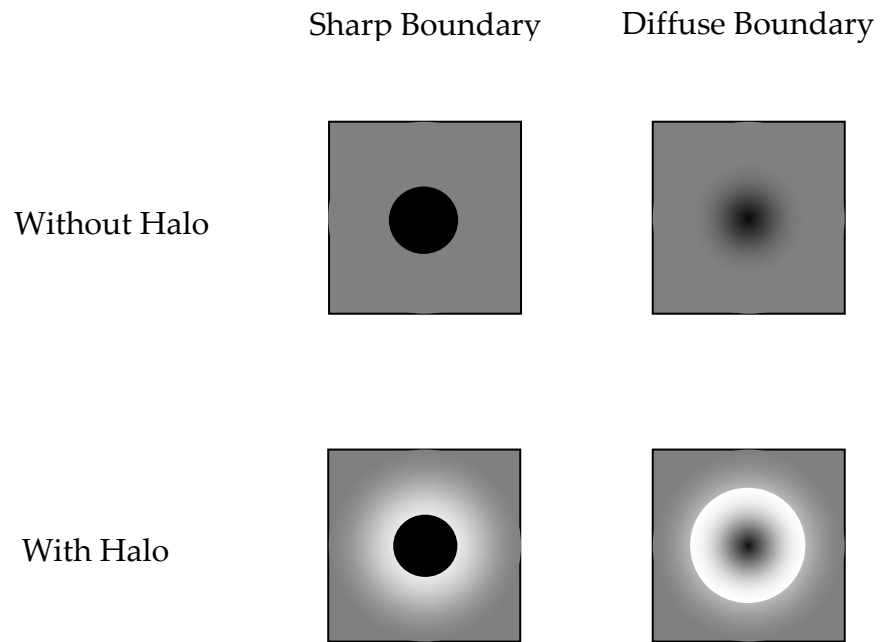


Figure 9. Boundary and halo are two different aspects of a high-chroma feature. The black-filled circle in the middle of each pane represent a high-chroma feature. The light ring or corona in the panes along the bottom row represents the halo. The dark gray surrounding the feature or halo represents the soil matrix.

Table 8. Hydromorphic classification of peds studied from each site. Drainage classes are from the OSDs of soils mapped at the sample site. Hydromorphic classes are as follows: W=weakly expressed; MW=moderate weak; M=moderate; MS=moderately strong; S=strongly expressed.

County/Site	Drainage class				Hydromorphic class				
	WD	MWD	SPD	PD	W	MW	M	MS	S
Kandiyohi	_____				_____				
Wright			_____			_____			
Carver	_____						_____		
Lincoln	_____						_____		
Hennepin	_____								_____

Peds from most sites that were selected for study expressed a range of hydromorphism encompassing no more than two classes (Table 8). Peds that contained no high-chroma features were not classified. The absence of features was interpreted as sampling variation. In retrospect, they should have been classified. Doing so may have extended the range of variation of hydromorphism within a site towards the weak side. More importantly, peds lacking in features may actually represent a formational environment that was not conducive to the formation of high-chroma features on a larger scale.

In general, the correlation between drainage class and hydromorphic class was poor (Table 8). Well-drained soils contained peds with moderate to strong hydromorphism and poorly drained soils contained peds with moderate to moderately weak hydromorphism. This is most likely the result of selecting peds for analysis from deeper horizons.

Kandiyohi County

Peds from the Kandiyohi site have dry colors of 2.5YR 7/3 to 2.5YR 7/4. Texture is sandy loam. Structure is platy. Occasionally, the platy structure is not evident at the macroscale. A drop of water placed on a ped fragment will cause the fragment to slake and reveal a platy structure under a low power microscope. Peds give strong to violent effervescence with 10% HCl. Hydromorphism is weak to moderately weak. Small intercalations of low chroma, some with hypocoatings of iron, are visible in many peds but have only faint contrast with the matrix (see Plate 5 for an example of intercalations).

Soils at the Kandiyohi County site are mapped as Sunburg-Wadenill complex (Table 6). Sunburg and Wadenill C-horizons seem to be a good match to ped morphology.

Wright County

Peds from the Wright County site have dry color 2.5YR 7/4. Texture is loamy. Structure is platy. Microstructure under saturation is subangular blocky to very weak platy. Peds give strong to violent effervescence with 10% HCl. Hydromorphism is weak to moderately weak. As with peds from Kandiyohi site, small intercalations of low chroma, some with hypocoatings of iron, are visible in some peds but again, these have only faint contrast with the matrix.

In the Wright County site, soils are mapped as Hamel loam (Table 6) with Reedslake-LeSueur complex to the north and Cokato-Storden to the south and east. Ped morphology was not a good match with Hamel loam. Hydromorphism in a ped taken from Hamel, a poorly to somewhat poorly drained Argiaquoll, should be more strongly expressed. Depletions were present in the peds but are not reported in the OSD for Hamel. Reedslake-LeSueur and Cokato-Storden complexes are better matches based on the presence of concentrations and depletions except that depletions are not reported in the OSD for Cokato. A clay increase was noted in auger samples between 55 and 84 cm, consistent with Le Sueur, Cokato, and Reedslake. Reedslake Bk2 and C-horizons seem to give the closest match.

Carver County

Peds from the Carver County site have dry colors of 2.5YR 7/3 to 2.5YR 7/4. Texture is sandy loam. Structure is platy. Microstructure under saturation is subangular blocky. The apparent platy structure may be the result of compaction related to disturbance at the site. Peds give strong to violent effervescence with 10% HCl. Hydromorphism is moderate. Small intercalations of low chroma,

some with hypocoatings of iron, are visible in most peds and have a more distinct contrast with the matrix.

The Carver County site was severely disturbed as the result of construction for a new housing development. It is possible that so much of the overlying soil had been removed that the lower horizons were present at the surface. Soils at the Carver County site are mapped as Lester-Kilkenny and Kilkenny-Lester (Table 6). The Bk2 and C-horizons of Lester seem to be the best match although the OSD does not report depletions in the Bk2 horizon.

Lincoln County

Peds from the Lincoln County site have dry colors of 2.5YR 7/3. Texture is loam. Structure is platy. Microstructure under saturation is weak platy to subangular blocky. Peds give strong to violent effervescence with 10% HCl. Hydromorphism is moderate to moderately strong. Large intercalations of low chroma, some with hypocoatings of iron, are visible in all peds and have a distinct contrast with the matrix.

Soils at this site are mapped as Buse-Wilno complex (Table 6) with adjacent areas of Hokans-Svea. No concentrations or depletions are reported in the OSD for Wilno. Buse Bk2 and C-horizons are a good match. Strong effervescence especially favors the Bk2 horizon as source.

Hennepin County

Peds from the Hennepin County site have dry colors of 2.5YR 7/2. Texture is loam. Structure is platy. Microstructure under saturation is weak platy to subangular blocky. Peds give strong to violent effervescence with 10% HCl. Hydromorphism is strong. Intercalations of low chroma, some with hypocoatings of iron, are visible in all peds and have a distinct to prominent

contrast with the matrix (Plate 5). Root channel and pore linings, often with iron and manganese hypocoatings, are also common.

The feature in Plate 4B bears a strong resemblance to Liesegang rings, features that have been recognized in the geological literature for many years. Although their origin is unknown, a common explanation is that reduced iron diffuses through a porous material such as a silicic acid gel, and alternately oxidizes (and precipitates) and solubilizes (depletes) with changing pH possibly in association with calcium carbonates (Hartman and Dickey 1932; Augustithis and Ottemann 1966). McBride (2003) suggested that oxygen diffusing through carbonate siltstones containing ferrous iron in pore water may be responsible for their formation. In soils, the precipitation/depletion mechanism may be fluctuations in redox potential. The dark bands in the feature in Plate 4B are precipitated manganese oxides. One explanation for their presence is that under reducing conditions, soil manganese became soluble and diffused through an iron-rich “gel” possibly of silicic acid. Whatever the exact origin, the appearance of such rings signals the almost certain existence, past or present, of an alternating oxidizing/reducing environment that results in strongly expressed hydromorphology.

The Angus and Lester series mapped at the Hennepin County site are “morainic” phases (Table 6), presumably recognizing the influence of their placement on the Altamont stagnation moraine. Both are potentially good matches to the peds taken from this site except that the Lester Bk2 horizon reportedly lacks depletions. The C-horizons of both Lester and Angus are a good match with ped hydromorphology. The Hennepin County site also was severely disturbed. As with the Carver County site, it is possible that so much of the

overlying soil had been removed that the lower horizons remain and are exposed at the present surface.

Soils at all collection sites were disturbed. Attempts to find undisturbed sites that would provide a sufficient quantity of features for characterization were unsuccessful. It therefore became necessary to rely on road or building construction to reveal sites that contained a suitable quantity of high-chroma features. Although not ideal, since interpretations were then limited, in the end the ability to recover high-chroma features in sufficient quantity for a more extensive characterization seems to justify the use of bulk samples from disturbed sites.

Characterization of high-chroma features

Occurrence

Field observations

High-chroma features have been found in well drained and poorly drained soils. Although not studied formally, features seem least abundant in moderately well drained soils on ground moraines. Depth to first occurrence, estimated by taking hand auger samples, for well-drained soils was from approximately 50 to 100 cm, with 75 cm being a reasonable average. Average depth to first occurrence at sites in Hennepin and Carver Counties was at or near the surface. This result is misleading because both sites have experienced severe disturbance, which likely exposed the subsurface horizons (Hennepin County) or substantially reduced the thickness of the surface horizon (Carver County). Field data are summarized in Table 9.

Table 9. Field data for soils in and near sample sites where high-chroma features were found. County abbreviations are as follows: LI=Lincoln; KA=Kandiyohi; WR=Wright; HE=Hennepin; CV=Carver. The column labeled “WD” includes well-drained and moderately well-drained soils; the column labeled “PD” includes somewhat poorly drained and poorly drained soils based on Soil Survey classifications.

Variable	WD	PD
Site (County)	LI, KA, HE, CV	WR
Depth (cm)	75 (50 to 100)†	Surface
Horizons	C and lower B	C and B
Hue	7.5YR	7.5YR
Value	5	5
Chroma	8	8
Abundance	—	—
Size	—	—
Contrast	Prominent	Prominent
Geographic setting	Convex Summit Shoulder/Backslope Backslope	Backslope Footslope
Physiographic feature	Alexandria and Altamont stagnation moraine and Bemis ground moraine.	Altamont stagnation moraine

† High-chroma features were found at the surface at the Hennepin County site. See text for discussion.

Significant differences in the size of features between sites were found in the field. Peds with more strongly expressed hydromorphology tended to contain larger features (see Table 11, page 153).

No differences in abundance were evident in the field. Even well-drained sites have abundant concentrations in localized areas of a profile. Measuring and comparing the ped-to-ped abundance of features is not likely to be accurate since smaller peds would be expected to have fewer concentrations than larger peds while the reliability of a per area or per volume comparison is dependent on the ability to accurately measure surface area or ped volume and count individual features. Since it was not possible in most cases to remove high-chroma features intact from their peds, counting features or estimating their population density per unit volume was impractical. An “appropriate scale of observation” (Davis 1986) as applied by Arocena and Ackerman (1998) of at least 5 observations per pre-defined frame, would have required a thin-section area several times what was possible to produce with the samples and equipment available. The relatively rare occurrence of high-chroma features in thin sections precluded the application of stereology to estimate volumes and other three-dimensional properties from two-dimensional observations.

Ped or soils with weakly expressed hydromorphology were found higher in the landscape: on a convex summit, shoulders, and backslopes. Peds with strongly expressed hydromorphology were taken from soils found on a lower backslope or footslope. The landscape position for the Hennepin and Carver County sites had to be inferred because of severe disturbance, but considering

that most interest is at or near the highest and lowest landscape positions, which are more easily located, the estimation seemed reasonable.

Four sites with high-chroma features were found on stagnation moraines. The occurrence of high-chroma features in ground moraines was unusual. Only the Lincoln County site was on a ground moraine. The Bemis ground moraine and more specifically the Bemis ground moraine in the southwestern part of the state in Lincoln County might be unusual given its narrow width and close proximity to the Bemis end moraine on the southwest and the Altamont stagnation moraine on the northeast. The Bemis ground moraine might be more similar to a stagnation moraine than are most ground moraines.

All samples were taken from soils formed in loamy Des Moines lobe till. The well-drained Kandiyohi County site was far enough north to be on or near the Alexandria stagnation moraine, possibly in an area of mixed Des Moines lobe and Wadena lobe tills or having a thin veneer of Des Moines over Wadena lobe. Although of slightly coarser texture, the presence of Cretaceous shale in these peds suggests the presence of Des Moines lobe till.

High-chroma features were never observed in any soil classified as excessively drained. That observation is consistent with other published observations that excess drainage removes reaction products preventing accumulation and nodule formation (Tsukunaga 1932; Winters 1938; Clark and Brydon 1963). It is possible that other environmental conditions such as pH and chemical and mineralogical composition are not conducive for their formation.

Analysis of data from Official Series Descriptions

Data pertaining to high-chroma features were collected from Official Series Descriptions from soils mapped at and near the sample sites (Table 10). In

Table 10. OSD data for soils in and near sample sites where high-chroma features were found. The column labeled “WD” includes well-drained and moderately well-drained soils; the column labeled “PD” includes somewhat poorly drained and poorly drained soils. Numbers are average values of all horizons. Numbers in parentheses are ranges (low and high value). Classes were assigned ordinal numbers as follows: Horizons: A=1, B1=2, B2=3, B3=4, C=5. Abundance: few=1, common=2, many=3; Size: fine=1, medium=2, coarse=3; Contrast: faint=1, distinct=2, prominent=3. These numbers were then averaged and recorded in the table along with low and high values.

Variable	WD	PD
Site (County)	LI, KA, HE, CV	WR
Depth (cm)	81.2 (18,102)	42.0 (41,43)
Horizons	4.2 (B3) (B,C)	3.0 (B2) (A,B,C)
Hue	9.2YR (5YR,2.5Y)	8.9YR (7.5YR,10YR)
Value	4.8 (4,5)	4.3 (4,5)
Chroma	6.4 (4,8)	5.0 (4,6)
Abundance	1.5 (1,2) few to common	2.6 (1,3) common to many
Size	1.4 (1,2) fine to medium	1.9 (1,3) medium
Contrast	2.5 (2,3) distinct-prominent	3.0 prominent
Till	Loamy, calcareous, Late Wisconsin	Loamy, calcareous, Late Wisconsin
Geographic setting	Convex slopes of ground moraines.	Concave footslopes and toeslopes on moraines
Permeability	Moderate to moderately slow	Moderate to moderately slow

this section, the terms “concentrations” and “features” are used with the understanding that they do not refer specifically to high-chroma features.

As a general observation, an informal study done prior to this research found no consistent association between concentrations and lithologic, textural, or structural discontinuities, or potentially restrictive layers. Although feature size and abundance sometimes increased near those types of discontinuities, their presence was not sufficient or necessary for concentrations to be reported in the profile.

Of all the soil series mapped at the sampling sites, Wilno is the only series that lacks concentrations. Wilno is thought to have formed in colluvium. The colluvium may have lost the pore structure and other environmental conditions necessary to form high-chroma features. Any concentrations present at the time of disturbance may have been destroyed.

Average depth to first-appearance of concentrations in well-drained soils (actually to the top of the horizon containing concentrations) averages 81 cm compared to only 42 cm in poorly drained soils. Well-drained soils have a greater range of depth of first occurrence than do poorly drained soils. Concentrations appear as high as 18 cm in the well-drained Storden to as deep as 127 cm in well-drained Lester, while the first-occurrence depths in the two poorly drained soils differ by only 2 cm. Typical first-appearance in field samples from well-drained soils was between 50 and 100 cm with an average close to 75 cm, which is consistent with the OSD data.

The appearance of concentrations deeper in the profile in well-drained soils also becomes evident by comparing the horizons in which concentrations first appear. In well-drained profiles, they are found on average in a “deep” B3

and C, while in poorly drained soils they are found on average in a B2 horizon. Concentrations were found in an A-horizon only in a poorly drained soil.

Depth results are consistent with the usual expectation that soils experience less drying at greater depths below the surface so remain wetter for longer periods of time or experience a fluctuating water that favors preservation and growth of concentrations. Another possible explanation of depth results applies if features have been inherited. Features nearer the soil surface, especially the surface of well-drained soils, will experience greater weathering than those farther below the surface. Conditions of feature preservation and growth exist nearer the surface of poorly drained soils, maintaining the existence of inherited features closer to the surface than in well-drained soils.

Well-drained soils with concentrations typically are found in soils developed on calcareous loamy till of Late Wisconsin age, on convex slopes of ground moraines, with moderate to moderately slow permeability. Poorly drained soils with concentrations are found in calcareous loamy till of Late Wisconsin age, on concave footslopes and toeslopes on moraines, with moderate to moderately slow permeability. Landscape position is what would be expected and does not differ from findings in the field. The reporting of concentrations in soils on ground moraines is inconsistent with findings in the field, but field results are based on limited sampling. Permeability does not differ significantly between the well-drained and poorly drained soils at the sampling sites, so they would not be expected to differ significantly in their respective removal rates of weathering products.

Colors of concentrations between those in well-drained and poorly drained profiles differ primarily in chroma. Average hue varies little between

well-drained and poorly drained soils, but the range of hue in well-drained soils includes one additional Munsell page on either side, from 5YR to 2.5Y, a range of 3 pages, while poorly drained soils have a range of 1 page, from 7.5YR to 10YR. Average Munsell value is greater by 0.5 chip in well-drained soils. Average chroma is higher in well-drained soils by almost 1.5 chips. The average chroma of concentrations in poorly drained soils is 5, which does not meet the definition of high-chroma (chroma greater than 5). Maximum chroma in well-drained soils is 8, while the maximum in poorly drained soils is only 6. The higher chroma of concentrations in well-drained soils might be the result of a greater concentration of iron than in features in poorly drained soils.

Abundance, size, and contrast of concentrations differ between well-drained and poorly drained soils. Concentrations are more abundant in poorly drained soils (common-to-many compared with few-to-common) and tend to be slightly larger (medium compared with fine-to-medium). Only poorly drained soils have horizons containing “many” or “coarse” concentrations. Significantly greater abundance of concentrations and a tendency for slightly larger sizes in poorly drained soils suggests formation in a wetter environment, possibly close to a water table. Greater contrast of concentrations with the soil matrix in poorly drained soils may be the result of poorly drained matrix colors having lower chromas than those of well-drained soils.

In all likelihood, not all concentrations with high-chroma described in the OSDs are high-chroma features as defined in this study. As a result, making generalizations about high-chroma features on the basis of OSDs must be done cautiously. Also, the discussion here is based on a very limited number of OSDs. A comparative study of this type could be expanded to cover a broader

geographic area and incorporate data on many more soils and their hydromorphic features.

Physical properties

Plates 1–35 document some of the physical properties of high-chroma features, their halos, and enclosing peds. The images are intended to be studied and the captions read as part of the text of the Results and Discussion section. Unless otherwise noted in the caption, all images are of peds or features taken from the Kandiyohi County site. Samples from the Kandiyohi site are representative of all other sites; no differences in the appearance of features between sites were found.

Tables 11 and 12 summarize the physical properties of high-chroma features. A more detailed discussion follows the presentation of the color plates. Note that reporting Munsell hues to “non-standard” pages (such as 9YR rather than 10YR) and value and chroma to one decimal place reflects the precision available from the measuring and conversion of RGB to Munsell. Increased accuracy does not necessarily follow the increase in precision.

Table 11. Summary of physical properties of high-chroma features by site. Numbers in the main body of the table are percentages of high-chroma features that possess the given characteristic (property and category). Counties are listed in order of increasing hydromorphism.

Property	Category	Kandiyohi (%) n = 30	Wright (%) n = 20	Carver (%) n = 20	Lincoln (%) n = 20	Hennepin (%) n = 20	Total (%) n = 110
Class 1	—	7	10	10	5	5	7
Class 2	—	47	35	35	30	10	33
Class3	—	20	25	40	35	45	32
Class 4	—	17	25	0	20	25	17
Class 5	—	10	5	15	10	15	11
Color†	2.5YR	33	0	0	0	—	2
“	5YR	0	11	—	21	—	15
“	7.5YR	67	84	—	79	—	80
“	10YR	0	0	—	0	—	0
“	2.5Y	0	5	—	0	—	2
Halo	Present	93	60	20	70	80	67
Cortex	Present	30	5	10	25	25	20
Transition	Sharp	100	100	100	100	100	100
Size	<0.5	40	30	20	45	15	31
“	≥0.5 to <1.0	43	35	25	15	25	30
“	≥1.0 to <1.5	7	20	30	15	0	14
“	≥1.5 to <2.0	3	5	15	5	15	8
“	≥2.0 to <2.5	3	0	10	5	5	5
“	≥2.5 to <3.0	3	0	0	0	15	4
“	≥3.0 to <4.0	0	5	0	0	15	4
“	≥4.0 to <6.0	0	5	0	10	5	4
“	≥6.0	0	0	0	5	5	2
Elongation	<1.5	67	70	65	45	60	62
“	≥1.5 to <2.0	23	15	25	25	20	22
“	≥2.0	10	15	10	30	20	16
Roundness	Round	70	55	80	60	45	63
“	Mixed	20	25	10	20	5	16
“	Angular	10	20	10	20	50	21
Form	Regular	73	70	90	40	90	73
“	Partial	7	15	0	15	0	7
“	Irregular	20	15	10	45	10	20
Surface	Rough	17	10	5	25	15	15
“	Moderate	40	25	10	20	20	25
“	Smooth	43	65	85	55	65	61
Induration	Weak	90	85	65	90	75	82
“	Moderate	7	15	20	0	10	10
“	Strong	3	0	15	10	15	8
Impregnation	Intrusive	100	100	100	100	100	100
	Impregnative	0	0	0	0	0	0

† Color data were not collected on all features; no color data are reported on features from Carver and Hennepin Counties.

Table 12. Summary of physical properties of high-chroma features and halos by class. Numbers in the main body of the table are percentages of high-chroma features that possess the given characteristic (property and category).

Property	Category	Feature Class					Halo†					Total
		1	2	3	4	5	1	2	3	4	5	
Color†	2.5YR	0	2	0	0	0	—	—	—	—	—	—
“	5YR	0	1	0	5	0	—	—	—	—	—	—
“	7.5YR	0	13	12	5	2	—	—	—	—	—	—
“	10YR	1	0	0	0	0	—	—	—	—	—	—
“	2.5Y	0	0	0	0	0	—	—	—	—	—	—
Halo	Present	11	68	77	86	50	—	—	—	—	—	—
Cortex	Present	33	10	11	46	8	0	0	0	0	0	0
Transition	Sharp	100	100	100	100	100	0	0	20	11	40	13
“	Diffuse	0	0	0	0	0	100	100	80	89	60	86
Size	<0.5	44	35	31	30	8	100	74	63	37	80	61
“	≥0.5 to <1.0	11	29	29	17	75	0	21	22	37	0	24
“	≥1.0 to <1.5	11	23	9	13	8	0	5	15	26	0	13
“	≥1.5 to <2.0	22	3	9	13	0	0	0	0	0	0	0
“	≥2.0 to <2.5	11	0	3	9	8	0	0	0	0	20	1
“	≥2.5 to <3.0	0	3	6	4	0	0	0	0	0	0	0
“	≥3.0 to <4.0	0	3	3	9	0	0	0	0	0	0	0
“	≥4.0 to <6.0	0	0	9	4	0	0	0	0	0	0	0
“	≥6.0	0	3	3	0	0	0	0	0	0	0	0
Elongation	<1.5	78	55	71	52	58	—	—	—	—	—	—
“	≥1.5 to <2.0	11	29	14	30	17	—	—	—	—	—	—
“	≥2.0	11	16	14	17	25	—	—	—	—	—	—
Roundness	Round	67	58	66	70	50	0	0	33	0	33	15
“	Mixed	11	19	14	9	33	100	91	58	100	67	82
“	Angular	22	23	20	22	17	0	9	8	0	0	3
Form	Regular	56	74	71	83	67	0	50	82	100	33	74
“	Partial	22	6	9	4	0	0	0	9	0	0	3
“	Irregular	22	19	20	13	33	0	50	9	0	67	24
Surface	Rough	0	16	14	9	33	—	—	—	—	—	—
“	Moderate	44	35	17	13	25	—	—	—	—	—	—
“	Smooth	56	48	69	78	42	—	—	—	—	—	—
Induration	Weak	78	97	91	87	8	100	33	17	0	33	18
“	Moderate	22	3	6	13	25	0	58	78	91	67	76
“	Strong	0	0	3	0	67	0	8	4	9	0	6
Impregnation	Intrusive	100	100	100	100	100	0	0	0	0	0	0
“	Impregnative	—	—	—	—	—	100	100	100	100	100	100
“	Strong	—	—	—	—	—	0	8	16	16	15	12
“	Medium	—	—	—	—	—	0	12	44	63	23	32
“	Weak	—	—	—	—	—	10	28	13	16	0	15
“	None	—	—	—	—	—	90	52	28	5	62	40

† Color and halo data were not collected on all features.

Plate 1A. Ped with weakly expressed hydromorphology. Ped lacks hydromorphic features with low chroma. Two high-chroma features are readily visible. A number of smaller features scattered below the upper larger feature are barely visible. Dry ped color is 2.5Y 6.6/2..4. Frame width is 25 mm.



Plate 1B. Enlargement of the upper feature in Plate 1A, a Class 5 feature. Core color is 10YR 3.4/2.1; inner halo is 7.7YR 5.4/7.4 with areas of 6.4YR 3.9/6.2; outer halo is 1.1Y 6.9/4.5. The darker core has a more yellow hue than the inner halo surrounding the core. The Munsell value of the outer halo is influenced by the high value of the matrix, but the slightly redder hue and higher chroma suggest a relationship with the inner halo. The two white spots over the inner core are loose quartz debris from handling the ped. Frame width is 2 mm.

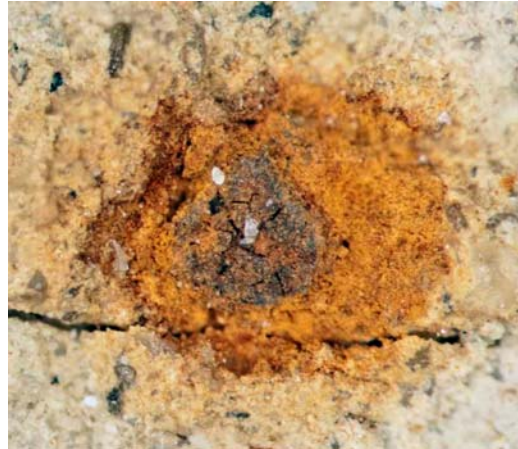


Plate 1C. Enlargement of lower feature in Plate 1A, a Class 4 feature. Inner core is 5.2YR 3.1/7.1; darker region to the upper left of the core is 8.0YR 1.7/4.0. Halo is 0.6Y 6.6/5.3. Again, the darker core areas have a more yellow hue than the lighter core area. Frame width is 3 mm.

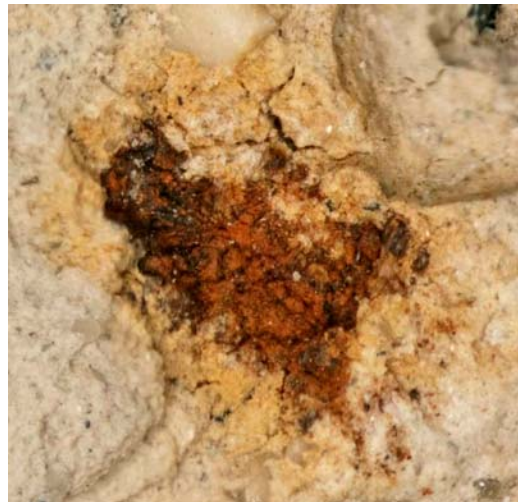


Plate 2A. Ped with strongly expressed hydromorphology from the Hennepin County site. Hydromorphism is manifested as medium-chroma reddish-brown and low-chroma gray mottling, and manganese concentrations at the bottom of the ped. Low chroma areas have a color of 9.1YR 6.1/1.9. Iron concentrations have a color of 8.8YR 5.5/3.6, while manganese concentrations are 7.0YR 3.6/2.8. Frame width is 50 mm.



Plate 2B. Enlargement of manganese concentrations in the lower center of Plate 2A. Iron and manganese typically appear in association with each other in peds with strongly expressed hydromorphology. Frame width is 15 mm.



Plate 3. A manganese-coated root channel in a ped from the Hennepin County site. Again, note the close association of iron and manganese.



Plate 4A. Ped with strongly expressed hydromorphology from the Hennepin County site. The most prominent feature is a root channel surrounded by a depletion, which is in turn surrounded by a ring of iron and manganese concentrations. Other areas of low chroma and some mottling are also visible.



Plate 4B. Enlargement of feature in upper center of ped of Plate 4A, a neoalban (A) with a quasiferran (F) and quasimangan (M). The alternating bands of iron and manganese concentrations resemble Liesegang rings. Frame width is 4 cm.

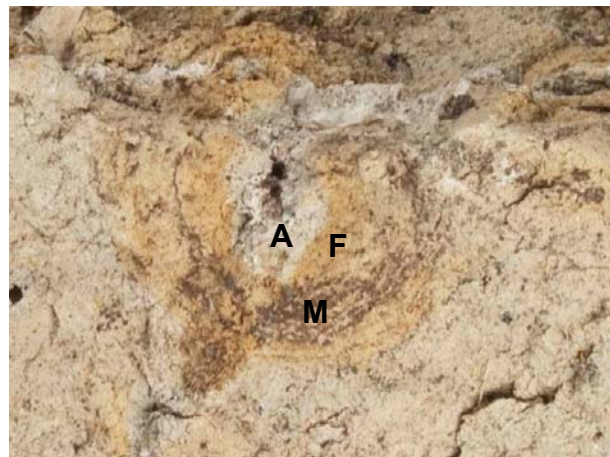


Plate 5. Another ped with moderately expressed hydromorphology from Carver County. Two intercalations, here recognized as areas of low chroma partially surrounded by yellowish brown iron concentrations with no pore or channel, are visible (I). The dark manganese concentration near the center is also surrounded by a yellowish brown halo. The chroma of ped matrix increased upon exposure to air.

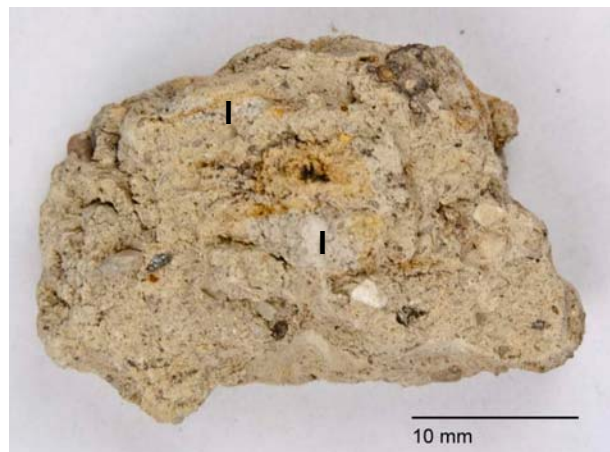


Plate 6. Ped from with weakly expressed hydromorphology showing high-chroma features and a platy structure.



Plate 7. Class 2 feature. Matrix color is 2.1Y 7.3/3.5. Feature is 8.8YR 4.6/8.7. Halo is 2.7Y 6.2/6.8. Smaller features to the right of the main feature have a similar color pattern. Such an extensive and well-defined halo is unusual. Frame size is 3 mm.

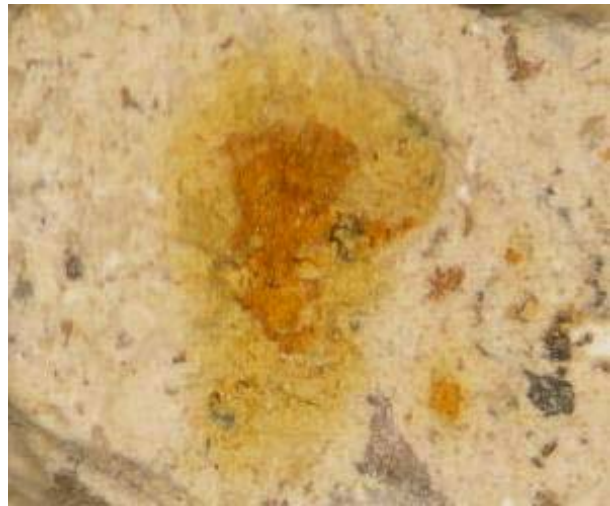


Plate 8. Class 2 feature with a partial cortex and full halo. Matrix color is 2.5Y 6.6/3.0. Feature color is 7.7YR 5.0/7.4 with a 7.2YR 4.4/6.2 cortex. Halo is 2.6Y 6.5/4.9. Frame width is 1 mm.

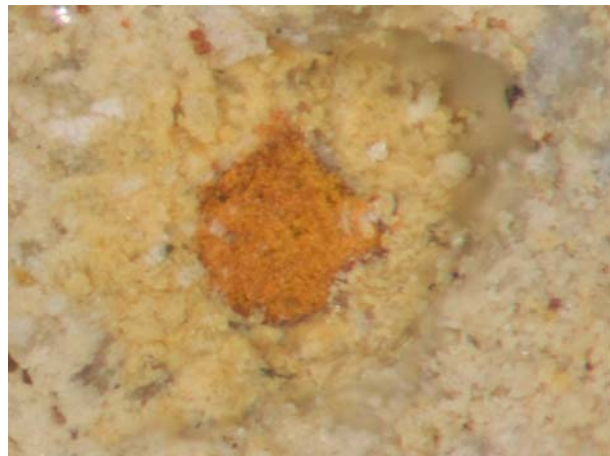


Plate 9. Class 2 feature. Matrix color is 5.3Y 8.0/2.6. Feature color is 7.6YR 5.6/8.6. Halo is 3.6Y 7.0 5.5. Dark zone surrounding the feature is a fissure not a cortex. Frame size is 1 mm.

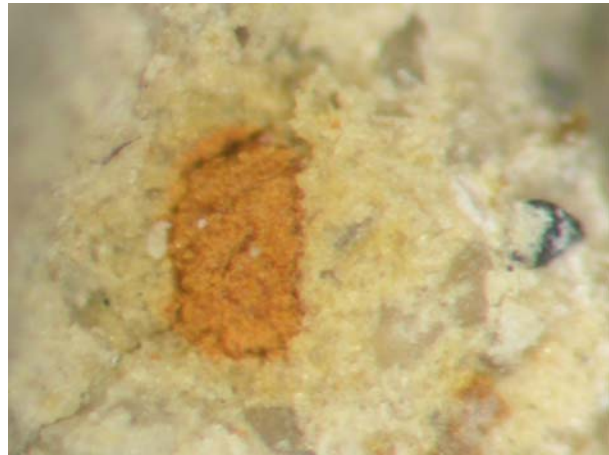


Plate 10. Class 2 feature. Feature color is 7.0YR 4.6/8.4. No distinct halo is distinguishable from the matrix. Surrounding color is 6.7Y 6.8/3.1, which is a yellower hue than is typical. Possibly the halo is extensive enough to cover most of the image frame or is indistinguishable from the matrix. Dark zone surrounding the feature is a fissure. Frame width is 2 mm.

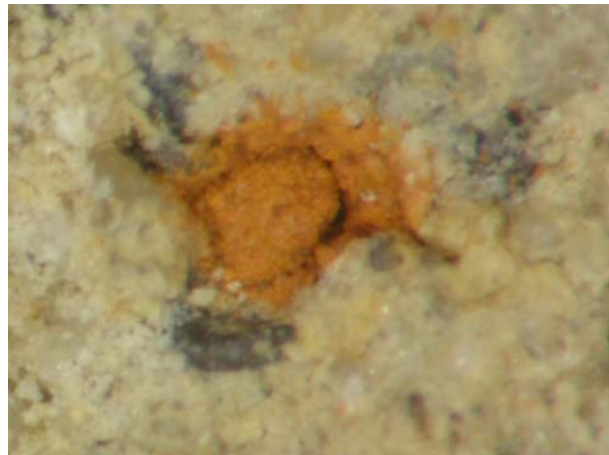


Plate 11. Class 2 feature. Some features remain intact when removed from the matrix. Note the crystalline or reticulate pattern characteristic of better cemented features. Feature color is 8.0YR 6.8/8.3. Small reddish inclusions are present with color 2.9YR 5.0/10.0. Although these features are better cemented than a typical high-chroma mottle, they are fragile as the small fragments above and to the right suggest.

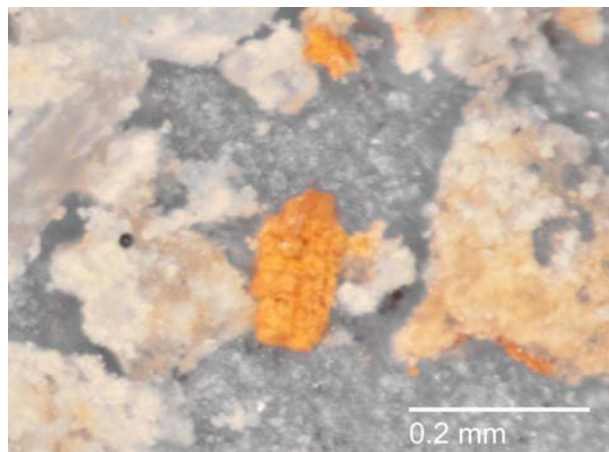


Plate 12A. Class 2 feature from a ped with weak-to-moderate hydromorphology. Matrix color is 1.9Y 7.0/4.2. Feature color is 7.4YR 5.2/8.4. Halo is 0.9Y 6.6/7.7. Note area of low chroma (9.4YR 7.7/2.0) in upper left and center.

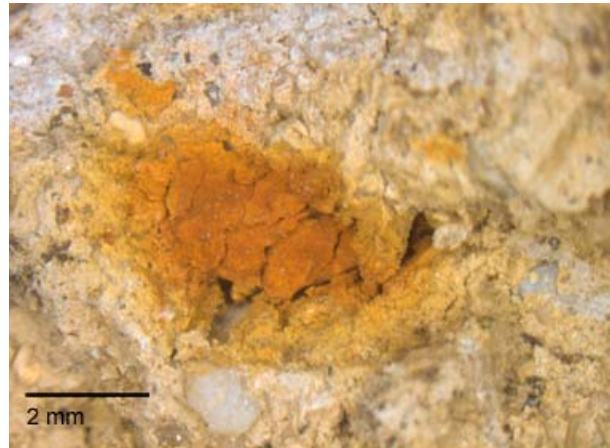


Plate 12B. Enlarged area of feature shown in Plate 12A. Loose structure and faint mottling are visible. Scattered white areas are loose fragments of matrix material from handling. Frame width is 2.5 mm.



Plate 12C. Detail from the center of image shown on Plate 12B. Loose structure is more evident. Mottling can be seen at the scale of the individual particle. Frame width is 1 mm.



Plate 12D. Another detail of Plate 12B. Individual dark fragments are visible. Frame width is 1 mm.



Plate 13. Class 3 feature with three square sides. This feature is somewhat cemented with a coarser texture, lacking the loose powdery structure of other features. Such features are still fragile and difficult to remove intact from the matrix. Matrix color is 1.9Y 7.7/2.7; feature is 6.4 YR 5.4/7.7 with darker mottles of 5.4YR 5.0/6.8; halo is 1.3Y 7.5/5.5. Feature is similar to the feature in Plate 11 above but with dark mottles. Bright area below feature is probably fractured quartz. Frame width is 1 mm.

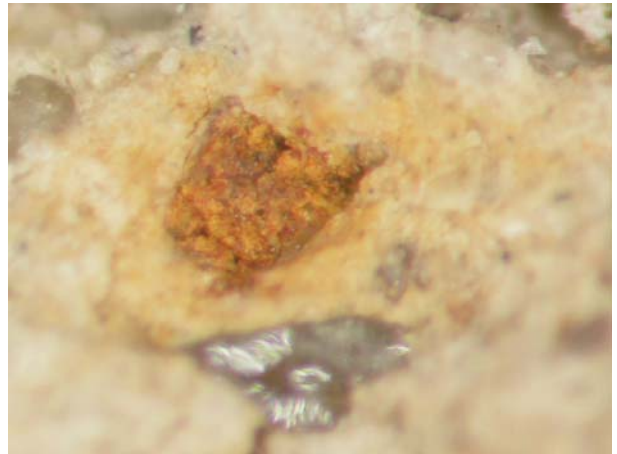


Plate 14. Class 2 feature of extreme red hue. Matrix color is 10YR 7.3/3.6. Feature color is 3.0YR 4.9/8.8. In some places, the transition between feature and matrix is very sharp with no halo while other places have a less pronounced transition and a weak halo. The feature has broken apart along the fracture line without scattering loose particles indicating that it is somewhat better cemented than is typical. Without being able to reconstruct the feature, it is difficult to say if the dark fragment to the upper left is related to the feature or to the matrix.

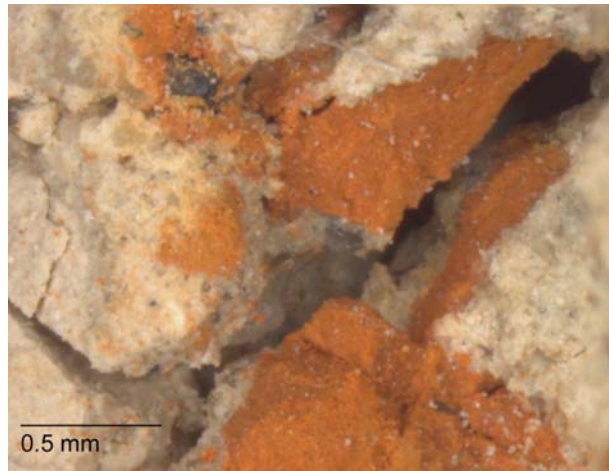


Plate 15. Class 2 feature similar to that shown in Plate 13. Matrix color is 0.1Y 7.8/3.2. Feature color is 3.8YR 5.4/8.1. Faint narrow halo is 8.8YR 7.5/4.8. The feature lacks depth so it may be a ped coating, a thin layer of oxide deposited in a void, or an outer remnant separated from a larger feature. Frame width is 1 mm.



Plate 16. Features labeled **A**, **B**, and **C** survived sieving and are present in a matrix of medium sand. Their identification as high-chroma features and not coated sand grains was confirmed after removal. **A** is a Class 3 feature (7.7R 5.0/8.4). Note the darker mottles within the feature. **B** is a Class 1 feature (1.8Y 5.6/7.1) lacking any dark material. **C** is unclassified. Dark blotchy areas on quartz and shale fragments as in **D** are manganese oxide coatings that effervesce in 3% hydrogen peroxide. Frame width is 2 mm.

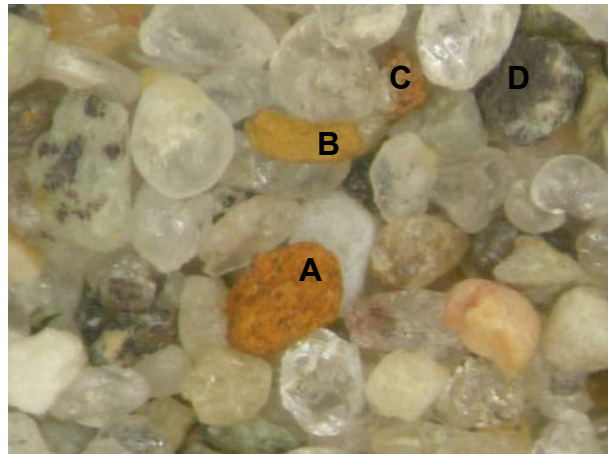


Plate 17. Section through a Class 5 feature. Darker round areas have color 2.7YR 5.1/2.1 with very small areas ranging in color from 7.1R 5.7/0.6 to 2.3R 5.5/0.5 to 3.1P 5.4/0.0. The color range might be the result of iridescence. Redder areas have color 5.6YR 5.6/8.5; yellow areas are 8.4YR 6.1/8.5. The exceptionally dark matrix surrounding the feature is the result of making the section thicker than 30 μm in order to preserve the feature. Epoxy has an amber to dark cast. Frame width is 1 mm.



Plate 18. Class 5 feature in thin section showing interior core of 5.1YR 4.6/2.0 with very small areas of 5.9R 2.5/2.6; red interior halo is 7.0YR 5.4/8.4; yellow exterior halo is 9.5YR 6.1/9.0. Dark matrix is from amber colored epoxy used to make the thick section as in Plate 17. Frame width is 1 mm.



Plate 19. Class 2 feature with an irregular boundary. Matrix color is 2.5Y 7.3/3.3. Feature color is 7.5 YR 4.8/8.9; darker mottled area near center of feature is 6.2YR 4.2/8.6. Halo color is 10YR 6.5/6.2. Frame width is 1 mm.

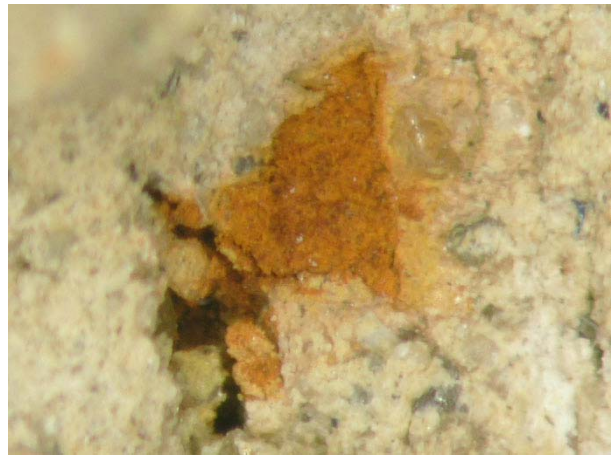


Plate 20. Class 2 feature with high elongation; round; smooth surface; and regular (elliptical) shape. Matrix color is 2.25Y 7.3/3.2. Feature color is 6.5YR 5.5/8.3. Narrow, faint halo has a color of 0.3Y 6.9/5.1. Frame width is 1 mm.



Plate 21. Class 2 feature with low elongation; round; medium surface; and regular (round) shape. Matrix color is 2.9YR 7.1/2.7. Feature color is 5.9YR 4.8/9.2. Feature lacks dark material. What appear as darker areas are packing voids or missing material. Small reddish spots scattered around the feature are loose feature material that was released when the ped was broken open. Halo color is 1.0Y 6.7/5.2. Feature in Plate 22 below is just out of the field of view to the right, less than 1 mm away. Feature diameter is 0.53 mm.

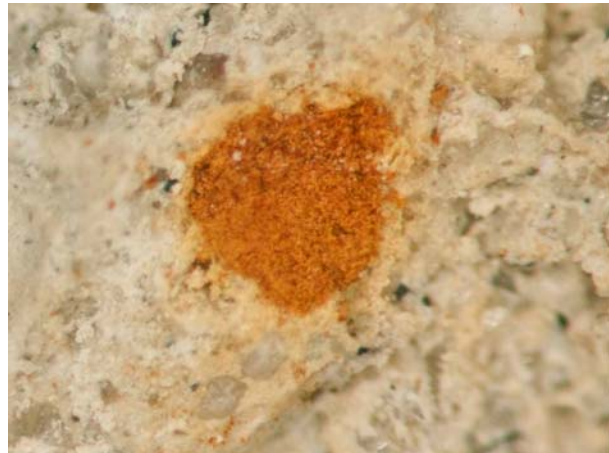


Plate 22. Matrix color is 2.4Y 7.0/2.1. Larger feature on the left is a Class 4 with interior color 7.6YR 4.5/5.3. Dark material is 5.2YR 3.2/4.4. Weak halo color is 2.5Y 6.6/5.0. Smaller feature to the immediate right has color 4.9YR 3.7/4.4 but lacks sufficient structure to permit classification. Smaller feature to the far lower right is an apparent Class 2 but small size makes classification unreliable. Note presence of a halo even on this small feature. The main body of the larger feature is about 0.25 mm diameter.

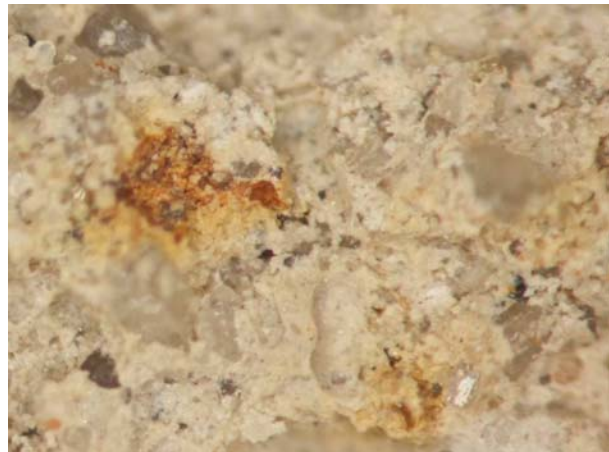


Plate 23. Class 4 feature. Matrix is 2.3Y 7.0/2.4; feature is 6.8YR 3.0/5.3 with dark areas of 8.6YR 2.5/4.2. Faint halo is 1.4Y 6.7/4.2. Classification as a 4 is made on the basis of the darker color of the feature. A partial rind of darker material is present, primarily at the very bottom and top of the feature. Again, the darker material has a yellower hue than the dominant reddish brown color. The halo incompletely surrounds the feature and extends into a small fissure above the feature. Diameter of feature is about 0.25 mm.



Plate 24. Class 2 feature with a fractured cortex. Matrix color is 2.6Y 6.9/3.0. Feature color is 8.8YR 4.9/7.4 with a darker mottle to the lower left. Cortex color is 8.8YR 3.9/5.3, the same hue as the feature. Halo color is 1.8Y 6.6/4.4. This feature is in the same ped as that in Plates 21, 22, and 23 Maximum dimension of the feature is about 0.3 mm.



Plate 25A. Class 4 feature with an unusual diamond shape. Matrix color is 2.6Y 7.2/3.4; halo is 2.7Y 6.6/6.1. The halo extends laterally (in this orientation) along what appears to be a crack or fissure. The half cylinder vertical groove is from a micro tool used to pry open the ped. Feature is approximately 2 mm wide.



Plate 25B. Enlarged area of the feature in Plate 25A. Feature color is 6.4 YR 4.9/8.5; dark areas are 9.8YR 4.2/5.8. Halo color is 2.8Y 6.7/6.0. Frame width is 2 mm.

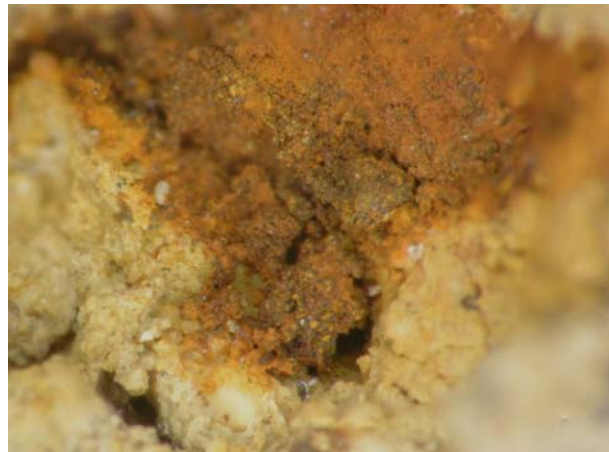


Plate 26. Feature color is 7.7YR 5.6/7.8; halo is 4.0Y 7.2/5.2. Dark material expresses a gradient of color, from lightest (1.8Y 3.8/2.3), to medium (2.6Y 3.2/1.2), to darkest (4.0Y 2.7/0.9). Munsell value and chroma both decrease along the gradient. Hue becomes more yellow as darkness increases (or more red as darkness decreases). This darkness trend suggests a weathering or transformation gradient. This feature resembles a Class 5 feature that has altered or is altering to a Class 4 (or a Class 4 that is altering to a Class 5). Frame width is 1 mm.

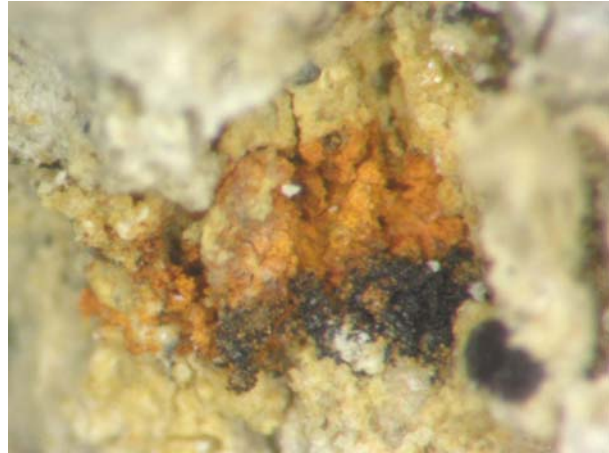


Plate 27. Unclassified. Matrix color is 2.1Y 7.7/2.6. The string of features is 0.3Y 6.8/6.8. The feature on the far right has a color of 7.2YR 5.5/8.6, more typical of high-chroma features but is connected to the main body of features by a narrow pathway of high-chroma material that is faintly visible. No halo is present on any of the features. The feature at the extreme lower right partially sitting in a shadow was not measured. Frame width is 15 mm.



Plate 28. Class 3 feature fully intact within the matrix. Matrix color is 2.6Y 7.6/4.6. Outer feature color is 5.8YR 5.5/7.2 partially covered by a 8.0YR 5.7/4.1 cortex. Halo is 0.7Y 6.4/6.3. Dark cortex has a yellower hue than the feature.



Plate 29. Smallest complete feature documented. Matrix color is 2.1Y 6.9/3.0. Feature color is 6.9YR 3.8/7.1. Cortex color is 4.4YR 2.2/5.5. Halo is faint and diffuse with color 2.6Y 6.8/4.3. A nearly complete cortex is rare.

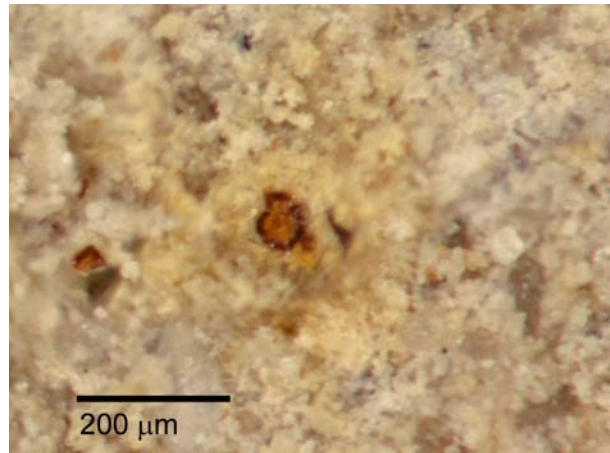


Plate 30. An unusual and unclassified feature removed from its ped. Matrix color, taken as the color of the material surrounding the feature is 1.1Y 8.3/3.8. The pinkish core is 5.1YR 6.6/4.5. Loose material surrounding the pink core and comprising the interior material in the two pieces in the upper right is 9.3YR 6.9/5.8. Some of the 5.1YR hue of a pink core is visible in those features.

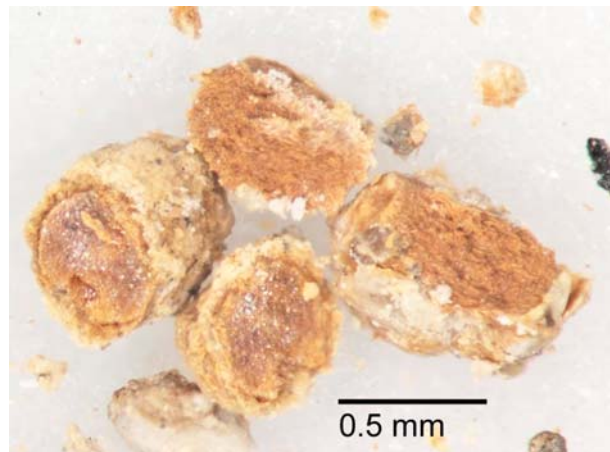


Plate 31. Class 5 feature removed from its ped. The outer coating color averages 5.4 YR 5.8/8.0. Redder areas are 3.8YR 5.2/7.8; orange-brown areas are 7.1YR 6.6/7.7. The dark core is 3.4Y 2.8/1.5. The core color of the fragment in the lower left is 9.4GY 3.5/1.4, an extreme yellow hue, but that color might be the result of a specular rather than a diffuse reflection off the broken surface.

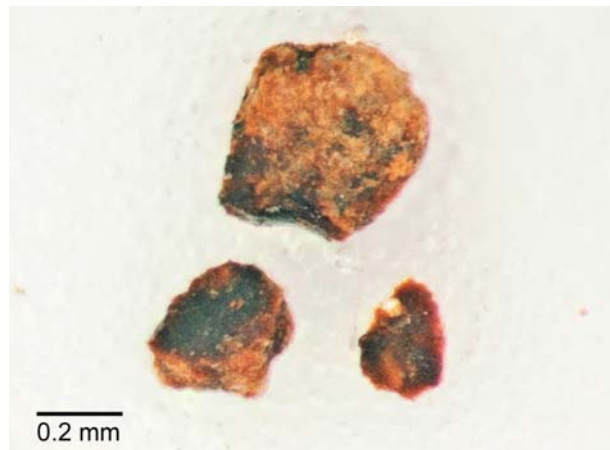


Plate 32. This feature in thick section has a metallic luster with color 5.6B 5.4/0.3 and a halo of 7.2YR 6.7/3.0. While not common, these types of features do appear occasionally. The mammillated boundary is unusual. The reddish halo surrounding the highly reflective metallic core may be oxidized material that has been lost from the outer rim of the feature. Frame width is 2 mm.

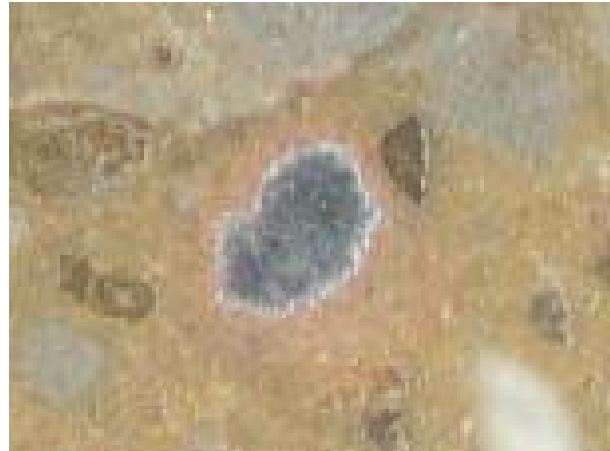


Plate 33. Result of ARS/NaOH stain test for dolomite/ankerite on a Class 2 feature from a ped with poorly expressed hydromorphology. Hues are red-purple (see main text). Rhombohedral shape of iron carbonates is visible on some particles.

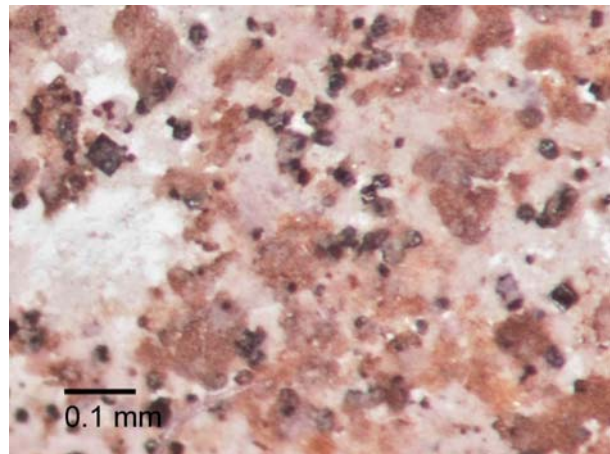


Plate 34. Class 3 feature stained with potassium ferricyanide without AAO pretreatment. The blue color developed after heating, which is indicative of siderite. Note rhomb shape of particle in the cluster at the lower center of the image. The nearly black color on the fragment in the far lower right is typical immediately after heating. Blue color becomes visible after the fragments are broken apart.

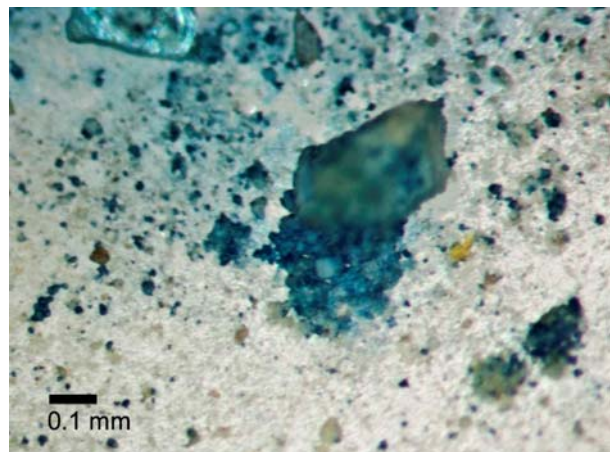


Plate 35A. A weak Class 3 feature as found in its ped. Slightly darker or redder mottles can be seen near the outer edges of the feature along the right and upper edges. A sharp boundary is clearly evident and separation cracks between the feature and matrix appear on the right and left sides of the feature. The halo is well-expressed and completely surrounds the feature.

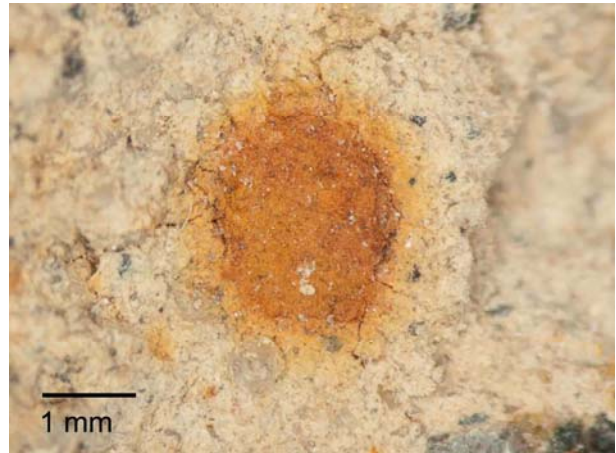


Plate 35B. Cavity remaining after removal of matrix material from the feature shown above. Loose material can be seen scattered around the cavity. Much of the halo was unintentionally removed along the sides along with the feature itself, resulting in a somewhat enlarged cavity. The cavity could be a mold of an inherited mineral fragment as in Plates 28, 30, and 31 (non-pedogenic hypothesis), a filled vesicle (pedogenic hypothesis), or a vug that was infilled after removal of soluble material (geode hypothesis).

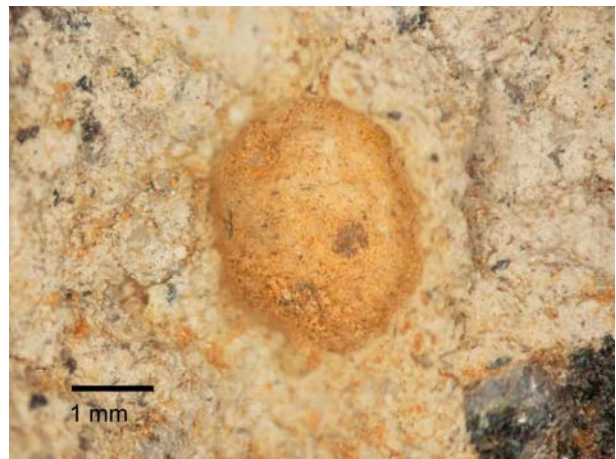


Plate 35C. Feature matrix material from the feature shown in Plate 35A. The feature was able to be removed nearly intact, an unusual occurrence. Material appears somewhat redder than in the ped, possibly because of surround effects of the white background. Mottles are visible as are some very small black fragments.



Feature

Size

Approximately 75% of the features measured were less than 1.5 mm in their largest dimension (Feret maximum). The range was from 0.2 to under 7 mm. The lower size limit may actually represent a resolution limit rather than a physical size limit imposed on the features. Actual feature sizes are probably understated by being measured in only two dimensions. It seems unlikely that a feature would break open exactly on its equator or a meridian. At least some smaller features, therefore, may actually be off-center sections of larger features. Some features, when extracted for analysis, appeared to be filled chambers or vugs that sometimes extended another 1 or 2 mm into the ped.

The largest features were found in peds with more strongly expressed hydromorphology. The trend is apparent in Table 11. Both Lincoln and Hennepin County sites contained features larger than 6 mm. Peds from Hennepin County contained features in all size categories except 1 to 1.5 mm. Peds with more strongly expressed hydromorphology retained the smaller features in addition to the larger features.

Intact nodules from 5 to 7 mm in diameter that had separated from the soil matrix were found at the Hennepin County site. They will be discussed later in more detail.

The end classes, Class 1 and Class 5, were consistently the smallest, never larger than 2.5 mm. The middle classes, Class 2, 3, and 4, contained the largest features.

Shape

Shape consists of the subcategory properties of elongation, roundness, form, and surface. Most features (62%) had an elongation of less than 1.5. Most (63%) also were round with a regular form. The properties of low elongation, high roundness, and a regular form, taken together, translate into the dominant shape being approximately round or spherical. Other features, based on combinations of elongation, roundness, and form, ranged from elliptical to square, to rectangular.

No consistent pattern of shape factors relating to hydromorphology or color class was apparent. Greater differences exist between sites than along a hydromorphic or color pattern classes.

Transition

All features have a sharp boundary with the matrix. This is true regardless of the degree of hydromorphology. In some cases, the feature and surrounding soil matrix or groundmass are separated by a crack or fissure.

Color

Feature color is more accurately considered to be a color pattern. Features themselves have an overall internal color that is, as is the case with soils generally, a visually weighted average of its individual colored components. While this measure of color is broadly useful, such an average fails to provide important clues about feature composition reflected in the variously colored components.

Feature color is most commonly 7.5YR 5/8 with some features having a redder hue of 5YR (Table 11). Internally, and visible only under a microscope, features often exhibit internal color variations ranging from subtle to obvious.

The more subtle variations of color can range from as red as 2.5YR with high chroma to as yellow as 10YR with low to moderate chroma. These variations appear as mottled patterns within the feature. Abrupt internal color changes result from the presence of black, white, and colorless materials that contrast with the primary feature color.

Areas of darkest color within the features range from black to a sometimes iridescent purple. They appear to be mineral fragments, possibly of the substrate material. Many of these fragments display striations on their surface.

Another aspect of feature color is the contrast between the feature and the soil matrix. Matrix colors are typically 2.5Y 7/2 dry and 2.5Y 5/3 moist resulting in a prominent feature-to-matrix contrast. Contrast is not a criterion for defining high-chroma features since high-chroma features could be present in a soil with a high chroma matrix thus giving a lower contrast. Identification of a feature as a high-chroma feature is based on absolute properties of the feature itself not on relative properties such as contrast. In the soils studied, however, contrast does provide a reliable indication of the presence of a high-chroma feature.

Color Class

Most features (65%) are Class 2 (33%) and Class 3 (32%) across all sites. The fewest number of features are Class 1 (7%) and Class 5 (11%). Class 1 and 5 often are difficult to see since they generally remain intact and coated with soil matrix material when the ped is broken open. They do not display the contrast with the matrix as do the other classes that make them more visible.

With only one exception, all color classes are found in peds from all sites. That exception is Class 4 in Carver County. Considering the relatively small sample sizes, it is perhaps more surprising that only one class of feature at one

site was not found. There is no theoretical explanation for the missing class, so its non-appearance seems to be attributable to sampling variation.

Class 1 and Class 5 features are evenly distributed across sites. Class 2 features show a decrease in abundance with increasing ped hydromorphism while Class 3 features show an increase in abundance with increasing ped hydromorphism.

Abundance estimates must be considered cautiously. Sampling of features from peds was not random, and some self-selection of classes on the investigator's part was inevitable.

Cortex

Twenty percent of all features observed have a cortex or rind. Nearly half of Class 4 features have a cortex (48%), while only 8% of Class 5 features, an adjacent category, have one. Although there appears to be no consistent trend in abundance across a hydromorphic gradient, the cortex tends to be thinner and less developed in features from peds with a more weakly expressed hydromorphism. A few features in peds with more highly expressed hydromorphism have a cortex that is composed of small, loose, individual grains or fragments that appear to surround the feature. These grains have a lower value and chroma than the feature itself but are often translucent, the darker color apparently originating from thin coatings on otherwise colorless grains.

Separation of the cortex from the feature was not practical before chemical analysis, nor was there an opportunity to examine them under the electron microscope. As a result, all samples submitted for chemical analyses include the cortex, if present, as well as the feature matrix.

Induration

Over 80% of features are poorly indurated, having a loose, poorly cemented internal structure. Features with loose structures are found across the hydromorphic gradient. Some features are somewhat better cemented than others. These will survive gentle sieving but still are fragile and not strongly cemented. In some cases, these better cemented features display a reticulate or accommodative crystalline pattern suggesting that they may be alteromorphic minerals inherited with the parent material. The presence of even a thin cortex might lend some stability to the feature. The other exception to the dominance of loose structure are a few large nodules found at the Hennepin County site. These large round nodules were found free of any peds and impregnated the soil matrix.

Moderately indurated features are those that could be just be removed from the groundmass intact. All classes contained some features that were considered moderately indurated. Despite being able to remove them from the ped, such features are still very fragile and easily broken up.

Two-thirds of Class 5 features are strongly indurated or hard. Of all other classes, only one Class 3 feature was classified as strongly indurated. That classification is questionable. With that exception in mind, only Class 5 features are strongly indurated.

Texture

Under the stereomicroscope, high-chroma features appear to be filled with rounded particles of relatively uniform size. Particle sizes range from coarse silt with a few particles of very fine sand, down to particles at least as small as 0.02 mm. Smaller particles may be present but are difficult to resolve under the low-

power stereomicroscope. Uniformity of particle size within features is confirmed by SEM, discussed later.

Some moderately indurated features often display a reticulate pattern that can be broken up into a collection of uniform particles of coarse silt or very fine sand.

Impregnation

All high-chroma features were classified as intrusive. Intrusive features form outside the groundmass with little or no incorporation of the soil matrix (Stoops 2003: 101, 103). The larger nodules from the Hennepin County site mentioned previously are impregnative, which seems to account for their greater induration. The higher clay content of the matrix compared to the feature is the likely cementing agent rather than an increase in the iron oxide content. Greater impregnation of the groundmass seems to correspond with an increase in feature size. These larger (exceeding 4 mm) and better impregnated features contain soft, loose, reddish-brown material and dark material typical of high-chroma features but that material is found only on the outside of the feature and serves to define the feature boundary. Despite being better cemented than high-chroma features, these features are somewhat fragile but are able to exist independently of the surrounding soil matrix. As free-standing nodules, these features are not included in the collection of observations reported in this study (Table 11) and are not considered high-chroma features since no information is available on the presence or absence of a halo or cortex or about the ped in which they were contained. They do represent an interesting variant and a possible extension of feature morphology worth including in the discussion and worthy of additional study.

Halo

Two-thirds of features in this study were surrounded by at least a partial halo. Only 20% of features from the Carver County site have halos. Features adjacent to areas of low-chroma lacked halos in those adjacent areas. Site-to-site differences in frequency and morphology are more pronounced than differences along a hydromorphology gradient.

Halos have a more yellow hue than the feature, most often 10YR when moderately to well-expressed, but when more weakly expressed are influenced by the color of the surrounding matrix. In such cases, the halo can be as yellow as 2.5YR but with a higher chroma than the matrix.

In general, their physical properties are more like the surrounding soil matrix than the feature itself. A gradient of induration sometimes occurs across the width of the halo, the halo being less indurated closer to the feature and more indurated farther from the feature. Otherwise, haloes have the same degree of induration as the soil matrix. All halos are impregnative, the soil matrix being clearly visible (per Stoops 2003:102). Halo composition will be discussed in the following section.

No trends across color classes are evident. Halos are most often present with Class 4 (83%), 3 (77%), and 2 (68%) features, while nearly 90% of Class 1 features have no halo.

Transitions with the soil matrix tend to be diffuse (86%) and sharp with the feature. All halos associated with Class 1 and 2 features have a diffuse boundary, while only 60% of halos associated with Class 5 features have a diffuse boundary.

Most halos (61%) extend into the soil matrix a distance of less than one-half the width of the feature. Only 14% of features have halos that extend more than one feature width into the soil matrix. Class 1 and Class 5 features have the narrowest halos overall, but a single Class 5 feature had the widest halo, between 2 and 2.5 times its associated feature width.

Nearly three-quarters of all halos follow the general shape of their associated feature. Irregular halos (24%) are those that are often interrupted by the presence of a mineral grain, usually quartz, adjacent to the feature boundary or in some cases, by a zone of low-chroma in the soil matrix.

Composition

Variable pressure SEM/EDS

Images from the Variable Pressure SEM revealed a difference in size and shape of particles between the feature and the surrounding matrix (Figure 10). The feature area was first located by the greater presence of iron compared to the surrounding areas as reported in real time by EDS. Particles within the feature are larger and of uniform size, averaging about 5 μ m. Particles in the matrix have a maximum size of about 5 μ m and have a greater range of sizes. Features appear to lack the smallest particle sizes that are present in the matrix. Associated pore spaces within the feature also are larger and more uniform. Particles in the feature also appear to be flatter and thinner with somewhat sharper, more angled corners, while the matrix particles are more rounded. An exception to this general pattern of size difference is the three larger grains of coarse silt that appear in the feature. The absence of larger particles in the matrix is most likely sampling variation. Larger grains are present in the features but typically do not

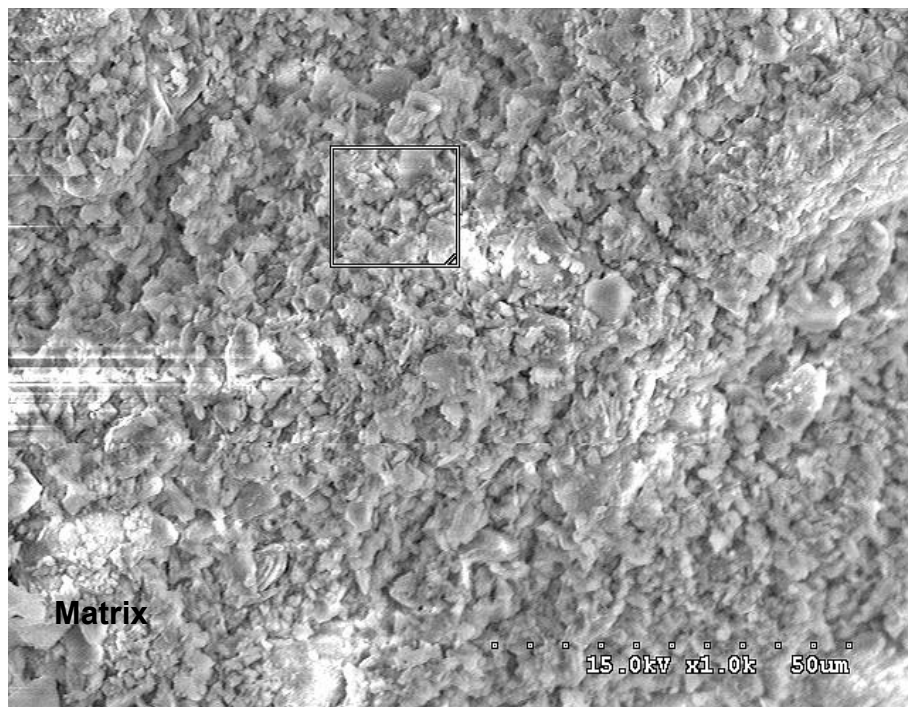
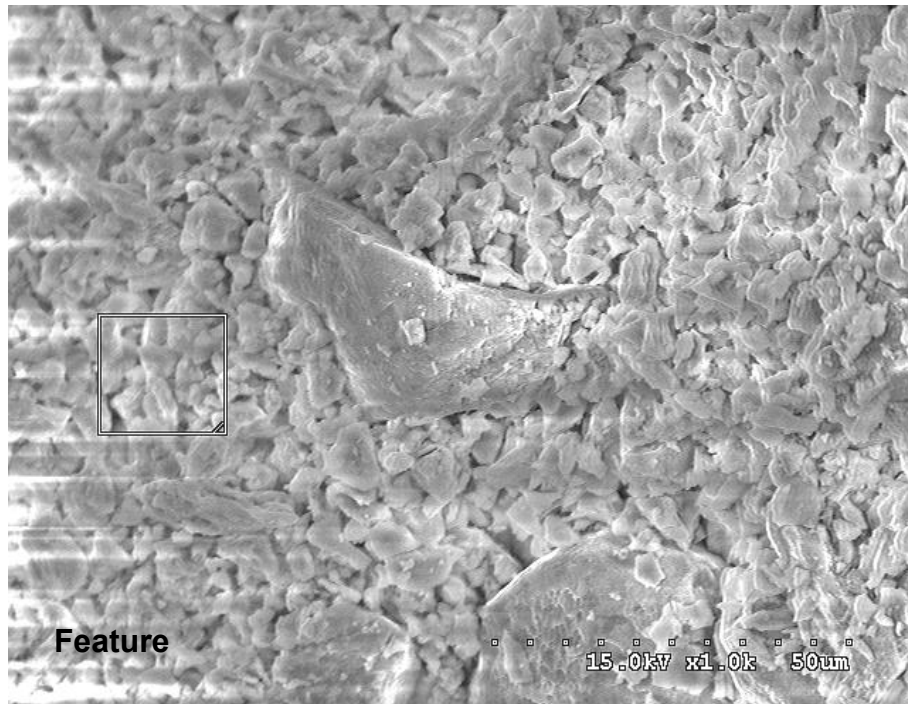


Figure 10. Upper image is on a high-chroma feature. Lower image is off-feature, on the matrix. The bright horizontal streaks near the edge of the images and the bright halos are from charging as a result of having no conductive coating on the sample. Sample is from Kandiyohi County site.

exceed coarse silt to very fine sand in size. Particles in the feature appear more rounded under the stereomicroscope than they do under the SEM.

EDS of the two areas studied under the VP-SEM found only slight differences in chemical composition. As expected, a higher Fe peak occurred in the feature area than the matrix area (Figure 11). All other peaks were considerably and consistently lower, including sodium, magnesium, aluminum, silicon, potassium, and calcium. Lower amounts of aluminum and silicon suggests a lack of clay minerals in the feature while the lower calcium suggests a lack of calcium carbonate. Since clays and carbonates act as cementing materials, their absence in the features could account for their loose, poorly indurated structure. No manganese or sulfur was found by EDS. These elements either are not present or are present in quantities below the detection limit of EDS.

Conventional SEM/EDS

Successful coating of a feature with platinum revealed an interesting morphology as viewed under the conventional SEM (Figure 12). Again, the particles in the feature are of a uniform size, with an average dimension of approximately 5 μ m, appear thinner and flatter, and with more angled corners than the surrounding material. At higher magnification, a surface texture appears (Figure 12, lower). These rods, about 50 nm in length and 10 nm in diameter, may be ferrihydrite coating on an unknown substrate such as a quartz or carbonate fragment. Similar morphologies of tubular deposits appear in the literature, which have been attributed to microbial activity (Zhang and Karathanasis 1997; Palumbo et al. 2001). These rods do not appear to be hollow tubes typical of microbial deposits. They also may be too small to be microbial,

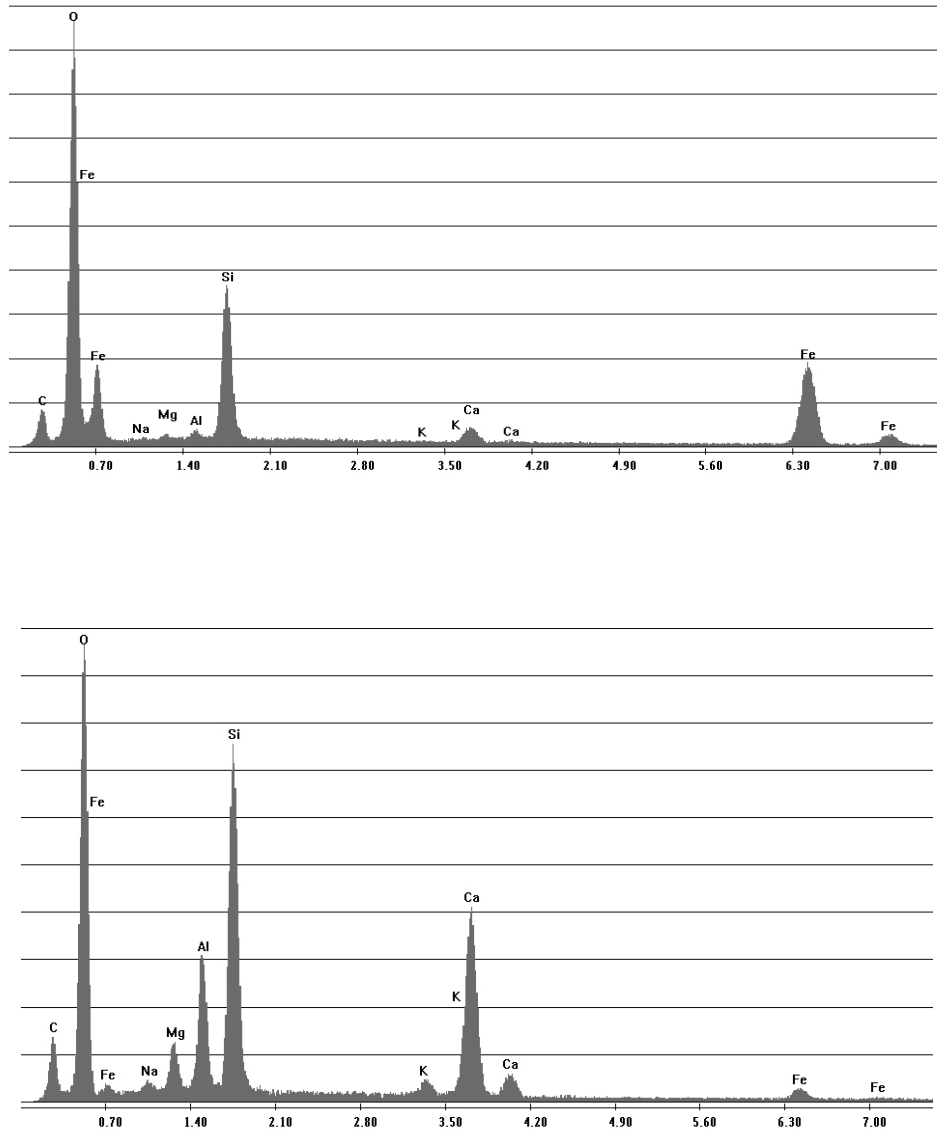


Figure 11. Upper spectrum is the result of an EDS analysis of the indicated area shown on the upper image (high-chroma feature) in Figure 10. Lower spectrum is the result of an EDS analysis of the indicated area shown on the lower image (matrix) in Figure 10.

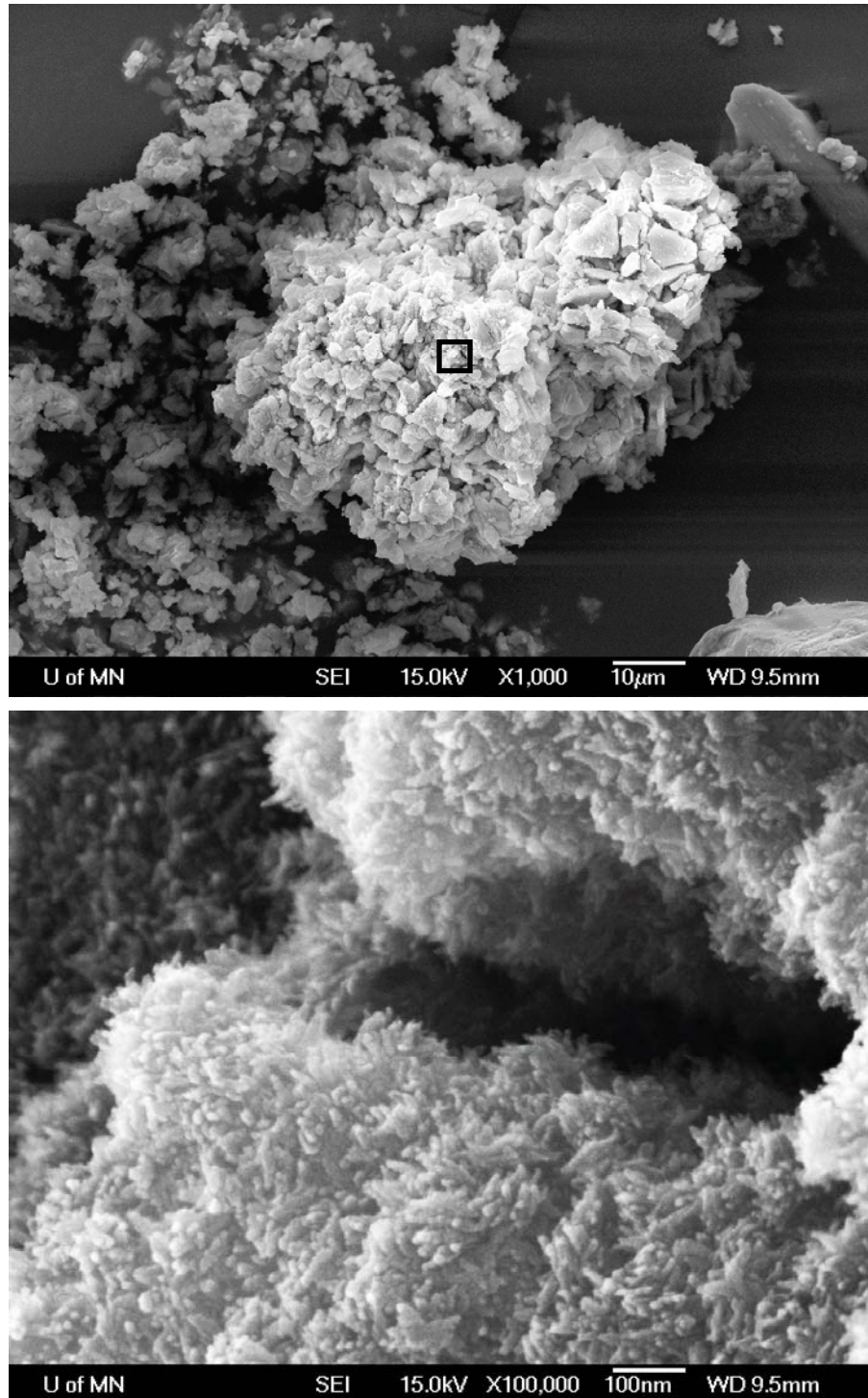


Figure 12. SEM image of high-chroma feature. Sample has been coated with 100 Å of platinum. Lower image is a magnification of the approximate area indicated in the upper image. Sample is from Kandiyohi County site.

their length being the approximate thickness of the Pt coating. The source of this surface morphology remains uncertain.

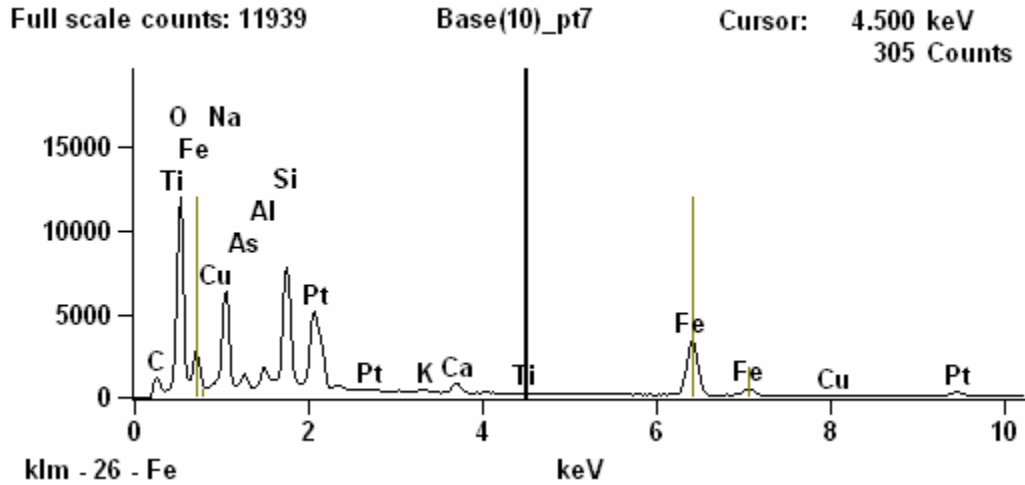
EDS of a similar sample again reveals difference in element content between locations (Figure 13). Higher Fe peaks are associated with lower magnesium, aluminum, silicon, and calcium peaks. A third sample, also coated with platinum, was investigated but the feature was not located with certainty. EDS of an area thought to be of the feature with longer count times, found additional elements of arsenic, copper, and nickel. Arsenic is known to be present in Des Moines lobe sediments.

Element mapping of a feature and its surrounding area confirmed other EDS results, most notably the depletion of calcium in the feature relative to the matrix. The element map is not shown.

TEM/ED

TEM revealed little information about the features. Only the largest features contained sufficient material to use the crush-and-float method but even then, recognition or identification of iron or manganese oxide particles or oxide coatings was not successful. The morphology of the material viewed in the TEM did not appear to be characteristic of any particular mineral (Figure 14, upper).

Electron diffraction (ED) revealed only a few weak reflections (Figure 14 lower). Identification of those reflections was ambiguous. Possible reflections are at 5.435, 4.529, 4.499, 4.476, 2.427, 2.205, and 1.542 Å. Although almost every mineral compared had at least one reflection that was an approximate match, no consistent set of matches were found, not even for quartz. The closest match overall was with romanèchite, a match that was not attempted until the results of



Thu Jun 11 14:25:11 2009

Filter Fit Chi-squared value: 11.835

Correction Method: Proza (Phi-Rho-Z)

Acc.Voltage: 15.0 kV Take Off Angle: 35.0 deg

Element	Atom %	Wt.%
C	4.05	9.87
O	31.27	57.14
Fe	19.15	10.03
Na	7.95	10.11
Si	5.83	6.07
As	1.06	0.41
Ca	1.01	0.73
Cu	0.54	0.25
Al	0.95	1.03
Ti	0.14	0.09
K	0.10	0.08
[Pt	27.93	4.19]

Total	100.00	100.00

Figure 13. EDS analysis of a feature *similar* to that in Figure 12. Pt peak is from the coating applied to the sample.

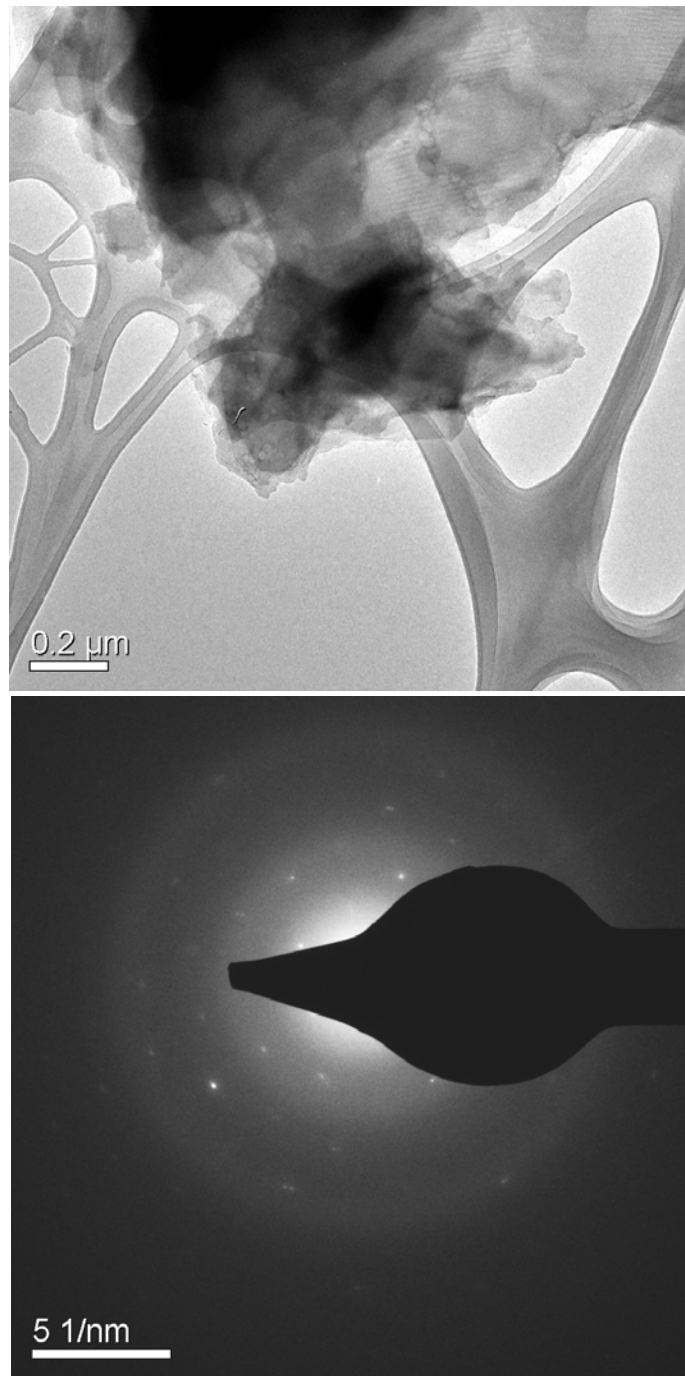


Figure 14. TEM image (upper) of a crushed fragment of material found in a feature. Bottom image is an electron diffraction pattern taken on the fragment.

the x-ray diffraction were obtained later. The closest d-spacings of romanèchite are at 2.415, 2.190, and 1.560 Å, not an altogether convincing match.

Manganese and sulfur were detected in a manganese nodule using EDS on the TEM in the Biological Imaging Center. The signal was very weak, however, and required an extended dwell time. No further investigation was undertaken.

X-ray diffraction

X-ray microdiffraction reported the possible existence of a variety of minerals. Quartz was the predominant mineral whose identity was virtually certain. The identity of most other minerals reported is less certain. Identification was based on a relatively large number of weak peaks rather than a few strong, diagnostic peaks. In general, peaks were narrow, an indicator that minerals present were crystalline but counts were low, an indication of low material quantity. Large reflections likely due to larger quartz grains interfered with some peaks. Hand grinding proved insufficient to reduce the particles to an acceptable size to avoid these reflections. Nevertheless, some patterns emerge. Summary results are given in Table 13.

The spectrum for Sample 1 was obtained by focusing the x-ray beam directly on an intact feature within the ped (Figure 15). Possible peaks that were identified include calcite, dolomite, quartz, and the iron (hydr)oxide minerals ferrihydrite, hematite, and goethite.

Only calcite, dolomite, hematite, and quartz were tentatively identified in the red material of Sample 2A. Sample 2B was material adjacent to Sample 2A but was described as less red and more brown in color, possibly from a halo. Sample 2B gave nearly identical peaks as Sample 2A but counts were

Table 13. Micro-X-ray diffraction results.

Sample	Reported Peaks	Sample	Reported Peaks	Sample	Reported Peaks
1	Calcite CaCO ₃ Dolomite CaMgCO ₃ Ferrhydrite Fe _{1.56} O _{2.3} (OH) _{0.08} Goethite FeOOH Hematite Fe ₂ O ₃ Quartz SiO ₂	4A	Calderite (Mn ⁺² ,Ca) ₃ (Fe ⁺³ ,Al) ₂ (SiO ₄) ₃ Magnetite (Fe ⁺² Fe ⁺³) ₃ O ₄ Quartz SiO ₂	6A	Dolomite CaMgCO ₃ Magnetite (Fe ⁺² Fe ⁺³) ₃ O ₄ Quartz SiO ₂ Rambertite MnS Reinhardbraunsite Ca ₅ (SiO ₄) ₂ (OH,F) ₂
2A	Calcite CaCO ₃ Dolomite CaMgCO ₃ Hematite Fe ₂ O ₃ Quartz SiO ₂	4B	Ankerite CaMgFe ⁺² Mn ⁺² (CO ₃) ₂ Fenaksite (K,Na)Fe(Si ₄ O ₁₀) ₂ (OH,F) Ferrhydrite FeO(OH) Hematite Fe ₂ O ₃ Quartz SiO ₂	6B	Dolomite CaMgCO ₃ Ferrhydrite Fe ₅ O ₇ (OH)·4H ₂ O Magnetite (Fe ⁺² Fe ⁺³) ₃ O ₄ Quartz SiO ₂ Rambertite MnS Reinhardbraunsite Ca ₅ (SiO ₄) ₂ (OH,F) ₂
2B	Calcite CaCO ₃ Dolomite CaMgCO ₃ Hematite Fe ₂ O ₃ Quartz SiO ₂	4C	Copper sulfide CuS ₂ Ferrhydrite Fe ₅ O ₇ (OH)·4H ₂ O Gedrite (Fe,Mn,Al)Al ₂ Si ₆ O ₂₂ (OH) ₇ Isocubanite CuFe ₂ S ₃ Manganese sulfide MnS Quartz SiO ₂	6C	Copper Sulfide CuS ₂ Ferrhydrite Fe ₅ O ₇ (OH)·4H ₂ O Ferrhydrite FeO(OH) Goethite Fe ⁺³ O(OH) Magnetite (Fe ⁺² Fe ⁺³) ₃ O ₄ Quartz SiO ₂
3A, 3B, 3C1	Calcite CaCO ₃ Dolomite CaMgCO ₃ Donpeacorite MgMnSi ₂ O Graphite C Hematite Fe ₂ O ₃ Quartz SiO ₂	5	Boron Iron BFe ₂ Calcite CaCO ₃ Copper Iron Sulfide CuFeS ₂ Cubanite CuFe ₂ S ₃ Quartz SiO ₂		
3C2 = 3C1+	Ankerite CaMgFe ⁺² Mn ⁺² (CO ₃) ₂ Boracite Mg ₆ B ₁₄ O ₂₆ Cl ₂ Na,Ca,MgF Romanèchite BaMnOH ₂ O				

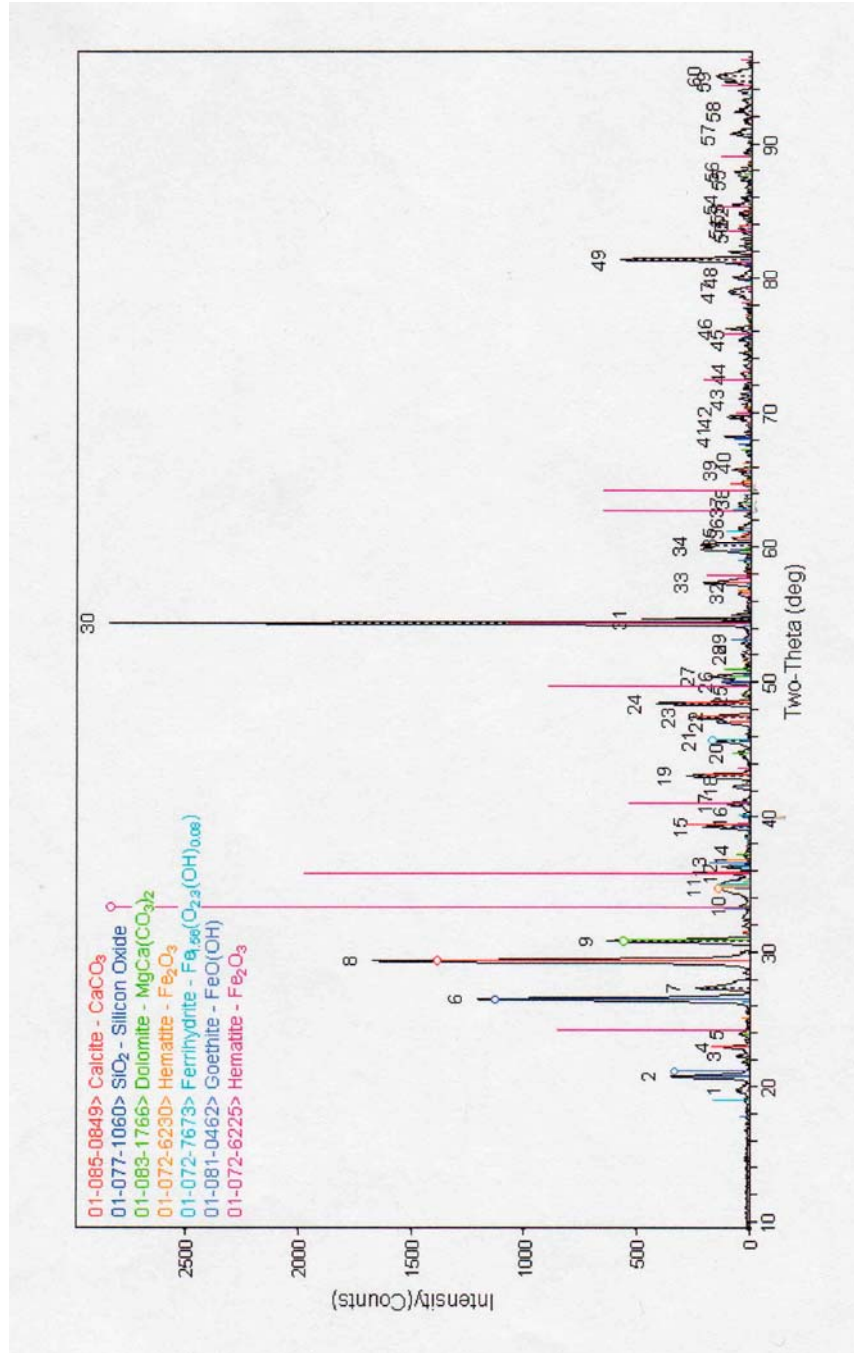


Figure 15. Micro-XRD spectrum from a high-chroma mottle.

substantially different, an indication that the relative quantities of calcite and dolomite are lower in Sample 2A than in Sample 2B (Figure 16).

Three samples of loose, powdered material were removed from a feature and analyzed (3A, 3B, 3C1). All three contained quartz, dolomite, calcite, hematite, graphite, quartz, and a mineral named donpeacorite, a magnesium-manganese silicate. An extended-time analysis (Sample 3C2) resulted in the tentative identification of ankerite, boracite, and romanèchite in addition to the minerals identified in Sample 3C1 (Table 13).

Sample 4A was a yellow feature with black spots. From the description it could be a Class 1 feature but was analyzed before the color pattern classification system was developed. Initial analysis tentatively identified calderite, magnetite, and quartz. Extended-time analysis (15 hours) of a high-chroma feature (Sample 4B) reported possible ankerite, fenaksite, ferrihydrite, hematite, and quartz. A feature described as reddish-brown (Sample 4C) was unusual. In addition to quartz and ferrihydrite, peaks for the sulfide minerals, copper sulfide, manganese sulfide, and isocubanite, and a manganese silicate mineral, gedrite, were identified (Table 13). Again these identifications are tentative and are based on only a few weak peaks.

Sample 5, identified as a red area, may have been composed of iron sulfide mineral cubanite and a generic copper iron sulfide, in addition to quartz and calcite (Table 13).

Sample 6A was a yellow feature similar to Sample 4A but with a more extensive black area on the margin. Sample 6B was taken just to the left of Sample 6A. Again, quartz and dolomite were present. The manganese sulfide mineral, rambergite, was also identified. Sample 6C was a black feature with

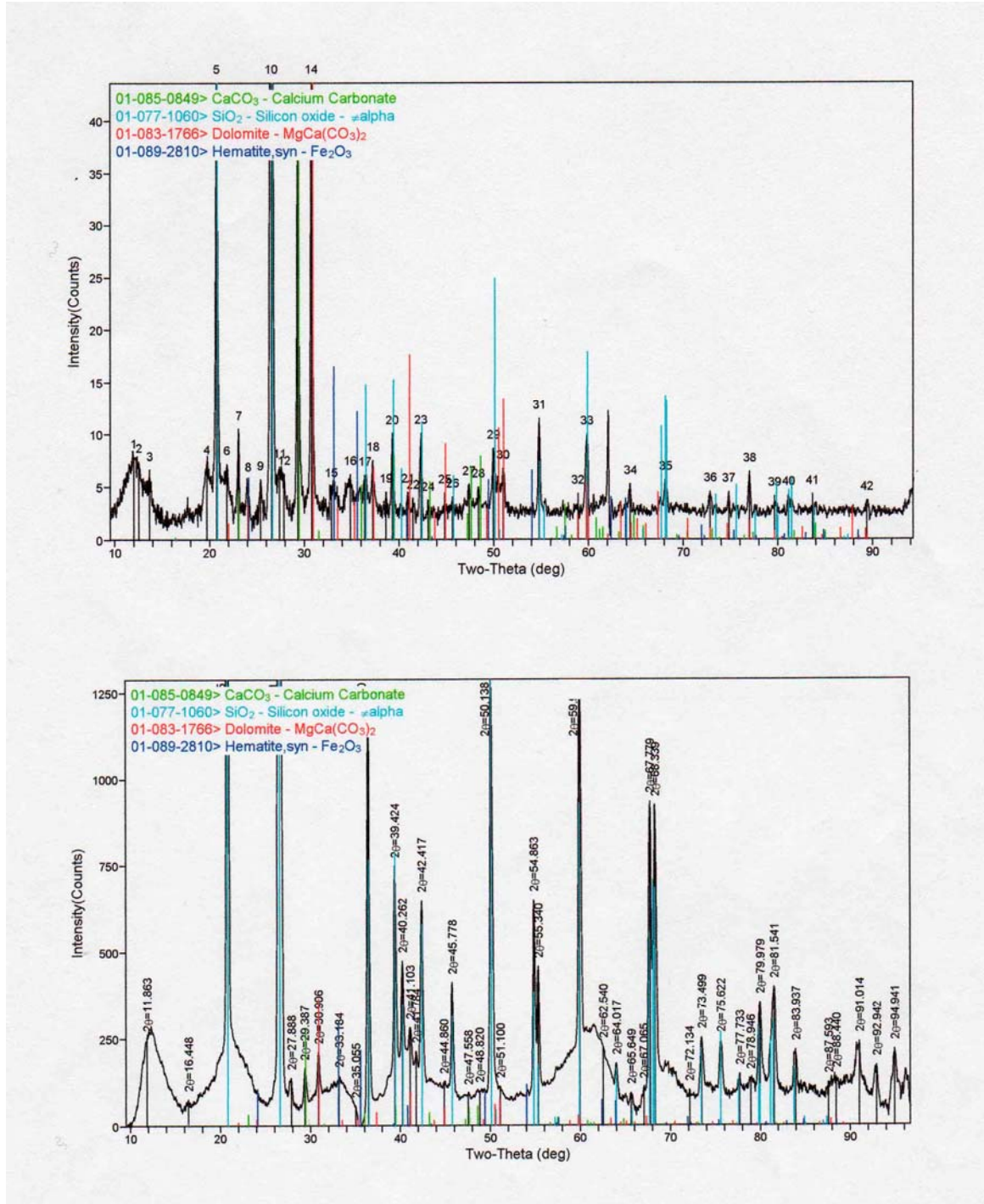


Figure 16. Micro-XRD spectra from Sample 2A (above), a red area, and Sample 2B (below), a more brownish colored area. Samples are very similar in composition but appear to differ in quantity based on relative counts.

small red spots on the surface. All three subsamples from Sample 6 appeared to contain quartz and magnetite and one of two forms of a metal sulfide mineral, either manganese or copper. Ferrihydrite (two forms), goethite, and dolomite were tentatively identified in two of the three samples.

All samples analyzed contained quartz and most contained a carbonate mineral, either calcite, dolomite, or both, and in some cases possibly ankerite. The composition of features varied considerably. All features contained some species of iron mineral, usually ferrihydrite, goethite, hematite, magnetite, or a combination. A few samples appeared to contain manganese minerals, a few sulfide minerals, and two samples possibly contained manganese sulfide as rambergite. Graphite, tentatively identified in Sample 3C1, was reportedly found in manganese deposits in Brazil by Spector (1941). Pyrite was not reported in any of the samples.

Some of the dolomite peaks reported on shorter scans may have been ankerite whose presence was revealed on longer scans. Some peaks are also close to lepidocrocite peaks but lepidocrocite was never reported even in the 15-hour scan that reported ankerite as well as ferrihydrite and hematite (Sample 4B).

None of the scans produced convincing evidence of the presence of the minerals identified, with the exception of quartz and possibly the carbonate minerals dolomite and calcite. This evidence, even though weak, when coupled with other supporting data and an explanatory hypothesis, becomes more significant and worthy of consideration in subsequent interpretations.

Raman spectroscopy

Raman spectroscopy produced the best results using synthetic or a relatively pure natural material. A Raman spectrum of obtained from a quartz

grain found within a high-chroma feature is shown in the upper spectrum in Figure 17. The closest matches obtained from the sample compared to a spectrum obtained from the RRUFF™ database (Downs 2006) implemented in the software CrystalSleuth (expected peaks are in parentheses) are at 211 (209), 404 (400), 468 (467), 699 (697), 802 (809), 1163 (1167) relative cm^{-1} , with expected but unmatched peaks at 133 and 358 relative cm^{-1} . A sample of synthetic goethite is shown in the middle spectrum of Figure 17. Matches are at 250 (248), 304 (302), 398 (404), 484 (482), 548 (548), 1002 (1000) relative cm^{-1} , with one expected peak at 211 relative cm^{-1} missing from the sample. The bottom spectrum in Figure 17 shows a more typical result of an analysis of a high-chroma feature. Fluorescence has overwhelmed any peaks that might otherwise be present except the peak at 404 relative cm^{-1} . Quartz and goethite reference spectra from CrystalSleuth are shown in Figure 18.

Methods used to eliminate or reduce fluorescence were unsuccessful. No useable spectra were gathered from either the longer-wavelength Krypton laser or with FT-Raman. FT-Raman produced a very nice spectrum of quartz on a sample of ASTM standard silica but no peaks were identifiable from spectra of natural samples.

Acid Ammonium Oxalate

Exposure to acid ammonium oxalate (AAO) for two hours resulted in the loss of approximately 50% of the oxidized material in Class 2, 3, and 4 features. This poorly crystalline material would most likely be ferrihydrite and possibly poorly crystalline goethite. Class 5 features produced the least color change. No trend across a hydromorphic gradient was found.

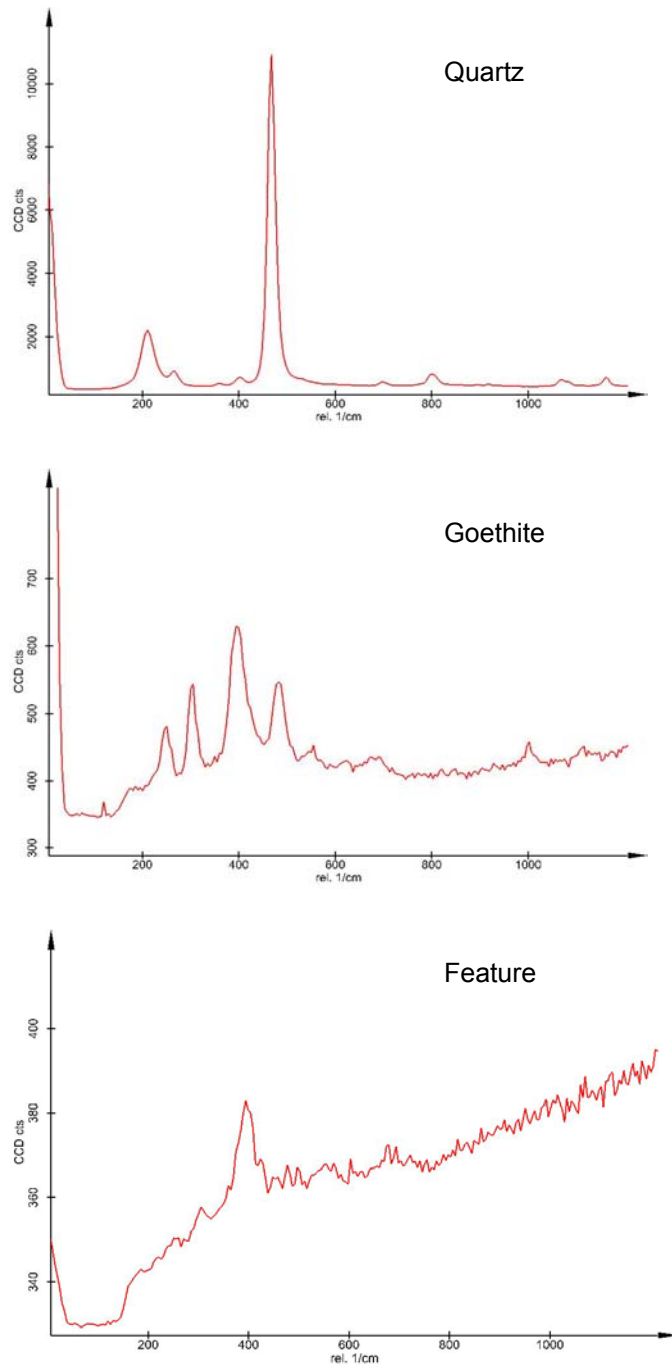


Figure 17. Raman spectra at 514 nm. Upper spectrum is from a grain of natural quartz found in a high-chroma feature. Middle spectrum is of *synthetic goethite. Some mild fluorescence is present. Bottom spectrum is of a high-chroma feature showing the effects of fluorescence. The characteristic strong goethite peak at 404 rel. 1/cm is the only peak not masked by fluorescence.

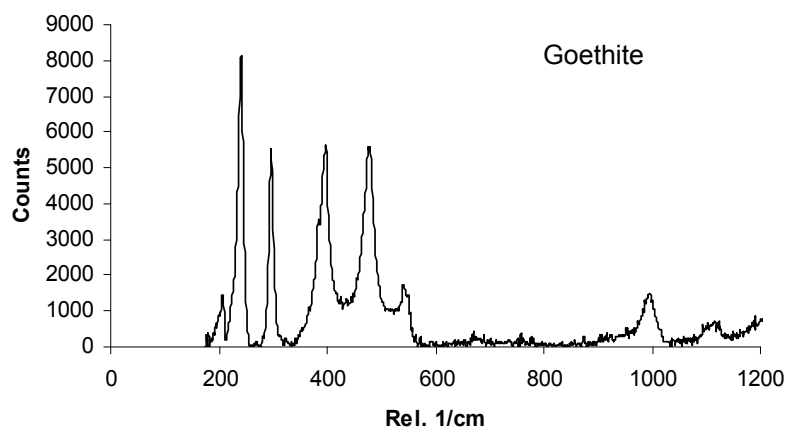
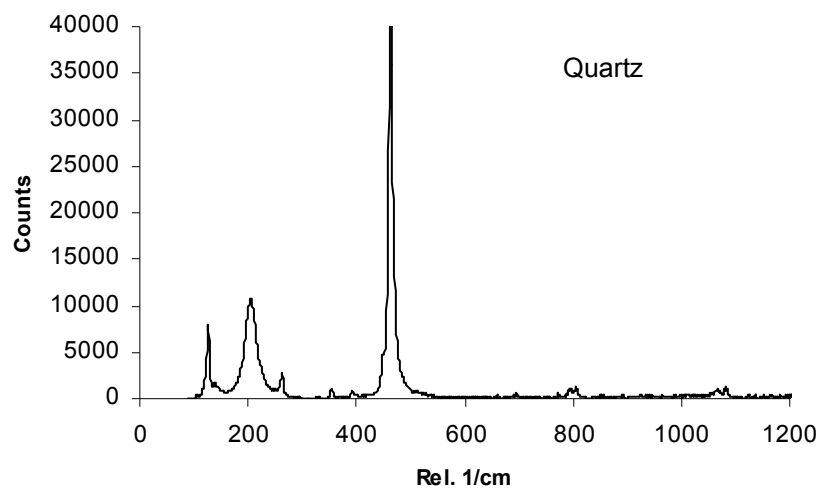


Figure 18. Raman reference spectra from RRUFF data files as implemented in CrystalSleuth software. Upper spectrum is a quartz reference at 514 nm. Lower spectrum is a goethite reference also at 514 nm. Comparison is with corresponding spectra in Figure 17.

The addition of ascorbic acid and heat removed most of the remaining material after the initial two-hour exposure, with the exception of the darkest material and crystalline silicate mineral grains.

AAO overnight resulted in most cases in the loss of nearly all the oxidized material in these features. Placing the AAO saturated sample under light and heat also removed nearly all the oxidized material, usually in less than two hours.

Of additional interest, however, was the observation that nearly all of the small individual grains that were cleared of oxides with AAO became soft and gelatinous after just two hours' exposure to the AAO solution. Only a very few grains remained hard and crystalline. These appeared to be silt or very-fine-sand size quartz. Upon drying, the soft fragments clump and consolidate somewhat, becoming a brittle, translucent mass that can be easily broken apart. This material does not react with or dissolve in dilute HCl even when heated so is unlikely to be a carbonate. They might be a form of amorphous silica, sufficiently crystalline to be identified with XRD but yet slightly soluble. The fragments do not dissolve in 5% NaOH, however.

Inductively Coupled Plasma (ICP)

Results are reported and plotted as an "enrichment factor" (Figure 19). After correcting the solution concentration against a blank, the enrichment factor is found by dividing the concentration of an element in the feature or in the halo by the concentration of that element in the matrix, minus 1. A depletion factor of zero means that the concentration of a particular element is the same as that of the matrix. A depletion factor less than zero means that the feature is depleted in that element relative to the matrix. An enrichment factor of -1 means that the

element was not detected in the sample. An enrichment factor greater than zero means that the feature is enriched in that element relative to the matrix. No data for Class 5 features or for halos associated with Class 1 features were collected. All Class 1 features lacked halos.

Zinc is a special case. Its concentration in the blank was very high (1079 ppm), which may have been the result of contamination. The corrected concentration of zinc in the matrix would be 0 ppm, since its concentration in the blank exceeded that in the matrix and concentration cannot be below zero. A zero concentration of zinc in the matrix would result in an infinite enrichment factor for features and halos. To avoid this situation, zinc was not corrected relative to the blank. Instead, its uncorrected value was standardized to the matrix value. Since zinc was reported in the C-horizon till in Kandiyohi County (Thorleifson et al. 2007), an assumption of its presence in the matrix seemed more justified than one of absence. Zinc appears to be highly concentrated in Class 4 features and Class 2 and 4 halos. This is possibly the result of contamination from brass sieves used to recover some features for analysis. Small fragments of brass in other sieved samples had been identified in other samples by the presence of copper and zinc using SEM/EDS. The enrichment of copper in Class 4 features correlates with the possibility of brass contamination. However, the enrichment of zinc in the haloes of Class 2 and 4 features is more difficult to explain as contamination since these samples were not sieved, nor was the blank. Because of the uncertainty of the zinc data, the results for zinc were discarded as were the data for copper for Class 4 features.

Class 1 features are significantly different in from classes 2, 3, and 4, being enriched in Cu, P, S, and slightly enriched in zinc compared to the matrix. Given

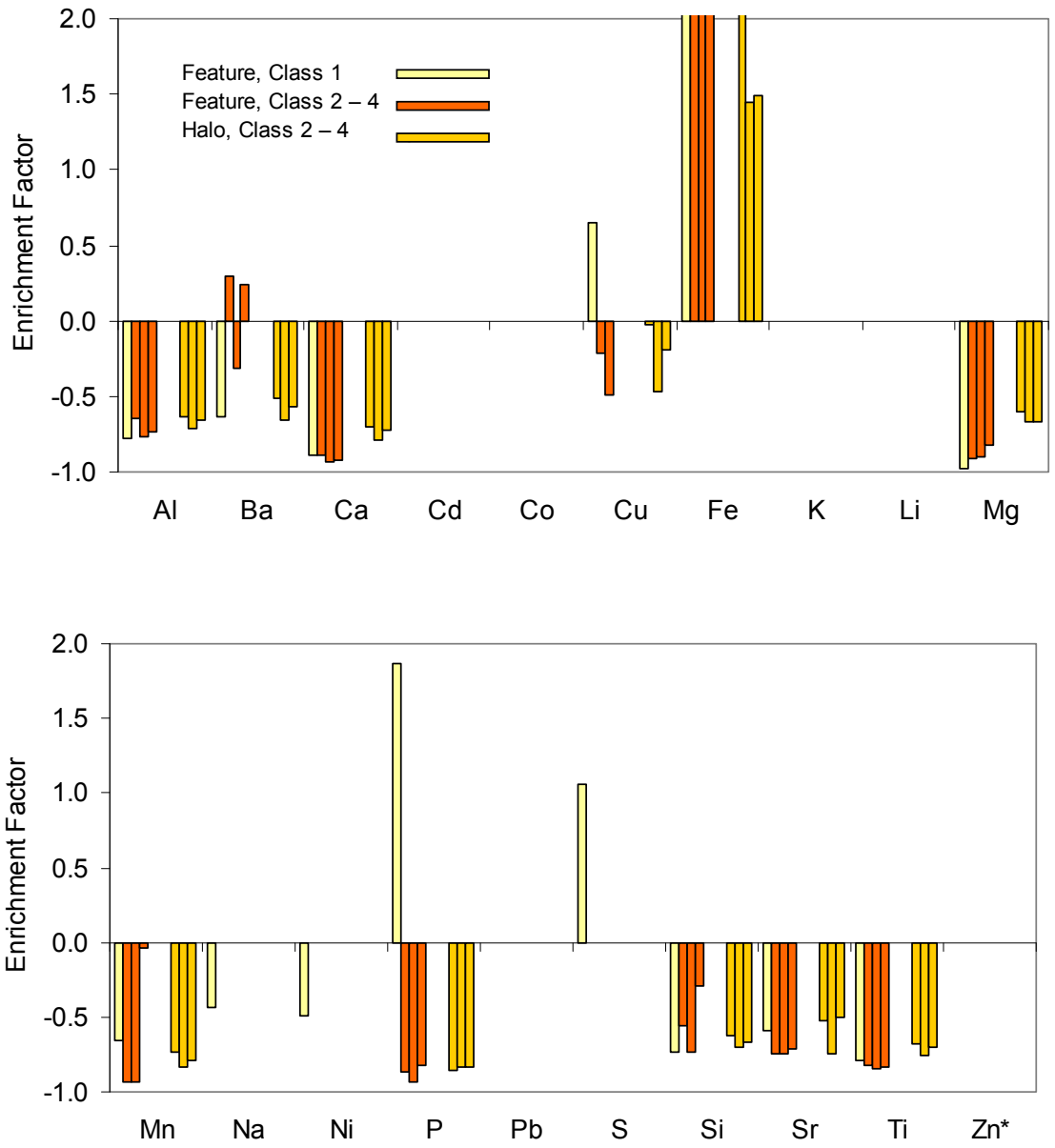


Figure 19. Enrichment factors from ICP results. Elements with factors greater than 0 are enriched relative to the matrix; those less than 0 are depleted relative to the matrix. The enrichment factor for Fe for Class 2 features is 2.7; Class 3 features is 5.0; Class 4 features is 8.0; for Class 2 halos is 2.1. *Data for zinc were deleted; see text for explanation.

their difference in color compared to the other feature classes, such compositional differences are not unexpected. No other trends or distinctions by color class are apparent.

As expected, the concentration of iron in features and their corresponding halos is very high, with enrichment factors of 2.7 to over 8 in the features and 1.5 to 2.1 in the halos. Cd, Co, K, Li, and Pb are absent from all features and halos while Na, Ni, and S, are absent from features and halos of Class 2, 3, and 4. A complete absence of Na, especially in the matrix, is unexpected. The depletion of Al, Ca, Mg, K, and Si, (and the apparent absence of Na) in all features suggests a lack of clay in the features but these same depletion patterns are found in their associated halos, which have physical properties that are much more similar to the matrix than to features. Since the matrix contains 15% to 20% clay based on their texture, and halos are impregnative, a reasonable expectation is that halos should more closely resemble the matrix than resemble features. EDS results are consistent with ICP results suggesting a lack of clay in features (lower magnesium, aluminum, silicon, and calcium in features compared with the matrix) as is the poor induration of features. Taken together, these considerations make the similarity of the chemical depletion pattern of the halo to the feature rather than to the matrix somewhat surprising. No satisfactory explanation of this unexpected relationship has been formulated.

On average across all classes (with the exception of Class 1) barium was the only element consistently enriched relative to the matrix, with the obvious exception of iron. Class 2 and Class 4 features were enriched in barium by 29% and 24% respectively. Barium is a component of two manganese minerals: romanèchite (BaMnOH_2O) and hollandite ($\text{Ba}(\text{Mn})_8\text{O}_6$), and sometimes

todorokite $((\text{Na,Ca,K,Ba,Mn}^{2+})_2\text{Mn}_4\text{O}_{12}\cdot 3\text{H}_2\text{O})$. Although manganese was not concentrated in features relative to the matrix, it is possible that barium is a stable indicator of the former presence of manganese. Electron diffraction and micro-XRD both provided some weak evidence for the presence of romanèchite in two different features so the possibility exists that the barium is residue from a weathered manganese mineral.

Stain tests

Stain test results follow the procedures outlined in Tables 14 and 15. The procedures in Table 14 are split into two groups: those that begin with alizarin red S in 0.2% HCl (ARS) at Stage 1 and are taken from Warne (1962), and those that begin with titan yellow in 30% NaOH (TY) based on Friedman (1959) Procedure II.

Alizarin red S at Stage 1 (Table 14 upper)

High magnesium calcite was common in halos and the matrix. Calcite was always present in the matrix, less so in halos, but was never detected in features.

Dolomite was common in halos, and the matrix, and occasionally in features. Staining with alizarin red S in 30% NaOH sometimes produced what appeared to be a weak dark brown or black stain, indicative of siderite, but it was not possible to distinguish with any reasonable certainty between a legitimate stain and a dark or black mineral fragment. Therefore, the test for siderite was at best inconclusive. It seems unlikely that siderite was present in any significant quantity. Benzidine produced areas of purple rather than blue as expected from rhodochrosite or a manganese carbonate in general. The purple stain might be a reaction with a metallic ion other than manganese, possibly iron.

Table 14. Stain test procedures for alizarin red S in 0.2% HCl (ARS) and titan yellow in 30% NaOH (TY). Sequence is from left to right. Columns labeled Stage 1, 2, 3, and 4 provide a list of the stain solutions used. The last column provides a list of mineral species reactive to each stain sequence. See text and Table B1 for details.

Stage 1	Color	Stage 2	Color	Stage 3	Color	Stage 4	Color	Mineral
ARS	Deep red	Feigl's solution	Black No color	ARS+30% NaOH	Purple No color			Aragonite† High Mg calcite Calcite Witherite†
ARS	No color	ARS + 30% NaOH	No color Dk brn/black Purple	ARS + 5% NaOH	No color Purple	Benzidine Mg reagent	Blue No color Deep blue No color	Anhydrite† Siderite‡ Rhodochrosite‡ Dolomite Magnesite‡§ Smithsonite†
ARS	Purple	ARS + 30% NaOH	Dark purple Dark red brn No color					Ankerite¶ Cerussite† Strontianite†
TY	Orange to red	TY + 5% NaOH	No color Orange to red	Hematoxylin	Purple No color			Dolomite High Mg calcite Magnesite‡§
TY	No color	Hematoxylin	No color Purple	Feigl's solution	Black No color			Anhydrite† Aragonite† Calcite

† Not found

‡ Possible

§ or gypsum

¶ or ferroan dolomite

Table 15. Colors of common carbonate minerals after staining with alizarin red S and potassium ferricyanide.†

Carbonate	Subgroup	Alizarin Red S	Potassium Ferricyanide	Combined
Aragonite	—	Pale pink to red	No color	Pale pink to red
Calcite	Fe ²⁺ free	Very pale pink to red	No color	Very pale pink to red
Ferroan calcite	Fe ²⁺ poor	Very pale pink to red	Light blue or turquoise to dark blue or turquoise	Mauve
Ferroan calcite	Fe ²⁺ rich	Very pale pink to red		Purple to royal blue
Dolomite	Fe ²⁺ free	No color	No color	No color
Ferroan dolomite	Fe ²⁺ /Mg ²⁺ <1	No color	Light blue or pale to deep turquoise	Light blue or pale to deep turquoise
Ankerite	Fe ²⁺ /Mg ²⁺ >1	No color	Dark blue	Dark blue or deep turquoise
Magnesite	—	No color	No color	No color
Rhodochrosite	—	No color	Very pale brown	Very pale brown
Siderite	—	No color	No color	No color
Witherite (BaCO ₃)	—	Red	No color	Red
Cerussite (PbCO ₃)	—	Mauve	No color	Mauve

† Sources: Evamy 1963; Dickson 1965; Dickson 1966; Hitzman 1999

Ferroan dolomite or ankerite was found in a feature after pretreating with AAO to remove the oxide coating. Treating the residue with alizarin red S in 30% NaOH gave a positive result after a weak purple color with alizarin red S only, the residual grains taking on a characteristic purple (red dominant) color (6.7RP 3.1/2.2, 6.1RP 3.6/1.6, 7.6RP 3.5/1.9) after heating (Plate 33). A number of the purple grains also showed the characteristic rhombohedral pattern of iron carbonates. No ferroan dolomite or ankerite were found in haloes or the matrix.

No evidence of aragonite, witherite, anhydrite, magnesite or gypsum, smithsonite, and strontianite was found. Testing for witherite (BaCO_3) required rhodozonic acid as a stain, which was not available. In view of the ICP results showing enrichment of barium in some features, the test would have been worthwhile to perform as would a stain test for barite (BaSO_4), which was unknown at the time.

Titan yellow at Stage 1 (Table 14 lower)

The Titan Yellow sequence confirmed the presence of high magnesium calcite in halos and the matrix and dolomite in the matrix and halos.

Alizarin red S and potassium ferricyanide (Table 15)

Alizarin red S alone or in combination with potassium ferricyanide produced results consistent with the previous stain test sequences.

Of most significance were the results of potassium ferricyanide alone, discussed in Warne (1962), Evamy (1963), and Dickson (1965). The test revealed the presence of Fe^{2+} as coatings on oxidized grains within the features after briefly exposing the grains to acid ammonium oxalate to remove oxidized iron. Longer exposure to acid ammonium oxalate reduced the amount of ferricyanide staining to localized residues on grain surfaces, indicating that the iron oxide was

actually a coating on grain surfaces. Without acid ammonium oxalate pretreatment, however, iron-oxide-coated grains within the feature turned very dark blue, in some cases nearly black, when heated to 90°C in the presence of potassium ferricyanide (Plate 34). Some of these grains produced a dark blue halo that slowly diffused away from the grain. If the black grains were disturbed with a probe, the dark material separated and revealed a strong blue color, again confirming the presence of an Fe²⁺ coating possibly an iron carbonate, between a less soluble substrate, possibly quartz, and the iron oxide coating. This phenomenon was never observed with untreated material from the matrix. Hitzman (1999) claims that pyrite and iron oxide minerals react with the staining solution to produce a dark blue-black precipitate. Since no reaction was evident between the stain solution and matrix grains, which most certainly contain iron oxide coatings, that explanation seems unlikely unless the stain solution is reacting to a specific type of iron oxide that is present only in features. Material underlying the iron oxide coating, visible after a brief exposure to acid ammonium oxalate, does not give the appearance of pyrite and is too soluble in acid ammonium oxalate. Material in the halo also formed a weak blue precipitate with hot potassium ferricyanide, although this result was less reliable than that from the features themselves, which gave a consistently positive response.

Rhodamine B and alizarin cyanine green

Despite the claim by Allman and Lawrence (1972) that rhodamine B base, titan yellow, and alizarin cyanine green are specific to gypsum, they failed to stain known gypsum samples. Alizarin cyanine green failed to give a positive response to any samples, while rhodamine B base and titan yellow did stain fragments of material in the features, halos, and matrix. ICP failed to find sulfur

in any samples suggesting that the stains might be reacting to a mineral other than gypsum.

Potassium hydroxide and hydrogen peroxide

Hallimond's (1925) test for siderite worked well with known siderite specimens. It failed to find any convincing evidence of siderite in features, halos, or the matrix as was the case with alizarin red S and sodium hydroxide discussed earlier.

Classification of high-chroma features

An accurate classification of high-chroma features as nodules, concretions, infillings, etc. could be useful since each type or class of feature may have a different origin. The characterization presented above provides the set of properties used to make as accurate a classification as possible with the information available.

An identification key was developed for field definitions of concentrations (Figure 20). The key is arranged so that organic features key out first, followed by inherited features, then by a series of pedogenic splits.

Applying morphological descriptors of high-chroma features to the key immediately reveals the shortcomings of using genetic definitions for feature identification. The first step requires that a decision be made based on strictly genetic criteria: interpreting the feature as being of biological or non-biological origin. As acknowledged by Bullock et al. (1985:133) the ability of micromorphologists to make that decision will vary greatly. It may not be possible even for an experienced micromorphologist to make an unequivocal decision. Furthermore, the question remains whether to include redoximorphic concentrations (assuming they actually could be identified as such) since the

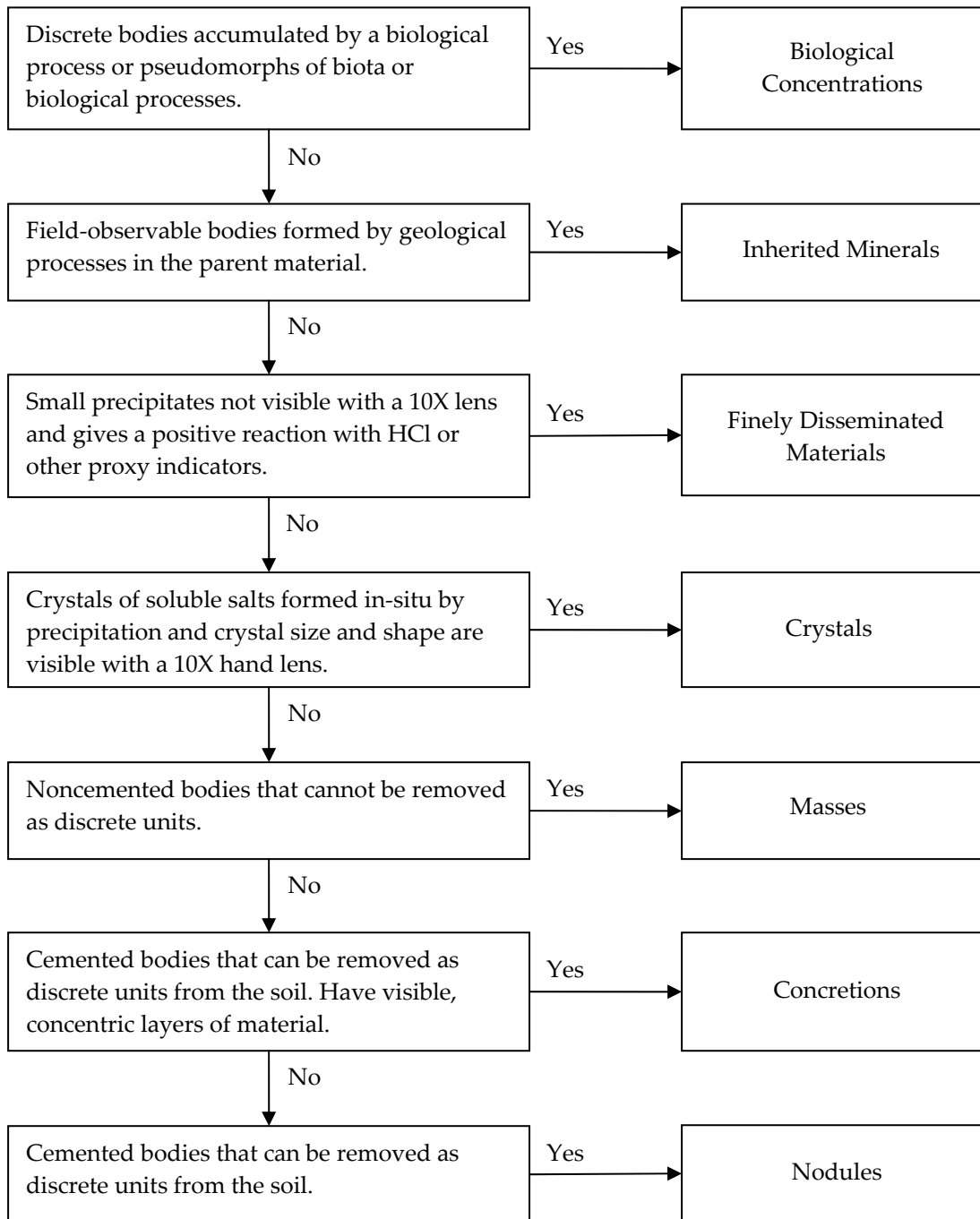


Figure 20. Field key to soil concentrations. Adapted from Schoeneberger et al. (2002).

processes of oxidation and reduction can be mediated by microbes, resulting in concentrations that have been “accumulated by a biological process” (Schoeneberger et al. 2002:2-18).

Absence of confirming evidence that concentrations are biological accumulations leads to the next level of the flow chart, which results in a similar problem: no descriptive criteria are provided to determine if a concentration is inherited. The question being asked at this level (whether inherited from the parent material or formed in the existing soil) defines one of the fundamental questions of feature analysis and one of the questions taken up by this dissertation. Again, lack of evidence that a feature is inherited moves the investigation to the next level, while still leaving open the questions of how one would establish if a concentration truly were inherited or biological.

The next five levels have criteria that are based primarily on descriptive or analytical criteria, with the exception of crystals. Since crystals within high-chroma features are not visible with a 10X hand lens and high-chroma features do not react positively with dilute hydrochloric acid, they fail tests for both finely disseminated material and crystals. If the shape and structure of the crystals were visible at 10X, a decision would need to be made as to whether or not they are crystals of soluble salts that formed in-situ by precipitation, a decision that is not always easy to make in the field.

At the next level of the flow chart (Figure 20), high-chroma features, being loose, uncemented, and not removable intact from the soil matrix, meet the stated criteria and key out as masses, although because an unequivocal decision could not be rendered as to biological or inherited origin, there is considerable uncertainty associated with that conclusion. The possibility of a biological or

inherited origin could be retained by using those two terms as adjectival modifiers of the base term “masses,” such as “biological masses” or “inherited masses” but since neither a biological nor inherited origin have been excluded, such combinatorics opens up the possibility of a feature being an “inherited biological mass,” an interesting combination that contributes nothing to resolving the issue. The term “masses” itself seems overly inclusive since any feature is a mass of something, known or unknown. Setting aside inherited and biological possibilities, the best-match of high-chroma features with any other field-defined concentrations is with the classification “masses.” Being uncemented, high-chroma features do not satisfy subsequent criteria for nodules and concretions.

Recall from the earlier discussion of masses in the Literature Review Part II, that the corresponding micromorphological features include infillings and nodules. Since cementation is not a consideration in micromorphology, the deciding criterion between infillings and nodules is whether or not the feature developed in a void, a determination of genesis that is not easily made. The loose fabric of high-chroma features could be described as “powdery,” suggesting similarity with Kubiëna’s (1938) concept of an efflorescence but also not excluding the possibility of an amygdalus formation or crystal chamber. Since any of these features can form by the *process* of efflorescence (although Kubiëna (1938) himself never specifically makes that claim) and the morphological evidence *points to* the process of efflorescence, then regardless of which type of feature might correspond, a high-chroma feature might be related to voids since efflorescence takes place in voids and on the interior surfaces of voids. Establishing that high-chroma features have completely filled voids leads to the

conclusion that high-chroma features are loose continuous infillings under a thin-section or micromorphological classification since infillings are defined as related to voids while nodules are not related to voids.

The classification systems of Bullock et al. (1985) and Stoops (2001) also address two other aspects of classification relevant to high-chroma features that the field classification of Schoeneberger et al. (2003) does not: texture and coatings. Bullock et al. (1985) discuss the concept of textural pedofeatures. Since high-chroma features consist predominantly of coarse-to medium silt-size grains, they could qualify as silty pedofeatures. Because many of the grains appear to be coated with iron (hydr)oxides, they should not be considered uncoated, although a reference is made specifically to clay coatings. Bullock et al. (1985:115) recognized the occurrence of silty pedofeatures in the form of loose infillings in albic horizons, most often associated with cappings and coatings. Stoops (2003) does not recognize textural pedofeatures as a distinct class but incorporates them into the concept of coatings, specifically in this case, silt coatings. Since silt has infilled more than 90% of the void, high-chroma features would not be considered silt coatings by Bullock et al. (1985:103). Regardless, the concept remains relevant because an internal silty texture is such a prominent feature of high-chroma features. A variety of terms has been used to describe silty pedofeatures leading Bullock et al. (1985) to declare that there is a “clear need for a structured classification.”

The final morphological property of high-chroma features relevant to classification is the presence of a halo. Brewer (1964:274) defined what he called “glaebular halos” as “weak accumulations of some fraction of the plasma surrounding much stronger glaebular features and having an undifferentiated

fabric and very diffuse to diffuse external boundaries.” He also considers that glaebular halos are accretionary, formed *in situ*, and indicate that the associated more distinct glaebule also formed *in situ* by accretion. This interpretation is offered without supporting evidence and is subject to the same criticisms offered earlier about Kubiëna’s unsupported conclusions. Bullock et al. (1985) considered a nodule with a halo to be a unique type of nodule. Stoops (2003:118) eliminated the term halo “because it belongs to a different level and partly corresponds to hypocoatings,” a term defined in Bullock et al. (1985) as features that immediately adjoin the surface with which they are associated. They may be external or internal. Hypocoatings correspond to the concept neocutans of Brewer (1964). Considering the relatively high iron concentrations of the halo, neocutans would be classified more specifically as neoferrans. Stoops (2003:106) defines hypocoatings as “matrix pedofeatures referred to a natural surface in the soil and immediately adjoining it.” They are considered to be impregnative, consistent with halos observed surrounding high-chroma features, which would be classified as external hypocoatings.

In a mixed system of Bullock et al. (1985) and Stoops (2003), high-chroma features could be classified as silty, loose continuous infillings with an open porphyric coarse/fine-related distribution at 50 μm of 1:9 (c/f_{50 μm} , 1:9), with an external ferric hypocoating. It is of some considerable relevance, however, that Stoops (2003:173) does not consider a feature with a porphyric c/f-related distribution to qualify as a loose continuous infilling. A porphyric c/f-related distribution consists of larger fragments within the feature surrounded by a dense mass of smaller fragments. Subtypes are defined based on the relative distances between the coarse fragments. Because of the spacing or relative

infrequency of coarser particles (coarse silt grains) to unaggregated fine particles (Figure 10 upper), the c/f-related distribution for high-chroma features is open porphyritic.

Classification as redoximorphic features

Before finishing the discussion of classification, it is necessary to return to the discussion of field classification of high-chroma features. In addition to the possibility of a biological or inherited origin, another problem exists with the field classification of high-chroma features as masses. Under the field definition, masses include “Redox Concentrations that do not qualify as nodules or concretions” (Schoeneberger et al. 2002:2-18). Redoximorphic features apparently are intended to “key out” before non-redoximorphic concentrations so a decision must be made early whether or not to declare a feature a concentration or a redoximorphic feature. A decision chart provided by Schoeneberger et al. (2002:2-7) uses color patterns to decide between matrix color, mottle, non-redoximorphic feature (e.g., a concentration), or redoximorphic feature until the final step of the decision process where the final deciding question is asked: “Is the feature formed by the processes of oxidation and reduction?”, a question whose answer leads directly back to the intractable problem of inferring origin. No objective criteria are provided to make the decision at that last crucial step.

At this point then, the question is whether or not high-chroma features are or should be considered redoximorphic features. There are particular morphological features that are considered to be “redox features” that have a defined morphology. Descriptions of what are now considered redoximorphic concentrations include a range of properties, occurrences, and compositions. Concentrations of Fe and Mn oxides are most commonly found in the subsurface

horizons of seasonally wet soils (Fanning et al. 1992:111). They are composed of relatively pure (hydr)oxides, may range in size from a few micrometers to a few centimeters, often coat the outsides of coarser grains or ped surfaces or the insides of channels and voids. They may include or exclude the groundmass. The boundary between the concentration and the soil matrix or the adjacent depletion may be diffuse or sharp.

Three different types of redoximorphic concentrations have been recognized: masses, pore linings, and nodules and concretions as described by Vepraskas (2001:167-8, 171). As defined by Vepraskas (2001:167) iron masses are poorly cemented masses of iron (hydr)oxides that are not associated with ped surfaces, root linings, or channels. Lack of cementation is the result of relatively low iron concentrations. Pore linings are accumulations of iron or manganese (hydr)oxides along root channels or ped surfaces. They may be cemented or loose depending on the amount of iron present. The shape and location of pore linings differentiate them from iron masses and nodules. Pore linings are found along root channels or in cracks between ped surfaces while soft masses are found within the matrix. Nodules and concretions are cemented masses of iron (hydr)oxides, are usually rounded, and of approximately the same size range as iron masses. Nodules and concretions appear to form slowly after repeated cycles of iron movement and oxidation at the same places in the soil where oxygen may be trapped (Vepraskas 2001). They may also require longer periods of saturation (Veneman et al. 1976) than do soft masses.

Iron concentrations of presumed redoximorphic features vary widely by internal fabric, grain size, color, porosity, and mineralogy. Combinations of these characteristics occur frequently, creating difficulties with identification,

definition, classification, and interpretation of formational processes responsible for each property or combination of properties (Brewer 1972). Since these features would now be considered redoximorphic concentrations, the impracticality of defining a redoximorphic concentration on the basis of morphology becomes apparent. The same is not necessarily true of redoximorphic depletions or concentrations when accompanied by clearly associated depletions.

As with the field classification of Schoeneberger et al. (2002), high-chroma features resemble the poorly cemented iron masses not associated with ped surfaces, root linings, or channels as described by Vepraskas (2001). Despite the resemblance, high-chroma features should not be considered “redoximorphic features” *sensu* Vepraskas (2001), Schoeneberger et al. (2002), and Vasilas et al. (2010).

All general definitions of redoximorphic features are genetic; no purely descriptive definition exists that includes any and all features that could be considered to be “redoximorphic.” This means that a potentially large number of features are eligible to be classified as redoximorphic features. Virtually any *pedogenic* concentration of iron and/or manganese could be considered a redoximorphic concentration. Although the requirement stated in Schoeneberger et al. (2002) that the composition and process of formation of a feature must be known or inferred before describing it as a redoximorphic feature seems reasonable and proper, doing so is not necessarily straightforward. Some evidence, color for example, might exist which implies that the concentration is composed of iron or manganese, which as is commonly accepted, requires an oxidation-reduction process to form, *if the feature is pedogenic*. The process that

actually produced the feature is invisible and unknown, proceeding too slowly for the process to be directly observable and hidden from view, underground and inaccessible to observation or measurement. Therefore, reliance is placed on the inference that the process is or was present at one time because the result or product of that process is visible: the feature itself. Using the feature itself to infer redoximorphism is dangerously close to becoming circular reasoning: trying to establish that the feature is a redoximorphic concentration by assuming that the feature is a redoximorphic concentration. The only way out of this logical fallacy is to have descriptive, morphological, or analytical criteria that identify a feature as redoximorphic with an acceptably high probability. Features do exist that are formed by processes of oxidation and reduction but unless their morphology is unequivocal, formation by oxidation and reduction must be demonstrated by independent evidence. Given the state of our knowledge at the present time, necessary, sufficient, and unique criteria to declare a feature to be “redoximorphic” do not exist. Use of existing descriptive, morphological terms, along with color, considered in a larger landscape and hydrological context, are preferable to using the vague term “redoximorphic feature.”

Hydric soil indicators, more formally called field indicators of hydric soils, developed by the Natural Resources Conservation Service, use only soil morphology to interpret process (see Vasilas et al. 2010). Hydric soil indicators have been based on carefully monitored studies that relate soil morphology to the processes that produce them. They establish a link between morphology and genesis.

Soils should be described using purely descriptive terms based on morphology. If interpretation is needed for a proposed land use, hydric soil

indicators should be used. Some indicators, for example A11 and A12, refer to “redox concentrations” but the adjective “redox” is superfluous and should be omitted. In fact, its inclusion should present a serious complication for using the Indicators since the process that produced the so-called redox concentration must be identified or inferred at the risk of invoking the circular argument discussed earlier. The adjectival term “redox” should be purged from the document. The noun “concentration” alone sufficiently conveys the desired meaning. At a more fundamental level, one can even question the need for the term “redoximorphic” or any of its variations.

In other applications, only depletions should be used to infer wetness in order to achieve any reasonable degree of reliability. Concentrations alone should not be used for reasons that are discussed below.

A contradiction regarding redoximorphic concentrations exists between field indicators and hydric soil indicators. By the field definition, redoximorphic concentrations are masses, nodules, or concretions (Schoeneberger et al. 2002:2-14). However, “for the purposes of the [hydric soil] indicators, nodules and concretions are excluded from the concept of redox concentrations unless otherwise specified by specific indicators” (Vasilas et al. 2010:39). Two reasons are given for their exclusion. First, because they are composed of iron and manganese oxides, they are resistant to weathering so may be relicts of past conditions when the soil was wetter. Second, they may have formed elsewhere and been transported to the present site (Vepraskas 1999:11). Either of these arguments against the inclusion of nodules and concretions apply equally to all other features considered to be redoximorphic concentrations. A third reason, not mentioned by Vasilas et al. (2010), is that a nodule may not be pedogenic,

having formed by the weathering of an iron-bearing mineral such as pyrite or siderite into limonite or other iron oxides. The concept of redoximorphic features appears to be seriously flawed.

Considering the efforts that have been expended to remove genetic terms and interpretations from the soil survey (see Smith 1986) and micromorphological or thin section descriptions (see Bullock et al. 1985), introduction of the purely genetic term “redoximorphic feature” and related terms seems like a significant step backwards.

As a descriptive field term, the concept of redoximorphic features or redoximorphic features is of no real value and may in some cases be detrimental to making proper soil interpretations. Its genetic basis does have explanatory value, however, and provides a useful framework for the study of concentration pedofeatures. The term should be replaced by the specific morphology of the feature being observed. The description should be non-genetic.

Redoximorphic features do exist as features that have formed, in the most general sense, through the processes of reduction and oxidation. In addition to requiring that the composition and process of formation for a soil color or color pattern must be known (and not just inferred), a key requirement in the definition of redoximorphic features is that translocation must accompany or “couple” removal and accrual that takes place by oxidation and reduction (Schoeneberger et al. 2002:2-14). Requiring that translocation take place eliminates the inclusion of inherited features that weather in-situ, features that oxidize to iron-manganese concentrations that should not be considered redoximorphic features for the purposes of establishing the suitability of a soil for a particular land use.

Comparison of data: non-pedogenic and pedogenic hypotheses

Any hypothesis proposed to explain the formation of high-chroma features must account for the physical, chemical and mineralogical properties, and the observed occurrence of the features within the profile and on the landscape. What follows is a brief overview of several of the most important and relevant results as they relate to potential formation hypotheses. The overview is followed by a more specific formulation and discussion of the resulting hypotheses. It is important to keep in mind that some, perhaps much, of the discussion that follows is based on informed speculation corroborated by observational data. The gaps in our knowledge of soil formation are plentiful and large. Some speculation becomes necessary to fill in those gaps.

Field and OSD data support a pedogenic hypothesis of feature formation, either inherited or coeval with modern soil development. If features are inherited rock or mineral fragments (substrates) that have weathered into iron oxide concentrations, they would most likely be distributed randomly throughout the glacial sediment, in the absence of any sorting mechanism such as flowing water or gravity. Instead, the average first appearance is at 50 to 100 cm. Size and abundance increase with depth according to the OSD data but it is unclear if the features reported in the OSDs are high-chroma features as defined in this project. Several explanations for the scarcity of high-chroma features above 50 cm can be formulated. Removal after formation in upper horizons seems unlikely because iron oxides tend to be stable in normal soil environments, requiring considerable periods of time for removal (Johnson and Swett 1974; Ping et al. 1993). The most likely explanation would seem to be the presence of factors that prevent formation from taking place.

Inherited substrates close to the surface would not have not experienced an environment that is favorable for the formation of high-chroma features. As substrates weather, weathering products are carried deeper into the soil profile before they are able to accumulate, as is the case in particular with excessively drained soils (see Winters 1938). Lower horizons, which might retain water longer than surface horizons, permit the accumulation of weathering products from inherited substrates.

Boulton and Dent (1974) found that till immediately beyond the ice margin is saturated. Also, a high void ratio in the upper horizon resulted in a higher water content compared to lower horizons. If that is the case in Minnesota tills, saturation and reduction at the surface may have resulted in removal of weathering products of iron-manganese nodules or other developed or developing high-chroma features at the surface. This effect was only observed for about a year, however, when near surface horizons of the till drain, surface voids collapse, and till consolidates.

Coniferous forest vegetation was present at the glacial margin so some degree of podzolization would be expected. Podzolization has been identified by several investigators as being active in permafrost and cryogenic soils (Pawluk and Brewer 1975; Ugolini 1986; Beyer and Bölter 1998; Blume et al. 2004) although not as a result of coniferous forest cover but from heath and other tundra vegetation. Mild podzolization may at least help prevent the accumulation of weathering products above 50 cm in the developing soil profile. Although chelating acids present in the decomposing coniferous litter would tend to be neutralized by the calcareous till, some chelation and decrease in the pH at the surface could reasonably be expected. Increased removal rates also

could be effected by reducing conditions that might have been present at or near the surface to a depth of 50 to 100 cm, possibly as the result of buried ice or extended periods of shallow frost. A combination of low pH and saturation/reduction would give an enhanced effect: lowered soil pH as a result of coniferous vegetative cover results in the reduction and solubilization of iron and manganese at a higher redox potential. All other indications of podzolization have since been removed from the soil profile over subsequent generations of non-podzolic conditions.

A third possibility is that a downward advancing freezing front excluded solutes behind the freezing front and concentrated them ahead of the freezing front (Kay and Groenevelt 1983; Ugolini 1986; Vogt and Larqué 1998). Solutes move ahead of the freezing front by diffusion and convection and may reach concentrations of 50 to 80 times the original concentration. Permafrost prevents further downward infiltration of solutes, leading to their concentration at the base of the active layer at a depth of approximately 20 to 60 cm (Alekseev et al. 2003). By analogy, an ice lens or buried ice block would have the same effect as permafrost.

Disturbance from fauna or alternating freeze-thaw cycles could contribute to the breakup and physical weathering of developing high-chroma features, either destroying them or making them more susceptible to chemical weathering.

The largest features were found in peds with strongly expressed hydromorphology, an observation that again favors a pedogenic hypothesis. In addition, the very largest features are more impregnative than the typical smaller features, and as a result, are more strongly indurated. These larger features may represent an as-yet unrecognized endpoint in the classification of high-chroma

features or might actually be a different type of feature. Since they do have a color very close to 7.5YR 5/8, and dark mottles have been found on their outer surfaces, they probably are related in some way to the high-chroma features of this study.

Poor induration is consistent with the concept of a loose infilling, most easily interpreted as the result of a pedogenic process, although extensive weathering of an inherited substrate could result in a soft, loose, entity resembling a pedogenic infilling formed by the deposition of dissolved or suspended material into a pore or void. Extensive weathering does not imply that long periods of time are required, only that weathering proceeds far into the weathering sequence as a result of favorable conditions or from the presence of an easily weathered substrate. Moderate to strong induration could favor either a pedogenic or inherited origin. An inherited mineral or rock fragment would be expected to retain at least its internal cohesiveness for some time as it weathers. Likewise, an inherited pedogenic feature that has increased in crystallinity or become more indurated over time will be more resistant to weathering and decomposition.

Shape suggests possible origin but not without ambiguity. Round versus square, rectangular, or other angular shapes would seem to favor a pedogenic hypothesis over a non-pedogenic one. Certainly, crystal fragments or rock fragments typically have sharp, angled corners, which support a non-pedogenic hypothesis, but transport by ice or water often results in a rounding of corners and edges giving an appearance more consistent with pedogenic formation.

Similarly, a sharp transition between the feature and the matrix supports the hypothesis of inherited substrates. Fragments of rocks and minerals have

sharp boundaries. Orthic nodules may have a gradual or sharp boundary (Stoops 2003:118). Pedogenic features such as infillings that form in well-defined voids or pore spaces would have sharp boundaries, especially if the interior boundary of the void is covered with a partially cemented lining. This type of lining may be visible as the cortex that was observed in about 20% of the features, although the cortex or lining would not have to be visible under an optical microscope to be effective. The presence of a cortex might then be evidence for a pedogenic hypothesis, but an inherited feature might have developed a cortex as it was formed as is the case with geodes, or the feature might form a cortex as it degrades.

Non-pedogenic inherited features are intrusive, having formed from material that is unlike the present soil material, under conditions different from those that currently exist, and may have been transported to their present site. Transported features have a sharp transition to the matrix unless material that has been removed by weathering grades uniformly into the surrounding soil matrix, a circumstance that would only be expected if weathering is at an advanced stage. Pedogenic features are intrusive if they form in a well-defined cavity or void (Stoops 2003:104), as discussed previously. The pedogenic feature contains material that is derived from the surrounding soil or parent material but differs from the soil or parent material either in composition or organization.

The presence within the features of coarse silt particles interspersed with very fine sand is difficult to explain pedogenically, whereas inherited non-pedogenic features may contain a significant quantity of well-sorted silt, which they incorporated from their original formational environment. Silt movement, or perversion, is possible under certain conditions, however, and will be

discussed later under the pedogenic inherited hypothesis. The presence of finer silt-size particles within the features, visible under the SEM, does not support any particular hypothesis but is relevant to all four hypotheses that will be discussed.

Color does not support one hypothesis over another but it does provide important clues about composition, compositional differences, and the relationship between components within the feature. The consistency of color and color patterns of the features and surrounding halo suggests a common environment and composition for all high-chroma features as they form or as they weather and degrade. The significance of color and color patterns to feature formation is discussed in the context of specific hypotheses.

Non-pedogenic and pedogenic hypotheses have support from the data and, more importantly, no hypothesis has been disproven and eliminated from consideration. All will be discussed in more detail.

Discussion of proposed formation hypotheses

Any interpretation of origin based on morphology alone must be approached with caution. Different minerals can have similar colors and morphology. Properties conveyed to pedofeatures by earlier processes can be modified or obscured by later processes. Distinctive crystal shapes can result from pseudomorphism, an alteration process whereby a mineral whose initial crystal form is retained even as its chemical composition and crystal structure are transformed into a different mineral, such as a cubic pyrite crystal altering to goethite, yet retaining the outward pyrite crystal shape.

As discussed earlier, the field classification of high-chroma features is ambiguous, being classed simply as “masses” in the absence of any defining

criteria for biological or inherited features. The micromorphological classification is only slightly more helpful but only if high-chroma features are classified as loose infillings, but that classification is only useful if the assumption is made that the term “infilling” refers a genetic process and is not a descriptive term only. If a porphyric c/f-related distribution disqualifies high-chroma features from being infillings, then it is unclear how high-chroma features would classify in that system. At the scale of the low-power stereomicroscope, high-chroma features classify as coarse monic, the coarse/fine split at coarse silt, because the individual fabric units appear more uniform in size than they do under the SEM. Under the SEM, a size difference between fabric units becomes visible and the c/f-related distribution becomes porphyric. Because the diagnostic property of loosely indurated matches the description of “loose infillings” and no other feature class provides a match, the classification of high-chroma features as loose infillings is allowed with reservation despite the question of the c/f-related distribution. As loose infillings, they are considered pedogenic.

Three general hypotheses have been proposed for the origin of high-chroma features: pedogenic, inherited, and inherited pedogenic. Pedogenic features are those that have formed by the surficial processes of addition, loss, transformation, or translocation. These correspond to Brewer's (1964:143) orthic pedological features. Inherited features are of two types: those that are derived from parent rock and retain the properties and structure of the rock, what Brewer (1964:145) refers to as “lithorelicts” and correspond to simple inherited features; and those that “formed by erosion, transport, and deposition ... of an older soil material or pedological features from it, or by preservation of some part of a previously existing soil horizon within a newly formed horizon.”

Brewer (1964:145) calls these pedofeatures “pedorelicts” and correspond to inherited pedogenic features.

After additional study, the proposed hypotheses discussed above have been refined and expanded into four hypotheses:

- (1) Non-pedogenic and inherited
- (2) Pedogenic and inherited
- (3) Pedogenic and coeval
- (4) Geodic

Non-pedogenic and pedogenic refer to the first appearance of the feature in the soil. Nonpedogenic features are inherited geologic features (lithorelicts) that have weathered in the soil. Once weathering proceeds to some arbitrary extent, the feature can arguably be considered to be pedogenic, having been acted upon and transformed by pedogenic processes in the soil. They may have been transported. Inherited pedogenic features formed as a result of pedogenic processes that may no longer be active or through preservation of an older soil or features within an older soil (pedorelicts). Coeval pedogenic features are pedogenic features that formed at the same time or approximately the same time as the surrounding soil and have not been displaced. They are sometimes referred to as “contemporary,” an unfortunate term that better describes a furniture style or historical figures than a pedological feature. Geodic features formed through a unique combination of the non-pedogenic and pedogenic hypotheses.

The hypotheses developed in the following sections are based on results and observations discussed earlier. In many cases, those results and observations

are insufficient or inconclusive for complete explanations. In those cases, it has been necessary to fill in the gaps with informed speculation.

The non-pedogenic inherited hypothesis is the simplest of the four so is discussed first. The inherited pedogenic hypothesis becomes more speculative and is the most complex and is discussed next. The coeval pedogenic hypothesis is similar in many ways to the inherited pedogenic hypothesis, differing primarily only in the timing of formational events. The geode hypothesis is discussed last.

Non-pedogenic, inherited

Hypothesis: High-chroma features are iron-manganese nodules or fragments of nodules inherited from bedrock sources, deposited in the Des Moines lobe till, and are degrading in the modern soil.

High-chroma features themselves are not inherited, only the substrate that weathers to high-chroma features. Under this hypothesis, that substrate is manganese nodules or fragments of nodules whose source is the manganeseiferous members of the Cretaceous Pierre shale bedrock found to the north and northwest of the study area. Another possible source of manganese nodules is the limestone-dolomite of Manitoba. Manganese nodules are common in limestone-derived soils (Dixon and White 2002:377). The composition of Des Moines lobe till was discussed rather extensively in Part I of the Literature Review, which established the presence of significant amounts of manganese and manganese nodules in the bedrock. Under this hypothesis, unweathered or slightly weathered nodules are identified as Class 5 features. As weathering proceeds, features would be reclassified as Class 4, Class 3, and finally Class 2, characterized by corresponding changes in the color pattern. Class 5 features are

strongly indurated as would be expected from an inherited nodule. An inherited nodule also makes its own filled cavity in the receiving soil, resulting in the intrusive characteristic of high-chroma features.

Coarse silt and very fine sand found in high-chroma features are also inherited with the nodule. The basal sandstone layer of the Sully Member, laying atop the Gregory Member of the Pierre Formation, consists of sub-angular quartz grains of “almost equal amounts of very fine sand and silt” cemented with calcium carbonate and heavily coated with iron oxide and clay (Gries and Rothrock 1941:15). Such a material might provide coarser matrix material of the shale that is incorporated into the iron-manganese nodules as they form in the sediment.

A strongly indurated nodule also establishes a sharp transition between it and the surrounding soil matrix. Some nodules tended to shatter upon weathering (Gries and Rothrock 1941:62). Brittle fracture would result in irregularly shaped fragments having a sharp transition between feature and soil matrix. Shatter also would result in fragments with sharp, angled corners but such corners are more susceptible to rounding during transport and subsequent weathering.

The specific details of actual nodule formation are of little interest since their formation took place before soil formation. Their composition and subsequent transformation are of interest, however. Formation will be discussed later under pedogenic hypotheses.

Internal properties of features would be expected to correlate with the internal properties of the original nodule. Manganese nodules found in the Pierre shale are thought to be composed of the minerals psilomelane (romanèchite),

manganite (MnOOH), and pyrolusite (MnO_2) (Gries and Rothrock 1941; Spector 1941:42). The nodules were described as having a black (Gries and Rothrock 1941:18–19, 27), a blue-black (Spector 1941:57) or purplish color, and weather to purplish black (Gries and Rothrock 1941:23, 26). Gries and Rothrock (1941:66 reported that “microscopic examination showed tiny, opaque black and blue-black specks with bright metallic lustre scattered through many of the samples. These possess the optical characteristics of pyrolusite and manganite” reaching their highest concentration in the most weathered zones that have a black metallic luster. Hanson (1932:16,18) defines an alteration sequence of psilomelane (romanèchite) to manganite to pyrolusite, so it is possible that all minerals could be present. Barite (BaSO_4) was also found in some deposits and is commonly found in manganese deposits (Hanson 1932:11; Gries and Rothrock 1941:21; Spector 1941:15), suggesting that barium is present in the bedrock till source and may have been incorporated into nodules. Barium was also reported in till in Minnesota in amounts of approximately 420 to 690 ppm (Thorleifson et al. 2007). These reports are entirely consistent with results observed and obtained analytically on high-chroma features.

Weathering or partial weathering of inherited nodules is responsible for the color and color pattern of high-chroma features. Most, if not all the dark material found in high-chroma features including the black, blue-black, and purple colors are manganese minerals of uncertain identity but most likely are manganite, romanèchite, or pyrolusite, or a combination of manganese minerals. Romanèchite was tentatively identified by μ -XRD and possibly by ED. The relative concentration of barium in features as found by ICP is additional evidence of the possible presence of romanèchite or other barium-containing

manganese minerals. The association of barium and manganese has been documented in the source area for the nodules. Another possible manganese mineral is birnessite. While not exclusively found with a platy morphology as in Figure 10 and Figure 12, Golden et al. (1988) synthesized platelets of birnessite approximately 2 to 3 μm in diameter. Reaction with Fe^{2+} resulted in an iron oxide pseudomorph of birnessite. XRD produced only two peaks that could both be assigned to ferrihydrite or ferroxhyte. Ferroxhyte was favored on the basis of its fibrous morphology.

Ferrihydrite typically has a granular morphology, but if precipitated through the action of microbes, it may have a tubular form similar to that in Figure 12. Although apparently lacking the hollow tubular morphology, the rod-like coating on the platelets might be microbial ferrihydrite deposited on flakes of a manganese or former manganese mineral that has weathered otherwise altered its appearance to take on its present form. A platy morphology is also typical of manganite, which might be a suitable substrate either for subsequent weathering or for alteration into an iron (hydr)oxide pseudomorph.

Manganese nodules of the Pierre Shale contain a significant amount of iron (see Literature Review Part I), a finding that is generally true of sedimentary manganese deposits (Hanson 1932:11). Iron oxides actually may be the main constituent of these deposits. This iron, along with manganese, is available for weathering. Fe^{2+} may be present as carbonate coatings on the silt particles within the nodule. These coatings dissolve into solution and reprecipitate as Fe^{3+} oxide coatings on silt and very fine sand particles within the feature, or surface oxidize directly to Fe^{3+} oxides when the soil and features dry out.

Oxidation of Fe^{2+} released from iron-manganese nodules is responsible for the dominant color, Munsell 7.5YR 5/8. Initial identification of the iron minerals present can be made on the basis of color but several factors, such as crystal size, induration, and element substitution influence mineral color (Schwertmann 1993), making identification on the basis of color alone unreliable. Also, different authors will associate slightly different colors and color ranges with the same minerals, complicating identification especially for colors at the margins.

Torrent and Barrón (2002) give medians and ranges of Munsell colors for a number of iron oxides and hydroxysulfates. A Munsell color of 7.5YR 5/8 is an immediate match to lepidocrocite and schwertmannite. Given the absence of sulfur in the features that were analyzed by ICP and the lack of a sulfur source, with the possible exception of localized pyrite crystals, schwertmannite seems unlikely. A hue of 7.5YR is on the low end of the range for goethite. A value of 5 is a good match, but a chroma of 8 is just slightly out of range on the high end. The hue is not sufficiently red to be hematite but is a good match to ferrihydrite although the chroma is about one unit out of range (too high). Similar results were obtained by comparison with results obtained by Scheinost and Schwertmann (1999). As a further complication, Torrent and Barrón (2002) note that the most frequent color of ferrihydrite is “strong brown” a descriptive term that includes 7.5YR 5/8, whereas schwertmannite and lepidocrocite are most frequently, “reddish-yellow.” Blume et al. (2004:443) found 7.5YR 5/8 colors in a Cryosol horizon that they attributed to organically bound ferrihydrite.

On the other hand, comparison with results reported by Cornell and Schwertmann (2003:133) gives a complete match only with schwertmannite. Lepidocrocite is a close match with the upper range of hue at 7.4YR, while value

of 5 and chroma of 8 are very good matches. Goethite hue is too yellow (lower bound at 8.1YR) but again value and chroma match. Ferrihydrite hue is too red (upper limit is 5.5YR), value matches, but chroma is too low.

Only ferrihydrite, goethite, and hematite were reported by μ -XRD as possible iron minerals present in features. No schwertmannite or lepidocrocite were reported. From the results of the acid ammonium oxalate test, approximately half of the iron oxides in a high-chroma feature are poorly crystalline, quite likely ferrihydrite, and half are more crystalline, possibly goethite.

The most likely explanation for the observed color of high-chroma features is that they contain a particular mixture of iron (hydr)oxide minerals. Ferrihydrite, as the poorly crystalline component, is responsible for a hue at or close to 7.5YR, possibly slightly redder. Goethite would bring a yellower hue to the mixture but hematite would bring a redder hue, so the mixed effects might cancel leaving hue at 7.5YR. If goethite dominates over hematite, which is likely, both from formational and color dominance considerations, the hue becomes more yellow favoring a shift from the somewhat redder ferrihydrite to more yellow as observed. Both goethite and hematite would increase the chroma above that of typical ferrihydrite, possibly to 7 or 8 as observed. A mixture of goethite and "a small amount of hematite" was suggested by Schwertmann (1993:60) to produce a hue of 7.5YR. Another possibility is that small but undetectable amounts of lepidocrocite present in a high-chroma feature could increase the chroma to 7 or 8. However, lepidocrocite is rarely found in calcareous soils or in association with hematite (Schwertmann 1993), therefore a

combination of ferrihydrite, goethite, and possibly hematite, all of which were reported as possible by μ -XRD seems most probable.

Small areas within Class 3 and 4 features often have pinkish mottles that appear within the dominant strong brown color. These areas might indicate the presence of Mn^{2+} , possibly as the pink mineral rhodochrosite ($MnCO_3$), which weathers to the black manganese oxides manganite or pyrolusite (Deer et al. 1992:636). The feature shown in Plate 30 resembles a Class 5 feature but has areas of 5.1YR 6.6/4.5 color rather than dark or black colors. This pinkish color is similar to that found in Class 3 and Class 4 features and frequently appears adjacent to a dark or black area. These particular features may represent a transition from Class 5 to a lower class without displaying the strong brown color, loose structure, and poor induration of a typical high-chroma feature. Those properties may require more time or more favorable conditions to develop.

Color classes might also provide information about the formational status of the features, that is, whether they are forming or degrading. As an example, Classes 2 through 5 could represent a hypothetical weathering sequence. If the correct sequence is from Class 5, most weathered, to Class 2, least weathered, the features are degrading. If the correct sequence is from Class 2 through 5, features are or have been recently forming. No unequivocal evidence has been found to confirm that one direction or the other is correct. Given what is known about the weathering of iron-manganese nodules and finding the observations made on high-chroma features to be consistent with expected weathering patterns of iron-manganese nodules, then *if* the defined feature classes *are* related sequentially, the sequence is from Class 5 to Class 2 and features are degrading.

The halo that at least partially surrounds most high-chroma features is also an indicator of feature degradation, as described by Rudeforth (1970). Vogt (1991) noted that loss of iron from biotite formed a halo. During brief periods of saturation and reduction as occur during high-precipitation events or snowmelt, iron oxide minerals partially dissolve, diffuse from the feature, and re-precipitate as a halo. Because there is a significant textural discontinuity between the soil matrix and the feature, if material that is dissolved or suspended in the soil solution moves towards a feature, that material would be expected to accumulate at the discontinuity just external to the feature where its movement is slowed as it reaches the discontinuity. The concentration of solute would increase at the discontinuity and then precipitate by oxidation when the soil dries. Instead, the halo is of uniform color and appearance, resembling the soil matrix more closely than the feature it surrounds, suggesting that the dissolved material is released from within the feature and then crosses the textural boundary.

Pedogenic, inherited

Hypothesis: High-chroma features are iron-manganese concentrations that formed as a result of pedogenic processes in an earlier soil or proto-soil and are degrading in the modern soil.

Under this hypothesis, five events take place immediately after retreat of the glacier leading to the formation of high-chroma features:

- (1) Formation of vesicles
- (2) Precipitation of iron and manganese within vesicles
- (3) Infilling of vesicles with silt
- (4) Re-precipitation and transformation of iron and manganese minerals
- (5) Weathering and degradation of features

(1) Formation of vesicles

Vesicles are very distinctive pores or voids, usually spherical with very smooth pore walls (Fox 1994). Vesicles are very common in all frost-susceptible soils (Van Vliet-Lanoë 1985) that under this hypothesis are taken to be early soils as they developed under periglacial conditions present shortly after deglaciation.

In coarse-textured soils that are highly thixotropic, vesicles are well-rounded and smooth, while in clay textured soils they are mamillated and irregular (Van Vliet-Lanoë et al. 1984; Pawluk 1988). Closed voids with irregular shapes are called vugs although their origin is regarded as different from that of vesicles (Brewer 1964:189; Stoops 2003:65). Shape alone does not seem a reliable criteria for distinguishing vesicles and vugs. Vesicles, normally round or spherical in ice, may become distorted in soil (Fitzpatrick 1956). Star-shaped vugs, usually triangular or quadrilateral with convex walls, form from the welding of convex aggregates (Stoops 2003:65) a process that could apply to partially collapsed vesicles as well. After thawing, ice leaves behind angular cavities (Van Vliet and Langohr 1981) a type of void that would satisfy the more narrow definition of vug. In calcareous sediments, vesicles may be preserved as microgeodes of calcite (Van Vliet-Lanoë et al. 1984).

Vesicles are a prominent characteristic of surface horizons of loam-textured Arctic soils, usually appearing in the upper 5 to 25 cm (Van Vliet-Lanoë et al. 1984; Harris and Ellis 1980). At greater depths "overburden pressure" and settling might collapse vesicles (Harris and Ellis 1980). In some cases, however, such as the presence of an underlying water table, they have been observed deeper in the profile (Van Vliet-Lanoë et al. 1984). Furthermore, well-compacted aggregates as would be expected at greater depth "are a thousand times more

stable than those occurring at the surface” and are very resistant to collapse. The additional pressure exerted by the air within the vesicle to overcome hydrostatic pressure and the increased viscosity of cold water may be responsible for the smoothness of the walls (Van Vliet and Langohr 1981). Vesicles have been observed along fissures formed by local superficial collapse of aggregates (Van Vliet-Lanoë et al. 1984). The vesicles shown in Figure 12 of Van Vliet-Lanoë et al. (1984) resemble those shown in Plate 27 after infilling. Direct evidence of vesicle formation at greater depths is provided by profile descriptions reported in the literature. Boulton and Dent (1974) found vesicles and platy structure in sandy loam to silt loam textures at depth from 48 to greater than 120 cm; Habecker et al. (1990) found vesicles and a platy structure in silt loams between 36 and 76 cm depth along with 7.5YR 5/6 mottles; Weisenborn and Schaetzl (2005) found very few to common fine vesicles, platy structures, fragipans, and proto-fragipans at depths of 44 to 160 cm in soils with five different textures ranging from sandy loam to silty clay loam.

In laboratory experiments with freeze-thaw cycles, vesicle sizes range from 0.2 to 2.5 mm (Coutard and Mùcher 1985) but have grown to 2 to 3 cm in length (tubular) (Van Vliet-Lanoë et al. 1984). Harris (1983) produced vesicles of 0.55 mm average diameter and 2.5 mm maximum at the surface of coarse thixotropic soils, and was even able to produce vesicles up to 3.6 mm in diameter. Naturally formed vesicles are generally smaller and decrease in diameter with depth, ranging from an average diameter of 0.66 mm at 5 cm depth to 0.39 mm at 25cm depth (Harris 1983). Maximum diameters were 4 mm and 1 mm respectively. Lack of illuvial coatings on vesicles walls and disruption of silt features have been attributed to recent vesicle formation, suggesting that

vesicles do not survive from season to season (Harris 1983). In other instances, vesicles may survive from year-to-year and continue growing.

The origin of vesicles is uncertain. Fitzpatrick (1956) attributed their abundance in Arctic soils to the expulsion of air during freezing. Gases dissolved in soil water are released as the water freezes and are trapped by the downward advance of the freezing front. The number and size of vesicles was found to increase with increasing carbon dioxide content in the soil water. Harris (1983), supported by later work of Van Vliet-Lanoë et al. (1984) suggested a different mechanism. His field observations and experiments showed that vesicles can form in thixotropic soils from thaw-consolidation as excess water is expelled and air present in voids or larger pores becomes bubbles. Liquifaction and vesicle formation occur as a result of thawing rather than freezing as suggested by Fitzpatrick (1956). Fitzpatrick's (1956) hypothesis has been generally accepted.

Vesicles are often associated with indurated layers having a platy structure or with fragipans in both natural environments (see for example, Fitzpatrick 1956; Boulton and Dent 1974; Habecker et al. 1990; Frenot et al. 1995) and laboratory settings (see for example, Van Vliet-Lanoë et al. 1984; Pawluk 1988; Coutard and Mùcher 1985). Platy structures and vesicles are often reported together in the profile descriptions mentioned earlier. Freeze-thaw is often mentioned as an important contributor to vesicle formation and the development of a platy structure (Van Vliet-Lanoë et al. 1984; Van Vliet-Lanoë 1985; Coutard and Mùcher 1985; Pawluk 1988; Fox 1994; Frenot et al. 1995).

(2) Precipitation of iron and manganese within vesicles

No examples of vesicles known to be infilled with iron or manganese minerals could be found in the literature. It is possible that infilled vesicles exist

but they might not be recognized or reported as such. However, the lack of data requires this section and others that follow to be rather speculative, based on limited observations that are combined with relevant published studies. A possible infilling process can be inferred from what is known about subglacial environments and the behavior of iron and manganese in those environments.

The exact chemistry and mineralogy of the sediment under the glacial ice and immediately upon exposure after glacial retreat is unknown and unknowable. Based on the composition of the bedrock sources of the till and their chemical and mineralogical composition given previously in the literature review, manganese, iron, calcium, magnesium, and silica would be expected to compose a significant portion of the solutes contained in the protosoil solution. At the pH likely to be found in the protosoil solution, approximately 7 to 8, bicarbonate is the most likely primary counter ion. Bicarbonate anion is common in soil solutions and groundwater (Robinson 1930; Spector 1941:11; Postma and Sine Brockenhuus-Schack 1987; Yershov 1998:120; Bohn et al. 2001:199).

Microorganisms are known to actively participate in subglacial biogeochemical cycling (Sharp et al. 1999; Laybourn-Parry 2009; Raiswell et al. 2009). Evidence of iron oxidation and reduction and the formation of mottles even in well-drained Cryosols indicate the presence of free water and active microbial populations at cryogenic temperatures (Tarnocai 1994; Beyer and Bölter 1998). Although microbial biomass is low compared to temperate soils, the metabolic rate is reported to be high. As further evidence of microbiological activity, so-called "redox concentrations" have been reported to form above a perched water table as water from rainfall and the seasonal melting of frost and

snow encounter an impermeable layer formed by thawing permafrost or from a rising permafrost layer (Ping et al. 1993).

Conditions under the glacier are predominantly saturated and anoxic with iron and manganese found in reduced and soluble form in the pore waters of glacial sediment. Likewise, conditions above a permafrost layer are saturated and waterlogged (Vogt and Larqué 1998). These conditions could be extended by analogy to exist above an ice lens or buried ice block present, for example, in a stagnation moraine. Vesicles may form at the first frost following ice melt. They represent the first introduction of oxygen into an otherwise anoxic environment containing relatively high concentrations of iron, manganese, and other solutes. The effect of their appearance is to cause the precipitation of dissolved material within the vesicle either by evaporation and drying of the solution or by the oxidation of iron and manganese.

Vesicles may be transient features produced only during the winter freeze (Harris and Ellis 1980). If so, precipitation of solutes from solution must have happened early in the formational history of the soil. Deep vertical movement of solutes dissolved in pore water or even their complete leaching to groundwater could have happened quickly considering the relatively large amount of meltwater present. Any vesicles that formed after the concentrations of iron and manganese decreased below a threshold value in the pore water remained either incompletely filled or even completely unfilled.

The exact chemical and mineralogical composition and the process responsible for the initial precipitation of solutes within a vesicle is unknown. An assumption is made at this point that the “main-event” cations such as iron, manganese, magnesium, calcium, and accompanying anions along with minor

constituents of the proto-soil solution such as silica were concentrated and precipitated within the vesicle. Exact identification of minerals and their formation process is actually of little importance at this point because of subsequent events that will be discussed below.

(3) Infilling of vesicles with glacially deposited silt

Abrasion and crushing during erosion and transport of tills produce large amounts of silt that are deposited on top of coarser till as glaciers retreat (Boulton and Dent 1974; Frenot et al. 1995) resulting in a bimodal grain size distribution with a major mode appearing in the silt fraction (Dreimanis and Vagners 1971; Sugden et al. 1987). In their study of tills in Iceland, Boulton and Dent (1974) found that 40% of the uppermost 40 to 50 cm of till was comprised of particles less than 4Φ (0.062 mm) while the underlying material contained only 20% to 25% of particles less than 4Φ . The overlying silt layer is produced entirely subglacially as a result of shearing and crushing in a zone up to 50 cm thick immediately beneath the glacial sole, a zone which is subject to shear stresses from the overriding ice (Boulton et al. 1974). A bimodal distribution appeared in the sheared zone with modes at 4Φ to 8Φ (0.062 mm to 0.004 mm) and -1Φ to -3Φ (2 mm to 8 mm) while a single mode from -1Φ to 2Φ (2 mm to 0.25 mm) was present in the un-sheared zone. Collins and O'Dubhain (1980) found silt-sized grains in some Irish Podzols that ranged from 5 to 35 μm . Silt-sized quartz was more uniform, ranging from 5 to 20 μm . Both ranges fall within the range found by Boulton et al. (1974) and include the smaller silt sizes found in high-chroma features but not the larger silt size.

Laboratory experiments confirm the results of field studies. After repeated freeze-thaw cycles, French (2007:75) found that grain sizes of 10 to 50 μm

diameter are the limit for the cryogenic disintegration of quartz, amphibole, and pyroxene. Under these conditions, quartz grains appear to be less resistant to abrasion than feldspar grains whose limit is 100 to 500 μm .

After the early removal of clays in suspension, particle movement is restricted to silts and fine sands (Frenot et al. 1995). They claim that pervection is the dominant process for the first 200 years but the authors are unclear whether pervection includes silt and clay or just silt. In the first year after ice retreat, there is a significant removal of fines in the upper 10-20 cm of till (Boulton and Dent 1974). Removal and transport of silt through voids and pores in the sediment is accomplished either by repeated freeze-thaw or by flooding meltwater as it percolates through the sediment (Boulton and Dent 1974; Van Vliet-Lanoë et al. 1984; Fox 1994; Frenot et al. 1995). Downward progress is often impeded by a platy layer and a silty accumulation develops over 10 to 40 years after which it degrades by pedoturbation unless stabilized by iron oxides (Collins and O'Dubhain 1980). No process was identified that specifically moves silt into vesicles or other closed pores.

Surfaces of vesicles are often coated with coarse clay and plate-like silt particles that have their flat surfaces tangent to the vesicle surface as a result of circumferential capillary pressures that develop during drying (Sullivan and Koppi 1991). In nearly all the discussions in the literature regarding the coating of vesicles, it is unclear if "coating" refers to a coating in the sense of Stoops (2003) as a coating on the internal wall of a void, cavity, or vesicle or to an external coating, a hypocoating. In either case, even a thin external coating or thin silty hypocoating could take on the appearance of a cortex and become integrated into the vesicle boundary. Sullivan and Koppi (1991:586) do make a

specific reference to the appearance of “composite layers of silt and oriented clay” that as they grow thicker “may eventually occupy a substantial portion of the vesicle and are better referred to as infillings rather than coatings.” Even if the assumption is made that the coating is along an internal wall, their study was done in the shallow layer of a desert loam soil. Their findings may not generalize to a deeper layer in a temperate till soil. Furthermore, clay and silt were involved in the infilling, whereas only silt, no clay, is observed in high-chroma features. If clay enters a vesicle that is later to become a high-chroma feature, it must be removed by a subsequent process.

Movement of silt through a soil profile or the regolith is well-documented, but unequivocal evidence of silty infillings of closed pores is not. Sullivan and Koppi (1991), discussed above, offer one possible example. Oliveira et al. (2010) found dense complete, loose continuous, and loose discontinuous void infillings in irrigated soils of Brazil. Again, the type of void was not specified. They described closed voids or vesicles that may in fact be cross sections through connected pores or channels. The voids shown are approximately 0.5 mm or less in diameter. Grain sizes of the infilling material can only be estimated from their scaled figures as silt-size, 4 to 15 μm . A greater proportion of quartz was found in the infilling material than the matrix along with grains of iron oxide, although the composition of the infilling was similar to the soil matrix. Void infillings in uncultivated soils were loose continuous or loose discontinuous whereas in cultivated sites, all infillings were dense complete or dense incomplete. All cultivated sites were under irrigation, which seemed to increase the frequency of infilling and resulted in a denser type of infilling. In this study, a simple increase in water flow through the soil resulted in an increase in movement of fines

without continuous cycles of freeze-thaw. Loose infillings, characteristic of high-chroma features, correspond with the uncultivated or undisturbed soils of Oliveira et al. (2010) as expected.

Note that a loose silty infilling accompanied by a nucleating grain of iron oxide, as found by Oliveira et al. (2010), has the potential to become a high-chroma feature under conditions of alternating oxidation and reduction that would mobilize the iron (and possibly manganese) and re-precipitate as iron and/or manganese (hydr)oxide coatings on the silt particles that have infilled the vesicle. Oliveira et al. (2010) might have found an example of the pedogenic hypothesis getting set up if the infilled pore is a closed vesicle (and weathering of the iron oxide grain proceeds).

Although silt is reported inside pores, no unequivocal evidence or theory of movement can be presented for the infilling of closed pores or vesicles by silt or very fine sand, especially in loamy soils. And once in, one could ask why the silt is not removed by the same process. A possible explanation is that whatever the specific process causing translocation of silt, it is buffered within the feature and is not capable of effecting particle movement out of the vesicle. Movement of silt into the vesicle is probably the weakest part of the pedogenic hypothesis.

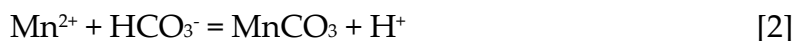
(4) Re-precipitation and transformation of iron and manganese minerals

Any discussion of events leading to the reprecipitation of solutes in vesicles is faced with an unknown mixture of iron, manganese, and other cations and anions, and possibly dissolved organic matter as well. This mixture interacts with the principle species of iron and manganese in complex and unknown ways, so any explanation of events involves considerable uncertainty.

In the discussion that follows, the term “vesicles” becomes a generalized reference to any closed pores or voids, including vesicles and vugs.

Precipitation

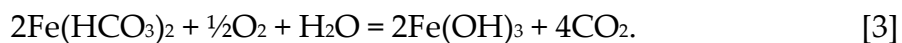
Reductive dissolution of minerals precipitated upon the formation of vesicles continues within the vesicle after arrival of the silt. Microbial activity will have consumed much of the oxygen and increased the carbon dioxide content in the protosoil. Eventually saturation is reached within the vesicle for one or more carbonate minerals. Under conditions of low redox potential and high P_{CO_2} , $FeCO_3$ (siderite), or $MnCO_3$ (rhodochrosite), precipitates onto the surface of the silt particles within the vesicle. Depending on local microenvironmental conditions within the vesicle, siderite, rhodochrosite, a mixture of the two, or a more complex mixed iron-manganese-magnesium-calcium carbonate similar to ankerite, or ferroan dolomite will precipitate. The process is similar to that described for the formation of siderite (Lindsay 1988:51). According to Matsunaga et al. (1993) and Mettler et al. (2001):



Upon dewatering of the protosoil, increasing redox potential causes Fe^{2+} in solution to precipitate as iron (hydr)oxides, the specific mineral dependant upon the particular conditions within the vesicle. While Fe^{2+} oxidizes readily in air, Mn^{2+} on its own does not oxidize readily in air except at high pH (McKenzie 1989). Aqueous solutions of Mn^{2+} even at a pH of 8.4 may take years to oxidize if uncatalyzed (Martin 2005). Only at a pH of 10 or higher will manganese oxidize readily without the help of a catalyst. Three possible catalysts that could be

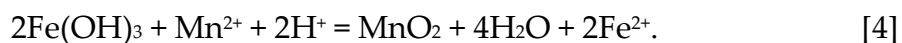
present in filled vesicles are iron oxides, manganese oxides, and oxidizing bacteria.

In a bicarbonate solution, Tillmans (1914) gives the oxidation of iron bicarbonate (in slightly modified form) as:



Ferric hydroxide is a stable compound that is precipitated rapidly from a bicarbonate solution by simple aeration (Savage 1936). The ferric hydroxide product can be taken as a generalized representation of a number of iron (hydr)oxides including what is now known to be ferrihydrite.

This initial oxidation and precipitation of iron (hydr)oxides may promote the oxidation of Mn^{2+} in a reaction similar that proposed by Hem (1964):



The reaction is normally displaced far to the left but under low Fe^{2+} activity, oxidation of Mn^{2+} could occur (McKenzie 1989). Low Fe^{2+} activity might exist in a vesicle immediately after the precipitation of iron carbonates. Manganese oxides produced from this reaction catalyze the oxidation of Mn^{2+} remaining in solution. The manganese mineral produced from this reaction may actually be a hydroxide and will be discussed later. Heterogeneous oxidation of Mn^{2+} takes place on Fe^{3+} surfaces, such as Mn^{2+} on FeOOH (Martin 2005). Upon oxidation of Mn^{2+} , Fe^{3+} is reduced to Fe^{2+} , which can return to solution and re-precipitate.

Once precipitated, manganese oxides are capable of autocatalysis. Mn^{2+} catalyzes on manganese (hydr)oxides such as MnOOH producing additional MnOOH (Martin 2005). All manganese is efficiently and effectively removed from solution through catalysis (Spector 1941). Once the precipitation reaction is

completed, oxides so formed are then available for further oxidation, which will be discussed later.

Although Fe^{3+} will oxidize manganese in the presence of oxygen, the failure of water supply systems to oxidize manganese while effectively removing iron by mechanical aeration (Zapffe 1931) suggests that the mechanism is not always active or effective.

Manganese is rapidly oxidized by microbes (Tebo et al. 1997). Both iron and manganese may be oxidized and precipitated by the activity of oxidizing bacteria. Biotic oxidation is not necessarily exclusive of abiotic processes and they may occur simultaneously (Zapffe 1931, 1933). Precipitation of iron and manganese from solution might also be the result of a combination of microbial oxidation and catalysis begun even before dewatering of the proto soil is complete.

Manganese oxides can promote the oxidation and precipitation of Fe^{2+} as iron (hydr)oxide minerals. Birnessite, cryptomelane, hausmannite, and pyrolusite were all found to oxidize Fe^{2+} in solution to goethite, akaganeite, and magnetite (Krishnamurti and Huang 1987, 1988). No precipitate formed at pHs below 5.0. Lepidocrocite did not form when manganese was present.

It appears, therefore, that iron oxides promote the oxidation of Mn^{2+} and manganese oxides promote the oxidation of Fe^{2+} . Zapffe (1933) makes reference to the close association of manganese and iron, the "rapidity with which they come out of solution in water mains, and the catalytic effect of the oxide of the one on the deposition of the other." Which process is active may depend on factors such as species activity and pH. Manganese tends to deposit where both manganese and iron are already present. Iron will deposit on manganese and on

previously deposited iron but since Fe^{2+} is oxidized more rapidly in the presence of MnO_2 , it tends to deposit on accumulating manganese rather than existing iron oxides (McKenzie 1989:453).

Overall, a likely scenario is that both microbial oxidation and auto-oxidation contributed to the precipitation of manganese (hydr)oxides, as suggested by Sullivan and Koppi (1992) and possibly iron (hydr)oxides as well. Regardless of the process, iron and manganese with their sometimes distinctive colors and morphologies along with silica precipitate out of solution. As an example of the possible variety that can exist in a sediment, ferric hydroxide, manganese oxyhydroxides, rhodochrosite, and an iron-manganese phosphate were identified in sediments of Elk Lake in Itasca State Park, Minnesota (Nuhfer et al. 1993).

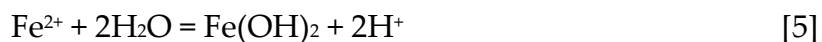
Iron transformations

As the till dewateres and oxygen re-enters the infilled vesicles, Fe^{2+} may be first to oxidize and precipitate as the redox potential increases. A homogeneous oxidation of iron would be expected to lead initially to ferrihydrite, generically $\text{Fe}(\text{OH})_3$ as in Eq. [3], with goethite, lepidocrocite, hematite and other iron (hydr)oxide minerals appearing later. The transformation pathway may actually begin earlier with the formation of what are called green rusts.

Green rusts are layered hydroxides consisting of stacked sheets of $\text{Fe}(\text{II})(\text{OH})_6$ octahedra in which some of the $\text{Fe}(\text{II})$ is oxidized to produce a positive layer charge (Bigam et al. 2002:327). This charge is balanced by interlayer cations including Cl^- , SO_4^{2-} , or CO_3^{2-} . Various divalent and trivalent cations may also be present leading to a range of possible combinations of pure or mixed phases (Taylor and McKenzie 1980). Green rusts are considered a

double hydroxide of the pyroaurite group, isostructural with hydrotalcite (Taylor 1980). In soils, the carbonate form, Fe(II)Fe(III)hydroxy-carbonate, is more likely to form than the sulfate or chloride variant. Stampfl (1969), in a study of metal corrosion, found the average composition of the carbonate to be $\text{Fe(II)}_4\text{Fe(III)}_2(\text{OH})_{12}\text{CO}_3$ but noted a variable Fe(II)/Fe(III) ratio. Variations in this ratio are responsible in part for variations in oxidation products of the hydroxy-carbonate.

The basic structural unit of Fe(II)Fe(III)hydroxy-carbonate is Fe(OH)_2 (Bigam et al. 2002:327), which appears as hydrolyzed Fe^{2+} under mildly alkaline conditions (formula based loosely on Martin 2005:65):



Ferrous hydroxide and siderite have been used to synthesize Fe(II)Fe(III)hydroxy-carbonate in aqueous solutions saturated in CO_2 (Taylor 1980). Fe(III) was added either as ferric nitrate or ferrihydrite. With Fe(III) added as nitrate, the main product was Fe(II)Fe(III)hydroxy-carbonate. Siderite appeared at higher Fe(II)/Fe(III) ratios while magnetite appeared at lower Fe(II)/Fe(III) ratios. When Fe(III) was added as ferrihydrite, the amount of Fe(II)Fe(III)hydroxy-carbonate was much lower, was poorly crystalline, and changed rapidly to a dark brown color. When no Fe(III) was added but was allowed to form through partial oxidation of Fe(II) in solution, siderite was the dominant phase especially at high Fe(II)/Fe(III) ratios. In general, Taylor (1980) found that Fe(II)Fe(III)hydroxy-carbonate, magnetite, siderite, and goethite formed as reaction products, either separately or in combination.

Green rusts are very unstable under oxidizing conditions. This instability may explain why they have not been found in soils (Schwertmann and Taylor

1989:394; Lewis 1997:354) until recently. They readily transform to goethite under slow oxidation in the presence of carbonates, lepidocrocite under rapid oxidation at pH from 5 to 7, or maghemite by oxidation of metastable magnetite that forms from slow oxidation of Fe^{2+} at a pH of 7 to 8 (Bigham et al. 2002:327,339). Taylor (1980) found that hydroxy-carbonate altered to ferrihydrite within seven days with some residual hydroxy-carbonate remaining after 31 days. Siderite with small amounts of hydroxy-carbonate altered to small amounts of ferrihydrite in air but to ferrihydrite and poorly crystalline goethite with small amounts of residual hydroxy-carbonate when oxidized in water. One sample of Fe(II)Fe(III)hydroxy-carbonate oxidized in water to poorly crystalline lepidocrocite. When the hydroxy-carbonate precipitate was held under vacuum, slight ferro-magnetism developed as the result of a solid-state transition to magnetite or maghemite. The transition to magnetic material took place between a few days and two months. Heating siderite and magnetite plus hydroxy-carbonate samples to 105° for 1 hour and 24 hours respectively changed the color to red-brown and changed the XRD spacings to a lower value indicating oxidation towards a maghemite end member. Diffraction lines of the siderite and hydroxy-carbonate disappeared, possibly having been replaced with hematite, but that finding was not confirmed.

The natural form of green rust is the mineral fougèrite, a layered double hydroxide clay mineral. Fougèrite can form by abiotic processes, by solution phase oxidation reactions, or biotically through reduction of Fe^{3+} oxides (Trolard et al. 2007:332). Fougèrite as a precursor mineral might have provided the substrate for the thin platy fine-silt material found in high-chroma mottles viewed under the SEM, although fougèrite crystals found in natural soils were

~400–500 nm (Trolard et al. 2007), one-tenth the size of the finest material found in high-chroma features.

Alteration of green rust or fougèrite in air could lead to the formation of the more stable iron oxide minerals ferrihydrite, goethite, or lepidocrocite. Ferrihydrite, a metastable mineral, typically alters to hematite or goethite, although despite favorable thermodynamics, kinetics often limits the rate and extent of the transformation (Schwertmann and Taylor 1989; Bigham et al. 2002). Hematite rather than goethite could form locally from ferrihydrite under suitable conditions, such as locally high pH. Changing environmental conditions could lead to the alternating formation of hematite and goethite and other iron (hydr)oxides, either from ferrihydrite or through solid-state or solution transformations. Ferrihydrite, goethite, and hematite were the only iron oxide minerals tentatively identified with μ XRD and all can form by the oxidation of a green rust precursor.

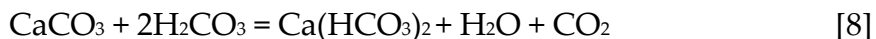
Ferrihydrite and goethite can also result from the oxidation of iron carbonates or may have formed on the carbonate-coated silt particles, either through precipitation or through reaction with Fe(II)Fe(III)hydroxy-carbonate present in solution. The oxidation of iron and manganese carbonate produces carbonic acid (Eq. [6] and [7]) that reacts with any calcite that might be present to produce soluble calcium bicarbonate (Eq. [8]). Calcium bicarbonate is removed easily from the developing feature. The oxidation of siderite is given by Postma (1983):



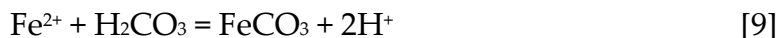
and by analogy, rhodochrosite:



The dissolution of calcite in carbonic acid forms additional CO₂:



Carbonic acid precipitates any remaining iron and manganese as their relatively insoluble carbonates shown in Eq. [9] and [10] (McBride 1994:243) before dissociation of carbonic acid into H⁺ and HCO₃²⁻ as in Eq. [1] and [2]:



Acidity produced by the above reactions has two consequences of relevance to the composition and formation of high-chroma features: calcite buffers the acidity and will be removed from the system with the formation of calcium bicarbonate and CO₂ and the production of CO₂ reduces the oxygen content in the vesicle and slowing the oxidation of iron and manganese. The presence of carbonates prevents the pH from rising much above 7 (McBride 1994:243).

It is not difficult to conceive of a mixed Fe(II)Fe(III) solution within the vesicles enclosing the developing high-chroma features leading to the formation of Fe(II)Fe(III)hydroxy-carbonate or green rusts as precursors for oxidation to subsequent iron (hydr)oxide minerals. Solution chemistry within vesicles would seem to favor the formation of a hydroxy-carbonate compatible with earlier carbonate and iron precipitation. Subsequent alteration to a variety of iron (hydr)oxide minerals under rapidly changing soil-environment conditions accounts for variations in iron mineral content found in high-chroma features.

Manganese transformations

Although manganese was not found in concentrations above that of the soil matrix, given its presence in the till, its reactivity, and similarity to iron it is

likely to be important for the formation of high-chroma features. Its relatively low concentration in high-chroma features might be a modern condition and does not represent most of the formational history of high-chroma features.

More than 30 manganese (hydr)oxides are known (Post 1999). Possible pathways to their formation and interconversion are even more diverse. The mineral species most relevant to the formation of high-chroma features are listed in Table 16. Convention in the literature seems to be that MnO_2 symbolizes any Mn^{4+} oxide of the basic form Mn_xO_{2x} , not just pyrolusite, and that convention will be followed here.

Synthesis experiments performed by Hem and Lind (1983) with different starting minerals and formation conditions illustrate some of the possibilities. With solutions of manganese chloride, manganese nitrate, and manganese perchlorate at a pH of 8.5 to 9.5, hausmannite formed at or above 25°C, while feitknechtite formed at temperatures near 0°C. Starting with a solution of manganese sulfate, under the same conditions, at temperatures near 0°C, the product was a mixture of manganite and groutite. Hausmannite altered spontaneously to manganite. Continued alteration to MnO_2 is slow at neutral pH and is hindered by the formation of manganite. Less stable feitknechtite readily altered to manganite under wider ranges of pH and manganese activity than for the hausmannite pathway. More than 25% of the original feitknechtite converted to MnO_2 in seven months with some manganite still remaining unaltered. In all cases, the final Mn^{4+} product, designated generically as MnO_2 , may be birnessite, ramsdellite, or conceivably pyrolusite, although pyrolusite is not specifically mentioned. Manganite is present in all pathways, whether as the initial precipitate, an intermediate, or the endpoint. The variety of reaction products

Table 16. Manganese minerals through ramsdellite are listed by increasing oxidation state of their manganese. Unknown or variable forms have been placed below ramsdellite. Iron minerals with an approximate corresponding composition are shown on the right. Data are from various sources and are provided as a reference only.

Manganese		Iron	
Mineral	Formula/Compound	Mineral	Formula/Compound
Manganosite	Mn^{2+}O		
Pyrochroite	$\text{Mn}^{2+}(\text{OH})_2$	Green rust§	$\text{Fe}^{2+}(\text{OH})_2$
Hausmannite	$\text{Mn}^{2+}\text{Mn}_2^{3+}\text{O}_4$	Magnetite	$\text{Fe}^{2+}\text{Fe}_2^{3+}\text{O}_4$
Groutite	$\alpha\text{-Mn}^{3+}\text{OOH}$	Goethite	$\alpha\text{-Fe}^{3+}\text{OOH}$
Feitknectite	$\beta\text{-Mn}^{3+}\text{OOH}$	Akaganeite	$\beta\text{-Fe}^{3+}\text{O}(\text{OH}, \text{Cl})$
Manganite	$\gamma\text{-Mn}^{3+}\text{OOH}$	Lepidocrocite	$\gamma\text{-Fe}^{3+}\text{OOH}$
		Feroxyhyte	$\delta'\text{-Fe}^{3+}\text{OOH}$
Todorokite	$(\text{Mn}^{2+}, \text{Ca}, \text{Na}, \text{K})(\text{Mn}^{4+}, \text{Mn}^{2+}, \text{Mg})_6\text{O}_{12} \cdot 3\text{H}_2\text{O}$		
Birnessite†	$(\text{Na}, \text{Ca})_{0.5}(\text{Mn}^{4+}\text{Mn}^{3+})_2\text{O}_4 \cdot 1.5\text{H}_2\text{O}$		
Romanèchite	$(\text{Ba}, \text{H}_2\text{O})_2(\text{Mn}^{4+}, \text{Mn}^{3+})_5\text{O}_{10}$		
Cryptomelane	$\text{K}_{1-1.5}(\text{Mn}^{4+}, \text{Mn}^{3+})_8\text{O}_{16}$		
Hollandite	$\text{Ba}(\text{Mn}^{4+}, \text{Mn}^{3+})_8\text{O}_{16}$		
Vernadite	$(\text{Mn}^{4+}, \text{Fe}^{3+}, \text{Ca}, \text{Na})(\text{O}, \text{OH})_2 \cdot n\text{H}_2\text{O}$		
Pyrolusite	$\beta\text{-Mn}^{4+}\text{O}_2$		
Ramsdellite	Mn^{4+}O_2		
Buserite	$\text{Na}_4\text{Mn}_{14}\text{O}_{27} \cdot 3\text{H}_2\text{O}$		
Bixbyite‡	$(\text{Mn}^{3+}, \text{Fe}^{3+})_2\text{O}_3$	Hematite	$\alpha\text{-Fe}_2^{3+}\text{O}_3$
		Maghemite	$\gamma\text{-Fe}_2^{3+}\text{O}_3$
		Ferrihydrite	$5\text{Fe}_2^{3+}\text{O}_3 \cdot 9\text{H}_2\text{O}$
		Fougèrite¶	$(\text{Fe}^{2+}, \text{Mg})_6\text{Fe}_2^{3+}(\text{OH})_{18} \cdot 4\text{H}_2\text{O}$

† Designated $\delta\text{-Mn}^{4+}\text{O}_2$ by Bricker (1965)

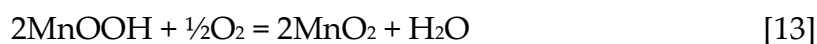
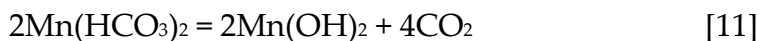
‡ or Mn_2O_3 (Bricker 1965)

§ A group of compounds with the basic $\text{Fe}(\text{OH})_2$ trioctahedral sheet structure. Positive layer charge from partial oxidation of Fe^{3+} is balanced by various inner layer cations as Cl^- , SO_4^{2-} , CO_3^{2-} , resulting in, for example, $\text{Fe}(\text{II})_4\text{Fe}(\text{III})_2(\text{OH})_{12}(\text{CO}_3) \cdot 3\text{H}_2\text{O}$ (Bigham et al. 2002:324; Ruby et al. 2010). Taylor (1980) refers to this compound as F(II)Fe(III)hydroxy-carbonate.

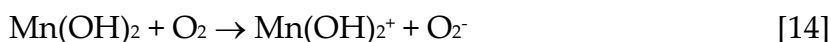
¶ A naturally occurring green rust that may contain Cl^- , SO_4^{2-} , CO_3^{2-} or other anions replacing (OH) (Hem and Lind 1983).

and metastable intermediates formed under differing conditions in the laboratory supports the conclusion that a variety of mineral species will also be found in soils that have changing physical and chemical environments (Vodyanitskii et al. 2003).

As with iron, the assumption is that manganese (hydr)oxides precipitate within a vesicle out of a bicarbonate solution. Again, Tillmans (1914) provided a sequence of reactions to account for the ultimate appearance of pyrolusite. They are presented here in somewhat modified form:



The sequence begins with $\text{Mn}(\text{HCO}_3)_2$, a species that exists only in solution. Once MnO_2 is formed, it acts as a catalyst producing more $\text{Mn}(\text{OH})_2$ and leaving the MnO_2 unchanged (Zappfe 1931:824) although MnOOH will also catalyze the oxidation of Mn^{2+} (Martin 2005). All the $\text{Mn}(\text{OH})_2$ produced eventually oxidizes to MnO_2 (Spector 1941:3). The sequence is consistent with increasing oxidation state of the manganese. Also consistent with the above sequence, Martin (2005) gives the oxidation of $\text{Mn}(\text{OH})_2$ as:



And noted that $\text{Mn}(\text{OH})_2^+$ polymerizes rapidly to a Mn-oxide precipitate such as MnOOH .

A similar pathway, romanèchite to manganite to pyrolusite, was proposed by Hanson (1932:16) and supported in part by Spector (1941). (Their term for romanèchite is the obsolete term, psilomelane.) Hanson (1932:18) based his sequence on the observation that vein manganese deposits in Canada began with

manganiferous calcite that oxidized to four zones each tens of feet thick, from most oxidized on top to least oxidized at the bottom. At the top he found hematite and hydrated iron oxides; below that, pyrolusite; below that, manganite, below that, psilomelane (romanèchite); and below that, manganiferous calcite and granite. Hanson's (1932) sequence is not consistent with the order of oxidation and reactivity (Table 16).

Noting that solid $Mn(OH)_2$ in Eq. [11] and [14] is the mineral pyrochroite, a speculative and more complex pathway for the precipitation and alteration of manganese minerals within vesicles can be worked out. The sequence follows the reactivity sequence and oxidation states of manganese (hydr)oxides in Table 16. Some parts of the alteration sequence are derived from information found in the Handbook of Mineralogy published by the American Mineralogical Society.

The sequence begins with pyrochroite. Pyrochroite oxidizes to feitknechtite or possibly to a mixture of groutite and feitknechtite, then to manganite, and finally to MnO_2 , which could be romanèchite or birnessite. Pyrochroite crystals are commonly tabular or rhombohedral, and as a lower manganese hydroxide, may appear pink to blue-purple (among other colors, including colorless). Although it darkens to brown to black, residual pyrochroite may account for some of the pink and pinkish-purple color observed in high-chroma features adjacent to black areas if its alteration to higher oxides is incomplete. Feitknechtite occurs as hexagonal platelets, often with hausmannite. Any of these forms, upon slight to moderate weathering, match to some degree the morphology of the fine silt platelets in high-chroma features. Platelets are lacking a clearly hexagonal shape, but that shape may never have formed well or was lost in subsequent weathering. Continued oxidation could result in the

formation of manganite possibly mixed with groutite. Both these minerals match the color and morphology of the larger dark iridescent fragments that appear in Class 4 features. Oxidation might then continue to the final product, pyrolusite.

Micro-XRD and TEM provided some evidence for the presence of romanèchite. Analysis by ICP found barium, an essential element of romanèchite, although barite is commonly present in sedimentary manganese deposits (Hanson 1932:11). The appearance of a dark, iridescent blue-black mineral with longitudinal striations visible in larger fragments of material found in high-chroma features suggests the possible presence of manganite. Reaction of the dark material with hydrogen peroxide was weaker than expected if the dark mineral were pyrolusite (Mn^{4+}O_2) or other Mn_xO_{2x} oxide. As a lower (hydr)oxide of manganese, manganite (Mn^{3+}OOH) may give only a weak reaction to dilute hydrogen peroxide. Some rhombs found in high-chroma features that react positively with potassium ferricyanide might be Fe-carbonate coated pyrochroite.

A question remains how far these transformations proceed in the 12,000 years since soil formation began. Under mildly alkaline conditions, $\text{Mn}(\text{OH})_2$ (pyrochroite) was oxidized in air to hausmannite and then to manganite but no further (Bricker 1965). Considerable time is required for manganite to convert to MnO_2 (Hem and Lind 1983; Martin 2005:65), although Savage (1936) states that it readily oxidizes to MnO_2 . If Hanson's (1932) sequence is correct, some romanèchite might still be present within high-chroma features with only minor amounts, if any, of pyrolusite. More likely, romanèchite formed towards the end of the sequence incorporating barium from weathered barite.

Microbial formation of feitknechtite and manganite at high Mn^{2+} concentrations and relatively high pH has been reported (Tebo et al. 1997:235). At lower Mn^{2+} concentrations and pH, Mn^{4+} minerals formed, suggesting that microbes are capable of oxidizing Mn^{2+} to Mn^{4+} without lower valence state intermediates. Other studies support direct microbial oxidation of Mn^{2+} to Mn^{4+} (Tebo et al. 1997; Wehrli et al. 1995).

Birnessite can form through microbial oxidation of Mn^{2+} as well as non-microbial oxidation (Sullivan and Koppi 1992). Abiotic formation by slow oxidation and crystallization results in a more ordered structure and larger crystals than microbially oxidized manganese minerals. Birnessite typically appears as aggregates of flakes (Chukhrov and Gorshkov 1981). As discussed earlier, birnessite flakes approximately 2 to 3 μm in diameter resembling those in Figures 10 and 12 were synthesized by Golden et al. (1988). Subsequent reaction with Fe^{2+} resulted in an iron oxide pseudomorph of birnessite.

Carbonates

A number of oxidation and dissolution reactions of both iron and manganese produce acidity and carbon dioxide, which decrease oxygen concentrations and when dissolved in the pore water solution, contribute acidity. Any calcite present will buffer the acidity and add CO_2 but overall the result may have been that any calcite initially present in a developing high-chroma feature has been dissolved and removed as bicarbonate and CO_2 (Eq. [7]).

Oxidation of the siderite-rhodochrosite-ankerite-like carbonate coating on silt particles within a high-chroma feature would produce either black manganese oxides that may be responsible for the black material in high-chroma features or the distinctive strong brown color of high-chroma features that results

from the presence of iron (hydr)oxides, depending on the local chemistry within the vesicle and the relative composition of the mixed cation carbonate.

(5) Weathering and degradation of iron-manganese features

Once formed, pedogenic iron-manganese concentrations will weather to high-chroma features through the same processes and result in essentially the same products as features that formed non-pedogenically. A number of the reactions given for the transformation of iron and manganese under the pedogenic hypothesis might also pertain to transformations that occur as non-pedogenic features transform and weather. Final weathering and transformation/degradation is discussed previously in the section on non-pedogenic features.

Summary of the pedogenic, inherited hypothesis

Vesicles matching the size and shape of high-chroma features form at depth (50 to 100 cm) in the protoil shortly after retreat of the glacier, possibly at initial freeze-thaw. Vesicle walls define the sharp boundary with the soil matrix and give the developing high-chroma feature its intrusive character. Overburden pressure may deform the otherwise round vesicle into an irregular shape.

The protoil solution within the pores of the saturated glacial sediment contains relatively high concentrations of Mn^{2+} , Fe^{2+} , Si, Mg, and Ca bicarbonates. This saturated solution enters the air-filled vesicles where solutes precipitate through oxidation or drying.

Large amounts of silt from the base of the glacier eluviate downward by the action of freeze-thaw and the gravitational movement of large amounts of melt-water. This glacial silt, along with some very fine sand, accumulates within the newly formed vesicles to form a poorly cemented, loose infilling. A

restrictive layer forms at depth by freeze-thaw and retards the downward flow of the silt, which aids vesicle infilling. This restrictive layer is weakly developed and later deteriorates until at most only a remnant weak platy structure remains as is observed in peds from some sites. Excess silt is eventually removed from the surrounding proto-soil matrix as are any silt caps that might have formed. Silt remains in the vesicles.

Water from glacial melt, snowmelt, rainfall, and melting of entrained ice within the stagnation moraine saturates the upper layers, especially the active layer above any buried ice blocks at a depth of at least 50 to 100 cm. The possible formation of high chroma features above buried ice blocks may help explain localized occurrences across the landscape. Inside the vesicles, during periods of saturation and reduction, the iron and manganese oxides that were initially precipitated in vesicles are reduced and dissolve into solution within the vesicle. Some iron and manganese diffuses out of the vesicle resulting in a slight increase in the concentration of iron and manganese around the vesicle periphery that later oxidizes, resulting in the first appearance of a halo around the feature.

Eventually saturation is reached for one or more carbonate minerals within vesicles. Under reducing conditions and the high P_{CO_2} expected at depth under these conditions, iron and manganese carbonates or an Fe-Mn-Mg-Ca carbonate similar to ankerite or ferroan dolomite precipitates onto the surfaces of the silt particles within the vesicle depending on micro-environmental conditions within vesicles. Upon dewatering of the proto-soil, rising redox potential causes Fe^{2+} in solution to precipitate as iron (hydr)oxides leading in turn to oxidation of Mn^{2+} and co-precipitation of iron and manganese. Precipitation of iron and manganese from solution might also be the result of a combination of microbial

oxidation and autocatalysis. Oxidation and precipitation of iron and manganese (hydr)oxides are at least partially responsible for the strong brown and black color observed in high-chroma features. Oxidation of the siderite-rhodochrosite-ankerite-like carbonate coating on silt particles also produces either black manganese oxides (from MnCO_3) or the distinctive strong brown color of iron (hydr)oxides (from FeCO_3 or ankerite) that are observed in high-chroma features. The vesicle now begins to take on the appearance of a high-chroma feature.

Iron and manganese (hydr)oxide minerals formed initially within the vesicle alter to more stable forms. Some of the original manganese minerals may become iron mineral alteromorphs. Some of these new forms may be responsible for the more subtle color patterns observed in high-chroma features.

Much of the original manganese and iron was quickly removed from the developing soil, either incorporated into vesicles or leached out of the developing soil profile and eventually into the groundwater. Continued drying of the soil and sustained oxidizing conditions introduced the onset of weathering. Features began to degrade primarily under seasonal cycles of oxidation and reduction and under present environmental conditions continue to degrade.

Pedogenic, coeval

Hypothesis: High-chroma features are iron-manganese concentrations that are actively forming through pedogenic processes in the modern soil and at the location in which they are presently found.

One version of this hypothesis states that the processes of formation that produce inherited pedogenic high-chroma features in the immediate post-glacial period are the same processes that produce high-chroma features coeval with

modern soil development. The difference is simply a matter of when the processes take place.

A second version is a classic “redox feature” hypothesis. Almost certainly, small amounts of manganese and iron continue to be mobilized during brief periods of saturation and reduction during and shortly after significant rainfall events and snowmelt. Upon encountering an air-filled void or an existing iron-manganese concentration acting as a nucleating site, dissolved iron and manganese oxidizes and precipitates. Dissolved iron (and manganese) in solution diffuse along a concentration gradient in the direction of lower Fe^{2+} concentration, a gradient set up by the oxidation of Fe^{2+} to Fe^{3+} at the nucleating site. The halo that is observed around many high-chroma features would then indicate movement of iron and manganese into the void, a seemingly unlikely situation discussed earlier.

Modern soils do not experience the long, deep cycles of oxidation-reduction and freeze-thaw of recently exposed glacial sediments and proto soils, and lack a silt source for infilling, all of which are required to form high-chroma features under the pedogenic hypothesis. The quantity of iron and manganese that is mobilized in modern soils probably is insufficient to form high-chroma features. Modern environmental conditions do not seem favorable for the neoformation or continued growth of existing high-chroma features.

One possibility, however, is that very small Class 2 features are recent, having formed in the absence of or with only a minimal amount of soil manganese, in a process similar to that described for “classic redox” but on a more limited scale. They could form in small voids adjacent to sand fragments, for example, that have been created by the action of freeze-thaw, but any small

void, especially an enclosed void could suffice. In this case, inflorescence of iron oxides into the void might account for the loose infilling and silty character of the new feature. Small, fragile, high-chroma concentrations have been observed occasionally in peds but are not common and would not be visible in the field. These very small features may represent one extreme of a natural size range of high-chroma features, while the largest features approach the other extreme, although it is unclear what might actually limit the sizes of high-chroma features, especially at the large end. The process or processes responsible for the formation of features at these two endpoints may be different.

Apart from the rather innocuous features described above, a more likely candidate for coeval status are brown, smooth, rounded lumps or nodules of manganese oxide, possibly birnessite, that have formed on the surfaces of sand-size fragments of shale and quartz (Plate 16). The external morphology of these features gives the appearance of their having been formed through microbial oxidation. Some of these features bear some similarity to Class 5 features, having adjacent areas of reddish and yellowish colors (Plate 26). These features have not been closely studied and any suggestions as to their origin and developmental chronology are purely speculative.

Geode hypothesis

Hypothesis: High-chroma features are degrading iron-manganese concentrations that formed by a combination of non-pedogenic void formation and pedogenic void filling processes and are now degrading in the modern soil.

The geode hypothesis combines a non-pedogenic precursor with subsequent pedogenic processes. Cavity or void formation is similar to the non-

pedogenic hypothesis but the process of filling the void is similar to that of the pedogenic hypothesis.

An initial cavity is a necessary prerequisite for the formation of a geode (Bassler 1908) as is true with the pedogenic hypothesis. Under this hypothesis, the initial cavity is a void made in the soil by the dissolution of a soluble fragment of a mineral such as calcite, dolomite, or gypsum. After dissolution of the soluble mineral, silt residue that had been incorporated in the mineral during its formation remains in the new- formed void. The silt particles acts as precipitation or crystallization nuclei during periods of oxidation following periods of reduction and mobilization of iron and manganese into the void.

As limestone fragments dissolve, they leave behind silt (Ugolini 1986). The silt is composed mostly of more resistant dolomite and quartz, whereas calcium carbonate is dissolved and removed. Much of the carbonate in these soils is secondary or pedogenic, suggesting that dissolution of limestone from bedrock sources incorporated into the till has been an active process. High-chroma features do not contain calcite but do contain dolomite and ferroan dolomite, possible residue from weathered limestone. The limestone fragments, however, would need to be well-rounded in many cases and of relatively uniform, generally sub-millimeter size, to match the size and shape of high-chroma features.

In calcareous sediments, vesicles may be preserved as microgeodes of calcite (Van Vliet-Lanoë et al. 1984). Calcium carbonate has an affinity for the surface adsorption of iron and manganese, sometimes lowering solution concentration below that expected for precipitation of the corresponding carbonate minerals and sufficiently low to induce iron chlorosis in crops grown

on calcareous soils (McBride 1979; Loeppert and Clarke 1984; Loeppert and Hossner 1984; Clarke et al. 1985; Loeppert 1986; Mania et al. 1989). Subsequent dissolution of the calcite substrate and transformation of the surface-precipitated iron and manganese oxides similar to processes described under the pedogenic hypotheses lead to the formation of high-chroma features. A carbonate enriched in iron and manganese such as ferroan dolomite or ankerite would be even more effective as a precipitation nucleus and also as an independent source of iron and manganese.

The “microgeode” hypothesis (Van Vliet-Lanoë et al. 1984) differs somewhat in that an existing vesicle becomes lined with calcite as soil solution enters the cavity and precipitates calcite on the inner cavity wall.

Uncertainty exists as to when dissolution and infilling of the resultant cavity would take place. Sediment and protosoil solutions before or immediately after deglaciation are likely to be at or near saturation for the most soluble minerals, yet filling the resulting pore with iron and manganese minerals must take place very early in soil formation in accord with the reasoning developed for the pedogenic hypotheses. Mineral dissolution would have to take place early before saturation prevents further dissolution.

The geodic hypothesis has important similarities to the non-pedogenic hypothesis. The required void is defined by the physical extent of the dissolved mineral fragment, which also supplies silt. Residual material such as iron and manganese (hydr)oxides and carbonates may supply iron and manganese directly and could also act as nucleating sites, oxidizing Fe^{2+} and Mn^{2+} in the soil solution causing them to precipitate as (hydr)oxides within the void. Microbial oxidation of iron and manganese may also play an important role under the

geode hypothesis. Partially filled voids high in CO₂ as a carbon source and sufficient manganese and iron as electron acceptors may provide a favorable environment for the establishment and maintenance of active lithotrophic bacterial colonies.

Geodes are considered to be very rare in soils (Stoops 2003) and only a few high-chroma features exhibit the morphology of a geode. Those with the best developed cortexes, especially those few whose cortex appears as an orderly arrangement of crystals (Plates 23, 24, 29), suggest geodic morphology and the presence of associated formation processes. A geodic hypothesis was not explored further but merits consideration for a complete study of high-chroma features.

Other hypotheses

Other hypotheses were considered during the course of this research. For completeness, brief mention is made here of several of those hypotheses. They are not developed further and are not thoroughly critiqued, but may serve as points of departure for further research.

An interesting hypothesis related to the formation of manganese oxides is based on the fungal weathering of manganese-containing siderite and rhodochrosite to produce concentrations of "a laminar oxide mineral of manganese which formed a characteristic form of open-fabric" (Golden et al. 1992:165). The mineral was identified as busserite. Busserite is very unstable and readily transforms to birnessite or todorokite, platy forms of manganese oxides. Todorokite has also been found as an oxidation product of siderite weathering in a lignite overburden in Texas (Senyaki et al. 1986). The loose open fabric of these minerals provides a large surface area for the reaction of Fe²⁺ with the manganese

oxide. Fe^{2+} in solution is oxidized to Fe^{3+} forming iron pseudomorphs of the manganese oxide mineral (Golden et al. 1988; Golden et al. 1992). The authors conclude that “the loose, fluffy aggregates of buserite are attractive speculations as centers for the formation of Fe-Mn nodules in soils” (Golden et al. 1992:167). The presence in Des Moines lobe till of siderite in the quantity and composition required for this hypothesis is questionable. Nevertheless, this hypothesis deserves more consideration and study.

The possibility exists that the precipitation of iron or manganese could take place in a small oxygenated void or at a nucleating site within the soil matrix. Local precipitation could also result from a localized increase in pH that would accompany the evolution of ammonia from decomposing organic matter, as suggested by Weeks (1953). As the feature grows, groundmass is pushed aside and the feature becomes intrusive. Thin sections show no stress or referred patterns around high-chroma features, however, and the presence of loose silt must still be explained.

A loose silty infilling accompanied by a nucleating grain of iron oxide, as found by Oliveira et al. (2010) and discussed earlier, has the potential to become a high-chroma feature if the void is a closed pore. During periods of saturation and reduction, iron and manganese present in the iron oxide grain would dissolve and enter the soil solution within the closed pore. When oxidizing conditions returned, the iron and manganese would precipitate as coatings on the silt particles. Under periods of extended oxidation, iron and manganese would alter to forms discussed previously.

A number of researchers have published on a topic variously called silt droplets and granules, silt clots or silt pellets, or clotted ice. These silt features are

found in a glacial facies “characterized by lenticular clots of silt and clay distributed through transparent ice” (Knight et al. 1994). Regardless of the name, these silt concentrations, if incorporated into the till and inherited by the parent material of the developing soil, have the potential to solve the problem of silt accumulation in high-chroma features. Questions of size, abundance, formation, and occurrence gave them a low priority and were not pursued further.

Kubiëna (1938:159) discussed the similarity of tests of the protozoa thecamoeba (tecamoeba) to granular shell-like structures in some chernozem soils (see Stout and Walker 1976; Patterson and Kumar 2002). Other biological molds include the remains of other protozoans, fresh-water ostracodes, or seeds such as pine or spruce that were present at glacial margins and resemble in several respects the size and shape of larger high-chroma features. These molds would infill in the same manner as do geodes or vesicles.

Pyrite or carbonate framboids could have been inherited from the bedrock source material by way of the till or as infillings of fossilized life forms (Krinsley et al. 1998: 45, 86, 87, et alia). Framboids are rounded microscopic spheroidal aggregates of smaller, individual crystals usually of pyrite (Ohfuji and Rickard 2005) although carbonate framboids have been produced in the laboratory (Fernández-Díaz et al. 2006; Katsikopoulos et al. 2009). Pyrite framboids are usually associated with sulfidic and saline soils (Rabenhorst and James 1992; Fitzpatrick et al. 1992). Formation of pyrite framboids seems unlikely in soils developed on Des Moines lobe till except possibly in wetland or peat soils having a sufficient supply of sulfur. Both pyrite and siderite framboids could be effective precursors, weathering to iron oxides and providing a well-defined nucleus of formation. Framboids are often small, less than 250µm in diameter and more

typically about 10 μ m in diameter (Ohfuji and Rickard 2005), too small for most of the high-chroma features that have been observed, unless growth occurred after their formation.

Considering their narrow formation requirements, occurrence, and morphology, these “other hypotheses” seem less likely than the proposed hypotheses to account for the formation of high-chroma features.

CONCLUSION

The hypothesis of choice is the non-pedogenic hypothesis of inherited precursors that weather to high-chroma features. Second choice is the geode hypothesis, and the third choice is the inherited pedogenic hypothesis. Fourth choice is the hypothesis of formation coeval with modern soil development. The first three hypotheses as ranked, consider high-chroma features to be degradational.

The inherited pedogenic hypothesis is based on a series of speculative events to explain the observations. If the probability of its being true is calculated as the combined probability of a sequence of improbable events, then the result is a very low probability that the inherited pedogenic hypotheses is a realistic explanation for the formation of high-chroma features.

To accept the non-pedogenic hypothesis and reject the inherited pedogenic hypothesis on the basis of their relative simplicity or complexity would be a misapplication of the principle of parsimony. Any individual model or hypothesis should be made as simple as possible without loss of explanatory power. A decision between competing models or hypotheses should be made on the basis of evidence and their ability to explain the observations rather than on relative complexity.

That the non-pedogenic hypothesis is simpler than the inherited pedogenic hypothesis is an illusion. The non-pedogenic hypothesis simply ignores the formation of iron-manganese nodule precursors, yet inherited nodules had to form somewhere, sometime, somehow. As with the inherited pedogenic hypothesis, their formation involved a sequence of probabilistic events that might have a low overall probability of occurrence but which must have taken place since their existence is the starting point of the hypothesis. If these lithogenic events are included in the non-pedogenic hypothesis, its apparent simplicity disappears. The events of nodule formation can be regarded as true and can be pared away (the razor of Occam's razor) from the hypothesis. Doing so does make for a simpler explanation but does not make it a more valid or accurate explanation. Only evidence, not simplicity, can decide accuracy. Evidence and explanatory power favors non-pedogenic explanations.

Probably the most challenging observation to explain is the presence of loose silt within high-chroma features. The proposed pedogenic hypothesis has considerable difficulty with this, most especially moving silt into the vesicle from outside, while the non-pedogenic hypothesis explains the presence of silt rather easily. An alternative explanation for the presence of loose, silty infilling material in pedogenic features is needed and might be found upon further examination. One possibility is that a feature is initially impregnative, but the soil matrix claimed by the growing feature has been disrupted in some way, chemically or physically, leaving behind only silt (and some very fine sand) as it becomes the internal fabric of the feature. No suitable mechanism for this hypothesis-within-a-hypothesis has been found. Discarding the pedogenic hypothesis entirely, however, may be premature.

Class 2 features and even some Class 3 features with a minimum amount of dark material may be pedogenic but have formed by means of a simpler and unknown version of the pedogenic hypothesis. Class 4 and 5 features, with their dark cores and relative abundance of dark fragments, seem most likely to be of non-pedogenic origin. More specifically, Class 3, 4, and 5 features form if manganese is present in relatively and increasingly high concentrations and Class 2 and Class 3 features form if the manganese concentration is relatively low.

High-chroma features seem unlikely to develop in modern soils. The quantity of iron present in high-chroma features relative to that in the modern soil matrix seems inadequate. Also, the need to invoke processes and environmental conditions associated with periglacial conditions at initial deglaciation excludes a recent origin. Present soil conditions are more favorable to weathering and degradation.

Although only a few features display geodic morphology, basic similarities of the geodic hypothesis to the non-pedogenic hypothesis make it a more attractive alternative in some cases than the pedogenic hypotheses. Again, the inheritance of silt from the dissolving mineral fragment and the initiation of the oxidation reaction by residual iron or manganese (hydr)oxides present in the dissolving fragment are more plausible explanations than those of the pedogenic hypotheses.

Existing classification systems provide little insight into genesis. Field definitions such as those of Schoeneberger et al. (2002) are useful despite inconsistencies with other systems but should be expanded to include descriptive terms to aid identification. The more detailed micromorphological

classification of features such as Bullock et al. (1985) allows greater resolution in classification but does not offer substantially greater insight into formation processes, although it should be noted that doing so was never their intent. Kubiëna (1938) offers some hypotheses and insights into formation processes but provides little help matching proposed genetic processes to descriptions since his descriptions are abbreviated or non-existent. Genetic definitions alone without descriptive or analytical criteria to confirm that the feature conforms to the genetic definition tend to confuse more than they clarify. Too much discretion is left to the individual micromorphologist making the interpretations, leading to inconsistencies and errors.

Given the present state of our understanding of soil and feature development, only physical, chemical, and mineralogical properties of a feature can be known with sufficient certainty to be used for identification and classification of pedofeatures. In most cases, and in particular for nodules and infillings, interpretations of genesis based on morphology are not linked closely and positively enough with genetic processes to provide reliable criteria for classification. Theoretical divisions and classes can be drawn up based solely on genetic factors, but when these are applied to actual features, the defining genetic criteria for those divisions prove to be inadequate, lacking any firm basis or justification for classification into the defined categories, as in the identification of biological and inherited concentrations in the field classification of Schoeneberger et al. (2002). That inability to link formational processes and observed morphology renders a genetic classification “useless and misleading” (Brewer 1972:87).

Rather than needing separate genetic and analytical/descriptive systems of classification, a classification system should be built in two steps. What is needed first is an adequate knowledge of genesis to provide the fundamental framework for a classification system. Each genetic class can then be defined by purely morphological terms that have a high correlation with the underlying genetic processes. These morphological terms can then be used to positively identify a particular feature as a true member of a predefined genetic class. For example, separating pedofeatures into those formed in voids and those not formed in voids defines a genetic framework. The morphological overlay to that genetic framework consists of descriptive criteria that positively identify which features formed in voids and which did not.

It is disappointing and rather remarkable that after so many years of discussing and studying nodules, concretions, and other common soil features, that no uniform definitions and terminology have been developed or have achieved widespread acceptance. Pettijohn's lament: "Rather obviously we are in need of better terminology" (Pettijohn 1975:462) remains true to this day.

High-chroma features should not be interpreted or classified as redoximorphic features; the argument for a non-pedogenic origin is too strong. Depletions are more reliable indicators of saturation and reduction than are concentrations. Although concentrations, including the high-chroma features of this study, may result from alternating periods of reduction and oxidation, they are ambiguous indicators of seasonal wetness and should not be used alone for making interpretations.

The possibility of misidentification of the minerals present in high-chroma features is a concern, especially manganese minerals, which are difficult to

identify under the best of circumstances. Identification based on morphology and color opens the way for interpretations that are ambiguous or contradictory. Although much of the identification, explanation, and interpretation presented here are based at least in part on color and morphology, assumption and speculation, what is presented seems the best that could be done at present.

Future research should include efforts to completely characterize the chemistry and mineralogy of high-chroma features. An important part of that effort would be to establish correlations with colors and color patterns and the reliability of those correlations. Doing so would greatly aid further studies by allowing interpretations and identification of minerals based on color within features. Alternative hypotheses should be studied, especially the geode and busenite-precursor hypotheses. Also, the very largest features that were found at sample sites but were not included in this study had the same color and color pattern as high-chroma features, yet were indurated and impregnative rather than loose and intrusive. Dark material was found on the outside of these features and was intimately associated with loose iron (hydr)oxide material in a manner identical with that of the smaller high-chroma features. The very smallest features also might have a somewhat different formational pathway than larger features. The process of formation appears to be different at opposite ends of the size range. A deliberate search should be made for high-chroma features that are found on ground moraines and the results compared to those found on stagnation moraines. Any difference might provide useful clues about their origin. Finally, more research should be done on the effects of freeze-thaw and seasonal changes in terms of past and present development of soils. Frost action, cryogenic weathering, and cryochemochemistry, whose effects are so evident

in the study of frozen soils, have influenced and continue to influence soil development in southern Minnesota.

This was a only a first look at these features; it is a beginning. Only time and the efforts of others will tell if this work has made a significant and lasting contribution to the understanding of high-chroma features and to the science of soil genesis.

REFERENCES

- Alekseev, A., T. Alekseeva, V. Ostroumov, C. Siegert, and B. Gradusov. 2003. Mineral transformations in permafrost-affected soils, North Kolyma Lowland, Russia. *Soil Sci. Soc. Am. J.* 67:596–605.
- Allman, M.A. and D.F. Lawrence. 1972. *Geological Laboratory Techniques*. Arco, New York.
- Anderson, J.L., J.C. Bell, T.H. Cooper, D.F. Grigal. 2001. *Soils and Landscapes of Minnesota*. Communication and Educational Technology Services, University of Minnesota Extension Service. Regents of the University of Minnesota.
- Aristovskaya, T.V. 1965. *Microbiology of Podzolic Soils*. Moscow-Leningrad: Nauka Publishing House. (Cited in Sokolova and Polteva 1968).
- Arms, K. and P.S. Camp. *Biology*. Holt, Rinehart and Winston, Orlando, FL.
- Arneman, H.F. and H.E. Wright. 1959. Petrography of some Minnesota tills. *Journal of Sedimentary Petrology* 29(4):540–554.
- Arocena, J.M. and J.D. Ackerman. 1998. Use of statistical tests to describe the basic distribution pattern of iron oxide nodules in soil thin sections. *Soil Sci. Soc. Am. J.* 62:1346–1350.
- Arocena, J.M. and S. Pawluk. 1991. The nature and origin of nodules in Podzolic soils from Alberta. *Can. J. Soil Sci.* 71:411–426.
- Arocena, J.M., S. Pawluk, M.J. Dudas. 1994. Iron oxides in iron-rich nodules of sandy soils from Alberta (Canada). p. 83–97. *In* A.J. Ringrose-Voase and G.S. Humphries (ed.) *Soil Micromorphology: Studies in Management and Genesis*. Proc. IX Int. Working Meeting on Soil Micromorphology, Townsville, Australia, July 1992. *Developments in Soil Science* 22, Elsevier, Amsterdam.
- Ashworth, A.C., D.P. Schwert, W.A. Watts, and H.E. Wright, Jr. 1981. Plant and insect fossils at Norwood in south-central Minnesota: A record of late-glacial succession. *Quaternary Research* 16:66–79.
- Augustithis, S.S. and J. Ottemann. 1966. On diffusion rings and sphaeroidal weathering. *Chemical Geology* 1:201–209.
- Bannatyne, B.B. 1988. *Dolomite Resources of Southern Manitoba*. Economic Geology Report ER85-1. Manitoba Energy and Mines, Geological Services.
- Barry, R.G. 1983. Late-Pleistocene Climatology. p. 390–407. *In* S.C. Porter (ed.) *Late Quaternary Environments of the United States*. The Late Pleistocene, Volume 1. University of Minnesota Press, Minneapolis.
- Bassler, R.S. 1908. The formation of geodes with remarks on the silicification of fossils. *Proc. U.S. Nat. Mus.* V. 35:133–154. (Cited in Pettijohn 1957:205).

- Bates, R.L. and J.A. Jackson (ed.) 1984. Dictionary of Geological Terms. American Geological Institute. Anchor Books, New York.
- Bennett, H.H. and R.V. Allison. 1928. The Soils of Cuba. Tropical Plant Research Foundation, Washington D.C. Monumental Publishing Company, Baltimore.
- Beyer, L. and M. Bölter. 1998. Formation, ecology, and geography of Cryosols of an ice-free oasis in Coastal East Antarctica near Casey Station (Wilkes Land). *Aust. J. Soil Res.* 37:209–244.
- Bigham, J.M., R.W. Fitzpatrick, and D.G. Schulze. 2002. Iron oxides. p. 323–366. *In* J.B. Dixon and D.G. Schulze (ed.) *Soil Mineralogy with Environmental Applications*. Soil Science Society of America Book Series Number 7. Chapter 2. Soil Science Society of America, American Society of Agronomy, Madison, WI.
- Birks, H.J.B. 1976. Late-Wisconsinan vegetational history at Wolf Creek, Central Minnesota. *Ecological Monographs* 46:395–429.
- Blume, H.P. 1968. Zum mechanismus der Marmorierung and Konkretionsbildung in Stauwasserböden. *Z. Pflanzenernaehr., Bodenkd.* 119:124–134. (Cited in Schwertmann and Fanning 1976).
- Blume, H.-P., J. Chen, E. Kalk, and D. Kuhn. 2004. Mineralogy and weathering of Antarctic Cryosols. p. 427–445. *In* J.M. Kimble (ed.) *Cryosols: Permafrost-Affected Soils*. Springer-Verlag, Berlin Heidelberg, Germany.
- Bohn, H.L., B.L. McNeal, G.A. O'Connor. 2001. *Soil Chemistry*. John Wiley & Sons, New York.
- Boulton, G.S. and D.L. Dent. 1974. The nature and rates of post-depositional changes in recently deposited till from south-east Iceland. *Geografiska Annaler* 56(3–4):135–145.
- Boulton, G.S., D.L. Dent, and E.M. Morris. 1974. Subglacial shearing and crushing, and the role of water pressures in tills from south-east Iceland. *Geografiska Annaler* 56(3–4):121–134.
- Borah, D., M.K. Baruah, and P.C. Gogoi. 2005. Model study of pyrite demineralization by hydrogen peroxide at 30°C in the presence of metal ions (Ni²⁺, Co²⁺, and Sn²⁺). *Fuel Processing Technology* 86:769–779.
- Brady, N.C. and R.R. Weil. 1999. *The Nature and Properties of Soils*. Prentice Hall, Upper Saddle River.
- Brewer, R. 1964. *Fabric and Mineral Analysis of Soils*. New York: John Wiley & Sons.
- Brewer, R. 1972. The basis of interpretation of soil micromorphological data. *Geoderma* 8:81–94.

- Brewer, R. and J.R. Sleeman. 1960. Soil structure and fabric: their definition and description. *Journal of Soil Science* 11(1):172–185.
- Bricker, O.P. 1965. Some stability relations in the system Mn–O₂–H₂O and one atmosphere total pressure. *Am. Min.* 50:1296–1354.
- Bronger, A. and J.A. Catt. 1989. Paleosols: problems of definition, recognition and interpretation. p. 1–7. *In* A. Bronger and J.A. Catt (ed.) *Paleopedology: Nature and Application of Paleosols*. Catena Supplement 16. Catena-Verlag, Cremlingen-Destedt, W. Germany.
- Bryan, W.H. 1952. Soil nodules and their significance. p. 43–53. *In* M.F. Glaessner and M.F. and E.A. Rudd (ed.) *Contributions to geology in honour of Professor Sir Douglas Mawson's 70th birthday anniversary presented by colleagues, friends, and pupils*. University of Adelaide.
- Bullock, P., N. Fedoroff, A. Jongerius, G. Stoops, T. Tursina, U. Babel. 1985. *Handbook for Soil Science Thin Section Description*. Prepared under the auspices of the International Society of Soil Science. Waine Research Publications, Albrighton, Wolverhampton.
- Burt, R. 2004. *Soil Survey Laboratory Methods Manual*. Soil Survey Investigations Report No. 42. Version 4.0. November 2004.
- Cescas, M.P. and E.H. Tyner. 1967. Chemical analysis of soil particles: a new approach to the study of climatic cycles, weathering, and soil formation. *Ill. Res.* 9(2):8–9.
- Cescas, M.P., E.H. Tyner, and R.S. Harmer III. 1970. Ferromanganiferous soil concretions: a scanning electron microscope study of their micropore structures. *Soil Sci. Soc. Am. Proc.* 34:641–644.
- Chamberlain, T.C. 1890. The Method of Multiple Working Hypotheses. *Science*. 15(366):92–96. 7 February 1890. Reprinted in *Science, New Series*, 148(3671):754–759. 7 May 1965.
- Chao, T.T. 1972. Selective dissolution of manganese dioxides from soils and sediments with acidified hydroxylamine hydrochloride. *Soil Sci. Soc. Am. Proc.* 36:764–768.
- Chao, T.T. and L. Zhou. 1983. Extraction techniques for selective dissolution of amorphous iron oxides from soils and sediments. *Soil Sci. Soc. Am. J.* 47:225–232.
- Chukhrov, F.V. and A.I. Gorshkov. 1981. Iron and manganese oxide minerals in soils. *Transactions of the Royal Society of Edinburgh: Earth Sciences*. 72:195–200.

- Ciolkosz, E.J. and R.R. Dobos. 1990. Color and Mottling in Pennsylvania Soils. Agronomy Series Number 108. Agronomy Department, The Pennsylvania State University, University Park.
- Clark, J.S. and J.E. Brydon. 1963. Characteristics and genesis of concretionary brown soils of British Columbia. *Soil Sci.* 96:410–417.
- Clarke, E.T., R.H. Loeppert, and J.M. Ehrman. 1985. Crystallization of iron oxides on calcite surfaces in static systems. *Clays and Clay Minerals* 33(2):152–158.
- Clayton, L., J.W. Attig, and D.M. Mickelson. 2001. Effects of late Pleistocene permafrost on the landscape of Wisconsin, USA. *Boreas* 30(3):173–188.
- Cleland, C.E. 2001. Historical science, experimental science, and the scientific method. *Geology* 29(11):987–990.
- Collins, J.F. and T. O'Dubhain. 1980. A micromorphological study of silt concentrations in some Irish Podzols. *Geoderma* 24:215–224.
- Coniglio, M. 2011. Manitoba's Tyndall Stone. <http://www.whaton.uwaterloo.ca/waton/s9911.html> Accessed 12 December 2011.
- Cornell, R.M. and U. Schwertmann. 2003. *The Iron Oxides: Structure, Properties, Reactions, Occurrences and Uses*. Wiley-VCH Verlag GmbH & Co. KGaA, Weinheim.
- Coutard, J.P and H.J. Mùcher. 1985. Deformation of laminated silt loam due to repeated freezing and thawing cycles. *Earth Surface Processes and Landforms* 10:309–319.
- Davis, J.C. 1986. *Statistics and data analysis in geology*. 2nd edition. John Wiley & Sons, New York.
- Davis, M.B. 1983. Holocene vegetational history of the Eastern United States. p. 166–181. *In* H.W. Wright (ed.) *Late Quaternary Environments of the United States. The Holocene, Volume 2*. University of Minnesota Press, Minneapolis.
- Davis, W.M. 1926. The value of outrageous geological hypotheses. *Science* 63(1636):463–468. May 7.
- Dawson, B.S.W., J.E. Fergusson, A.S. Campbell, and E.J.B. Cutler. 1985. Distribution of elements in some Fe-Mn nodules and an iron-pan in some gley soils of New Zealand. *Geoderma* 35:127–143.
- Dean, W.E. 1999. The carbon cycle and biogeochemical dynamics in lake sediments. *Journal of Paleolimnology* 21:375–393.
- Deer, W.A., R.A. Howie, and J. Zussman. 1992. *An Introduction to the Rock-Forming Minerals*. Longman, London; Halsted Press, New York.

- de Faria, D.L.A., S.V. Silva, and M.T. de Oliveira. 1997. Raman microspectroscopy of some iron oxides and oxyhydroxides. *J. Raman Spectrosc.* 28:873–878.
- Dickson, J.A.D. 1965. A modified staining technique for carbonates in thin section. *Nature* 4971:587. 6 February 1965.
- Dickson, J.A.D. 1966. Carbonate identification and genesis as revealed by staining. *Journal of Sedimentary Petrology* 36(2):491–505.
- Dixon, J.B. and G.N. White. 2002. Manganese oxides. p. 367–388. *In* J.B. Dixon and D.G. Schulze (ed.) *Soil Mineralogy with Environmental Applications*. Soil Science Society of America Book Series Number 7. Chapter 11. Soil Science Society of America, American Society of Agronomy, Madison, WI.
- Downs, R.T. 2006. The RRUFF Project: an integrated study of the chemistry, crystallography, Raman and infrared spectroscopy of minerals. Program and Abstracts of the 19th General Meeting of the International Mineralogical Association in Kobe, Japan. O03-13.
- Dreimanis, J.A. and U.J. Vagners. 1971. Bimodal distribution of rock and mineral fragments in basal tills. *In* R.P. Goldthwaite (ed.) *Till: a symposium*. Ohio State University Press.
- Drosdoff, M., and C.C. Nikiforoff. 1940. Iron-manganese concretions in Dayton soils. *Soil Sci.* 49:333–345.
- Edwards, R.J. 1968a. Soil Survey of Wright County, Minnesota. United States Department of Agriculture, Soil Conservation Service, in cooperation with the University of Minnesota Agricultural Experiment Station.
- Edwards, R.J. 1968b. Soil Survey of Carver County, Minnesota. United States Department of Agriculture, Soil Conservation Service, in cooperation with the University of Minnesota Agricultural Experiment Station.
- Estes, J.E., E.J. Hajic, and L.R. Tinney. 1983. Fundamentals of image analysis: analysis of visible and thermal infrared data. p. 987–124. *In* R.N. Colwell (ed.) *Manual of remote sensing*, 2nd edition. American Society of Photogrammetry, Falls Church, VA.
- Evamy, B.D. 1963. The application of a chemical staining technique to a study of dedolomitisation. *Sedimentology* 2:164–170.
- Fanning, D.S., M.C. Rabenhorst, and M.L. Thompson. 1992. Micro-Macromorphology of wet soils in relation to classification. pp. 106-112. *In* J. M. Kimble (ed.) *Characterization, classification and utilization of wet soils*. Proc. 8th Int. Soil Correlation Meeting (VIII ISCOM), 6-21 October 1990, at Baton Rouge, LA and College Station, TX. USDA-SCS Publ. Natl. Soil Surv. Center, Lincoln, Nebraska.

- Feigl, F. 1972. Spot tests in inorganic analysis, 6th edition. Elsevier, New York.
- Fernández-Díaz, L., J.M. Astilleros, and C.M Pina. 2006. Chemical Geology 225:314–321.
- Fitzpatrick, E.A. 1956. An indurated soil horizon formed by permafrost. *Journal of Soil Science* 7(2):248–257.
- Fitzpatrick, E.A. 1993. *Soil Microscopy and Micromorphology*. John Wiley & Sons, West Sussex, England.
- Fitzpatrick, R.W., R. Naidu, and P.G. Self. 1992. Iron deposits and microorganisms in saline sulfidic soils with altered soil water regimes in South Australia. p. 263–286. *In* H.C.W. Skinner and R.W. Fitzpatrick (ed.) *Biomining Processes of Iron and Manganese: Modern and Ancient Environments*. Catena Supplement 21. Catena-Verlag, Cremlingen-Destedt, Germany.
- Fox, C.A. 1994. Micromorphology of permafrost-affected soils. p. 51–62. *In* J.M. Kimble and R.J. Ahrens (ed.) *Proceedings of the Meeting on the Classification, Correlation, and Management of Permafrost-Affected Soils*. July 1994. USDA, Soil Conservation Service, National Soil Survey Center, Lincoln, NE.
- French, H.M. 2007. *The Periglacial Environment*. John Wiley & Sons, West Sussex, England.
- Frenot, Y., B. Van Vliet-Lanoë, and J-C. Gloaguen. 1995. Particle translocation and initial soil development on a glacier foreland, Kerguelen Islands, Subantarctic. *Arctic and Alpine Research* 27(2):107–115.
- Friedman, G.M. 1959. Identification of carbonate minerals by staining methods. *Journal of Sedimentary Petrology* 29(1):87–97.
- Frodeman, R. 1995. Geological reasoning: geology as an interpretive and historical science. *GSA Bulletin*, 107(8):960–968.
- Froment, F., A. Tournié, and P. Colomban. 2008. Raman identification of natural red to yellow pigments: ochre and iron-containing ores. *J. Raman Spectrosc.* 39:560–568.
- Gallaher, R.N., H.F. Perkins, and D. Radcliffe. 1973. Soil concretions: I. X-ray spectrograph and electron microprobe analyses. *Soil Sci. Soc. Am. Proc.* 37:465–469.
- Gallaher, R.N., H.F. Perkins, K.H. Tan, and D. Radcliffe. 1973. Soil concretions: II. Mineralogical analysis. *Soil Sci. Soc. Am. Proc.* 37:469–472.
- Gasparatos, D., D.Tarenidis, C. Haidouti, G. Oikonomou. 2005. Microscopic structure of soil Fe-Mn nodules: environmental implication. *Environ. Chem. Lett.* 2:175–178.

- Gaudette, A. and G.J.F. Millette. 1975. Proprietes chimiques et physiques des concrections dans certain sols du Quebec. *Can. J. Soil Sci.* 55:269–278. (Cited in Schwertmann and Fanning 1976).
- Giencke, A.G. 1987. Soil Survey of Kandiyohi County, Minnesota. National Cooperative Soil Survey. United States Department of Agriculture, Soil Conservation Service, in cooperation with the Minnesota Agricultural Experiment Station.
- Golden, D.C., C.C. Chen, J.B. Dixon, and Y. Tokashiki. 1988. Pseudomorphic replacement of manganese oxides by iron oxide minerals. *Geoderma* 42:199–211.
- Golden, D.C., D.A. Zuberer, and J.B. Dixon. 1992. Manganese oxides produced by fungal oxidation of manganese from siderite and rhodochrosite. p. 161–168. *In* H.C.W. Skinner and R.W. Fitzpatrick (ed.) *Biom mineralization Processes of Iron and Manganese: Modern and Ancient Environments*. Catena Supplement 21. Catena-Verlag, Cremlingen-Destedt, Germany.
- Goldstein, B.S. 1998. Quaternary Stratigraphy and History of the Wadena Drumlin Region, Central Minnesota. *In* Patterson, C.J. and H.E. Wright (editors), *Contributions to Quaternary Studies in Minnesota*. Minnesota Geological Survey, Report of Investigations 49. Saint Paul: University of Minnesota. pp. 61-84.
- Gowan, A.S. 1998. Methods of till analysis for correlation and provenance studies in Minnesota. p. 159–178. *In* C.J. Patterson and H.E. Wright (ed.) *Contributions to Quaternary Studies in Minnesota*. Minnesota Geological Survey, Report of Investigations 49. University of Minnesota, Saint Paul.
- Grabau, A.W. 1904. On the classification of sedimentary rocks. *American Geologist* 33:228–247.
- Grabau, A. W. 1913. *Principles of Stratigraphy*. Seiler, NY.
- Gries, J.P. and E.P. Rothrock. 1941. Manganese Deposits of the Lower Missouri Valley in South Dakota. State of South Dakota. State Geological Survey. Report of Investigations No. 38. University of South Dakota, Vermilion.
- Habecker, M.A., K. McSweetney, and F.W. Madison. 1990. Identification and genesis of fragipans in Ochrepts of north central Wisconsin. *Soil Sci. Soc. Am. J.* 54:139–146.
- Hallimond, A.F. 1925. Iron ores: bedded ores of England and Wales. *Petrography and Chemistry*. Special reports on the mineral resources of Great Britain. Volume 29. *Memoirs of the Geological Survey*.

- Hanesch, M. 2009. Raman spectroscopy of iron oxides and (oxy)hydroxides at low laser power and possible applications in environmental magnetic studies. *Geophys. J. Int.* 177:941–948.
- Hanson, G. 1932. Manganese Deposits of Canada. Economic Geology Series No. 12. Canada Department of Mines, Geological Survey. F.A. Acland, Ottawa.
- Harris, C. 1983. Vesicles in thin sections of periglacial soils from north and south Norway. p. 445–449. *In* International Conference on Permafrost (4th: 1983 : Fairbanks, Alaska) Permafrost: Fourth International Conference. Proceedings July 17–22, 1983. Organized by University of Alaska and National Academy of Sciences. National Academy Press, Washington, D.C.
- Harris, C. and S. Ellis. 1980. Micromorphology of soils in soliflucted materials, Okstindan, northern Norway. *Geoderma* (23):11–29.
- Hartman, R.J. and R.M. Dickey. 1932. The Liesegang phenomenon applied to the Lake Superior iron formations. *Journal of Physical Chemistry* 36(4):1129–1135.
- Hem, J.D. 1964. Deposition and solution of manganese dioxides. U.S. Geol. Surv. Water-Supply Pap. 1667B. (Cited in McKenzie 1989:453).
- Hem, J.D. and C.J. Lind. 1983. Nonequilibrium models for predicting forms of precipitated manganese oxides. *Geochimica et Cosmochimica Acta.* 47:2037–2046.
- Hewitt, D.F. 1930. Memo for Press. February 5, 1930. (Cited in Gries and Rothrock 1941:20)
- Hitzman, M.W. 1999. Routine staining of drill core to determine carbonate mineralogy and distinguish carbonate alteration textures. *Mineralium Deposita* 34:794–798.
- Hobbs, H.C. 1998. Use of 1–2 millimeter sand-grain composition in Minnesota Quaternary studies. p. 193–208. *In* C.J. Patterson and H.E. Wright (ed.) Contributions to Quaternary Studies in Minnesota. Minnesota Geological Survey, Report of Investigations 49. University of Minnesota, Saint Paul.
- Hobbs H.C. and J.E. Goebel. 1982. Geologic Map of Minnesota, Quaternary Geology. State Map Series S-1. Minnesota Geological Survey, University of Minnesota.
- Hokanson, H.L., W.W. Anderson, D.W. Calkins, K.W. Hein, F.D. Lorenzen, J.J. Murray, R.O. Paulson, R.F. Peterson. 1970. Soil Survey of Lincoln County, Minnesota. United States Department of Agriculture, Soil Conservation Service, in cooperation with the University of Minnesota Agricultural Experiment Station.

- HPRCC. 2011. High Plains Regional Climate Center. Available at <http://www.hprcc.unl.edu/wrcc/states/mn.html>. Accessed 24 May 2011.
- InPhotonics. 1999. An introduction to Raman for the infrared spectroscopist. Technical Note 11. Available at <http://www.inphotonics.com/technote11.pdf>. Accessed 8 May 2011.
- Jeffrey, E.C. 1924. The origin and organization of coal. Mem. Amer. Acad. Arts and Sci. 15: No. 1. (Cited in Robinson 1930).
- Jirsa, M. and D. Southwick. 2011. Mineral potential and geology of Paleozoic and Mesozoic rocks in Minnesota. Minnesota Geological Survey. Available at <http://www.mngs.umn.edu/mnpot/paleozoic.html>. Accessed 9 December 2011.
- Johnson, D.B. and K. Swett. 1974. Origin and diagenesis of calcitic and hematitic nodules in the Jordan Sandstone of northeast Iowa. *Journal of Sedimentary Petrology* 44(3):790–794.
- Kay, B.D. and P.H. Groenevelt. 1983. The redistribution of solutes in freezing soil: exclusion of solutes. p. 584–588. *In* International Conference on Permafrost (4th: 1983 : Fairbanks, Alaska) Permafrost: Fourth International Conference. Proceedings July 17–22, 1983. Organized by University of Alaska and National Academy of Sciences. National Academy Press, Washington, D.C.
- Katsikopoulos, D., Á. Fernández-González, and M. Prieto. 2009. Crystallization behaviour of the (Mn,Ca)CO₃ solid solution on silica gel: nucleation, growth and zoning phenomena. *Mineralogical Magazine* 73(2):269–284.
- Kendall, A.C. 1977. Origin of dolomite mottling in Ordovician limestones from Saskatchewan and Manitoba. *Bulletin of Canadian Petroleum Geology* 25(3):480–504. June.
- King, H.B., J.K. Torrance, L.H. Bowen, and C. Wang. 1990. Iron concretions in a Typic Dystrachrept in Taiwan. *Soil Sci. Soc. Am. J.* 54:462–468.
- Kingma, K.J. and R.J. Hemley. 1994. Raman spectroscopic study of microcrystalline silica. *American Mineralogist* 79:269–273.
- Kirk, S.R. 1929. Cretaceous stratigraphy of the Manitoba Escarpment. Sum. Rept. Part B, Geological Survey, Canada. p. 114. (Cited in Spector 1941:44)
- Klein, C. and C.S. Hurlbut, Jr. 1993. *Manual of Mineralogy* (after James D. Dana). John Wiley and Sons, Inc., NY.
- Knight, P.G., D.E. Sugden, and C.D. Minty. 1994. Ice flow around large obstacles as indicated by basal ice exposed at the margin of the Greenland ice sheet. *Journal of Glaciology* 40(135):359–367.

- Kolesov, B.A. and C.A. Geiger. 2004. A Raman spectroscopic study of Fe-Mg olivines. *Phys. Chem. Minerals* 31:142–154.
- Krinsley, D.H., K. Pye, S. Boggs, Jr., N.K. Tovey. 1998. *Backscattered Scanning Electron Microscopy and Image Analysis of Sediments and Sedimentary Rocks*. Cambridge University Press, United Kingdom, New York, Australia.
- Krishnamurti, G.S.R. and P.M. Huang 1987. The catalytic role of birnessite in the transformation of iron. *Can. J. Soil Sci.* 67:533–543.
- Krishnamurti, G.S.R. and P.M. Huang. 1988. Influence of manganese oxide minerals on the formation of iron oxides. *Clays and Clay Minerals* 36(5):467–475.
- Krynine, P.D. 1948. The megascopic study and field classification of sedimentary rocks. *J. Geol.* 56(2): 130-165.
- Kubiěna, W.L. 1938. *Micropedology*. Collegiate Press, Ames, IA.
- Last, W.H. and W.W. Shum. 1991. Diagenesis of the Winnipeg Formation in Manitoba: a regional petrographic study. p. 14–20. *In* J.E. Christopher and F.M. Haidl (ed.) *Sixth International Williston Basin Symposium*. Proceedings of a symposium held in Regina, Saskatchewan 7, 8, 9, October 1991. Special Publication Number 11 Saskatchewan Geological Society, Regina.
- Laybourne-Parry, J. 2009. No place too cold. *Science* 324:1521–1522. 19 June 2009.
- Lehr, J.D. 1990. *Aggregate Resources and Quaternary Geology Wright County Minnesota*. State of Minnesota. Department of Natural Resources. Division of Minerals. Available at http://files.dnr.state.mn.us/lands_minerals/wrigqgeo.pdf Accessed 26 November 2012.
- Leonard, A.G. 1906. Stratigraphy of North Dakota clays. p. 71–74 and 131–138. *State Geological Survey of North Dakota, Fourth Biennial Report*. A.G. Leonard, State Geological Survey, Bismark.
- Lewis, D.G. 1997. Factors influencing the stability and properties of green rusts. p. 345–372. *In* K. Auerswald, H. Stanjek, and J.M. Bigham (ed.) *Soils and Environment: Soil Processes from Mineral to Landscape Scale*. *Advances in Geocology* 30. Catena Verlag. Reiskirchen, Germany.
- Liedmann, W. and H. Quader. 1991. Optical analysis of geologic structures by confocal laser scanning microscopy. *Naturwissenschaften* 78:413–414.
- Lindbo, D.L., F.E. Rhoton, W.H. Hudnall, N.E. Smeck, J.M. Bigham, and D.D. Tyler. 2000. Fragipan degradation and nodule formation in Glossic

- Fragiudalfts of the lower Mississippi River valley. *Soil Sci. Soc. Am. J.* 64:1713–1722.
- Lindsay, W.L. 1988. Solubility and redox equilibria of iron compounds in soils. p. 37–62. *In* J.W. Stucki, B.A. Goodman, and U. Schwertmann (ed.) *Iron in Soils and Clay Minerals*. NATO ASI Series C: Mathematical and Physical Sciences Volume 217. Proceedings of the NATO Advanced Study Institute on Iron in Soils and Clay Minerals, Bad Windsheim, West-Germany, July 1–3, 1985. D. Reidel Publishing Company, Dordrecht, Holland.
- Liu, F., C. Colombo, P. Adamo, J.Z. He, and A. Violante. 2002. Trace elements in manganese-iron nodules from a Chinese Alfisol. *Soil Sci. Soc. Am. J.* 66:661–670.
- Loeppert, R.H. 1986. Reactions of iron and carbonates in calcareous soils. 9(3–7):195–214.
- Loeppert, R.H. and E.T. Clarke. 1984. Reactions of Fe²⁺ and Fe³⁺ in calcareous soils. *Journal of Plant Nutrition* 7(1–5):149–163.
- Loeppert, R.H. and L.R. Hossner. 1984. Reactions of Fe²⁺ and Fe³⁺ with calcite. *Clays and Clay Minerals* 32(3):213–222.
- Loeppert, R.H. and W.P. Inskeep. 1996. Iron. p. 639–664. *In* D.L. Sparks et al. (ed.) *Methods of Soil Analysis, Part 3: Chemical Methods*. Soil Science Society of America Book Series Number 5. Chapter 23. Soil Science Society of America, American Society of Agronomy, Madison, WI.
- Lueth, R.A. 1974. Soil Survey of Hennepin County, Minnesota. United States Department of Agriculture, Soil Conservation Service, in cooperation with the University of Minnesota Agricultural Experiment Station.
- Lusardi, B.A. 1998a. Salisbury Hill road cut: a deformed multiple-till section near Henderson, Scott County, Minnesota. p. 141–154. *In* C.J. Patterson and H.E. Wright (ed.) *Contributions to Quaternary Studies in Minnesota*. Minnesota Geological Survey, Report of Investigations 49. University of Minnesota, St. Paul.
- Lusardi, B.A. 1998b. Surficial geologic map of the Victoria quadrangle, Carver County, Minnesota, M-88. Minnesota Geological Survey, St. Paul. Available at <http://reflections.mndigital.org/cdm/singleitem/collection/mgs/id/966/rec/27> Accessed 26 November 2012.
- Lusardi, B.A., C.E. Jennings, and K.L. Harris. 2011. Provenance of Des Moines lobe till records ice-stream catchment evolution during Laurentide deglaciation. *Boreas* 40(4):585–597.

- MGIO. Minnesota Geospatial Information Office. Minnesota Land Use and Cover: 1990s Census of the Land. Map. Minnesota Department of Natural Resources, Forestry Division. Based on *Minnesota Land Use and Cover: 1990s Census of the Land* authored by Association of Minnesota Counties in 1998 and published by St. Paul: Association of Minnesota Counties. Available through CURA, University of Minnesota (<http://www.cura.umn.edu/publications/catalog/19801>). <http://www.mngeo.state.mn.us/landuse/> Accessed 2 October 2011.
- Mania, J., P. Chauve, F. Remy, and P. Verjus. 1989. Evolution of iron and manganese concentrations in presence of carbonates and clays in the alluvial groundwaters of the Ognon (Franche-Comté, France). *Geoderma* 44:219–227.
- Manitoba Geological Survey. 2011a. Manitoba Geology. Province of Manitoba. <http://www.manitoba.ca/iem/mrd/geo/exp-sup/mbgeology.html>. Accessed 10 December 2011.
- Manitoba Geological Survey. 2011b. Industrial Minerals. Province of Manitoba. <http://www.manitoba.ca/iem/mrd/busdev/industrial/marble.html>. Accessed 10 December 2011.
- Martin, S.T. 2005. Precipitation and dissolution of iron and manganese oxides. p. 61–68. *In* V.H. Grassian (ed.) *Environmental Catalysis*. CRC Press, Boca Raton.
- Matsch, C.L. 1972. Quaternary geology of southwestern Minnesota. p. 548–560. *In* P.K. Sims and G.B. Morey (ed.) *Geology of Minnesota – A Centennial Volume*. Minnesota Geological Survey.
- Matsunaga, T., Karametaxas, H.R. von Gunten, and P.C. Lichtner. 1993. Redox chemistry of iron and manganese minerals in river-recharged aquifers: a model interpretation of a column experiment. *Geochimica et Cosmochimica Acta* 57:1691–1704.
- Mazzetti, L. and P.J. Thistlethwaite. 2002. Raman spectra and thermal transformations of ferrihydrite and schwertmannite. *J. Raman Spectrosc.* 33:104–111.
- McBride, E.F. 2003. Pseudofaults resulting from compartmentalized Liesegang bands: update. *Sedimentology* 50(4):725–730.
- McBride, M.B. 1979. Chemisorption and precipitation of Mn²⁺ at CaCO₃ surfaces. *Soil Sci. Soc. Am. J.* 43:693–698.
- McBride, M.B. 1994. *Environmental Chemistry of Soils*. Oxford University Press, New York, NY.

- McKenzie, R.M. 1989. Manganese oxides and hydroxides. p. 439–465. *In* J.B. Dixon and S.B. Weed (ed.). *Minerals in Soil Environments*. Soil Science Society of America Book Series Number 1. Chapter 9. Soil Science Society of America, Madison, WI.
- Mettler, S., M. Abdelmoula, E. Hoehn, R. Schoenenberger, P. Weidler, and U. von Gunten. 2001. Characterization of iron and manganese precipitates from an in situ ground water treatment plant. *Ground Water* 39(6):921–930.
- Meyer, G.N. 1986. *Subsurface Till Stratigraphy of the Todd County Area, Central Minnesota*. Minnesota Geological Survey, Report of Investigations 34. University of Minnesota, St. Paul.
- Meyer, G.N. and B.A. Lusardi. 2000. Surficial geology of the St. Paul 30 x 60 minute quadrangle, Minnesota, M-106. Minnesota Geological Survey, St. Paul. Available at <http://reflections.mndigital.org/cdm/singleitem/collection/mgs/id/1145/rec/1> Accessed 26 November 2012.
- Mickelson, D.M., L. Clayton, D.S. Fullerton, and H.W. Borns, Jr. 1983. The Late Wisconsin glacial record of the Laurentide Ice Sheet in the United States. p. 3–37. *In* S.C. Porter (ed.) *Late Quaternary Environments of the United States. The Late Pleistocene, Volume 1*. University of Minnesota Press, Minneapolis.
- Miller, J. *Microscopical Techniques: I. Slices, slides, stains, and peels*. 1988. p. 86–107. *In* M. Tucker (ed.) *Techniques in Sedimentology*. Ch. 4. Blackwell, Oxford.
- Minnesota Geological Society. 2011. Images posted at <http://www.mngs.umn.edu/pebbles.htm>. Accessed 10 October 2011.
- MnDOT. 2011. Frost and Thaw Depths. Available at http://www.mrr.dot.state.mn.us/research/seasonal_load_limits/thawindex/frost_thaw_graphs.asp Accessed 24 May 2011.
- Moore, E.S. and J.E. Maynard. 1929. Solution, transportation and precipitation of iron and silica. *Econ. Geol.* Parts I–III 24(3,4,5). (Cited in Zapffe 1933).
- Moran, S.R., M. Arndt, J.P. Bluemle, M. Camara, L. Clayton, M.M. Fenton, K.L. Harris, H.C. Hobbs, R. Keatinge, D.K. Sackreiter, N.L. Salomon, and J. Teller. 1976. Quaternary Stratigraphy and History of North Dakota, Southern Manitoba, and Northwestern Minnesota. p.133–158. *In* W.C. Mahaney (ed.) *Quaternary Stratigraphy of North America*. Dowden, Hutchinson & Ross, Stroudsburg, PA.
- Morey, G.B., R.S. Lively, and G.N. Meyer. 2000. Utility of Geochemical Data in Correlation and Provenance Studies of Pleistocene Materials: A Case

- Study in Stearns County, Central Minnesota. Minnesota Geological Survey. Information Circular 45. University of Minnesota, Saint Paul.
- Mossler, J.H. 1978. Results of subsurface investigations in northwestern Minnesota, 1972. Report of Investigations 19. Minnesota Geological Survey. University of Minnesota, Saint Paul.
- Mossler, J.H. 1985. Sedimentology of the Middle Ordovician Platteville Formation southeastern Minnesota. Report of Investigations 33. Minnesota Geological Survey. University of Minnesota, Saint Paul.
- MRCC. 2011. Midwest Regional Climate Center. Climate Summaries. http://mrcc.isws.illinois.edu/climate_midwest/mwclimate_data_summaries.htm Accessed 24 May 2011.
- Nikiforoff, C.C. 1937. Soils of the phaneropodzolic group in western Oregon. *Soil Science* 44:447–465.
- Nuhfer, E.B., R.Y. Anderson, J.P. Bradbury, and W.E. Dean. 1993. Modern sedimentation in Elk Lake, Clearwater County, Minnesota. p. 75–96. *In* J.P. Bradbury and W.E. Dean (ed.) *Elk Lake, Minnesota: Evidence for Rapid Climate Change in the North-Central United States*. Geol. Soc. Am. Spec. Paper 276. (Cited in Dean 1999:387).
- Ohfuji, H. and D. Rickard. 2005. Experimental synthesis of framboids—a review. *Earth-Science Reviews* 71:147–170.
- Ojakangas, R.W. and C.L. Matsch. 1982. *Minnesota's Geology*. University of Minnesota Press, Minneapolis.
- Oliveira, T.S., N.B. Lacerda, R.J. Gilkes. 2010. Infillings in irrigated soils cultivated with annual and perennial crops in the Apodi Plateau, Northeastern Brazil. 19th World Congress of Soil Science, Soil Solutions for a Changing World. 1–6 August 2010, Brisbane, Australia. Available at <http://www.iuss.org/19th%20WCSS/Symposium/pdf/1668.pdf> Accessed 11 January 2012.
- Pai, C.W., M.K. Wang, H.C. Chiang, H.B. King, J.-L. Hwong, and H.T. Hu. 2003. Formation of iron nodules in a Hapludult of central Taiwan. *Can. J. Soil Sci.* 83:167–172.
- Palumbo, B., A. Bellanca, R. Neri, and M.J. Roe. 2001. Trace metal partitioning in Fe-Mn nodules from Sicilian soils, Italy. *Chemical Geology* 173(4):257–269.
- Pannekoek, A.J. 1956. *Geologie als wetenschap en als kunst*. Inaugural lecture. University of Leiden, February 3, 1956. (Cited in van Bemmelen 1961).

- Patterson, C. (Jennings). 1996. The Glacial Geology of Southwestern Minnesota with Emphasis on the Deposits and Dynamics of the Des Moines Lobe. Unpublished Ph.D. dissertation. University of Minnesota, Minneapolis.
- Patterson, C.J. 1995. Surficial Geologic Map. Regional Hydrogeologic Assessment, Quaternary Geology–Southwestern Minnesota. RHA–2, Part A. Minnesota Department of Natural Resources, Division of Waters, and the Minnesota Environment and Natural Resources Trust Fund.
- Patterson, R.T. and A. Kumar. 2002. A review of current testate rhizopod (thecamoebian) research in Canada. *Palaeogeography, Palaeoclimatology, Palaeoecology* 180:225–251.
- Pawluk, S. 1988. Freeze-thaw effects on granular structure reorganization for soil materials of varying texture and moisture content. *Can. J. Soil Sci.* 68:485–494.
- Pawluk, S. and R. Brewer. 1975. Investigations of some soils developed in hummocks of the Canadian Sub-Arctic and Southern-Arctic regions. 2. Analytical characteristics, genesis and classification. *Canadian Journal of Soil Science* 55:321–330.
- Pawluk, S. and J. Dumanski. 1973. Ferruginous concretions in a poorly drained soil of Alberta. *Soil Sci. Soc. Am. Proc.* 37:124-127.
- Pettijohn, F.J. 1949. *Sedimentary Rocks*. Harper & Brothers, New York, NY.
- Pettijohn, F.J. 1957. *Sedimentary Rocks*. Second edition. Harper & Brothers, New York, NY.
- Pettijohn, F.J. 1975. *Sedimentary Rocks*. Third edition. Harper & Row, New York, NY.
- Péwé, T.L. 1983. The Periglacial environment in North America during Wisconsin time. p. 157–189. *In* S.C. Porter (ed.) *Late Quaternary Environments of the United States. The Late Pleistocene*, volume 1. University of Minnesota Press, Minneapolis.
- Phillippe, W.R., R.L. Blevins, R.I. Barnhisel, and H.H. Bailey. 1972. Distribution of concretions from selected soils of the Inner Bluegrass Region of Kentucky. *Soil Sci. Soc. Am. Proc.* 36:171–173.
- Ping, C.L., W. Lynn, and C.A.S. Smith. 1993. Redoximorphic features in permafrost soils. p. 233–244. *In* D.A. Gilichinsky (ed.) *Joint Russian-American Seminar of Cryopedology and Global Change. Post-seminar proceedings*. November 15–16. Russian Academy of Sciences, Pushchino Research Center.
- Post, J.E. 1999. Manganese oxide minerals: crystal structures and economic and environmental significance. *Proc. Natl. Acad. Sci., USA* 96:3447–3454.

- Postma, D. 1983. Pyrite and siderite oxidation in swamp sediments. *Journal of Soil Science* 34:163–182.
- Postma, D. and B. Sine Brockenhuus-Schack. 1987. Diagenesis of iron in proglacial sand deposits of late- and post-Weichselian Age. *Journal of Sedimentary Petrology* 57(6):1040–1053.
- Rabben, E.L. 1960. Fundamentals of photointerpretation. p. 99–168. *In* R.N. Colwell (ed.) *Manual of photographic interpretation*. American Society for Photogrammetry, Washington, D.C.
- Rabenhorst, M.C. and B.R. James. 1992. Iron sulfidization in tidal marsh soils. p. 203–217. *In* H.C.W. Skinner and R.W. Fitzpatrick (ed.) *Biom mineralization Processes of Iron and Manganese: Modern and Ancient Environments*. Catena Supplement 21. Catena-Verlag, Cremlingen-Destedt, Germany.
- Raiswell, R., L.G. Benning, L. Davidson, M. Tranter, and S. Tulaczyk. 2009. Schwertmannite in wet, acid, and oxic microenvironments beneath polar and polythermal glaciers. *Geology* 37(5):431–434.
- Raman, C.V. and K.S. Krishnan. 1928. *Nature* 121:501.
- Robinson, W.O. 1929. Detection and significance of manganese dioxide in the soil. *Soil Sci.* 27:335–350.
- Robinson, W.O. 1930. Some chemical phases of submerged soil conditions. *Soil Sci.* 30:197–217.
- Rodgers, J. 1950. The nomenclature and classification of sedimentary rocks. *Am. J. Sci.* 248(5): 297-311.
- Rudelforth, C.C. 1970. The micromorphology of surface-water gley soils. p. 69–81. *In* D.A. Osmond, and P. Bullock (ed.) *Micromorphological Techniques and Applications*. Agricultural Research Council, Soil Survey, Technical Monograph No. 2. Harpenden.
- Ruhe, R.V. 1983. Aspects of Holocene pedology in the United States. p. 12–25. *In* H.W. Wright (ed.) *Late Quaternary Environments of the United States. The Holocene, Volume 2*. University of Minnesota Press, Minneapolis.
- Sanz, A., M.T. Garcia-Gonzalez, C. Vizcayno, R. Rodriguez. 1996. Iron-manganese nodules in a semi-arid environment. *Australian Journal of Soil Research* 34(5):623–634.
- Savage, W.S. 1936. Solution, transportation and precipitation of manganese. *Economic Geology* 31(3):278–297.
- Schaetzl, R.J. and S. Anderson. 2005. *Soils: Genesis and Geomorphology*. Cambridge University Press, New York.

- Scheinost, A.C. and U. Schwertmann. 1999. Color identification of iron oxides and hydroxysulfates: use and limitations. *Soil Sci. Soc. Am. J.* 63:1463–1471.
- Schoeneberger, P.J., D.A. Wysocki, E.C. Benham, and W.D. Broderson. (ed.) 2002. *Field Book for Describing and Sampling Soils, Version 2.0*. Natural Resources Conservation Service, National Soil Survey Center, Lincoln, NE.
- Schumm, S.A. *To Interpret the Earth: Ten Ways to be Wrong*. 1991. Cambridge University Press.
- Schwertmann, U. 1993. Relations between iron oxides, soil color, and soil formation. p. 51–69. *In* J.K. Bigham and E.J. Ciolkosz (ed.) *Soil Color. Proceedings of a symposium sponsored by Divisions S-5 and S-9 of the Soil Science Society of America in San Antonio, Texas, 21–26 October 1990*. SSSA Special Publication No. 31. Soil Science Society of America, Madison, WI.
- Schwertmann, U. and D.S. Fanning. 1976. Iron-manganese concretions in hydrosequences of soils in loess in Bavaria. *Soil Sci. Soc. Am. J.* 40:731–738.
- Schwertmann, U. and R.M. Taylor. 1989. Iron oxides. p. 379–438. *In* J.B. Dixon and S.B. Weed (ed.) *Minerals in Soil Environments*. Soil Science Society of America Book Series Number 1. Chapter 8. Soil Science Society of America, Madison, WI.
- Senkayi, A.L., J.B. Dixon, and L.R. Hossner. 1986. Todorokite, goethite, and hematite: alteration products of sidertite in East Texas lignite overburden. *Soil Science* 142(1):36–42.
- Sharp, M., J. Parkes, B. Cragg, I.J. Fairchild, H. Lamb, M. Tranter. 1999. Widespread bacterial populations at glacier beds and their relationship to rock weathering and carbon cycling. *Geology* 27(2):107–110.
- Shuman, L.M. 1982. Separating soil iron- and manganese-oxide fractions for microelement analysis. *Soil Sci. Soc. Am. J.* 46:1099–1102.
- Shuman, L.M. 1985. Fractionation method for microelements. *Soil Science* 140(1):11–22.
- Smith, E. and G. Dent. 2005. *Modern Raman Spectroscopy: A Practical Approach*. John Wiley and Sons, Ltd, Chichester, West Sussex, England.
- Smith, G.D. 1986. *The Guy Smith Interviews: Rationale for Concepts in Soil Taxonomy*. SMSS Technical Monograph No. 11. Soil Management Support Services, Soil Conservation Service, U.S. Department of Agriculture. New York State College of Agriculture and Life Sciences. Cornell University Department of Agronomy.
- Smith, W.O. 1936. Sorption in an ideal soil. *Soil Science* 41:209–230.

- Soil Science Society of America. 2001. Glossary of Soil Science Terms. Soil Science Society of America, Madison, WI.
- Sokolova, T.A. and R.N. Polteva. 1968. The study of iron-manganese concretions from a strongly podzolic soil profile. p. 459-466. Transactions 9th International Congress of Soil Science. Adelaide, Australia. Vol. IV. International Society of Soil Science and Angus and Robertson.
- Spector, I.H. 1941. Manganese Deposits in the Riding Mountain Area, Manitoba. M.S. Thesis. University of Manitoba.
- Stampfl, P.P. 1969. Ein basisches Eisen-II-III-Karbonat im Rost. *Corros. Sci.* 9:185-187. (Cited in Taylor 1980)
- Steno, Nicolaus. 1687. The prodromus of Nicolaus Steno's dissertation concerning a solid body enclosed by process of nature within a solid. Hafner, New York.
- Stolt, M.H., C.M. Ogg, J.C. Baker. 1994. Strongly contrasting redoximorphic patterns in Virginia valley and ridge paleosols. *Soil Sci. Soc. Am. J.* 58:477-484.
- Stoops, G. 2003. Guidelines for Analysis and Description of Soil and Regolith Thin Sections. Soil Science Society of America, Madison, WI.
- Stoops, G. 2009. Seventy years' "micropedology" 1938-2008: the past and future. *J. Mt. Sci.* 6:101-106. DOI: 10.1007/s11629-009-1025-3
- Stoops, G. and H. Eswaran. 1985. Morphological characteristics of wet soils. p. 177-189. In S.J. Banta and C.V. Mendoza (ed.) *Wetland Soils: Characterization, Classification, and Utilization*. Proceedings of a workshop held 26 March to 5 April 1984 under the joint sponsorship of the International Rice Research Institute; Soil Management Support Services, Agency for International Development and United States Department of Agriculture; Bureau of Soils, Philippine Ministry of Agriculture. International Rice Research Institute, Los Baños, Laguna, Philippines.
- Stoops, G., V. Marcelino, F. Mees (ed.). 2010. Interpretation of Micromorphological Features of Soils and Regoliths. Elsevier, Amsterdam.
- Stout, J.D. and G.D. Walker. 1976. Discrimination of mineral particles in test formation by thecamoebae. *Trans. Amer. Micros. Soc.* 95(3):486-489.
- Subramanyan, V. 1927a. Biochemistry of water-logged soils: I. The effect of water-logging on the different forms of nitrogen, on the reaction, on the gaseous relationships, and the bacterial flora. *Jour. Agr. Sci.* 27(4):429-448. (Cited in Robinson 1930).

- Subramanyan, V. 1927b. Biochemistry of water-logged soils: II. The presence of a deaminase in water-logged soils and its rôle in the production of ammonia. *Jour. Agr. Sci.* 27(4):449–467. (Cited in Robinson 1930).
- Sugden, D.E., P.G. Knight, N. Livesey, R.D. Lorrain, R.A. Souchez, J.-L. Tison, and J. Jouzel. 1987. Evidence for two zones of debris entrainment beneath the Greenland ice sheet. *Letters to Nature. Nature* 328:238–241. July.
- Sullivan, L.A. and A.J. Koppi. 1991. Morphology and genesis of silt and clay coatings in the vesicular layer of a desert loam soil. *Aust. J. Soil Res.* 29:579–586.
- Sullivan, L.A. and A.J. Koppi. 1992. Manganese oxide accumulations associated with some soil structural pores. I. Morphology, composition and genesis. *Aust. J. Soil Res.* 30:409–427.
- Tarnocai, C. 1994. Genesis of permafrost-affected soils. p. 143–154. *In* J.M. Kimble and R.J. Ahrens (ed.) *Proceedings of the Meeting on the Classification, Correlation, and Management of Permafrost-Affected Soils.* July 1994. USDA, Soil Conservation Service, National Soil Survey Center, Lincoln NE.
- Taylor, R.M. 1980. Formation and properties of Fe(II)Fe(III) hydroxyl-carbonate and its possible significance in soil formation. *Clay Minerals* 15(4):369–382.
- Taylor, R.M. and R.M. McKenzie. 1980. The influence of aluminum on iron oxides. VI. The formation of Fe(II)-Al(III) hydroxyl-chlorides, -sulfates, and-carbonates as new members of the pyroaurite group and their significance in soils. *Clays and Clay Minerals* 28(3):179–187.
- Taylor, R.M. and U. Schwertmann. 1974. The association of phosphorus with iron in ferruginous soil concretions. *Aust. J. Soil Res.* 12:133-145.
- Tebo, B.M., W.C. Ghiorse, L.G. van Waasbergen, P.L. Siering, R. Caspi. 1997. Bacterially mediated mineral formation: insights into manganese(II) oxidation from molecular genetic and biochemical studies. p. 225–266. *In* J.F. Banfield and K.H. Nealson (ed.) *Geomicrobiology: Interactions between Microbes and Minerals. Reviews in Mineralogy, Vol. 35.* Mineralogical Society of America, Washington, D.C.
- Teng, W.L., E.R. Loew, D.I. Ross, V.G. Zsilinszky, C.P. Lo, W.R. Philipson, W.D. Philpot, and S.A. Morain. 1997. Fundamentals of photographic interpretation. p. 49–113. *In* W.R. Philipson (ed.) *Manual of photographic interpretation.* American Society for Photogrammetry and Remote Sensing, Bethesda, MD.

- Thiel, G.A. 1925. Manganese precipitated by microorganisms. *Economic Geology* 20:301–310.
- Thorleifson, L. H., K. L. Harris, H. C. Hobbs, C. E. Jennings, A. R. Knaeble, R. S. Lively, B. A. Lusardi, G. N. Meyer. 2007. Till Geochemical and Indicator Mineral Reconnaissance of Minnesota. Minnesota Geological Survey Open File Report OFR-07-01. 512 p. 15 pdf digital files, 5 digital images.
- Thresh, M. 1902. Manganese nodules in Essex. *Essex Naturalist* 12:137–139.
- Tillmans, J. von. 1914. Ueber die Entmangung von Trinkwasser. *Jour. Gasbel. U. Wasser* 57:713. (Cited in Savage 1936).
- Todd, J.E. 1903. Concretions and their geological effects. *Bull. Geol. Soc. Am.* 14:353–360.
- Torrent, J. and V. Barrón. 2002. Diffuse reflection spectroscopy of iron oxides. *Encyclopedia of Surface and Colloid Science*. p. 1438–1446.
- Trolard, F., G. Bourrié, M. Abdelmoula, P. Refait, F. Feder. 2007. Fougérite, a new mineral of the pyroaurite-iowaite group: description and crystal structure. *Clays and Clay Minerals* 55(3):323–334.
- Tsukunaga, K. 1932. Studies on the formation of iron concretions in Manchurian soils. *Manchuria Agricultural Experiment Station*. 7:43–80.
- Ugolini, F.C. 1986. Pedogenic zonation in the well-drained soils of the Arctic regions. *Quaternary Research* 26:100–120.
- United States Geological Survey. 2011. Pierre Shale. <http://tin.er.usgs.gov/geology/state/sgmc-unit.php?unit=MTKp%3B0> Accessed 9 December 2011.
- Van Bemmelen, R.W. 1961. The scientific character of geology. *Journal of Geology* 69:453–463.
- Van Vliet, B. and R. Langohr. 1981. Correlations between fragipans and permafrost with special reference to silty Weichselian deposits in Belgium and Northern France. *Catena* 8:137–154.
- Van Vliet-Lanoë, B., J-P. Coutard, and A. Pissart. 1984. Structures caused by repeated freezing and thawing in various loamy sediments: a comparison of active, fossil, and experimental data. *Earth Surface Processes and Landforms* 9:553–565.
- Van Vliet-Lanoë, B. 1985. Frost effects in soils. p. 117–158. *In* J. Boardman (ed.) *Soils and Quaternary Landscape Evolution*. John Wiley & Sons, Ltd., New York.
- Vasilas, L.M., G.W. Hurt, and C.V. Noble (ed.) 2010. *Field Indicators of Hydric Soils in the United States, Version 7.0*. United States Department of

- Agriculture, Natural Resources Conservation Service. USDA, NRCS, in cooperation with the National Technical Committee for Hydric Soils.
- Veneman, P.L.M., M.J. Vepraskas, and J. Bouma. 1976. The physical significance of soil mottling in a Wisconsin toposequence. *Geoderma* 15:103-118.
- Veneman, P.L.M., D.L. Lindbo, and L.A. Spokas. 1998. Soil moisture and redoximorphic features: A historical perspective. p. 1–23. *In* M.C. Rabenhorst, J.C. Bell, and P.A. McDaniel (ed.) *Quantifying Soil Hydromorphology*. Proceedings of a symposium sponsored by Divisions S-5 and S-10, and Committee S-884 of the Soil Science Society of America in Indianapolis, Indiana, 4 November 1996. SSSA Special Publications Number 54. Soil Science Society of America, Inc. Madison, WI.
- Vepraskas, M.J. 1999. Redoximorphic Features for Identifying Aquic Conditions. North Carolina Agricultural Research Service, North Carolina State University, Raleigh, North Carolina. Technical Bulletin 301.
- Vepraskas, M.J. 2001. Morphological features of seasonally reduced soils. p. 163–182. *In* J.L. Richardson and M.J. Vepraskas (ed.) *Wetland Soils: Genesis, Hydrology, Landscapes, and Classification*. CRC Press, Boca Raton, FL.
- Vodyanitskii, Y.N., S.N. Lesovaya, and A.V. Sivtsov. 2003. Iron hydroxidogenesis in forest and steppe soils of the Russian plain. *Eurasian Soil Science* 36(4):420–429.
- Vogt, T. 1991. Cryogenic physico-chemical precipitations: iron, silica, calcium carbonate. *Permafrost and Periglacial Processes* 1:283–293.
- Vogt, T. and P. Larqué. 1998. Transformations and neoformations of clay in the cryogenic environment: examples from Transbaikalia (Siberia) and Patagonia (Argentina). *European Journal of Soil Science* 49:367–376.
- Waksman, S.A. 1932. *Principles of Soil Microbiology*, ed. 2. Williams and Wilkins, Baltimore. (Cited in Drosdoff and Nikiforoff 1940).
- Warne, S. St.J. 1962. A quick field or laboratory staining scheme for the differentiation of the major carbonate minerals. *Journal of Sedimentary Petrology* 32(1):29-38.
- Watson, R.A. 1969. Explanation and prediction in geology. *Journal of Geology* 77:488–494.
- Watts, W.A. 1983. Vegetational History of the Eastern United States 25,000 to 10,000 years ago. p. 294–310. *In* S.C. Porter (ed.) *Late Quaternary Environments of the United States. The Late Pleistocene, Volume 1*. University of Minnesota Press, Minneapolis.
- Webb, T., III, E.J. Cushing, H.E. Wright. 1983. Holocene changes in the vegetation of the Midwest. p. 142–165. *In* H.W. Wright (ed.) *Late Quaternary*

- Environments of the United States. The Holocene, Volume 2. University of Minnesota Press, Minneapolis.
- Webers, G.F. 1972. Paleogeology of the Cambrian and Ordovician strata of Minnesota. p. 474-484. *In* P.K. Sims and G.B. Morey (ed.) *Geology of Minnesota: A Centennial Volume*. Minnesota Geological Survey, Saint Paul.
- Weeks, L.G. 1953. Environment and mode of origin and facies relationships of carbonate concretions in shales. *Journal of Sedimentary Petrology* 23:162–173. (Cited in Pettijohn 1957, 1975).
- Wehrli, B., G. Friedl, A. Manceau. 1995. Reaction rates and products of manganese oxidation at the sediment-water interface. *In* C.P. Huang, C.R. O'Melia, J.J. Morgan (ed.) *Aquatic chemistry: interfacial and interspecies processes*. American Chemical Society, Washington, D.C. (Cited in Tebo et al. 1997).
- Weisenborn, B.N. and R.J. Schaetzl. 2005. Range of fragipan expression in some Michigan soils I: morphological, micromorphological, and pedogenic characterization. *Soil Sci. Soc. Am. J.* 69:168–177.
- Welch, S.A., A.G. Christy, D. Kirste, S.G. Beavis, F. Beavis. 2007. Jarosite dissolution I – Trace cation flux in acid sulfate soils. *Chemical Geology* 245:183–197.
- Welch, S.A., D. Kirste, A.G. Christy, F.R. Beavis, S.G. Beavis. 2008. Jarosite dissolution II – Reaction kinetics, stoichiometry and acid flux. *Chemical Geology* 254:73–86.
- Wheeting, L.C. 1936. Shot soils of western Washington. *Soil Sci.* 41:35–45.
- White, G.N. and J.B. Dixon. 1993. Iron and manganese distribution in nodules from a young Texas Vertisol. *Soil Sci. Soc. Am. J.* 60:1254–1262.
- Whittig, L.D., V.J. Kilmer, R.C. Roberts, and J.G. Cady. 1957. Characteristics and genesis of Cascade and Powell soils of northwestern Oregon. *Soil Sci. Soc. Am. Proc.* 21:229–232.
- Winters, E. 1938. Ferromanganiferous concretions from some podzolic soils. *Soil Sci.* 46:33–40.
- Wright, H.E., Jr. 1972. Quaternary History of Minnesota. p. 515–547. *In* P.K. Sims and G.B. Morey (ed.) *Geology of Minnesota: A Centennial Volume*. Minnesota Geological Survey, Saint Paul.
- Wright, H.E., Jr. 1976. Ice retreat and revegetation in the Western Great Lakes area. p. 119–132. *In* W.C. Mahaney (ed.) *Quaternary Stratigraphy of North America*. Dowden, Hutchinson & Ross, Stroudsburg, PA.
- Yershov, E.D. 1998. *General Geocryology*. Cambridge University Press, UK.

- Zanner, C.W. 1998. Late-Quaternary Landscape Evolution in Southeastern Minnesota: Loess, Eolian Sand, and the Periglacial Environment. Ph.D. dissertation. University of Minnesota, St. Paul.
- Zapffe, C. 1931. Deposition of manganese. *Economic Geology* 26(8):799–832.
- Zapffe, C. 1933. Catalysis and its bearing on origin of Lake Superior iron-bearing formations. *Economic Geology* 28(8):751–772.
- Zhang, M. and A.D. Karathanasis. 1997. Characterization of iron-manganese concretions in Kentucky Alfisols with perched water tables. *Clays and Clay Minerals*. 45(3):428–439.

APPENDICES

Appendix A

Table A1. ICP data corrected against a blank. All values are in mg/kg. KD1 denotes a sample from the Kandiyohi County site; C1 through C4 refer to color class; F, H, M denote feature, halo, and matrix respectively.

Sample	Element									
	Al	Ba	Ca	Cd	Co	Cu	Fe	K	Li	Mg
KD1C1F	1451	45	6207	0	0	112	46890	0	0	1365
KD1C2F	2279	152	6043	0	0	53	75770	0	0	3861
KD1C3F	1496	82	3633	0	0	34	48010	0	0	4598
KD1C4F	1726	145	4272	0	0	94	114940	0	0	7868
KD1C2H	2347	59	16126	0	0	66	39400	0	0	16870
KD1C3H	1864	43	11706	0	0	36	31160	0	0	13890
KD1C4H	2221	52	15276	0	0	55	31680	0	0	14200
KD1M	6399	118	54556	0	0	68	12710	0	0	41650
Sample	Mn	Na	Ni	P	Pb	S	Si	Sr	Ti	Zn
KD1C1F	147	591	25	4064	0	372	5130	18	63	0
KD1C2F	30	0	0	271	0	0	8395	12	51	0
KD1C3F	29	0	0	184	0	0	5110	12	45	0
KD1C4F	411	0	0	332	0	0	13657	13	50	251
KD1C2H	111	0	0	297	0	0	7129	20	93	124
KD1C3H	69	0	0	325	0	0	5730	12	72	0
KD1C4H	88	0	0	320	0	0	6388	21	87	530
KD1M	425	0	0	1478	0	0	19157	41	288	0

Appendix B

Table B1. Reagents and stains. For details see references in text.

Reagent, Extractant, or Stain	To make 20 ml of solution in DI water or as indicated
Ammonium oxalate, 0.2 M	5.68 g in DI water
Ammonium oxalate + oxalic acid	Mix 4:3 to obtain a pH of 3
Acetic acid, 2 N	2.3 ml glacial (17.4 N) in DI water
Alizarin cyanin green (Acid Green 25)	0.4 g in 50 ml methanol
Alizarin Red S	0.03 g in 30 ml 0.2% HCl
Alizarin Red S + 5% NaOH	Mix in equal proportions
Alizarin Red S + 30% NaOH	Mix in equal proportions
Alizarin Red S + Potassium ferricyanide	Mix in equal proportions
Ascorbic acid, 0.1 M	3.5 g in DI water
Benzidine	0.2 g in 10 ml of 1% HCl (saturated)
Feigl's solution	1.44 g $\text{MnSO}_4 \cdot \text{H}_2\text{O}$, 0.2 g Ag_2SO_4 , 1 drop 5% NaOH†
Harris' Hematoxylin, Modified	Commercially available; full strength
Hydrochloric acid, 0.25 N	0.41 ml of 12.1N HCl in DI water
Hydrochloric acid, 0.2%	0.04 ml of 12.1 N HCl in DI water
Hydrochloric acid, 0.2% (alt. method)	0.4 ml of 10% HCl in DI water
Hydrochloric acid, 10%	2 ml of 12.1N HCl in DI water
Hydrochloric acid, 2%	0.4 ml of 12.1N HCl in DI water
Hydrogen peroxide, 3%	Commercially available
Hydrogen peroxide, 30%	Commercially available
Hydroxylamine hydrochloride	3.47 g (0.25 M) in 20 ml of 0.25 N HCl
Hydroxylamine hydrochloride, pH2	1.39 g (0.1 M) in 20 ml of 0.01 N HNO_3
Magnesium reagent	Commercially available; full strength
Nitric acid, 0.01 N	0.3 ml of 15.6 N HNO_3 in DI water
Nitric acid, 6 N	7.7 ml of 15.6 N HNO_3 in DI water
Oxalic acid, 0.2 M	5.0 g in DI water
Potassium ferricyanide	0.1 g in 20 ml of 0.2% HCl‡
Potassium hydroxide, concentrated	24.2 g in DI water (saturated)
Potassium hydroxide + 3% H_2O_2	Mix in equal proportions
Rhodamine B Base	0.2 g in 25 ml methanol
Sodium bismuthate	Powder added directly to test solution
Sodium hydroxide, 5%	5 g in 95 ml DI water
Sodium hydroxide, 30%	30 g in 70 ml DI water
Sodium hypochlorite (NaOCl)	Commercial laundry bleach; full strength
Sodium(meta)periodate	2.9 g in DI water (saturated)
Tetrabase, 1%	0.2 g in 19.8 g chloroform
Titan yellow	0.2 g in 25 ml methyl alcohol
Titan yellow + 30% NaOH	Mix in equal proportions

† In 20 ml of DI water

‡ Potassium ferricyanide and hydrochloric acid mixture is unstable. For longer shelf life, mix 1% potassium ferricyanide and 0.4% hydrochloric acid separately. Combine in equal amounts shortly before using.

Appendix C

Discussion and evaluation of analytical methods

A variety of analytical methods were considered in an attempt to obtain a useful basis for characterization and comparison of high-chroma features. A brief discussion of each method that was considered, whether used or not, is given below. Specific results, when obtained, can be found in the section titled "Characterization of high-chroma features." The purpose of this section is to share some thoughts about and experiences with selected analytical methods in a way that might prove useful to subsequent investigators who are considering further work on high-chroma or similar pedofeatures.

Optical microscopy

As suggested by Schaetzl and Anderson (2005:25–26), low-power stereomicroscopy proved to be one of the most useful and effective techniques for characterizing, describing, and classifying features. The ability to visualize in color and dissect features with specialized microtools for further analysis was crucial. Several physical properties were readily observed, measured, and recorded while the features remained in the ped, but the loose structure of features meant that some disturbance of features was unavoidable when breaking peds open while searching for features within peds.

The ability to view features in three-dimensions revealed a perspective seldom appreciated in optical microscopy. Additional capabilities were provided by image analysis software. Recent software enhancements, specifically the ability to stack images in the z-axis using Photoshop™ and other software results in an extended depth of field capability that greatly enhanced documentation and image interpretation that had not been possible previously. Readily available software easily converted the RGB of screen pixels to Munsell color notation, although calibration of colors with an acceptable balance throughout the color range proved to be problematic.

Thin sectioning was hindered by the extreme friability of the features, difficulties with impregnating the peds with epoxy, and the low probability of intersecting a feature contained within the ped. Poor epoxy impregnation was most likely the result of the relatively high clay content of the soil together with the collection technique, which tended to close the already small pores of these fine-textured loamy soils. Many of these extremely friable features were lost during the grinding and polishing of sections as a result of poor epoxy

impregnation. Water also had to be excluded from any grinding, polishing, or cleaning operations.

Despite the difficulties, some usable sections were obtained (Plates 17, 18, 32). Professionally prepared samples produced no better and sometimes worse results than thin sections prepared internally. Results depended on the amount of experience the vendor had working with soils.

Scanning electron microscopy and microanalysis

Since electrons produce images only in black and white, concentrations were difficult and sometimes impossible to locate under the scanning electron microscope. Best results were obtained by mapping the location of a feature on an image taken with an optical microscope and then combining electron imaging with EDS to find iron peaks stronger than those from the surrounding soil matrix. Optimal resolution in electron microscopy, both for imaging and EDS, requires the application of conductive coatings to drain away the accumulating electrical charge from the electron beam. These coatings were not always effective because of the uneven texture, high relief, and small openings in the features and peds that prevented the coating from penetrating into the feature. Backscattered electron imaging met with no better success than secondary electron imaging.

Despite the obvious textural contrast between features and matrix when viewed under the optical microscope, SEM did not always reveal a detectable contrast difference.

Manganese was never detected in any sample with the SEM/EDS. This result was not entirely surprising since manganese content of the features was expected to be low, likely below the detection limit for EDS.

Backscattered imaging with the variable-pressure SEM was somewhat more successful at locating features but in the end, was not a reliable solution. As with conventional SEM/EDS, the combination of imaging and chemical analysis to confirm the location, was the most reliable method of locating features.

Variable-pressure SEM did produce some interesting and useful images but it too, failed to detect manganese in any sample, even with extended dwell times.

Transmission electron microscopy and microanalysis

Transmission electron microscopy also images only in black-and-white. TEM requires a sample that is sufficiently thin so electrons are able to pass through, making sample preparation considerably more time-consuming than with SEM. Again, even using a relatively straightforward method of sample preparation, lack of color contrast made locating features a time consuming,

inefficient, hit-or-miss proposition. Using EDS to complement the image view, as was done with SEM, was the only option.

Iron minerals were intermixed with quartz and other minerals, none of which produced a unique identifiable morphology, chemical spectrum, or electron diffraction (ED) pattern. Poor crystallinity of iron minerals may have contributed to the lack of success identifying minerals using selected area electron diffraction with the TEM. At best, the results were ambiguous. Most of the measurable spacings belonged to quartz. Some spacings fell between goethite and quartz. No positive identification of any mineral was possible.

Ion milling was considered as a possible method of thinning a feature in-situ to make it electron transparent for the TEM. The time and expense required was prohibitive and the uncertainty of locating small colored features that could be viewed only in the black-and-white of electron imaging made the procedure impractical.

X-ray diffraction

Conventional and micro-XRD were found to be of limited value for identifying iron or manganese minerals. Conventional XRD was limited by the small quantity of material available. In many cases, the quantity of iron, manganese, and other minerals may have been below the detection limit of XRD. In other cases, poor crystallinity may have contributed to unsuccessful attempts at identification. Much of the iron oxide in high-chroma features occurs as thin coatings on silt-sized quartz or silica, making separation impractical and detection unlikely. The micro-diffraction methods used in this study offer the greatest potential for future work.

Raman spectroscopy

Raman spectroscopy through an optical microscope, called micro-Raman spectroscopy, has the potential for identifying and characterizing minerals present even in the small volumes associated with high-chroma features. Virtually no sample preparation is needed. All samples, however, exhibited substantial fluorescence that obscured any underlying Raman spectra. In some cases, only one or two weak peaks were resolved. These peaks were not by themselves diagnostic, leaving mineral identification inconclusive. The fluorescence problem persisted with all natural samples. Synthetic samples produced useable spectra as did pure natural minerals, such as quartz. For example, a sample of ASTM standard silica produced an excellent quartz spectrum with Fourier-Transform Raman (FT-Raman). Fluorescence remained a problem even at the longer wavelengths of a krypton laser instead of the shorter wavelength argon-ion laser. Although fluorescence was reduced using FT-

Raman, the lower sensitivity of the longer wavelength laser contributed to its inability to resolve any spectral peaks, so produced no useable information about the composition of high-chroma features.

Fluorescence is a commonly acknowledged problem using Raman spectroscopy with many materials, including iron minerals. Its presence is attributed in many cases to impurities within the sample but colored samples or colored molecules are also known to cause a variety of problems. At the present time, the best solution seems to be the use of a pico- or nanosecond pulsed laser with a Kerr-gated system. Only the first few pico- or nanoseconds of emission following the laser pulse are collected. Since the Raman scattering takes place faster than fluorescence, the incoming signal is predominately from Raman scattering. Filtering by the Kerr-gate, essentially a polarization device, rejects fluorescence signals. These short, filtered pulses are accumulated over a period of time to produce a fluorescence-free spectrum (Smith and Dent 2005: 149–150, 197–198). Such a system was unavailable for this project.

Although expensive pulsed Kerr-gated systems are most successful in reducing fluorescence, some researchers have reported successfully producing Raman spectra and identifying iron minerals using more conventional systems (Kingma and Hemley 1994; Kolesov and Geiger 2004; Hanesch 2009) but significant reductions in power and greatly increased counting times are necessary to decrease fluorescence to an acceptable degree (Froment et al. 2008). Consistent with results obtained in this study, synthetic laboratory prepared samples or at least relatively pure natural samples give the best results (for example Kingma and Hemley 1994; de Faria et al. 1997; Mazetti and Thistlethwaite 2002). It is unclear why some are successful and some are not.

Another common problem is that many iron minerals will transform when subjected to a high-energy laser beam either through thermal or photodegradation. A transformation of iron coatings, apparently from goethite to hematite, was observed in some samples. Low power and longer dwell times are necessary to prevent such unwanted transformations while still permitting the collection of sufficient data to produce a useable Raman spectrum.

Raman imaging and mapping are related techniques that also have considerable potential but were not explored.

Despite the setbacks, Raman is a promising technology worthy of continued development and pursuit. Raman is a highly sensitive technique, capable of identifying samples 1 μm diameter or smaller with a minimum of sample preparation. Portable field systems are being developed but their

widespread successful use for iron minerals and other materials that tend to fluorescence awaits further development.

Laser Scanning Confocal Microscopy

Since fluorescence proved to be a fatal flaw with Raman spectroscopy, the idea of using fluorescence to advantage with Laser Scanning Confocal Microscopy (LSCM) was explored. As with Raman spectroscopy, little or no sample preparation is required. Samples can be impregnated and polished sections or loose material. Liedmann and Quader (1991) used LSCM imaging to study the dedolomitization of dolomites and the alteration of limonite in carbonate using optical sectioning.

In LSCM, coherent laser light is scanned across a sample. Secondary fluorescence emitted by the sample passes through an aperture to remove the out-of-focus light and is collected by a sensitive detector. Multiple wavelength lasers can be used simultaneously to collect a full spectrum of fluorescent images of the sample. As applied to geologic and soil samples, each mineral would produce a unique spectrum, thus providing a relatively simple way to identify and characterize various minerals.

Mineral identification with LSCM would have required constructing specific spectra based on emission patterns of known standard minerals. The absence of a database, however, would not preclude the collection of spectra for the comparison of different samples.

Iron and manganese minerals are actually expected to quench fluorescence. While this was not the case with Raman, it was true of LSCM. High-chroma features were located but appeared only as black areas devoid of any internal detail. The inability to produce a spectrum from iron and manganese minerals removed any incentive to pursue further work with LSCM.

Ultraviolet-Visible-Near Infrared microspectroscopy

Ultraviolet-Visible-Near Infrared (UV-Vis-NIR) microspectroscopy is a relatively new technique that can non-destructively measure absorbance, reflectance, fluorescence, and polarization in samples less than about 1 μm in diameter. The equipment needed is relatively compact and the principles involved are straightforward. An ultraviolet, visible, or near infrared light source is directed onto or through a sample, passing through a standard microscope objective and focused on the spectrophotometer aperture. Electromagnetic energy collected from the sample enters the spectrophotometer through the aperture and is separated into its component wavelengths by a diffraction grating. The separated light is then focused onto a detector where the intensity of each wavelength is measured and sent to a computer to produce a spectrum that

displays the intensity of each wavelength of light. As with LSCM, fluorescence can be used to advantage, but in most cases, as with many new analytical methods, characteristic spectra must be developed for the particular material being studied. A sample was brought to a workshop on campus conducted by Craic Technologies and Ebatco and sponsored by the Characterization Facility.

No spectra were obtained using UV-Vis-NIR on any samples of high-chroma features. Although these results were disappointing, as with Raman spectroscopy, the technique should be considered as a potentially useful analytical technique.

Electron microprobe analysis

Electron microprobe analysis (EMPA) was another micro-beam technique that was considered. The electron microprobe is essentially an electron microscope optimized for analysis rather than imaging. Along with conventional EDS, the microprobe is equipped with more sensitive Wavelength Dispersive Spectrometers (WDS). Another advantage of EMPA is that the microprobe is also equipped with an optical microscope, making it possible to locate and position the beam over a colored feature for WDS analysis. Since quantities of iron and manganese especially were expected to be low, the greatly enhanced sensitivity of WDS over EDS was attractive. Poor impregnation of the epoxy made it impossible to produce a sample that could be polished to the required 0.1 μm finish required to access the full benefits of WDS. Commercially prepared sections were of no better quality than those prepared in-house. EMPA was pursued no further and no actual analysis was attempted with EMPA.

Magnetics

Magnetic methods offer a number of advantages for soil analysis including ease of sample preparation and relative simplicity of the procedures themselves. These methods, however, require a larger quantity of sample material than was available from submillimeter-size high-chroma features.

A few peds with strongly expressed hydromorphology had concentrations and depletions containing sufficient material to submit for magnetic analysis. Features submitted were ped and root channel linings, not high-chroma features. Sample masses ranged generally from 50 to 150 mg. Results using the Vibrating Sample Magnetometer suggested that a large, soft, yellow-brown concentration could be a mixture primarily of goethite and magnetite and possibly a very small amount of hematite but no ferrihydrite. This result suggests that the sample could be very old, any ferrihydrite that formed initially having transformed into goethite and hematite. Later work with Mössbauer spectroscopy found only goethite with lattice defects but the

concentration of magnetite was below the detection of level for Mössbauer. Iron, possibly in the form of magnetite, was also present in neoalbans surrounding root channels. Some magnetic order was detected in all samples and all samples appeared to contain at least some magnetite.

The smallest sample submitted (11.0 mg) produced very noisy results most likely as a result of the small sample size. Since high-chroma features contain only a fraction of this quantity of material even in the very largest features, and those occur only in limited quantity and in restricted locations, neither a characterization of nor a comparison between features that occur in pedes having differing hydromorphology would have been possible. Consequently, no further work with magnetics was pursued.

Wet Chemical Methods

Wet chemical tests were among the most successful. Acid ammonium oxalate, used to estimate the degree of crystallinity of iron minerals, was used also as a partial extractant for subsequent ICP analysis.

Classic stain tests, principally for carbonates, were also successful but the number of tests performed on any sample was limited by the small quantity of sample available. Spot tests to identify specific elements were of limited success. In most cases the reagent used for extraction interfered with the action of the indicator.

ICP analysis was also successful. ICP was the only analytical technique that was able to identify manganese in the features. Only limited work with ICP was completed due to lack of resources. Additional work needs to be continued to complete the analysis on a full set of samples. In addition, the element cerium should be added to the suite of trace elements in the analysis. Cerium, like barium, is often closely associated with manganese. More discussion on that point follows in a subsequent section.

Characterizing high-chroma features requires analysis of sub-millimeter sized features that are difficult to distinguish from the surrounding soil matrix except by color. They are poorly cemented, making them difficult to separate completely from the ped without contamination from the surrounding soil matrix, are often weakly crystalline, and contain concentrations of iron, manganese, and other elements and minerals that are below the detection limit of many conventional micro-analysis methods. Taken together, these factors limited the success of x-ray and electron beam analysis.